The Basal Opisthokonts *Nuclearia* spp. with Associated Bacterial Symbionts: Aspects of Diversity and Ecology

Dissertation

zur

Erlangung der naturwissenschaftlichen Doktorwürde

(Dr. sc. nat.)

vorgelegt der

Mathematisch-naturwissenschaftlichen Fakultät

der

Universität Zürich

von

Sebastian Dirren

von Unterbäch VS

Promotionskomitee

PD Dr. Thomas Posch

Prof. Dr. Jakob Pernthaler

Prof. Dr. Leo Eberl

Zürich, 2016

‘Now, a composite is composed of something in such a way that the whole thing is one, not as a heap is, but as a syllable is. A syllable is not the same as its letters – for instance, B and A are not the same thing as BA, nor is flesh fire and earth.’

Aristotle

Table of contents

Summary

The diverse group of the Opisthokonta includes beside Metazoa (animals) and Fungi about 300 described protists (i.e. unicellular eukaryotes). The family Nucleariidae, one of these protistan taxa, is the sister group of Fungi. It is represented by the single genus *Nuclearia*, which is made up of 11 described species. Nine of these nucleariids were described during the 19th century, when descriptions exclusively relied on morphological characteristics. Unfortunately, the limited number of good diagnostic characters led to misidentifications and re-descriptions. Nowadays, morphological characterisation in combination with sequencing of the 18S rRNA gene allows more holistic species descriptions. This is the basis for phylogenetic analyses and facilitates the identification of isolates. While typical nucleariid species were isolated from different freshwater lakes, their diversity has never been addressed systematically. For this PhD thesis, 17 *Nuclearia* spp. strains were isolated from five Swiss lakes and characterised morphologically as well as by their 18S rRNA genes. Surprisingly, an unexpected high diversity of nucleariid species was found even in single lakes. Isolates from Lake Zurich, for example, belonged to four different phylogenetic clusters.

An interesting aspect of nucleariids is their association with prokaryotic symbionts. Especially two species (*N. thermophila* and *N. delicatula*) are frequently associated with ecto- as well as endosymbiotic bacteria. Many nucleariid species have a characteristic glycocalyx which can be colonised by ectosymbionts. Endosymbionts on the other hand are located inside the cytoplasm either freely or surrounded by a host derived membrane. Although symbionts of *N. radians* were observed by transmission electron microscopy already in the year 1979, only recently the identification of symbiotic bacteria became technically feasible. Phylogenetic affiliation based on the 16S rRNA gene made it possible, for the first time, to address the diversity of symbionts. After a single identification of the endosymbiont found in *N. pattersoni*, this thesis represents the first systematic quest for symbiotic bacteria of 17 *Nuclearia* spp. isolates. My studies led to the identification of six different symbionts, but it seems that we still are only scratching the surface of symbionts' diversity. The phylogenetic assignment of the two observed ectosymbionts was possible, however, no close relatives of the four endosymbionts were found in public data bases. Thus, the provisional status of *Candidatus* species was proposed for these bacteria and they were named as following: *Ca.* Endonucleariobacter rarus, *Ca*. Ovatusbacter abovo, *Ca.* Turbabacter delicatus and *Ca.* Intestinusbacter nucleariae.

Apart from the diversity of nucleariids and their symbionts, it was the aim of this PhD thesis to address also ecophysiological aspects. Despite its possible ecological importance, the ability of many nucleariid species to feed on and digest toxic cyanobacteria has not been investigated systematically up to now. Although exact functions of symbionts remained unexplored, feeding experiments revealed instead a pivotal role of accompanying bacteria. The bacterial assemblage in the culture medium affected not only the growth of nucleariid amoebae but it had also an impact on the degradation of microcystins, the cyanobacterial toxin. This finding again pointed to intimate interactions of these eukaryotic cells with prokaryotic species. Experiments with 'isolated' protists are often used to address physiological aspects. Results from nucleariid amoebae emphasised the need to carefully draw conclusions from experiments, in which organisms are investigated separated from their natural 'microbiota'.

Zusammenfassung

Die heterogene Gruppe der Opisthokonta beinhaltet neben den Metazoa (Tiere) und Fungi (Pilze) schätzungsweise 300 beschriebene Arten von Protisten (einzellige Eukaryoten). Einige dieser einzelligen Opisthokonten gehören zur Familie der Nucleariidae, welche eine Schwestergruppe zu den Pilzen darstellt. Sie enthält einzig die Gattung *Nuclearia* mit 11 beschriebenen Arten. Neun Artbeschreibungen aus dem 19. Jahrhundert beschränken sich ausschliesslich auf morphologische Merkmale. Unglücklicherweise führte das Fehlen guter diagnostischer Merkmale dazu, dass einerseits Arten falsch bestimmt wurden und andererseits neue Artbeschreibungen von schon bekannten Spezies entstanden. Heutzutage werden morphologische Untersuchungen mit Analysen der 18S rRNA Gensequenz kombiniert. Dies ermöglicht sowohl phylogenetische Rekonstruktionen, als auch zuverlässigere Artbestimmungen. Nichtsdestotrotz hat noch keine vorherige Studie die Diversität der Nucleariiden systematisch untersucht. Für diese Dissertation wurden erstmals 17 *Nuclearia* spp. Stämme aus fünf Schweizer Seen isoliert, morphologisch charakterisiert und deren 18S rRNA Gene sequenziert. Die gefundene Diversität von *Nuclearia* Arten war überraschend hoch, beispielweise gehörten die Stämme vom Zürichsee zu vier phylogenetischen Gruppen.

Ein interessanter Aspekt der Nulceariiden ist deren Assoziation mit prokaryotischen Symbionten. Zwei Arten (*N. thermophila* und *N. delicatula*) sind besonders oft sowohl mit Ekto- als auch mit Endosymbionten assoziiert. Während ektosymbiotische Bakterien die bei vielen nucleariiden Arten vorhandene Glykokalyx besiedeln, findet man die Endosymbionten entweder frei im Zytoplasma oder in Symbiosomen (umhüllt von einer zusätzlichen Membran). Schon im Jahre 1979 wurden symbiotische Bakterien von *N. radians* mit Transmissionselektronenmikroskopie beobachtet, aber erst seit kurzem ist es möglich, diese Symbionten exakt zu identifizieren. Mit Hilfe phylogenetischer Analysen basierend auf 16S rRNA Genen konnte erstmals die Diversität der Symbionten untersucht werden. Nach einer einzigen Arbeit über die Endosymbionten von *N. pattersoni* aus dem Jahr 2003, stellt diese Doktorarbeit erstmals eine systematische Suche nach symbiotischen Bakterien in 17 *Nuclearia* spp. Isolaten vor. Obwohl sechs Symbionten identifiziert wurden, scheint dies erst ein kleiner Teil der gesamt vorhandenen Diversität zu sein. Während sich die zwei Ektosymbionten phylogenetisch zuordnen liessen, wurden für die vier Endosymbionten keine nahen Verwandten gefunden. Diese neuen Arten bekamen daher den provisorischen Status ‚*Candidatus*' und wurden folgendermassen benannt: *Ca.* Endonucleariobacter rarus, *Ca*. Ovatusbacter abovo, *Ca.* Turbabacter delicatus and *Ca.* Intestinusbacter nucleariae.

Neben der Diversität von Nucleariiden und deren Symbionten befasst sich diese Doktorarbeit auch mit ökophysiologischen Aspekten. Die Fähigkeit sich von toxischen Cyanobakterien zu ernähren wurde bei den nucleariiden Arten, trotz der möglichen ökologischen Bedeutung, nicht gänzlich untersucht. Während die Funktion der Symbionten noch unklar ist, zeigten meine Experimente, dass den Begleitbakterien im Kulturmedium eine entscheidende Rolle zukommt. Die Zusammensetzung der bakteriellen Gemeinschaft beeinflusste nicht nur das Wachstum der nucleariiden Amöben, sondern auch den Abbau von Microcystinen, den Toxinen von Cyanobakterien. Diese Resultate verdeutlichen, wie wichtig Interaktionen zwischen eukaryotischen Zellen und prokaryotischen Arten sind. Um physiologische Aspekte zu untersuchen, werden in vielen Studien Experimente mit ‚isolierten' Protisten durchgeführt. Experimente mit Organismen, die von ihrem natürlichen ‚Mikrobiom' getrennt wurden, bergen daher stets ein erhebliches Risiko zur Fehlinterpretation. Die Ergebnisse dieser Doktorarbeit zeigen am Beispiel der nucleariiden Amöben eindrücklich, wie wichtig eine vorsichtige Interpretation von Resultaten solcherart Experimente ist.

Preface

According to the Protist Working Group (Pawlowski et al., 2012), approximately 74 400 described protistan species are catalogued. Remarkably, estimates about the real species richness range from 140 000 to 1.6 million. This great discrepancy between the number of described species and estimates about the real diversity points to huge amount of 'protists dark matter'. Studies using Next Generation Sequencing methods continuously generate environmental sequences of marker genes (i.e. DNA barcodes), which at present cannot be assigned to any known species. It is thus the challenge of this century to give a 'face' to these nameless sequences.

Aspects of diversity and ecophysiology of nucleariid species and their symbionts represent the main part of this PhD thesis. My work resulted in two published articles in the peer-reviewed journals *Protist* (Dirren et al., 2014) and *FEMS Microbiology Ecology* (Dirren and Posch, 2016), and an additional manuscript, which is currently in preparation. Beside these three articles about nucleariids, I had the opportunity to work on a forth publication describing a recently discovered ciliate. Although the newly described species belongs to a different phylogenetic taxon (i.e. Alveolata), this study had several aspects in common with my previous work. It is the first ciliate of the genus *Tetrahymena*, which was found to harbour endosymbiotic green algae. My main contribution to this article was the phylogenetic analysis of endosymbiotic algae. The state of the art approach using sequence-structure information from the 18S rRNA gene combined with the ITS2 region allowed for the affiliation of algae to the genus *Micractinium* (Chlorellaceae). This forth article was accepted by the *Journal of Eukaryotic Microbiology* and will be published soon.

> **Article I**: Dirren S, Salcher MM, Blom JF, Schweikert M & Posch T (2014) Ménage-à-trois: The amoeba *Nuclearia* sp. from Lake Zurich with its ecto- and endosymbiotic bacteria. *Protist* **165**: 745-758.
>
> **Article II**: Dirren S & Posch T (2016) Promiscuous and specific bacterial symbiont acquisition in the amoeboid genus *Nuclearia* (Opisthokonta). *FEMS Microbiology Ecology* **92**.
>
> **Article III**: Dirren S, Pitsch G, Da Silva M & Posch T (in prep.) Feeding of *Nuclearia thermophila* and *Nuclearia delicatula* (Nucleariidae, Opisthokonta) on the toxic cyanobactetrium *Planktothrix rubescens*.
>
> **Article IV**: Pitsch G, Adamec L, Dirren S, Nitsche F, Šimek K, Sirová D & Posch T (accepted) The green *Tetrahymena utriculariae* n. sp. (Ciliophora, Oligohymenophorea) with its endosymbiotic algae (*Micractinium* sp.), living in traps of a carnivorous aquatic plant. *Journal of Eukaryotic Microbiology*.

On the following pages I try to add an 'historical perspective' to this PhD thesis. I decided to honour contributions from former scientists rather than repeat the introductions of my included articles. Not only that their pioneering work represents a perquisite for modern research, this 'antique' literature is still a resource of fascination and inspiration. After the included articles, I will wrap up my work of the last years pointing out the core findings. The text is organised in chapters related to methodological issues and implications for further studies. For a better understanding of how and why experiments were designed, I will include some unpublished data.

Introduction

Symbiosis

It is hard to imagine a life without the phenomenon of symbioses. Organisms tend to build up interconnections by establishing associations. This tendency seems to be one of the driving forces of innovation, adaption and diversification, which are the fundamental pillars of evolution. Although Charles Darwin did not integrate symbiosis as a driving force in his theory about 'The origin of species', this ubiquitous phenomenon does not contradict his fundamental assumptions. This was already realized by the German biologist Heinrich Anton de Bary (1879), who set the concept of symbiosis into a biological context. He simply defined symbiosis as a close association of dissimilar organisms and emphasised the need to perceive this phenomenon as a general principle including parasitism, commensalism and mutualism. De Bary named symbioses between parasitic fungi and insects in the same breath as those between epiphytic orchids and their trees, pollinating insects and their plants, buffalos and their nose cleaning birds, fungi and their algal symbionts (i.e. lichens) and so on. Consequently, by this broad definition independent biological disciplines were 'suddenly' forced to communicate and to exchange knowledge with each other. It is thus not surprising that de Bary's generalisation came under criticism at its very beginning. Among others, especially lichenologists felt offended. Their favourite organisms were not valued as independent specimens anymore, but rather *'degraded'* to creatures originating from *'an illegitimate relationship between a fungus and one or even two algae'* (Bary, 1879). Although de Bary pointed to the difficulties to draw clear boundaries between different types of symbioses, he mentioned the possibility to at least distinguish between extreme cases by their very nature. For example highly pathogenic interaction (e.g. human trichinosis) can be classified as antagonistic, whereas obviously beneficial or even obligate interactions (e.g. lichens) should be characterised as mutualistic.

The next milestone in the history of symbiosis research can be dated back to the beginning of the 20th century. The Russian biologist Konstantin Sergejewitsch Mereschkowsky formulated his symbiogenesis theory (Mereschkowsky, 1910). Although the significance of the work has not been appreciated at that time, his revolutionary perspective on the importance of symbiosis for the origin of higher life forms amazes even today. Already in the year 1905, Mereschkowsky argued that any plant cell has to be considered as a product of an ancient endosymbiosis between an animal cell and a cyanobacterium (Mereschkowsky, 1905). Five years later, he integrated his former assumptions about the 'chromatophores' into the general symbiogenesis theory, which he illustrated with a revolutionised phylogenetic tree of life (Fig. 1). According to his theory, two ancient endosymbioses gave rise to the formation of nuclei and chloroplasts, respectively. Although the origin of the nucleus is still under debate today (Martin et al., 2015), molecular analyses proved that plastids have evolved from an ancestral cyanobacterial endosymbiont (Rodríguez-Ezpeleta et al., 2005).

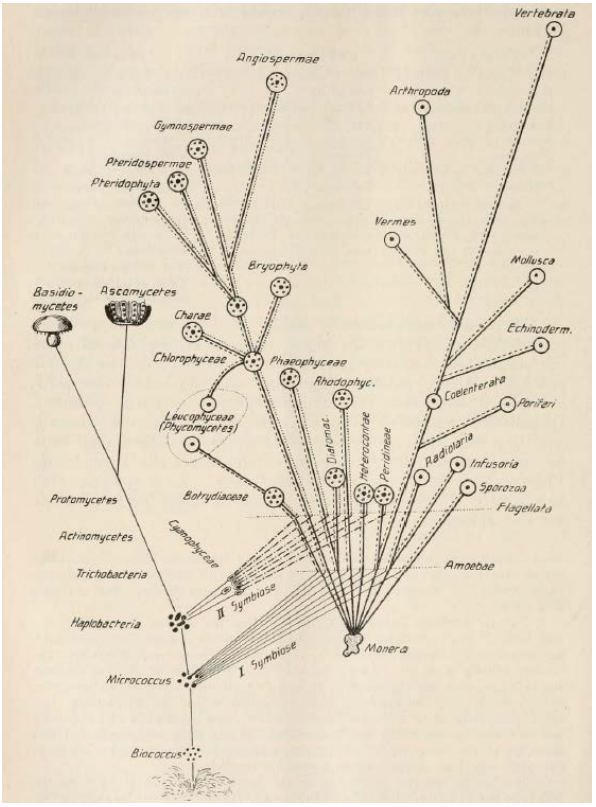

Fig. 1: Phylogenetic tree form Mereschkowsky (1910) illustrating his theory about the two symbiotic events (I and II) which led to the origin of nuclei and 'chromatophores' (i.e. chloroplasts).

About 50 years later Lynn Margulis followed the ideas of Mereschkowsky and others to formulate the well elaborated 'endosymbiotic theory' (Sagan, 1967). Specifically, she postulated the symbiotic origin of mitochondria, flagella and plastids. As mentioned above, it is generally accepted that plastids have evolved from formerly free-living cyanobacteria. Similarly, we have now good evidences, that the alphaproteobacterial clade SAR11 and mitochondria share a common ancestor (Thrash et al., 2011). In contrast, the suggested emergence of flagella through the endosymbiosis with spirochaete-like bacteria could not be verified. It is more likely that the underlying structures evolved from a simpler cytoplasmic microtubule-based transport system (Mitchell, 2007). Nevertheless, Margulis's lifework contributed overwhelmingly to the today's awareness of symbiosis in biology. Her question about *'how one can talk about the evolution of the cow without mentioning its cellulose-digesting microbes'*, illustrates probably this topic at best (Margulis, 1992).

In this context, one can argue that no multicellular organism should be studied isolated from its associated microbial community. During the last decade the pivotal role of the microbiota for human ontology and physiology gained much attention, not at least due to the pathogenic outcome of disruptions to the normal balance (Huttenhower et al., 2012; Lozupone et al., 2012). Although huge steps towards a more comprehensive understanding have been made, it is still challenging to study interactions between trillions of microbes and their host. Less complex examples of associations between eukaryotic and prokaryotic cells can be found for phylogenetically more basal animals like corals (Lema et al., 2014) and cnidarians (Franzenburg et al., 2013). Nonetheless, in these cases their microbiota is estimated to consist of several hundred bacterial species.

Symbioses are not at all restricted to multicellular organisms. Many protistan species are known to be transiently or permanently associated with bacteria. In these cases the number of symbionts is usually much lower. Thus, instead of microbiota the term ectosymbionts is used for the description of extracellularly associated microbes. Whereas intracellular bacteria (i.e. endosymbionts) are rather seldom for animals, they can be found in many protists (Nowack and Melkonian, 2010). These associations between a eukaryotic cell and usually one or two prokaryotic species represent a great opportunity for studying inter-domain symbioses.

During the last years I worked with rather exotic protists belonging to the genus *Nuclearia*. Associations with endo- as well as ectosymbiotic bacteria seem to be a common phenomenon for certain nucleariid species. Therefore, they represent uniquely suited model organisms to study the basic principles of symbiosis between eukaryotes and prokaryotes.

The 'filose' amoeba *Nuclearia*

About 150 years ago, Cienkowski published his pioneering work entitled 'Beiträge zur Kentniss der Monaden' (1865). Supported with descriptions and drawings he presented 9 'monads', which were, as he stated, either new or formerly lumped together in the chaotic genus *Amoeba*. He used the term monads for amoebae with flagellated life stages and / or cysts. Fine hyaline pseudopodia (i.e. filopodia), were a special feature of two newly established groups *Vampyrella* and *Nuclearia*. These 'filose' genera had another character in common, namely they were feeding on algal cells. The 'vampire amoeba' *V. spirogyrae* typically attacked healthy filaments of *Spirogyra* sp. by penetrating the cell walls and 'sacking' their cell content. In contrast, representatives of the genus *Nuclearia* were observed to feed mainly on dead algae. Cienkowski described two species of the new taxonomic group, the uninucleate *N. simplex* and the multinucleate *N. delicatula*. Whereas he found cysts (Fig.2A) of the former species, for *N. delicatula* (Fig. 2B-D) he pointed out that they were either missing or have not been discovered yet. In his eyes, lack of this life stage even questioned their affiliation to the monads. One of Cienkowsky's drawings strikingly illustrates *N. delicatula* extracting the cell content of a filamentous alga by means of a long tube-like pseudopodium (Fig.2D).

Three decades later, Artari reported further observations on the feeding behaviour of a nucleariid species (1889). In addition to the filamentous green algae (e.g. *Spirogyra* sp.) he documented cyanobacterial filaments (e.g. *Oscillatoria* sp.) to be suited as food source for *N. delicatula* (Fig. 2E). Beside new insights into the feeding behaviour of this organism, Artari reported other striking observations. The fusion of individuals to form a syncytium and the 'unidentified' granules (Fig. 2E) inside the mucous layer (i.e. glycocalyx of the cell), are probably the most remarkable ones.

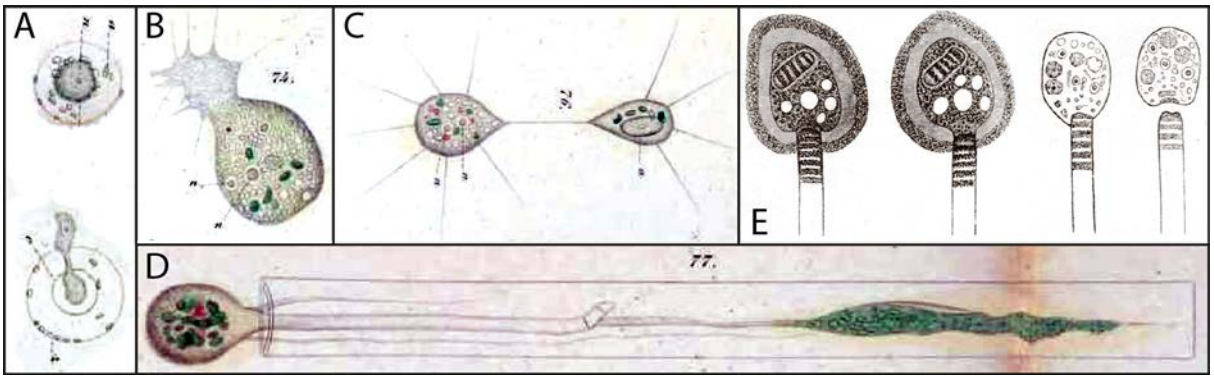

Fig. 2: Drawings of *Nuclearia simplex* and *Nuclearia delicatula* from Cienkowski (1865) and Artari (1889). A: Cyst (above) and excystment (below) of *N. simplex*. B: Multinucleate cell of *N. delicatula*. C: Binary fission of *N. delicatula*. D: Cell content of a dead algal filament extracted by *N. delicatula*. E: Feeding of *N. delicatula* on filamentous cyanobacteria. Note the mucous layer with unidentified 'granules' (two drawings left). A-D: from Cienkowski. E: from Artari.

During the following 90 years, only few studies have reported occasional observations of *Nuclearia* spp.. This changed when Cann and Page (1979) presented detailed light and transmission electron microscopy (TEM) investigations of a new nucleariid species: *Nucleosphaerium tuckeri*. Later the proposed genus disappeared and the newly described species was revised as homonym for *N. radians* (Patterson, 1984). Nonetheless, the ultrastructural observations gave important first insights into the structure of cellular compartments and uncovered the presence of symbiotic partners. TEM preparations revealed, for example, the ultrastructure of the nucleus with its nucleolus, the Golgi apparatus and the flattened mitochondrial cristae. The 'unidentified' granules were recognized for the first time to be Gram-negative bacteria colonizing the 'mucilaginous' coating of the cell. Beyond that, 'endozoic' bacteria (i.e. endosymbionts) were detected in all region of the cytoplasm. In the same year, Mignot and Savoie (1979) published further ultrastructural observations of another nucleariid species, namely *N. simplex*. In contrast to the association of *N. radians* with endo- and ectosymbiotic bacteria, symbionts were present neither in the cell nor inside the glycocalyx of *N. simplex*. These findings already suggested a species-specific interaction with symbiotic bacteria but taxonomic affiliations of bacterial symbionts were still unexplored. Although a morphological characterisation allowed more or less for the discrimination of different *Nuclearia* species, molecular methodologies (e.g. based on the small subunit of the ribosomal RNA encoding gene) were still in their infancy.

In the early 1980es, the two families Nucleariidae and Vampyrellidae were generally assigned to the large class Filosea, established by Leidy (1879). The main character to include organisms into this class was their delicate thread-like pseudopodia (filopodia). The 'heavy weight attached to the presence of thin hyaline pseudopodia' was later criticised by Patterson (Patterson, 1984). He expressed his serious doubts about the monophyly of a class, which comprised a large variety of distinct protistan groups (e.g. dinoflagellates, euglenid flagellates, slime moulds and so forth). Moreover, he even stated his concerns about the close realness of the genera *Nuclearia* and *Vampyrella*. Based on ultrastructural features (e.g. different mitochondrial cristae) he considered the two groups to be only distantly related. In addition to this clear separation from the vampyrelids, he reviewed the family Nucleariidae. In his overview he listed all described species together with homonyms and invalid re-descriptions. Finally he accepted nine species to belong to the genus *Nuclearia* but he was not sure, if

N. delicatula with its peculiar features (e.g. multinucleate, formation of syncytia, ectosymbiotic bacteria) should be considered as type species.

After the studies by Patterson it lasted another 20 years until molecular information from the 18S rRNA encoding gene has resolved the phylogenetic affiliation of the Nucleariidae. Whereas the similar Vampyrellidae were later assigned to the Cercozoa (Hess et al., 2012), nucleariid amoebae were placed at the animal-fungal boundary (Zettler et al., 2001). Phylogenetic analyses based on multiple genes confirmed their assignment to the Opisthokonta (Liu et al., 2009; Steenkamp et al., 2006). Beside animal and fungi this diverse taxon consists of several protistan groups (e.g. Chanoflagellates, Ichthyosporea and Filasterea), which are the closeted living unicellular relatives of the two formerly mentioned multicellular linages.

Since the revision of the genus by Patterson in the 1980es, only two new descriptions of *Nuclearia* species have been published. Both studies were based on morphological and molecular characterisations. Whereas morphological features were addressed with light and electron microscopy, 18S rDNA served as marker gene for phylogenetic tree reconstructions. *N. pattersoni* (Dykova et al., 2003) was isolated from a rather atypical habitat, namely from the gills of roach (*Rutilus rutilus*). While TEM analysis revealed the presence of endosymbionts in the cytoplasm, molecular methods allowed for the first time an identification of the harboured symbiont. Based on its 16S rRNA gene sequence the endosymbiont was placed within the genus *Rickettsia*, whose members are well known for their obligate symbiotic lifestyle. *N. thermophila* (Yoshida et al., 2009), isolated from a thermal spring in Japan, was the last described species in the genus. Neither endo- nor ectosymbionts were detected for this nucleariid amoeba. Yoshida and colleagues listed the morphological features of all 11 valid *Nuclearia* spp. in a comparative table (see Table 1 in the reference) additionally indicating available 18S rRNA gene sequences. At that time only six sequences of isolates assigned to five different species were available in public data bases.

Article I

Dirren S, Salcher MM, Blom JF, Schweikert M & Posch T (2014) Ménage-à-trois: The amoeba *Nuclearia* sp. from Lake Zurich with its ecto- and endosymbiotic bacteria. *Protist* **165**: 745-758.

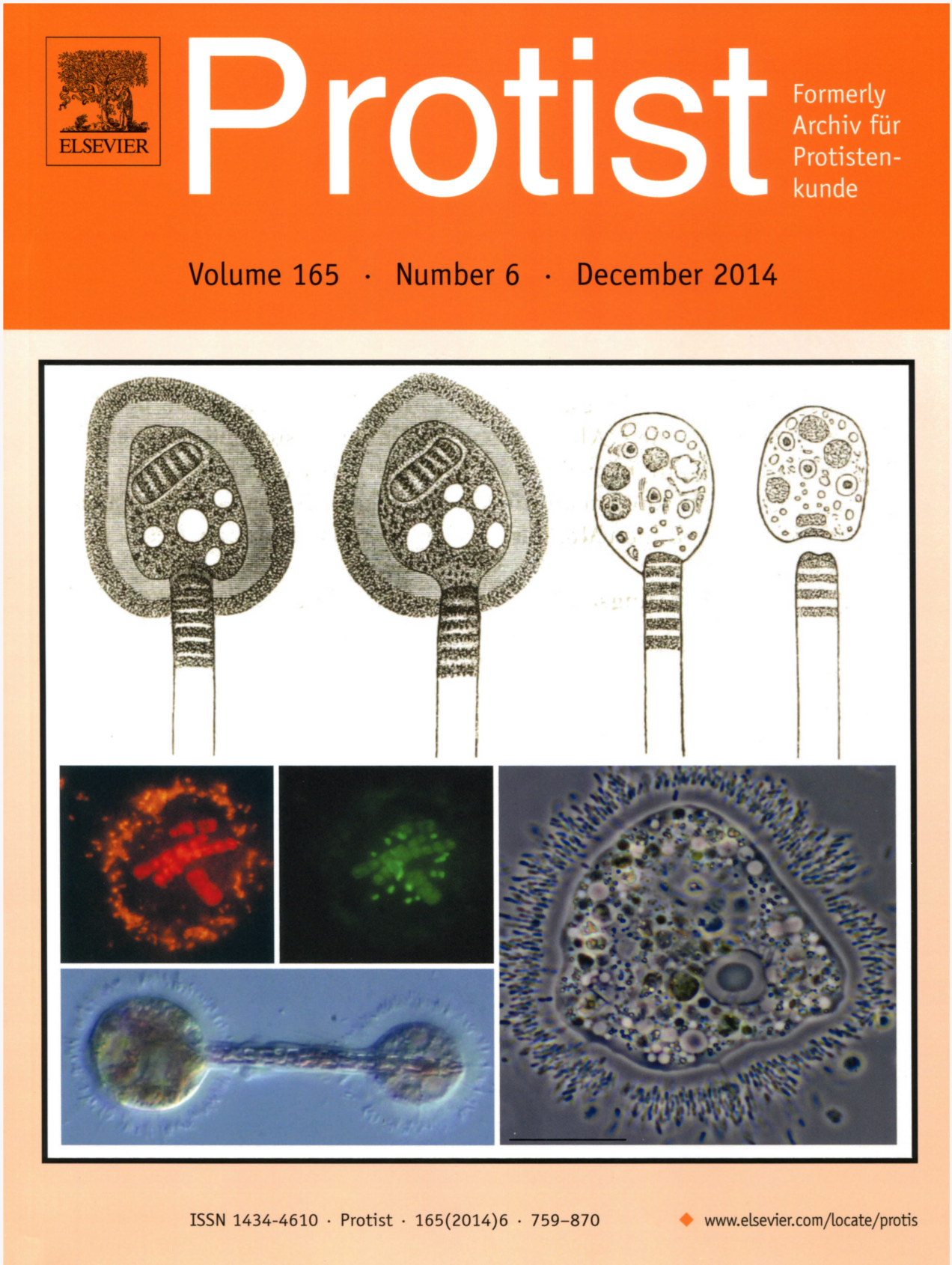

Images from the publication '*Ménage-à-trois*: The amoeba *Nuclearia* sp. from Lake Zurich with its ecto- and endosymbiotic bacteria.' on the cover of the Journal Protist, December 14.

Protist, Vol. 165, 745–758, xx 2014
http://www.elsevier.de/protis
Published online date 28 August 2014

Protist

ORIGINAL PAPER

Ménage-à-trois: The Amoeba *Nuclearia* sp. from Lake Zurich with its Ecto- and Endosymbiotic Bacteria

Sebastian Dirren[a], Michaela M. Salcher[a,b], Judith F. Blom[a], Michael Schweikert[c], and Thomas Posch[a,1]

[a]Limnological Station, Institute of Plant Biology, University of Zurich, Seestrasse 187, CH-8802 Kilchberg, Switzerland
[b]Biology Centre of the Academy of Sciences of the Czech Republic, Institute of Hydrobiology, Na Sádkách 7, CZ-37005 České Budějovice, Czech Republic
[c]Department of Zoology, Institute for Biomaterials and biomolecular Systems, University of Stuttgart, Pfaffenwaldring 57, D-70569 Stuttgart, Germany

Submitted April 29, 2014; Accepted August 19, 2014
Monitoring Editor: Sandra L. Baldauf

We present a fascinating triad relationship between a eukaryotic amoeba and its two bacterial symbionts. The morphological characteristics of the amoeba allowed for a confident assignment to the genus *Nuclearia* (Opisthokonta, Nucleariidae), but species identification resulted in an ambiguous result. Sequence analysis indicated an affiliation to the species *N. thermophila*, however, several morphological features contradict the original description. Amoebal isolates were cultured for several years with their preferred food source, the microcystin-producing harmful cyanobacterium *Planktothrix rubescens*. Symbioses of the amoeba with ecto- and endosymbiotic bacteria were maintained over this period. Several thousand cells of the ectosymbiont are regularly arranged inside a layer of extracellular polymeric substances produced by the amoeba. The ectosymbiont was identified as *Paucibacter toxinivorans* (Betaproteobacteria), which was originally isolated by enrichment with microcystins. We found indications that our isolated ectosymbiont indeed contributed to toxin-degradation. The endosymbiont (Gammaproteobacteria, 15-20 bacteria per amoeba) is enclosed in symbiosomes inside the host cytoplasm and represents probably an obligate symbiont. We propose the name "*Candidatus* Endonucleariobacter rarus" for this bacterium that was neither found free-living nor in a symbiotic association. Nucleariidae are uniquely suited model organisms to study the basic principles of symbioses between opisthokonts and prokaryotes.

Key words: Bacteria-protist symbioses; ectosymbionts; endosymbionts; feeding; Nucleariidae; *Paucibacter toxinivorans*.

Introduction

Two billion years of co-evolution between eukaryotes and prokaryotes has led to the establishment of numerous symbiotic associations (Moya et al.

[1]Corresponding author; fax +41 44 634 9225
e-mail posch@limnol.uzh.ch (T. Posch).

http://dx.doi.org/10.1016/j.protis.2014.08.004

2008). Essentially, all higher animals and plants live in symbiosis with several, up to thousands of prokaryotic species (Marx 2004; Paracer and Ahmadjian 2000; Ruby et al. 2004). Nevertheless, symbioses with bacteria are not restricted to multicellular organisms. Bacterivorous protists live in intimate contact with bacteria, and this spatial co-occurrence is a potential playground for novel symbioses (Görtz and Brigge 1998; Nowack and Melkonian 2010; Schmitz-Esser et al. 2008). Symbiotic bacteria of protists (Gast et al. 2009) are either attached to extracellular structures (ectosymbionts) or inside the host itself (endosymbionts).

In this article the term symbiosis is used as it was first mentioned in a biological context by Heinrich Anton de Bary in the year 1879 (see Appendix 1 in Paracer and Ahmadjian (2000)). Symbiosis includes any kind of coevolutionary-based 'living together' of 'dissimilar individuals'. Thus it comprises the whole spectrum of possible interactions reaching from parasitism to mutualism.

So far, only a few associations of bacteria with protists have been characterized in detail, as symbiotic bacteria are often uncultivable when separated from their hosts. Probably in many cases the appropriate cultivation methods and media for a successful isolation of symbionts have not been found. However, cultivation outside an obligate host has still to be considered challenging or even impossible with the available methods. Nowadays, culture-independent techniques like PCR, cloning and sequencing of marker genes, metagenomics, and fluorescence in situ hybridization (FISH) ease at least the identification of symbiotic microorganisms.

Here we present a triad relationship, in which an amoeboid host is associated with endo- as well as ectosymbiotic prokaryotes. The amoeba belongs to the genus *Nuclearia*, the type genus of the family Nucleariidae, which was originally assigned to the class Filosea by Cann and Page (1979). Based on molecular phylogenetic analyses, nucleariid amoebae are a sister group of Fungi (Brown et al. 2009) belonging to the diverse group of Opisthokonta (Liu et al. 2009; Steenkamp et al. 2006; Zettler et al. 2001). This phylogenetic position makes them uniquely suited model organisms to study the basic principles of symbiosis between opisthokont eukaryotes and prokaryotes. One typical feature of some *Nuclearia* species is the excretion of extracellular polymeric substances (EPS) that form a mucous sheath around the cell - already observed by Artari (1889). A positive periodic acid-schiff (PAS) staining of the EPS, indicating its polysaccharide character, was shown for *N. radians* (described as *Nucleosphaerium tuckeri* by Cann and Page (1979)), for *N. delicatula* (Cann 1986) and for *N. simplex* (Pernin 1976). The EPS can be colonized by ectosymbiotic bacteria that are arranged regularly a few micrometres from the cell membrane (Cann 1986; Cann and Page 1979; Patterson 1984). So far, endosymbiotic bacteria have been detected in two nucleariid species. *N. radians* harbours endosymbionts that are surrounded by a peribacterial membrane in the cytoplasm (Cann and Page 1979), and the amphizoic *N. pattersoni* has a rickettsial endosymbiont (Dyková et al. 2003).

Besides being already a complex community of three microorganisms, several nucleariid amoebae have a peculiar feeding behaviour with respect to prey ingestion and selection (Artari 1889; Cann 1986; Cann and Page 1979). These *Nuclearia* species can ingest toxic filamentous cyanobacteria as their sole source of food. The herein presented *Nuclearia* species isolated from Lake Zurich (Switzerland) preferentially feeds on the filamentous cyanobacterium *Planktothrix rubescens*, which is the main primary producer in this ecosystem (Posch et al. 2012). *P. rubescens* produces and stores several toxic secondary metabolites intracellularly, e.g., microcystins (MCs), that are released into the surrounding when the cell wall is broken. Although the ecological role of MCs is still under debate, they seem to be the primary defence of cyanobacteria against grazers (Blom et al. 2001; Kurmayer and Jüttner 1999). However, some invertebrates (Galanti et al. 2013) and even vertebrates (Pflugmacher et al. 1998) might detoxify these cyanotoxins by the formation of glutathione-MC conjugates. In contrast to the limited knowledge about eukaryotic detoxification pathways of MCs, efficient biological degradation of toxins was reported for various aquatic bacterial strains - see review by Dziga et al. (2013). A possible biodegradation of MCs was also described for a few xenic (plus bacteria) protistan isolates (Combes et al. 2013; Ou et al. 2005; Zhang et al. 2008). Thus, protists living in close association with bacteria might profit from the presence of prokaryotic symbionts that are able to degrade toxins.

In this study, we give an example of a symbiotic interaction that is formed by three organisms (a microbial 'ménage-à-trois'). (i) We present an accurate morphological and phylogenetic analysis of the eukaryotic host. (ii) The phylogenetic affiliation of the two prokaryotic symbionts was determined. (iii) We document the growth of the triple microbial community seen as one single organism as well as the dynamics of each player. (iv) Finally, we discuss the

role of the ectosymbiont in the degradation of cyanotoxins, with which amoebae are faced via their toxic food.

Results

Morphological and Molecular Identification of *Nuclearia* sp. Strain N

According to morphological traits (including behaviour), the amoebae were undoubtedly classified to the genus *Nuclearia* (Opisthokonta, Nucleariidae). However, the determination at the species level was ambiguous (Table 1). We documented several mismatches in morphological features of already described species (see the summary in Yoshida et al. 2009) and our *Nuclearia* sp. strain N (Table 1). Cells of our isolate were often spherical (d = 10 to 37 μm; mean: 16.9 μm; n = 718) while floating freely (Fig. 1A, D, G-I), but adopted a flattened form when attached to a surface (Fig. 1B, C, F). Fine hyaline pseudopodia (filopodia), sometimes branched and knobbed (Fig. 1J), could be elongated and retracted. Filopodia were either evenly distributed around the cell (floating form) or concentrated in the frontal part during locomotion (attached form). Cells divided by binary fission. Cysts were repeatedly observed when environmental conditions changed rapidly or during starvation (Fig. 1E). Cysts were resistant to desiccation, and excystment was stimulated by adding new medium and prey organisms. The formation of syncytia (i.e., fusion of two or more cells) was rarely observed (Supplementary Material Fig. S1), but multinucleated cells appeared more frequently at the end of the log-phase (Fig. 1F). The subsequent division of multinucleated syncytia (~2 to 30 nuclei) was also documented. The EPS, only visible after Alcian blue staining (Fig. 1G), was usually present but could be lost during starvation periods. The EPS was colonized by a distinct bacterial morphotype that showed a highly regular arrangement (Fig. 1A-D, G). Amoebae without ectosymbionts or a different colonisation pattern were rarely found (Fig. 1H-I). Two different feeding modes were observed. In one mode, cells used a thick filopodium to engulf the tip of a cyanobacterial filament (consisting of up to 100 single cells). In this way, *P. rubescens* cells were ingested sequentially (Fig. 1D). Alternatively, short fragments of filaments could be ingested by phagocytosis (Fig. 1A). Occasionally, we also observed amoebae that could bend and finally break down a long filament into two parts.

Table 1. A comparison of the features of *Nuclearia* sp. strain N versus those described for *Nuclearia thermophila.* Note that the two isolates show 99.6% sequence identity for 18S rDNA (1804 bp). Morphological features in bold indicate differences between the two isolates.

	Nuclearia sp. strain N	*Nuclearia thermophila*
Original description	This study	Yoshida et al. (2009)
Spherical form*	Observed	Described
Flattened form*	Observed	Described
Nucleus*	Uninucleate, **Multinucleate syncytia**	Uninucleate
Nucleolus*	Evident	Evident
Extracellular matrix*	**Observed** (polysaccharide mucous layer)	No matrix
Cyst producing*	**Observed**	Not described
Branching of filopodia*	Observed	Described
Typical body diameter*	16.9 μm (n=718, spherical), 28.6 μm (n=424, spherical with ectosymbionts)	25-40 μm (spherical), 30-65 μm (elongated)
Registered SSU rDNA sequence*	HG530253	AB433328
Ectosymbiotic bacteria	**Observed** (several thousand per amoeba)	Not described
Endosymbiotic bacteria	**Observed** (15-20 bacteria per amoeba)	Not described
Formation of syncytia	**Observed**	Not described
Other features*	Knobbed filopodia	Knobbed filopodia

*These features were listed in table 1 in Yoshida et al. (2009) for the description of *N. thermophila*.

Ultrastructural features investigated by TEM showed that food vacuoles with undigested remains (e.g., cell walls) of *P. rubescens* cells dominated the cytoplasm (Fig. 2A). Outside the eukaryotic cells several ectosymbiotic bacteria colonized the EPS (Fig. 2A). No microtubules supported the filopodia, mitochondria had discoidal cristae, and membrane stacks of the dictyosome showed a regular pattern

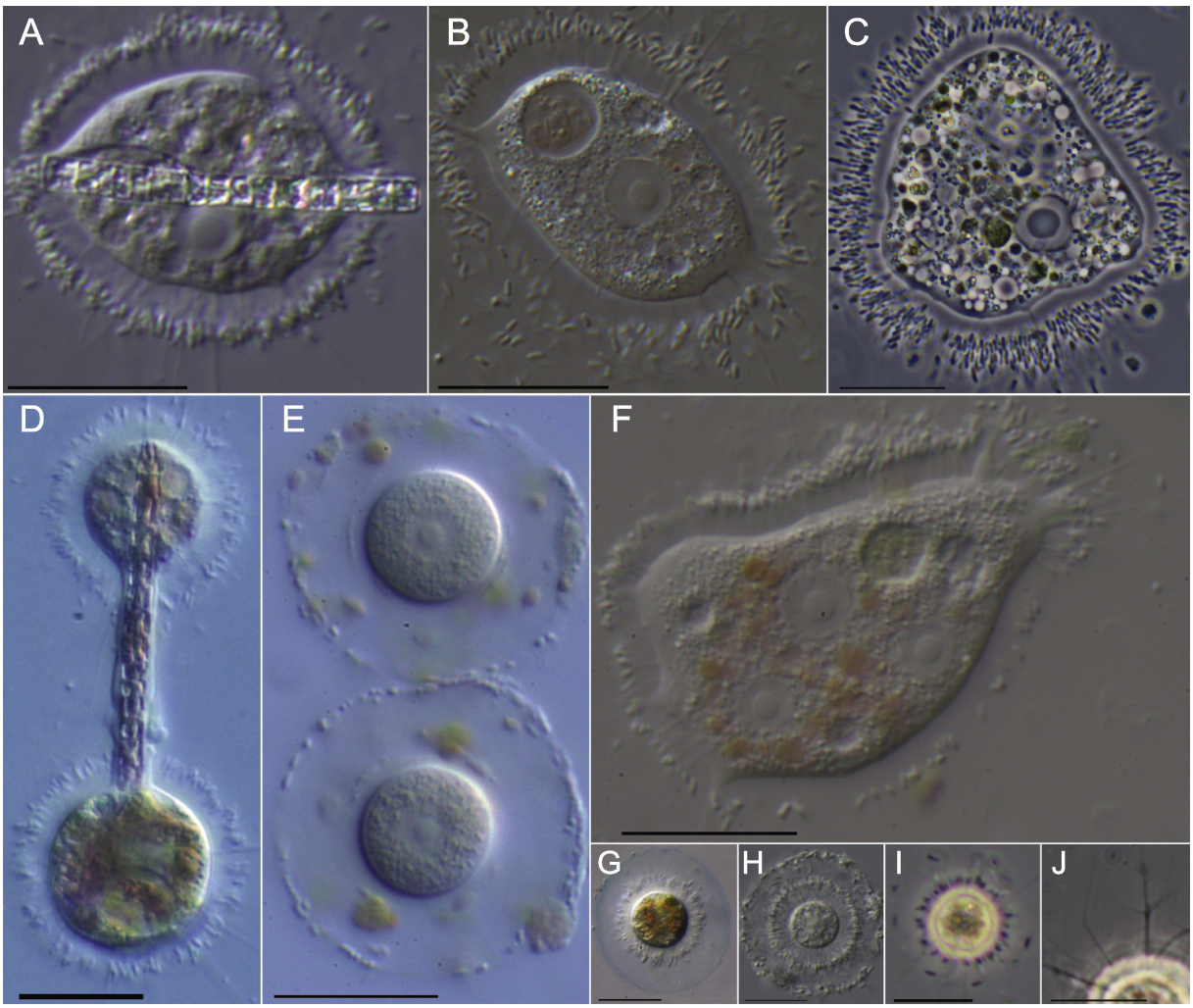

Figure 1. *Nuclearia* sp. strain N isolated from Lake Zurich, Switzerland. (**A**) Spherical shape ingesting a short cyanobacterial filament (*Planktothrix rubescens*) surrounded by well-arranged bacteria in the extracellular matrix, (**B**) and (**C**) flattened body form attached on surfaces, (**D**) two amoebae feeding on the same cyanobacterial filament, (**E**) two cysts with still intact extracellular matrix, (**F**) multinucleated (3 nuclei) syncytium, (**G**) Alcian blue staining of the extracellular matrix, (**H-I**) different colonization patterns of ectosymbiotic bacteria, (**J**) fine hyaline pseudopodia (filopodia), sometimes branched and knobbed. (C, I, J) Phase contrast pictures, all others: differential interference contrast (DIC) pictures. Scale bar: 20 μm in (A-J).

(Fig. 2B). Endosymbiotic bacteria in the cytoplasm had a typical Gram-negative cell wall and were surrounded by a peribacterial membrane (Fig. 2C, D).

Phylogenetic analysis of 18S rDNA sequences (1804 bp) of our isolate (accession number: HG530253) confirmed a close relationship to *N. thermophila* (99.6% sequence identity, Fig. 3A). Further, two monophyletic groups (one including the species *N. delicatula*, *N. simplex* and *N. moebiusi*, and the second group including another *N. simplex* and *N. patterson*i) were closely related to our isolate (~5% and ~6% sequence divergence in conserved regions, respectively).

The Endosymbiont "*Candidatus* Endonucleariobacter rarus"

Endosymbionts (length: 0.86 μm; n = 125) were initially identified by CARD-FISH as Gammaproteobacteria (probe GAM42a, Supplementary Material Fig. S2 and S3). We constructed a clone library of 16S rDNA sequences from the *Nuclearia* culture. This library was screened with primers specific for Gammaproteobacteria, resulting in 9 relevant sequences (Fig. 3B): *Pseudomonas fluorescens* (1), *Acinetobacter johnsonii* (1), *Stenotrophomonas acidaminiphila* (1), *S. maltophilia* (3), and a novel

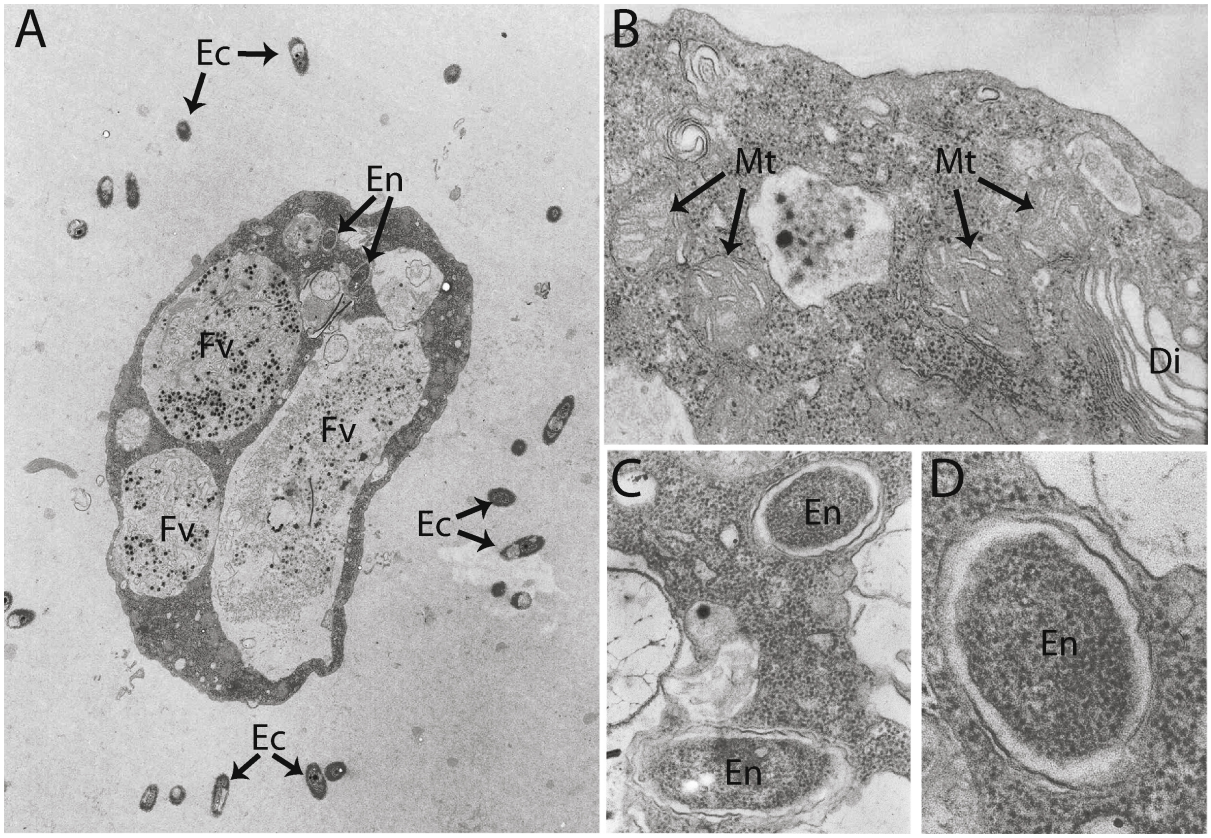

Figure 2. Transmission electron micrographs of the amoeba *Nuclearia* sp. strain N. (**A**) Whole cell overview showing several food vacuoles (Fv) with partly digested cyanobacterial material. Note the two endosymbiotic bacteria (En) in the upper part of the cytoplasm. The extracellular matrix is transparent in TEM preparations (low electron density). A few ectosymbiotic bacteria (Ec) arranged around the amoebae are visible. (**B**) Detailed view of the cytoplasm of the amoeba, showing several mitochondria (Mt) with discoidal cristae and parts of the dictyosome (Di). (**C-D**) Detailed views of endosymbiotic bacteria (En) in symbiosomes, i.e. surrounded by peribacterial membranes.

Table 2. Oligonucleotide probes designed in this study. FA% = Formamide concentration.

Probe	Specificity	Sequence (5′ to 3′)	FA %
Pauci995	*Paucibacter toxinivorans*	AATCTCTTCGGGATCTCTGACATG	70
CoNuc67	"*Candidatus* Endonucleariobacter rarus"	ATTGCTACACACTCTGTTACCG	70

deeply branching cluster related to Ectothiorhodospiraceae / *Beggiatoa* (3). CARD-FISH with the oligonucleotide probe SteMal-439 for the detection of *S. maltophilia* gave no positive hybridization signals. Therefore, we focussed on the cluster related to Ectothiorhodospiraceae / *Beggiatoa.* Sequences of this cluster were used as templates to design the specific oligonucleotide probe 'CoNuc67' (Fig. 3B, Table 2). This probe was used for CARD-FISH analyses, which resulted in a positive signal for all bacterial cells lying within the *Nuclearia* cytoplasm, even at 70% formamide concentration (Fig. 4A, B and Supplementary Material Fig. S3).

All recovered sequences of this cluster showed strong similarity (Fig. 3B) to only one public database sequence corresponding to an uncultured bacterium (DQ984555; ~97.5% sequence identity). Otherwise, the closest described relatives to our sequence was in the family Ectothiorhodospiraceae (AY298904 *Ectothiorhodosinus mongolicus* and FR733667 *Ectothiorhodospira shaposhnikovii*), which showed a sequence divergence

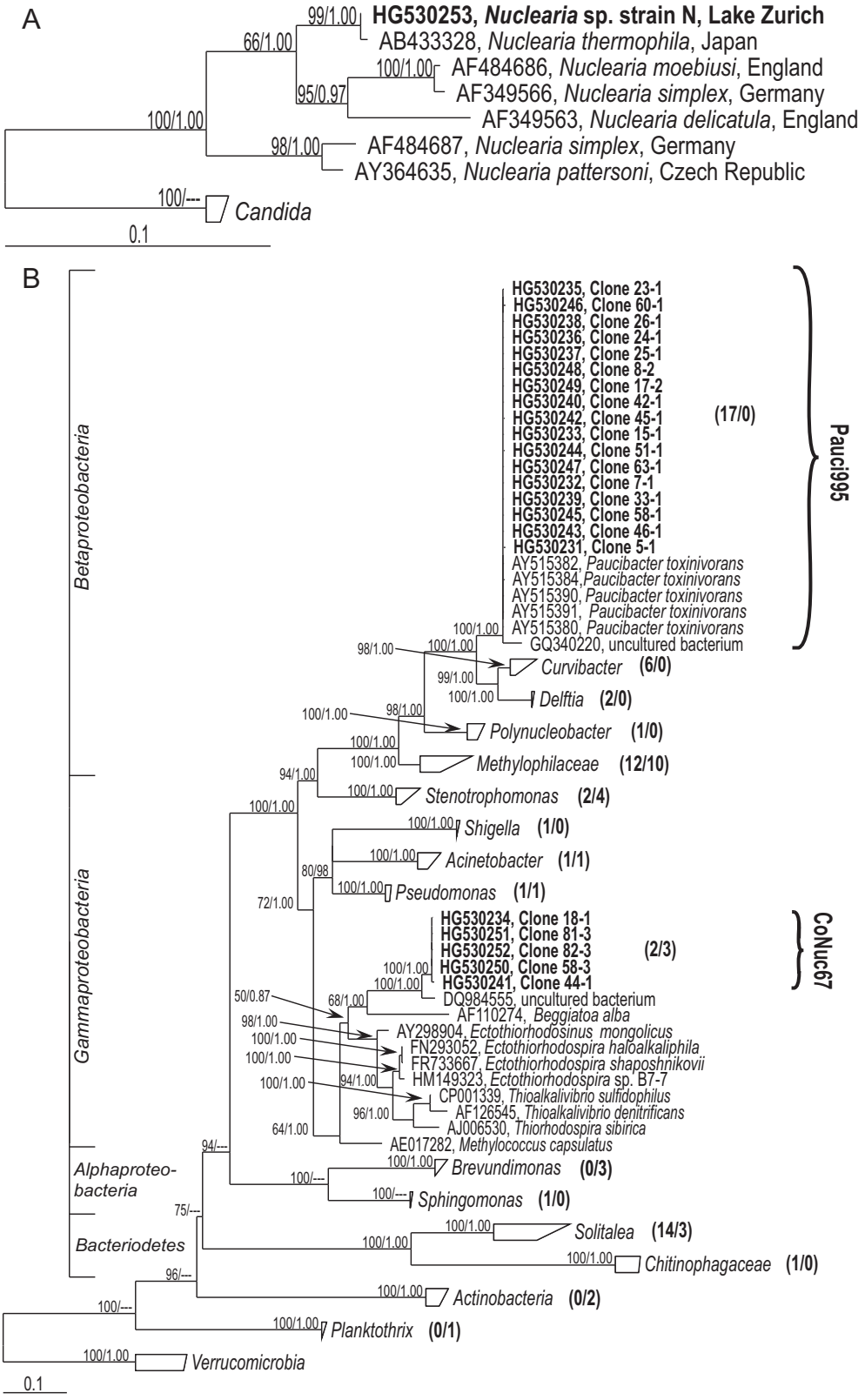

Figure 3. Phylogenetic analysis of the amoeboid host and its ecto- and endosymbiotic bacteria. Bootstrapped Maximum Likelihood (ML) trees (1000 iterations) with posterior probabilities from the Bayesian inference (BI)

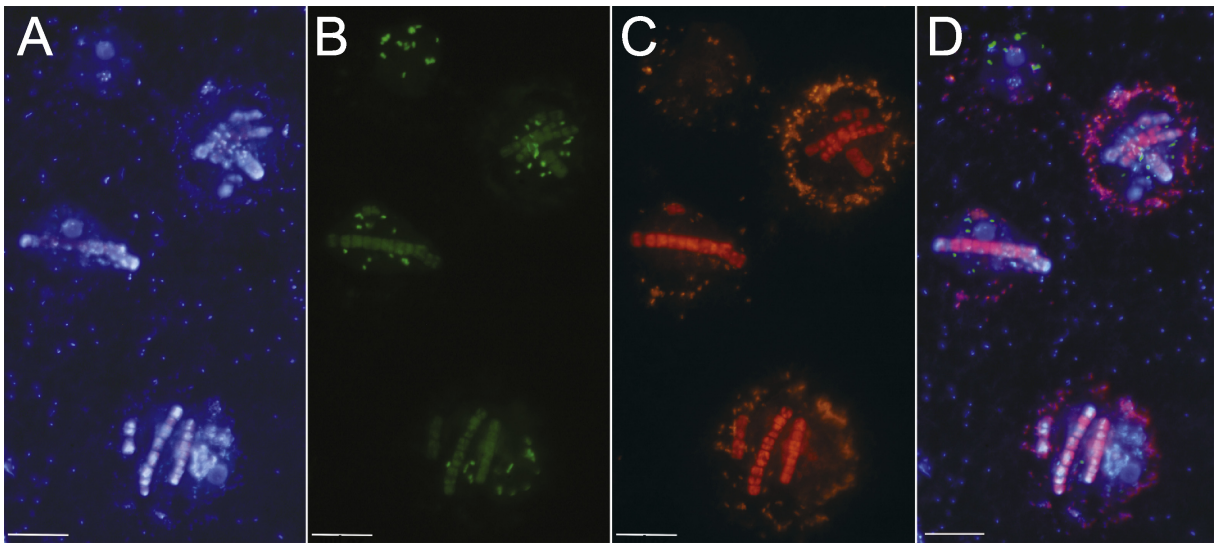

Figure 4. CARD-FISH double hybridization of four *Nuclearia* sp. strain N individuals. (**A**) DAPI staining, (**B**) hybridization of endosymbiotic bacteria with the probe CoNuc67 and fluorescein-labelled tyramides, (**C**) hybridization of ectosymbiotic bacteria with the probe Pauci995 with Alexa546-labelled tyramides, (**D**) overlay of (A-C). Note the strong auto-fluorescence of ingested cyanobacterial filaments in three amoebae in (B-D). Scale bars: 20 μm.

of about 10%. Therefore, we propose the establishment of a new genus, i.e., "*Candidatus* Endonucleariobacter rarus" (HG530234) for this endosymbiont.

Identification of Ectosymbiotic Bacteria

Molecular identification based on 16S rDNA was also done for the dominant rod-shaped bacteria (length: 0.92 μm; n = 125) found in a regular spherical arrangement around *Nuclearia* sp. strain N cells (Fig. 1A-D). Screening of a universal ('general') 16S rDNA clone library resulted in 42 full length and 19 partial sequences after chimera check. A cluster of 17 of these sequences was found to be closely related to *Paucibacter toxinivorans* (Betaproteobacteria, Fig. 3B). We first applied CARD-FISH with general oligonucleotide probes (Manz et al. 1992), which resulted in a positive signal for Betaproteobacteria (Supplementary Material Fig. S4). To confirm that our sequences related to *P. toxinivorans* corresponded to the ectosymbionts, we designed a new oligonucleotide probe 'Pauci995' (Table 2, Supplementary Material Fig. S4) specific for our *P. toxinivorans* sequences and published ones (Fig. 3B). Hybridization with this specific probe resulted in positive signals with the ectosymbionts, even at 70% formamide concentration (Fig. 4C).

Growth of the Microbial Consortium

Two parallel cultures (N1 and N2) of *Nuclearia* sp. strain N reached the stationary phase after 300 h with ~1.2 x 10^4 cells ml^{-1} (Fig. 5A). Maximal growth rates μ_{max} were 0.34 d^{-1} for N1 and 0.29 d^{-1} for N2, respectively. Regularly arranged ectosymbiotic bacteria (usually several thousand per amoeba) in the EPS were found on ~99% of amoebae, except during the death phase, when the EPS and ectosymbionts disappeared. We observed a rather conservative median of 11 to 18 endosymbionts per amoeba during the growth phase of both N1 and N2 (Fig. 5B, C).

consensus trees (4 chains, 100000 generations). Node labels: ML bootstrap in %/BI posterior probabilities. Incongruent topology is indicated with —: (**A**) 18S rDNA of *Nuclearia* ap. strain N isolated from Lake Zurich (Switzerland) related to all published *Nuclearia* spp. sequences with *Candida* as outgroup. (**B**) 16S rDNA phylogeny of sequences from the clone library together with related sequences from the Silva database and *Verrucomicrobia* as outgroup. Clusters with sequences from the symbionts are shown in detail. On the left hand higher taxonomic affiliations are indicated. Numbers in the brackets represent the number of sequences from the clone library affiliated with the respective cluster (# general screening / # gamma-screening). Curly brackets show the coverage of the CARD-FISH probes Pauci995 and CoNuc67. Scale bars: number of nucleotide substitutions per site.

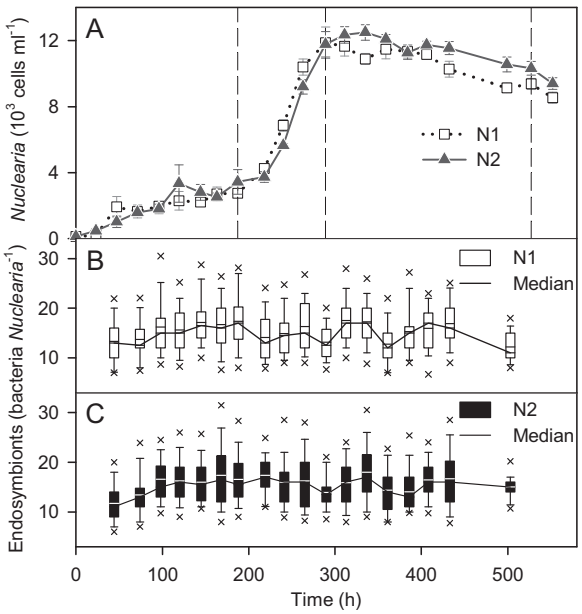

Figure 5. Growth of *Nuclearia* sp. strain N and its endosymbiotic bacteria. (**A**) Growth curves of two replicate amoebal cultures (N1 and N2). Dashed lines indicate the succession of the four growth phases: lag, log, stationary and death phase. Shown are means ± standard errors, n ≥ 100 cells sample^{-1}. (**B, C**) Numbers of endosymbiotic bacteria determined form CARD-FISH preparations with probe GAM42a in N1 and N2, respectively. n = 24 to 84 inspected amoebae sample^{-1}. Boxes indicate the 25th to 75th percentiles, whiskers the 10th to 90th and crosses the 5th and 95th percentiles.

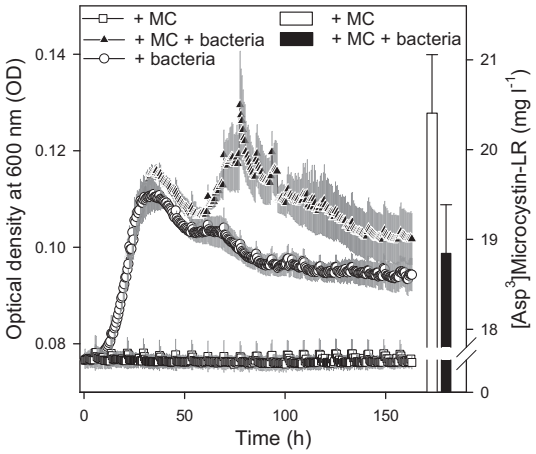

Figure 6. Growth dynamics (optical density values at 600 nm) of the isolated ectosymbiotic bacterium *Paucibacter toxinivorans* strain SD41 with and without the addition of [Asp^3]microcystin-LR to the culture medium. Additionally, three control runs containing only the medium and [Asp^3]microcystin-LR but no bacteria were measured. Bars show the difference of microcystin concentrations after 163 h in the treatments with and without bacteria. Shown are means ± standard errors.

Isolation of Ectosymbionts and Bacterial Degradation of Microcystins (MC)

Our isolated *P. toxinivorans* strain SD41 (HG792253) showed a positive hybridization with the probe Pauci995, and the recovered strain's 16S rDNA sequence was identical to six sequences from our clone library (HG530232; HG530236; HG530238; HG530239; HG530243; HG530247). We analysed the growth of the isolate with and without the addition of [Asp^3]MC-LR (Fig. 6). Bacterial cultures with [Asp^3]MC-LR in the medium reached higher ODs after only 40 hours, indicating that bacteria benefited from this cyanotoxin. After 163 hours, we compared the [Asp^3]MC-LR concentrations in bacterial treatments with the ones where we added [Asp^3]MC-LR to the medium but no bacteria. Although the statistical analysis (t-test) showed no significant difference between the MC concentrations in the different treatments, we found a relatively large decrease (1570 μg L^{-1}) of [Asp^3]MC-LR in the treatments with bacteria (Fig. 6), and calculated a degradation rate of 231 μg [Asp^3]MC-LR L^{-1} d^{-1}.

Discussion

Morphological Versus Molecular Identification

Analysing phenotypic traits in combination with genomic information from conserved genes (e.g. 18S rDNA) is needed for a holistic species description of protists (Caron 2013). Morphological features of the isolated filose amoeba revealed striking similarities with described species belonging to the Nucleariidae (Cann and Page 1979). Nevertheless, the comparison of our isolate with all former species descriptions showed an incongruity in at least two morphological features (see summary in Yoshida et al. (2009)). The closest morphological similarity was found between *Nuclearia* sp. strain N and *N. simplex*. However, *N. simplex* differs in two points: it is always uninucleated, and the cell size is usually much larger (~30 μm versus ~17 μm of *Nuclearia* sp. strain N).

To our knowledge, the formation of syncytia in the genus *Nuclearia* has been documented only once,

which was for the permanently multinucleated *N. delicatula* (Artari 1889). The fusion of *Nuclearia* sp. strain N cells was rarely observed; however, at the end of the log phase, syncytia were more frequent (Fig. 1F). Thus, multinucleated cells cannot be considered as an exclusive trait of *N. delicatula* anymore. For *Nuclearia* sp. strain N, the formation of syncytia seemed to be a coordinated process, suggesting that it might be beneficial, e.g. under harsh environmental conditions. During food depletion periods, the larger dimensions of syncytia most probably increased the encounter rate with *P. rubescens* filaments, and syncytia also ingested much longer filaments. A subsequent division of syncytia into uninucleated cells occurred when food was available at saturating levels, again suggesting that syncytia are a response to starvation.

As an exact morphotype-based species determination was not possible, we expected that phylogenetic analyses of the 18S rDNA would result in a stringent determination. Surprisingly, *N. thermophila* was the closest relative of *Nuclearia* sp. strain N (99.6% sequence identity). However, there are several mismatches in the described morphological features of the two 'species' (Table 1): *N. thermophila* has no extracellular matrix, does not build cysts nor syncytia, has a different mean cell size, and harbours no bacterial symbionts (Yoshida et al. 2009). One could argue that those characters (Table 1) are very flexible and can easily be lost or gained. However, we kept *Nuclearia* sp. strain N in culture for more than 3 years and did not observe a loss of symbionts, the EPS, or the ability to form cysts and syncytia. There are three explanations for the observed differences between the two isolates. First, they could represent two ecoytpes of the same species that drastically differ in phenotypic features. Second, conditions in which the *N. thermophila* was originally grown differed markedly from our approach. Yoshida et al. (2009) kept the amoebae at 25 °C on AF6 medium with traces of sterilized flour, a diet that might affect distinct phenotypic traits. Unfortunately, the original isolate of *N. thermophila* is not in culture and is no longer available (Yoshida, pers. com.). Finally, we are aware that a phylogenetic classification based only on 18S rDNA might not be sufficient to resolve a possible 'genetic distance' between *N. thermophila* and *Nuclearia* sp. strain N. However, the fact that sequences of *N. thermophila*, *N. delicatula*, *N. simplex*, and our isolate formed a monophyletic cluster in the ML tree is consistent with the morphologically determined closest relatives of *Nuclearia* sp. strain N.

The Endosymbiotic Bacterium "*Candidatus* Endonucleariobacter rarus"

The endosymbiont was exclusively localized inside peribacterial membranes (symbiosomes; sensu Schweikert and Meyer (2001)), whereas food vacuoles merely contained *Planktothrix* remnants and no other bacteria. These observations in combination with the fact that we never observed endosymbiont-free amoebae clearly pointed to an obligate interaction. The 16S rDNA of the endosymbiont affiliated with a so far uncharacterized deep branching cluster of Gammaproteobacteria, which had a sequence divergence of about 10% to the closest described relative of the genus *Ectothiorhodosinus* (Fig. 3B). The low numbers of endosymbionts inside *Nuclearia* host cells and the possible absence of free-living populations could explain the lack of this organism in public databases. Hence, we propose the establishment of a new genus and a new species for the endosymbiont of *Nuclearia* sp. strain N: "*Candidatus* Endonucleariobacter rarus".

A Mutualistic, Commensalistic or Parasitic Endosymbiont?

To further elucidate the symbiotic character, we focused on the growth of both the amoeba and its endosymbiont in parallel (Fig. 5). In the case of a pathogenic interaction, we would have expected an overgrowth of the host by the endosymbiont. However, numbers of endosymbionts per amoeba were stable during the entire growth phase (Fig. 5B, C). Thus, the two microbial partners seemed to be well synchronized, which points to a mutualistic or commensalistic symbiosis. Nevertheless, the low number of endosymbionts per host cell is rather exceptional for protists with intracellular bacteria, and this fact could have important implications for the stability of this symbiosis. This is particularly true if we consider the tight bottleneck that might occur when bacteria are vertically transmitted and single amoebae get dispersed (Moya et al. 2008). The resulting genetic drift affecting the genome of the symbiont might be important for the fate of this interaction (Sachs et al. 2011). Hence, it will be interesting to describe this potentially 'fast evolving' interaction on a genomic level.

P. toxinivorans Strain SD41 and the Degradation of Cyanotoxins

The regularly arranged bacteria surrounding *Nuclearia* sp. strain N pointed to a coordinated

interaction. Since the amoeboid growth followed the typical phases, there was no indication for a negative influence by the closely associated prokaryotes. Phylogenetic analysis showed an affiliation to *P. toxinivoran*s (Fig. 3B), which was originally described to degrade the cyanotoxins MC-LR and -YR (Rapala et al. 2005). These secondary metabolites may act as defence against predators (Blom et al. 2001). Although *Nuclearia* spp. were in direct contact with endotoxins when cyanobacteria were digested, we found no indication that amoebae were harmed by their food. Thus, *Nuclearia* must have developed strategies to cope with MCs. There is evidence that some protists, such as ciliates (e.g. *Paramecium* strains), have protein phosphatases other than PP1 and PP2A, which are not inhibited by MCs (MacKintosh et al. 1990). However, the protein phosphatases of *Nuclearia* spp. are currently not known. Moreover, amoebae might use multiple drug resistance-like transporters to export toxins into the surrounding medium. Therefore, MCs might be made available for bacteria specialized in their degradation (Dziga et al. 2013). The discovery of ectosymbiotic *P. toxinivorans* supports this theory. To test this, a widely distributed MC variant ([Asp^3]MC-LR) was offered as a substrate to the bacterium, and the presence of this variant was found to increase bacterial growth. Moreover, the observed bacterial induced degradation rate of 231 μg [Asp^3]MC-LR L^{-1} d^{-1} is in accordance to degradation rates of other MCs (96-384 μg L^{-1} d^{-1}) described for *P. toxinivorans* (Rapala et al. 2005). Compared to other strains, *P. toxinivorans* has a moderate capability to degrade MCs. Degradation rates of more than 10,000 μg L^{-1} d^{-1} have been found for *Sphingomonas* species and *Ralstonia solanacearum*, but also much lower values (1-120 μg L^{-1} d^{-1}) have been described, e.g., for different *Sphingopyxis*, *Sphingomonas*, or *Burkholderia* species (for review see Dziga et al. (2013)).

Conclusions

We present a triad relationship between a eukaryotic amoeba and its two bacterial symbionts. The three microorganisms were successfully identified based on their morphology and a phylogenetic marker, and we give some unique initial insights into this microbial 'Ménage-à-trois'. Future genomic and proteomic analysis may help to unravel metabolic pathways and interconnections between the three microorganisms.

Description of "*Candidatus* Endonucleariobacter rarus"

Endonucleariobacter rarus. Gr. adj. *endo*, within*;* N. L. fem. n. *nuclearia*, the amoeboid genus *Nuclearia*; N.L. masc. n. *bacter*, a rod; N.L. masc. n. *Endonucleariobacter*, a rod-shaped bacterium living inside the amoeboid genus *Nuclearia*. L. masc. adj. *rarus*, rare, referring to the low number of endosymbionts per amoebal cell.

Rod-shaped bacterium (length: 0.86 μm; n = 125), always surrounded by a vacuolar membrane (symbiosome). Gram negative cell-wall organization. Basis of assignment: 16S rDNA sequence (accession number: HG530234) and positive signal with the general FISH oligonucleotide probes EUBI-III, GAM42a and the specific probe CoNuc67 (5′- ATT GCT ACA CAC TCT GTT ACC G -3′, this study). Up to now only identified in the cytoplasm of the *Nuclearia* sp. strain N (accession number: HG530253), isolated from Lake Zurich, Switzerland. Uncultured so far.

Methods

Strains and cultures: *Nuclearia* sp. strain N was isolated from the benthic zone of Lake Zurich, Switzerland (47°19′11.5″N, 8°33′10.1″E) in February, 2011. Monoclonal xenic (i.e. plus bacteria) amoebal cultures were established by washing single cells in sterile water, and kept in Tissue Culture Flasks 25 cm^2 (TPP$_®$) at 18 °C on autoclaved mineral water (Cristalp). Cultures were grown under a 12 h light (irradiance of 5-15 μmol m^{-2} s^{-1}) / 12 h dark cycle. Axenic cultures of the cyanobacterium *Planktothrix rubescens* BC 9307 isolated from Lake Zurich (Blom et al. 2001; Walsby et al. 1998) served as sole food source for the amoebae. Batch cultures (10 ml) of amoebae were fortnightly renewed by adding cyanobacterial stock cultures (~1 ml) to new culture medium inoculated with 200 μl of an older culture. *Nuclearia* sp. strain N has been deposited in the Culture Collection of Algae and Protozoa (CCAP; http://www.ccap.ac.uk/) with the strain number CCAP 1552/5.

Sequencing of the 18S rDNA (*Nuclearia* sp. strain N): Aliquots (1.5 ml) of dense *Nuclearia* cultures were centrifuged (15 min; 16,000 x *g*), pellets were subjected to several freeze-thaw cycles, and DNA was isolated with the GenElute^{TM} Bacterial Genomic DNA Kit (Sigma). The 18S rDNA was amplified by PCR with the eukaryote-specific primers Euk328f and Euk329r (Moon-van der Staay et al. 2001), PCR products were purified with the QIAquick PCR Purification Kit (Qiagen), and subsequently sequenced with ABI BigDye chemistry on an ABI 3130x Genetic Analyzer (Applied Biosystems). Additionally, the primers SR4f and SR8r (Nakayama et al. 1998) were used for sequencing, and partial sequences were assembled with the software DNA Baser v3.5.0 (Heracle BioSoft).

Clone library and sequencing of 16S rDNA (symbionts): Four hundred individuals of *Nuclearia* sp. strain N were picked with a micropipette, washed in sterile water, centrifuged (30 min; 16,000 x *g*), and DNA was extracted either by several freeze-thaw cycles or with the GenElute

™ Bacterial Genomic DNA Kit (Sigma). Bacterial 16S rDNA was amplified with primers GM3f and GM4r (Muyzer and Ramsing 1995), products were purified, pooled, and concentrated with the DNA Concentrator Kit (Epigentek). PCR products were cloned into competent *Escherichia coli* cells using a pGEM®-T Vector (Promega) according to the manufacturer's instructions. The obtained clone library was screened with plasmid primers (general screening) and additionally with a two-step nested PCR approach (Boutin et al. 2012) with a second primer pair specific for Gammaproteobacteria (Klein et al. 2007). These primers were slightly modified by the insertion of wobbles (S-Sc-gProt-0382-a-S-18_f_wobble 5′-AGGCAGCAGTGGGGAATM-3′ and S-Sc-gProt-0946-a-A-18_r_wobble 5′-GCCCCCGTCAATTCMTTT-3′). Positive clones were purified with a GenElute™ Five-Minute Plasmid Miniprep Kit (Sigma) and sequenced as above with primers GM3f, GM4r, and GM1f (Muyzer and Ramsing 1995). Partial sequences were assembled and chimeric sequences were detected with the software Mallard and Pintail (Ashelford et al. 2005).

Screening with a second primer pair specific for Gammaproteobacteria showed that only 9 sequences of 28 positive clones (Fig. 3B) indeed belonged to Gammaproteobacteria, i.e., *Stenotrophomonas maltophilia* (3), *Stenotrophomonas acidaminiphila* (1), a novel deeply branching cluster related to Ectothiorhodospiraceae / *Beggiatoa* (3), *Pseudomonas fluorescens* (1), and *Acinetobacter johnsonii* (1).

Phylogenetic analyses: Analyses were performed with the ARB software (Ludwig et al. 2004) using the SILVA database SSU Ref 111 (Pruesse et al. 2007). The 18S rDNA sequence from *Nuclearia* sp. strain N was first automatically aligned (FAST_ALIGNER tool) to the sequence of *N. thermophila* (AB433328), and all available complete 18S rDNA sequences of described *Nuclearia* spp. were subsequently added. This allowed for proper alignment of the conserved regions, but long inserts that are typical for Nucleariidae had to be aligned manually. The beginning and ends of all alignments were trimmed to the length of the shortest sequence.

Bacterial 16S rDNA sequences were aligned with the SINA web aligner (www.arb-silva.de/aligner/) and manually refined. Only full-length sequences (*E. coli* position 8 – 1507) from the clone library and related sequences from the ARB database (quality scores $\geq$ 88) were used for calculation of the phylogenetic tree.

Maximum Likelihood (ML) and Bayesian inference (BI) methods were used for the phylogenetic reconstructions. Two bootstrapped ML trees (*Nuclearia* spp. and clone library) were calculated (1000 iterations) using the RAxML algorithm on a dedicated web server (Stamatakis et al. 2008) using the GTR (General Time Reversible) model with a Γ distribution for rate heterogeneity among sites, with 4 discrete rate categories. Additionally BI consensus trees were constructed (4 chains; 100,000 generations) using the ExaBayes software package (©The Exelixis Lab). The posterior probabilities from the BI trees were added to the ML trees where identical topography for both methods was found. All complete 16S rDNA sequences from the clone library and the 18S rDNA sequence of *Nuclearia* sp. strain N have been deposited in the EMBL database with accession numbers HG530231-HG530253 and HG973425-HG973449.

CARD-FISH and probe design: Two CARD-FISH probes (Table 2) specific for *Paucibacter toxinivorans* and for a novel cluster of Gammaproteobacteria were designed with the dedicated ARB tools. The resulting probes were tested in silico in the Ribosomal Database Project (RDP) (www.rdp.cme.msu.edu), and hybridization efficiencies and mismatch stability were analysed with the web tool Mathfish (Yilmaz et al. 2011). The newly designed oligonucleotide probes were tested on *Nuclearia* sp. cultures at different formamide concentrations until highest stringency was achieved (Table 2). Additionally the already published (Manz et al. 1992) general probes EUB I-III, BET42a, GAM42a (Supplementary Material Figs S3 and S4) and the specific probe SteMal-439 (Piccini et al. 2006) were used. The probe NON338 was applied to check for non-specific staining (Supplementary Material Fig. S2). The best preservation of amoeboid and bacterial morphologies was determined by testing different fixatives (i.e., formaldehyde, Lugol's solution, glutaraldehyde). Finally, cells were fixed on ice with Lugol's solution (0.5% final. conc.), formaldehyde (2% final. conc.), and followed by decolourization with a few drops of Na-thiosulfate (3% stock solution). Samples were filtered onto white polycarbonate filters (0.2 μm pore size, Millipore) placed on a support filter (Sartorius). Filters were rinsed with distilled water, air dried, and stored at -22 °C until further processing. CARD-FISH with fluorescein- and, in case of double hybridization, with Alexa546-labeled tyramides was done for filter sections as described by Sekar et al. (2003). Hybridization took place at 35 °C on a rotation shaker for a minimum of 2 h. After hybridization filter sections were counterstained with DAPI (1 μg mL^{-1}).

Microscopy and photographic documentation: Living specimens were observed with differential interference and phase contrast with an Axio Imager.M1 microscope (Zeiss). The extracellular polymeric substances (EPS) of amoebae were visible in brightfield microscopy after staining with Alcian Blue (Logan et al. 1994). CARD-FISH preparations were analysed with epifluorescence on the same microscope. The following optical filter sets (Zeiss) were used: set 01, set 10, set 14, set 43. All photographs were taken with a Canon EOS1000D controlled by the software AxioVision 4.8.2 (Zeiss).

Transmission electron microscopy (TEM): Cells of *Nuclearia* sp. strain N cultures were fixed on ice for 1 h with 2.5% glutaraldehyde in 0.1 M cacodylate buffer (pH = 7.6) followed by embedding in low melting agar (2%). After cutting the agar block in small pieces (~2-3 mm^3), cells were washed by exchanging the cacodylate buffer (3X) and postfixed for 1 h with 1% osmium tetroxide (OsO_4). Subsequently, samples were dehydrated in an acetone series (30%, 50%, 75%, 90% and 100%) and embedded in Spurr's resin. Ultrathin sections were made with an Ultracut UCT (Leica) and stained with 1% (aq.) uranylacetate for 6 min and lead citrate (Venable and Coggeshall 1965) for 4 min. TEM preparations were analysed with a Zeiss EM 10 at 60 kV (Schweikert and Meyer 2001).

Growth curves: We monitored the growth of *Nuclearia* sp. strain N in a duplicate setup (N1 and N2) simultaneously with their per cell number of endosymbiotic bacteria during a 3-week period. In addition, cell sizes of living amoebae were measured interactively with an image analysis system (AxioVision 4.8.2, Zeiss) and distribution patterns of ectosymbionts in the EPS were documented. Cultures were grown in Tissue Culture Flasks 75 cm^2 (TPP®) in 100 ml of autoclaved mineral water (Cristalp). *P. rubescens* was added as food source at the beginning (10 ml of stock culture), together with an inoculum of *Nuclearia* sp. strain N (~130 cells ml^{-1}). We determined abundances of amoebae from live counts in 6 drops of 15 μl (n $\geq$ 100 individuals counting^{-1}) on a daily basis. Aliquots (1.5 ml) for CARD-FISH preparations were taken daily from day 3 to day 21. The number of endosymbiotic bacteria was counted after hybridization with probe GAM42a (Manz et al. 1992) in 24 to 84 amoebae per preparation (total n of inspected *Nuclearia* sp. = 2952).

Isolation of ectosymbionts and bacterial degradation of microcystins: Single *Nuclearia* sp. strain N cells with a densely colonized EPS were picked with a micropipette under a

dissection microscope, transferred onto R2A plates (Reasoner and Geldreich 1985) and incubated at 18 °C. After several days bacterial colonies were repeatedly picked and streaked on fresh agar plates to obtain clonal isolates of different bacterial strains. CARD-FISH with the probe Pauci995 (Table 2) allowed for a screening of isolates. One isolate with positive hybridization signal was subsequently grown in liquid R2 medium. DNA was extracted from the liquid culture with the GenElute ^{TM} Bacterial Genomic DNA Kit (Sigma) and the 16S rDNA gene was amplified, purified, and sequenced as described above (*P. toxinivorans* strain SD41, accession number: HG792253). Pure cultures of the isolate were cryopreserved (30% glycerol, -80 °C).

Cells were re-grown on R2A plates until visible colonies appeared. One colony was picked and transferred to liquid R2 medium and grown to a density of ~4 x 10^8 cells ml^{-1}. For the experiment, cells were grown in R2 medium diluted (1:9) with artificial lake water (ALW) medium (Zotina et al. 2003) that was amended with vitamins (thiamine 0.593 μM, niacin 0.08 μM, cobalamine 0.000074 μM, para-amino benzoic acid 0.005 μM, pyridoxine 0.074 μM, pantothenic acid 0.081 μM, biotin 0.004 μM, folic acid 0.004 μM, myo-inositol 0.555 μM). The microcystin variant [Asp^3]microcystin-LR (abbreviated as [Asp^3]MC-LR) was isolated in high purity (> 99%, HPLC) from *Microcystis aeruginosa* PCC 7806. HPLC purification was performed on a Shimadzu 10AVP system equipped with a photodiode array detector (PDA) on a C-18 Grom-Sil 120 ODS-4 HE reversed phase column (Stagroma, Germany), using solvent A: UV-treated H_2O containing 0.05% trifluoroacetic acid (TFA, Merck) and solvent B: acetonitrile and 0.05% TFA. A gradient was achieved by applying linear increases in three steps (solvent B from 30% to 35% in 10 min, from 35% to 70% in 30 min, and from 70% to 100% in 2 min). Further details on the purification process are given in Blom and Jüttner (2005).

In four parallel experimental set-ups, ~6 x 10^4 cells of *P. toxinivorans* strain SD41 were inoculated to 200 μl of R2 and ALW medium (1:9) containing pure [Asp^3]MC-LR (20.4 mg l^{-1} final concentration). Eight bacterial control treatments were prepared in the same way but without the addition of [Asp^3]MC-LR. Three additional replicates contained only 200 μl medium and 20.4 mg l^{-1} of [Asp^3]MC-LR but no bacterial inoculum, to check for any contamination or chemical degradation of the toxin during the incubation period. All treatments were incubated at 26 °C for 163 h and optical densities (OD at 600 nm) were recorded every 30 min with a microplate reader (SpectraMax 190, Molecular Devices). At the end of the experiment, 150 μl each of the 4 replicates with bacteria and of the 3 controls (only medium and [Asp^3]MC-LR) were diluted with methanol to achieve a 60% aqueous MeOH solution. For the quantification of [Asp^3]MC-LR, calibration curves were established using a Hydrosphere C18 column (YMC, 4.6 x 250 mm, Stagroma, Switzerland). The specific molar absorption coefficient of [Asp^3]MC-LR was used to prepare accurate standard solutions between 1 and 10 μg (Blom et al. 2001). Quantification was based on the peak area recorded at 239 nm on a HPLC system (Shimadzu 10AVP) equipped with a photodiode array detector (PDA).

Acknowledgements

This study was financed by the Swiss National Fund (SNF 31003A_138473). We thank Marie-Ève Garneau for correcting our funny Austrian-Swiss English. We are thankful to Stefan Neuenschwander, Kasia Piwosz and Jakob Pernthaler for fruitful discussions and Bettina Eugster for cultivating *Planktothrix rubescens*.

Appendix A. Supplementary data

Supplementary data associated with this article can be found, in the online version, at http://dx.doi.org/10.1016/j.protis.2014.08.004.

References

Artari A (1889) Morphologische und biologische Studien über *Nuclearia delicatula* Cienk. Zool Anz **12**:408–416

Ashelford KE, Chuzhanova NA, Fry JC, Jones AJ, Weightman AJ (2005) At least 1 in 20 16S rRNA sequence records currently held in public repositories is estimated to contain substantial anomalies. Appl Environ Microbiol **71**:7724–7736

Blom JF, Jüttner F (2005) High crustacean toxicity of microcystin congeners does not correlate with high protein phosphatase inhibitory activity. Toxicon **46**:465–470

Blom JF, Robinson JA, Jüttner F (2001) High grazer toxicity of [D-Asp^3,(*E*)-Dhb^7]microcystin-RR of *Planktothrix rubescens* as compared to different microcystins. Toxicon **39**:1923–1932

Boutin S, Sevellec M, Pavey SA, Bernatchez L, Derome N (2012) A fast, highly sensitive double-nested PCR-based method to screen fish immunobiomes. Mol Ecol Resour **12**:1027–1039

Brown MW, Spiegel FW, Silberman JD (2009) Phylogeny of the "forgotten" cellular slime mold, *Fonticula alba*, reveals a key evolutionary branch within Opisthokonta. Mol Biol Evol **26**:2699–2709

Cann JP (1986) The feeding behavior and structure of *Nuclearia delicatula* (Filosea: Aconchulinida). J Protozool **33**:392–396

Cann JP, Page FC (1979) *Nucleosphaerium tuckeri* nov. gen. nov. sp. - A new freshwater filose amoeba without motile form in a new family Nucleariidae (Filosea: Aconchulinida) feeding by ingestion only. Arch Protistenkd **122**:226–240

Caron DA (2013) Towards a molecular taxonomy for protists: Benefits, risks, and applications in plankton ecology. J Eukaryot Microbiol **60**:407–413

Combes A, Dellinger M, Cadel-six S, Amand S, Comte K (2013) Ciliate *Nassula* sp. grazing on a microcystin-producing cyanobacterium (*Planktothrix agardhii*): impact on cell growth and in the microcystin fractions. Aquat Toxicol **126**:435–441

Dyková I, Veverková M, Fiala I, Macháčkova B, Pecková H (2003) *Nuclearia pattersoni* sp. n. (Filosea), a new species of amphizoic amoeba isolated from gills of roach (*Rutilus rutilus*), and its rickettsial endosymbiont. Folia Parasitol **50**:161–170

Dziga D, Wasylewski M, Wladyka B, Nybom S, Meriluoto J (2013) Microbial degradation of microcystins. Chem Res Toxicol **26**:841–852

Galanti LN, Amé MV, Wunderlin DA (2013) Accumulation and detoxification dynamic of cyanotoxins in the freshwater shrimp *Palaemonetes argentinus*. Harmful Algae **27**:88–97

Gast RJ, Sanders RW, Caron DA (2009) Ecological stratgies of protists and their symbiotic relationships with prokaryotic microbes. Trends Microbiol **17**:563–569

Görtz HD, Brigge T (1998) Intracellular bacteria in protozoa. Naturwissenschaften **85**:359–368

Klein AN, Frigon D, Raskin L (2007) Populations related to *Alkanindiges*, a novel genus containing obligate alkane degraders, are implicated in biological foaming in activated sludge systems. Environ Microbiol **9**:1898–1912

Kurmayer R, Jüttner F (1999) Strategies for the co-existence of zooplankton with the toxic cyanobacterium *Planktothrix rubescens* in Lake Zürich. J Plankt Res **21**:659–683

Liu Y, Steenkamp E, Brinkmann H, Forget L, Philippe H, Lang BF (2009) Phylogenomic analyses predict sistergroup relationship of nucleariids and Fungi and paraphyly of zygomycetes with significant support. BMC Evol Biol **9**: 272

Logan BE, Grossart HP, Simon M (1994) Direct observation of phytoplankton, TEP and aggregates on polycarbonate filters using brigthfield microscopy. J Plankt Res **16**: 1811–1815

Ludwig W, Strunk O, Westram R, Richter L, Meier H, Yadhukumar, et al. (2004) ARB: a software environment for sequence data. Nucleic Acids Res **32**:1363–1371

MacKintosh C, Beattie KA, Klumpp S, Cohen P, Codd GA (1990) Cyanobacterial microcystin-LR is a potent and specific inhibitor of protein phosphatases 1 and 2A from both mammals and higher plants. FEBS Lett **264**:187–192

Manz W, Amann R, Ludwig W, Wagner M, Schleifer KH (1992) Phylogenetic oligodeoxynucleotide probes for the major subclasses of *Proteobacteria*: Problems and solutions. Syst Appl Microbiol **15**:593–600

Marx J (2004) The roots of plant-microbe collaborations. Science **304**:234–236

Moon-van der Staay SY, De Wachter R, Vaulot D (2001) Oceanic 18S rDNA sequences from picoplankton reveal unsuspected eukaryotic diversity. Nature **409**:607–610

Moya A, Peretó J, Gil R, Latorre A (2008) Learning how to live together: genomic insights into prokaryote–animal symbioses. Nature Rev Genet **9**:218–229

Muyzer G, Ramsing NB (1995) Molecular methods to study the organization of microbial communities. Water Sci Technol **32**:1–9

Nakayama T, Marin B, Kranz HD, Surek B, Huss VAR, Inouye I, Melkonian M (1998) The basal position of scaly green flagellates among the green algae (Chlorophyta) is revealed by analyses of nuclear-encoded SSU rRNA sequences. Protis **149**:367–380

Nowack ECM, Melkonian M (2010) Endosymbiotic associations within protists. Philos Trans R Soc B **365**:699–712

Ou D, Song L, Gan N, Chen W (2005) Effects of microcystins on and toxin degradation by *Poterioochromonas* sp. Environ Toxicol **20**:373–380

Paracer S, Ahmadjian V, eds (2000) Symbiosis. An Introduction to Biological Associations. Oxford University Press, New York, 291 p

Patterson DJ (1984) The genus *Nuclearia* (Sarcodina, Filosea): Species composition and characteristics of the taxa. Arch Protistenkd **128**:127–139

Pernin P (1976) Étude sur le vivant d'une amibe a pseudopodes filosa: *Nuclearia simplex* Cienkowski 1865 (Protozoa, Rhizopodea, Filosia, Aconchulinida). Protistologica **12**: 555–562

Pflugmacher S, Wiegand C, Oberemm A, Beattie KA, Krause E, Codd GA, Steinberg CEW (1998) Identification of an enzymatically formed glutathione conjugate of the cyanobacterial hepatotoxin microcystin-LR: the first step of detoxication. Biochim Biophys Acta **1425**:527–533

Piccini C, Conde D, Alonso C, Sommaruga R, Pernthaler J (2006) Blooms of single bacterial species in a coastal lagoon of the Southwestern Atlantic Ocean. Appl Environ Microbiol **72**:6560–6568

Posch T, Köster O, Salcher MM, Pernthaler J (2012) Harmful filamentous cyanobacteria favoured by reduced water turnover with lake warming. Nature Clim Change **2**:809–813

Pruesse E, Quast C, Knittel K, Fuchs BM, Ludwig W, Peplies J, Glöckner FO (2007) SILVA: a comprehensive online resource for quality checked and aligned ribosomal RNA sequence data compatible with ARB. Nucleic Acids Res **35**:7188–7196

Rapala J, Berg KA, Lyra C, Niemi RM, Manz W, Suomalainen S, Paulin L, Lahti K (2005) *Paucibacter toxinivorans* gen. nov., sp. nov., a bacterium that degrades cyclic cyanobacterial hepatotoxins microcystins and nodularin. Int J Syst Evol Microbiol **55**:1563–1568

Reasoner DJ, Geldreich EE (1985) A new medium for the enumeration and subculture of bacteria from potable water. Appl Environ Microbiol **49**:1–7

Ruby E, Henderson B, McFall-Ngai M (2004) We get by with a little help from our (little) friends. Science **303**: 1305–1307

Sachs JL, Skophammer RG, Regus JU (2011) Evolutionary transitions in bacterial symbiosis. Proc Natl Acad Sci USA **108**:10800–10807

Schmitz-Esser S, Toenshoff ER, Haider S, Heinz E, Hoenninger VM, Wagner M, Horn M (2008) Diversity of bacterial endosymbionts of environmental *Acanthamoeba* isolates. Appl Environ Microbiol **74**:5822–5831

Schweikert M, Meyer B (2001) Characterization of intracellular bacteria in the freshwater dinoflagellate *Peridinium cinctum*. Protoplasma **217**:177–184

Sekar R, Pernthaler A, Pernthaler J, Warnecke F, Posch T, Amann R (2003) An improved protocol for the quantification of freshwater *Actinobacteria* by fluorescence *in situ* hybridization. Appl Environ Microbiol **69**:2928–2935

Stamatakis A, Hoover P, Rougemont J (2008) A rapid bootstrap algorithm for the RAxML web servers. Syst Biol **57**:758–771

Steenkamp ET, Wright J, Baldauf SL (2006) The protistan origins of animals and fungi. Mol Biol Evol **23**:93–106

Venable JH, Coggeshall R (1965) A simplified lead citrate stain for use in electron microscopy. J Cell Biol **25**:407–408

Walsby AE, Avery A, Schanz F (1998) The critical pressure of gas vesicles in *Planktothrix rubescens* in relation to the depth of winter mixing in Lake Zürich. Switzerland. J Plankt Res **20**:1357–1375

Yilmaz LS, Parnerkar S, Noguera DR (2011) mathFISH, a web tool that uses thermodynamics-based mathematical models for *in silico* evaluation of oligonucleotide probes for fluorescence *in situ* hybridization. Appl Environ Microbiol **77**: 1118–1122

Yoshida M, Nakayama T, Inouye I (2009) *Nuclearia thermophila* sp. nov. (Nucleariidae), a new nucleariid species isolated from Yunoko Lake in Nikko (Japan). Eur J Protistol **45**:147–155

Zettler LAA, Nerad TA, O'Kelly CJ, Sogin ML (2001) The nucleariid amoebae: More protists at the animal-fungal boundary. J Eukaryot Microbiol **48**:293–297

Zhang X, Hu H-Y, Hong Y, Yang J (2008) Isolation of a *Poterioochromonas* capable of feeding on *Microcystis aeruginosa* and degrading microcystin-LR. FEMS Microbiol Lett **288**:241–246

Zotina T, Köster O, Jüttner F (2003) Photoheterotrophy and light-dependent uptake of organic and organic nitrogenous compounds by *Planktothrix rubescens* under low irradiance. Freshwater Biol **48**:1859–1872

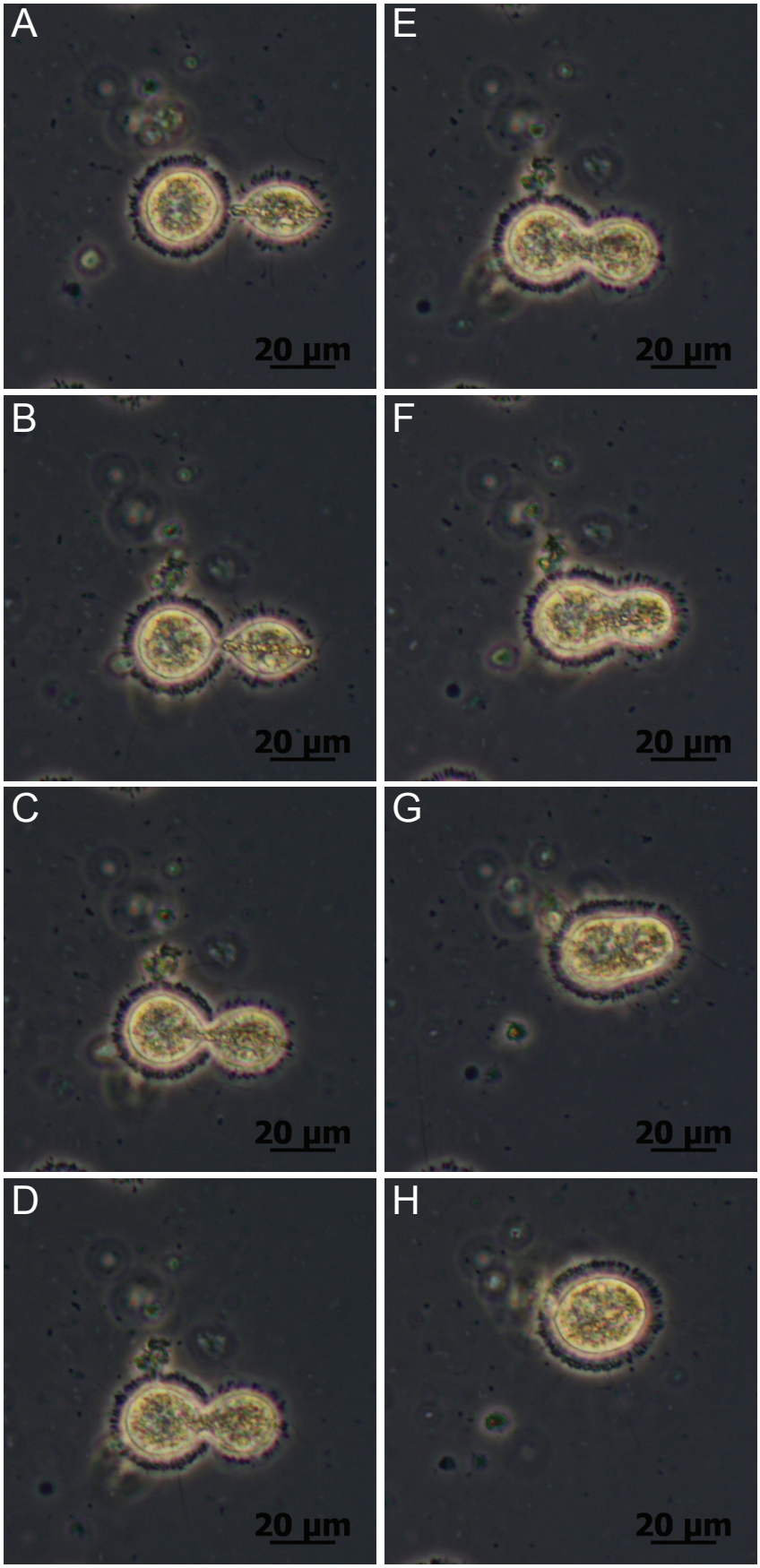

Figure S1. Photographic sequence (**A-H**, covering a time span of 6 minutes) showing the fusion of two *Nuclearia* sp. strain N cells, resulting in a multinucleated syncytium. Note that the right cell in (**A**) contained an ingested cyanobacterial filament (*Planktothrix rubescens*). During the fusion of cells, the two rings of ectosymbiotic bacteria are combined to one layer. Phase contrast pictures.

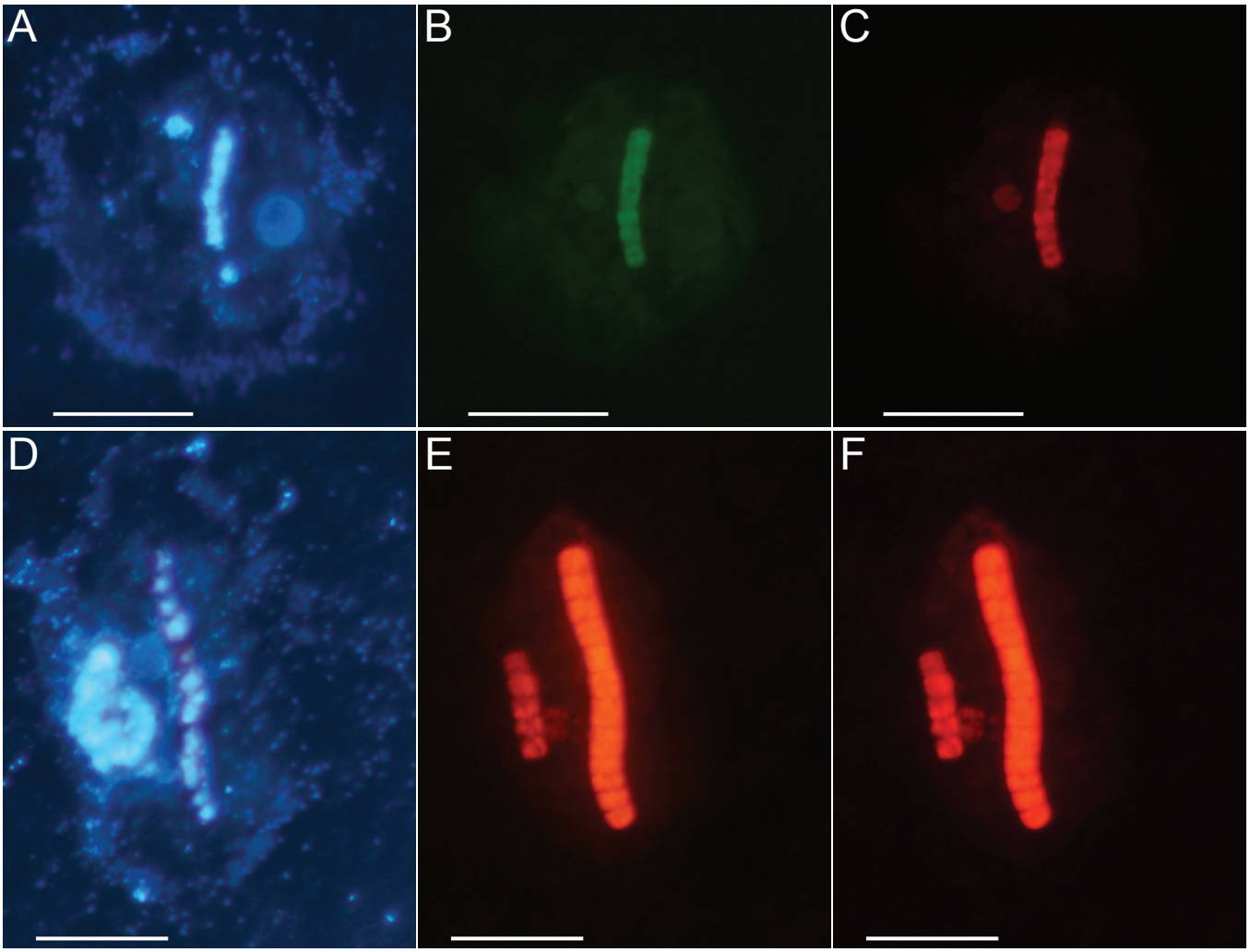

Figure S2. Two different CARD-FISH hybridization of *Nuclearia* sp. strain N cells with the probe NON338. **A-C**: Fluorescein-labelled tyramides. **D-F**: Alexa546-labelled tyramides
A and **D**: DAPI staining (analyzed with Zeiss Filter set 01).
B Hybridization with the probe NON338 and fluorescein-labelled tyramides (Zeiss filter set 10).
E Hybridization with the probe NON338 with Alexa546-labelled tyramides (Zeiss filter set 43).
C and **F**: Analysis of the same objects with wide green exciation (Zeiss filter set 14).
Note the strong autofluorescene of ingested *Planktothrix rubescens* filaments in **B**, **C**, **E** and **F**.
Scale bars: 20µm.

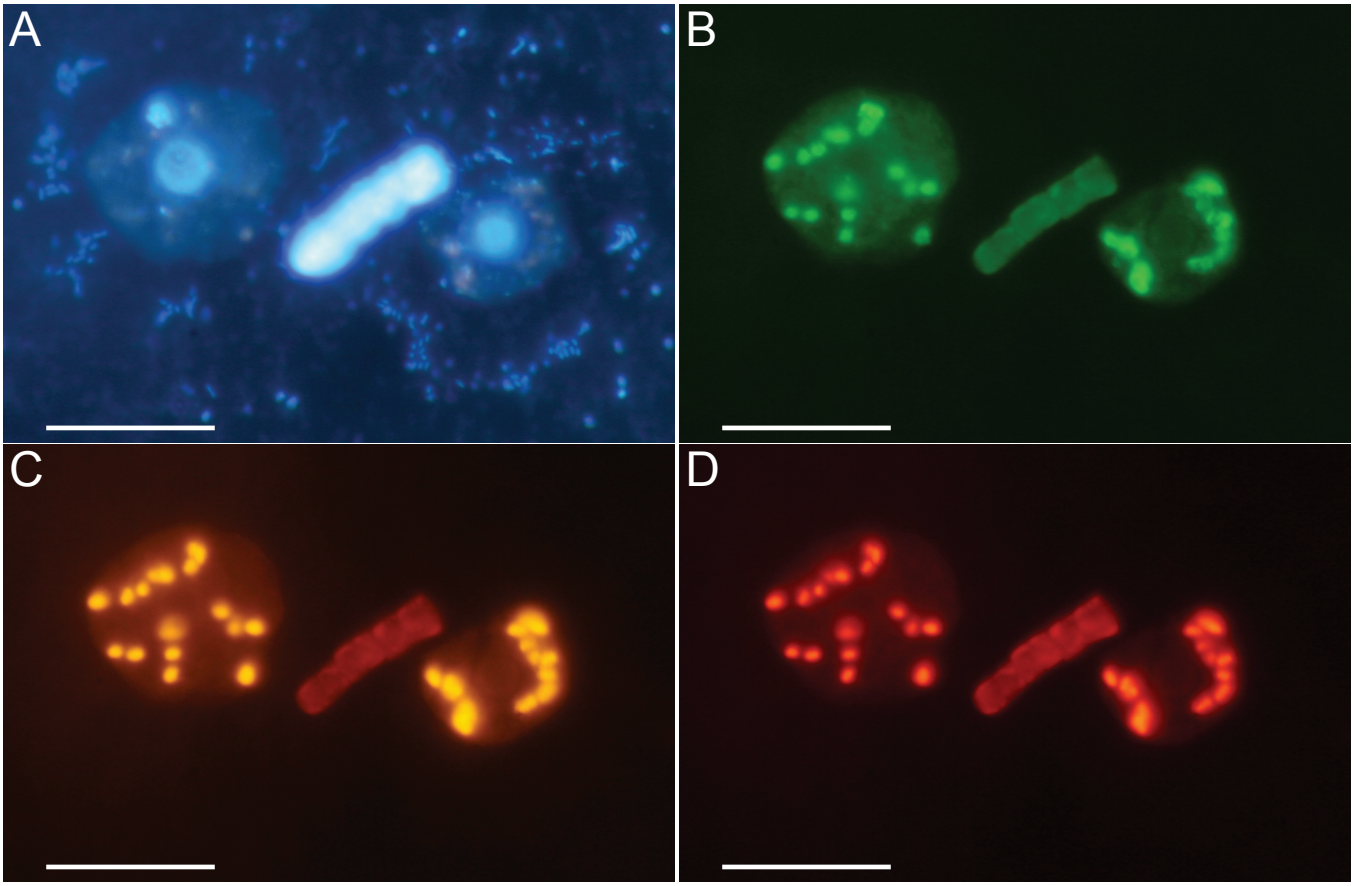

Figure S3. CARD-FISH double hybridization of endosymbionts of two *Nuclearia* sp. strain N.
A. DAPI staining (analyzed with Zeiss Filter set 01).
B. Hybridization of endosymbiotic bacteria with the specific probe CoNuc67 and fluorescein-labelled tyramides (analyzed with Zeiss Filter set 10).
C. Hybridization of endosymbiotic bacteria with the general probe Gam42a and Alexa546-labelled tyramides (analyzed with Zeiss Filter set 43).
D. Same objects analyzed with wide green exciation (Zeiss Filter set 14). Scale bars: 20µm.

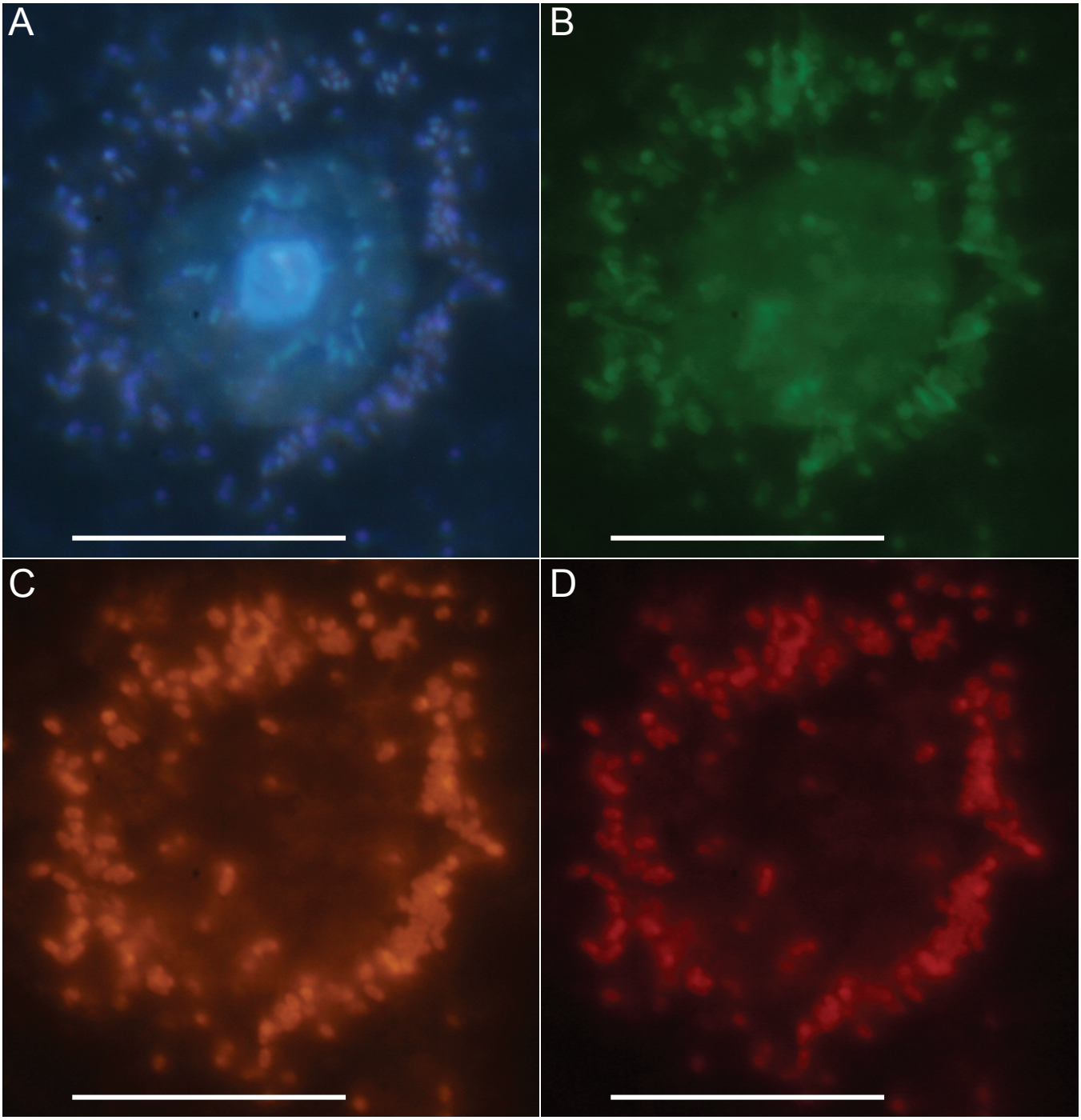

Figure S4. CARD-FISH double hybridization of ectosymbionts of a *Nuclearia* sp. strain N cell.
A. DAPI staining (analyzed with Zeiss filter set 01).
B. Hybridization of ectosymbiotic bacteria with the specific probe Pauci995 and fluorescein-labelled tyramides (Zeiss filter set 10).
C. Hybridization of ectosymbiotic bacteria with the probe general Bet42a and Alexa546-labelled tyramides (Zeiss filter set 43).
D. The same object analyzed with wide green excitation (Zeiss filter set 14). Scale bars: 20µm.

Article II

Dirren S & Posch T (2016) Promiscuous and specific bacterial symbiont acquisition in the amoeboid genus *Nuclearia* (Opisthokonta). *FEMS Microbiology Ecology* **92**.

FEMS Microbiology Ecology, 92, 2016, fiw105

doi: 10.1093/femsec/fiw105
Advance Access Publication Date: 18 May 2016
Research Article

RESEARCH ARTICLE

Promiscuous and specific bacterial symbiont acquisition in the amoeboid genus *Nuclearia* (Opisthokonta)

Sebastian Dirren and Thomas Posch*

Limnological Station, Department of Plant and Microbial Biology, University of Zurich, Seestrasse 187, CH-8802 Kilchberg, Switzerland

*Corresponding author: Limnological Station, Department of Plant and Microbial Biology, University of Zurich, Seestrasse 187, CH-8802 Kilchberg, Switzerland. Tel: 0041-44-634-9224; Fax: 0041-44-634-9225; E-mail: posch@limnol.uzh.ch

One sentence summary: Many amoeboid species of the genus *Nuclearia* (Opisthokonta) feed on filamentous cyanobacteria and live together with ectosymbiotic and/or endosymbiotic bacteria.

Editor: Julie Olson

ABSTRACT

We isolated 17 strains of the amoeboid genus *Nuclearia* (Opisthokonta) from five Swiss lakes. Eight of these nucleariid isolates were associated with bacterial endosymbionts and/or ectosymbionts. Amoebae were characterized morphologically and by their 18S rRNA genes. Phylogeny based on molecular data resulted in four established monophyletic branches and two new clusters. A heterogeneous picture emerged by highlighting nucleariids with associated bacteria. Apart from one cluster which consisted of only isolates with and three groups of amoebae without symbionts, we also found mixed clusters. The picture got even more 'blurred' by regarding the phylogeny of symbiotic bacteria. Although seven different bacterial strains could be identified, it seems that we still are only scratching the surface of symbionts' diversity. Furthermore, types of symbioses might be different depending on host species. Strains of *Nuclearia thermophila* harboured the same endosymbiont even when isolated from different lakes. This pointed to a specific and obligate interaction. However, two isolates of *N. delicatula* were associated with different endosymbiotic bacteria. Here the symbiont acquisition seemed to be rather promiscuous. This behaviour regarding symbiotic associations is especially remarkable considering the phylogenetic position of these basal opisthokonts.

Keywords: bacteria-protist symbioses; ectosymbionts; endosymbionts; *Nuclearia*; Nucleariidae; glycocalyx

INTRODUCTION

Intimate associations between unicellular or invertebrate eukaryotes and prokaryotes are ubiquitous, and their importance for the evolution of 'higher' life forms is increasingly recognized (Smith 1989; McFall-Ngai *et al.* 2013; Alegado and King 2014; Kiers and West 2015). We can intuitively argue that the probability of interactions increases if the spatial distance between hosts and potential symbionts is small, which is often the case for protists and bacteria. Knowing that such interactions are manifold, we use the term symbiosis in a very general way. We call the phenomenon of a close association of dissimilar organisms a 'symbiosis', thus we follow the original definition of this term by de Bary (see Appendix 1 in Paracer and Ahmadjian 2000). On an evolutionary scale, symbioses between eukaryotes and prokaryotes may emerge and disintegrate constantly and only a minute part will turn into 'stable associations'. The most stated and intensively studied examples are mitochondria and plastids that originated from the endosymbiosis of a host cell

Received: 28 January 2016; **Accepted:** 15 May 2016

with alphaproteobacteria (Thrash *et al.* 2011) and cyanobacteria (Rodríguez-Ezpeleta *et al.* 2005), respectively. Beside the fundamental functions of respiration and photosynthesis, we know several traits which bacterial symbionts may provide to their eukaryotic hosts, e.g. they can be important for the host's nutrition, defence, competition and adaption to the environment (Gast, Sanders and Caron 2009). Associated bacteria can also be involved in the production (Freeman *et al.* 2012) or degradation of secondary metabolites including toxins (Kikuchi *et al.* 2012; Dirren *et al.* 2014).

Here we focus on members of the amoeboid genus *Nuclearia* (Opisthokonta, Nucleariidae) which can live in symbiosis with ecto- and endosymbiotic bacteria. *Nuclearia* is a single genus in the family Nucleariidae which is a sister group to Fungi (Zettler *et al.* 2001; Steenkamp, Wright and Baldauf 2006; Liu *et al.* 2009). As far as we know, there is only one documented case of an opisthokont protist with prokaryotic symbionts. Wylezich *et al.* (2012) described the choanoflagellate *Codosiga balthica*, which harboured two different endosymbiotic bacteria inside the cytoplasm. This lack of evidence is remarkable considering the importance of symbiotic interactions for multicellular opisthokonts. Nucleariid amoebae are usually surrounded by a glycocalyx (Moran, Gupta and Joshi 2011; Ouwerkerk, de Vos and Belzer 2013), which can be colonized by ectosymbiotic bacteria (Artari 1889; Cann and Page 1979; Patterson 1984; Cann 1986). In a previous study, we characterized *Nuclearia* sp. strain N (hereafter named *Nuclearia thermophila* strain N) which harboured the bacterial ectosymbiont (*Paucibacter toxinivorans*) nicely arranged inside the glycocalyx (Dirren *et al.* 2014). The interaction between *N. thermophila* strain N and this prokaryote seemed to be specific and stable.

Multicellular organisms usually are associated with more than one bacterial species. Ectosymbionts form entire assemblages which are designated as microbiota of the respective host. The microbiota of very 'simple' animals like the cnidarians *Hydra* (Fraune and Bosch 2007; Franzenburg *et al.* 2013) and corals (Lema, Bourne and Willis 2014) seem to be relatively distinct and even species specific. In higher animals including humans (Huttenhower *et al.* 2012), the microbiota is more diverse and variations between individuals within the same population are pronounced. However, in contrast to the taxonomic variability, the functional roles of such assemblages seem to be conserved. Thus, composition and function of the microbiota is essential for the organism's well-being. A multitude of diseases are consequently caused by regime shifts to unhealthy and unstable states (Lozupone *et al.* 2012). The 'simplicity' of the *Nuclearia* system could be a great benefit for the fundamental understanding of interactions of prokaryotes with their opisthokont hosts.

Symbiotic interactions of Nucleariidae are not restricted to ectosymbiotic associations but amoebae may additionally harbour bacterial endosymbionts. For example, *N. radians* (described as *Nucleosphaerium tuckeri* by Cann and Page 1979) may be associated with ectosymbiotic and endosymbiotic bacteria. In recent studies, the rickettsial endosymbiont of *N. pattersoni* (Dykova *et al.* 2003) and *Candidatus* Endonucleariobacter rarus (Dirren *et al.* 2014) of *N. thermophila* strain N were characterized. Endosymbiotic bacteria are not at all as common in higher life forms as ectosymbionts. The barrier for bacteria to enter metazoans' cells is rather rigid and well protected (e.g. by the immune system). In vertebrates, mainly pathogens are able to enter cells causing infections and pathological states (Casadevall 2008). From an evolutionary point of view, this is of great interest as multicellular organisms seem to 'outsource' their bacterial associations to preserve their integrity. Consequently, the glycocalyx can be regarded as a kind of 'external organ' harbouring the symbiotic assemblage. This arrangement not only allows benefiting from the microbiota but also ensures a minimal physical distance and thus protection (Fraune *et al.* 2015).

To sum up, from a phylogenetic perspective, Nucleariidae might be good model organisms to verify hypotheses about symbioses in general. In order to study these interactions, it is the first step to elucidate the diversity of Nucleariidae and to characterize in parallel their symbionts. In this study, (i) we report on the morphology and taxonomic affiliation (18S rRNA genes) of 17 *Nuclearia* strains; (ii) all isolates were screened for bacterial symbionts both in the glycocalyx and inside amoebae; (iii) finally, we focused on symbionts of *N. delicatula* and *N. thermophila* strains, and analysed the ultrastructure and the intracellular localization of endosymbiotic bacteria via transmission electron microscopy (TEM). Additionally, we sequenced the bacterial 16S rRNA genes for phylogenetic analyses.

METHODS

Strains and cultures

A total of 17 *Nuclearia* strains were isolated from benthic and pelagic water samples of five Swiss lakes (Table 1). Single cells were picked with a glass pipette and washed in sterile water to generate monoclonal xenic amoebal cultures. Finally, isolates were cultured in autoclaved mineral water (Cristalp) and the cyanobacterium *Planktothrix rubescens* was added as sole food source. *Planktothrix rubescens* BC 9307 was isolated from Lake Zurich (Walsby, Avery and Schanz 1998) and is kept as axenic stock culture. *Nuclearia* cultures were maintained at a 12 h light (irradiance: 5–15 μmol m^{-2} s^{-1})/12 h dark cycle in Tissue Culture Flasks 25 cm^2 (TPP) at 18°C. Cultures were fortnightly renewed by adding 1 ml of the axenic cyanobacterial stock culture to 10 ml of new culture medium inoculated with 200 μl of an older culture. For all analyses, we included the dataset about *N. thermophila* strain N and its bacterial ectosymbiont *P. toxinivorans* strain SD41 (HG792253), originating from our previous study (Dirren et al. 2014). *Nuclearia delicatula* strain G (CCAP 1552/6), *N. moebiusi* strain K (CCAP 1552/7), *N. thermophila* strain N (CCAP 1552/5) and *N. pattersoni* strain A2 (CCAP 1552/8) were deposited in the Culture Collection of Algae and Protozoa (CCAP).

Morphological analysis and cladistic tree

Morphological characters were observed by light microscopy on living specimens. Features like multinucleate/uninucleate, evident/not evident nucleolus and branching of filopodia were observed when cells adapted a flattened form under the compression of the cover slip. Cells were considered 'spherical' if floating individuals in the water column could be observed (even if they were not always 'perfect' spheres). Strains were classified as being able to adapt a 'flattened form' when cells have ever attached to and moved on surfaces. The formation of syncytia was defined as the fusion of two or more cells. In addition, we checked all culture flasks for the appearance of cysts. The glycocalyx was either seen with phase contrast as translucent halo surrounding cells or after staining with Alcian blue. Ectosymbionts were defined as bacteria inside the glycocalyx located close to the cell membrane (loosely attached bacterial cells on the outer border of the glycocalyx were not classified as symbionts). Endosymbionts were detected with epifluorescence microscopy after DAPI staining and by in situ hybridization (CARD-FISH). The body diameter of spherical cells was

Table 1. Features of *Nuclearia* isolates. The following features were observed for all strains and thus are not listed: spherical form, flattened form, nucleolus, glycocalyx and branching of filopodia. If not stated otherwise, strains were isolated from benthic samples. Strains are listed according to the phylogenetic tree shown in Fig. 1A. In case that bacterial symbionts could be identified with CARD-FISH, the adequate oligonucleotide probes are listed (see Table 2 for probes abbreviations). Lake Zurich: 47°19′11.5″N, 8°33′10.1″E, Lake Hallwil: 47°18′16.3″N, 8°13′03.3″E, Lake Sempach: 47°08′15.8″N, 8°08′25.8″E, Lake Baldegg: 47°11′38.9″N, 8°15′46.6″E, Lake Soppi: 47°05′25.6″N, 8°04′51.5″E.

Nuclearia sp. strain	Nucleus	Ectosymbiont	Endosymbiont	Cysts	Mean size (range); n (sizes in μm)	18S rRNA sequence	Isolation date; source
N. delicatula strain G	Multinucleate	Bu154	Del1424 and Le827	–	26 (17.2–45.8); $n = 100$	LN875119	Oct 2012; Lake Zurich
N. delicatula strain D	Multinucleate	+ (lost)[a]	AlRick85	–	20.4 (10.7–82.2); $n = 133$	LN875118	Feb 2012; Lake Zurich
N. delicatula strain S4	Multinucleate	+ (lost)[a]	Del1424	–	24.5 (12.8–104.8); $n = 100$	LN875117	Oct 2014; Lake Sempach
N. delicatula strain D4	Multinucleate	+ (lost)[a]	Del1424	–	24 (13.8–42.6); $n = 100$	LN875116	Oct 2014; Lake Sempach
N. delicatula strain B6	Multinucleate	+ (lost)[a]	–	–	26.7 (15–45.6); $n = 107$	LN875115	Sep 2014; Lake Hallwil
N. moebiusi strain K	Uninucleate	–	–	–	9.8 (3.8–15.1); $n = 100$	LN875108	Oct 2012; Lake Zurich
N. thermophila strain B1	Uninucleate	–	–	+	15.4 (9.5–23.2); $n = 100$	LN875121/22	Nov 2013; Lake Zurich
N. thermophila strain D6	Uninucleate	–	CoNuc67	+	15.7 (9.4–22.7); $n = 100$	LN875109	Sep 2014; Lake Hallwil
N. thermophila strain A	Uninucleate and multinucleate syncytia	+ (lost)[a]	CoNuc67	+	17.7 (9.8–28.3); $n = 270$	LN875106	May 2011; Lake Zurich
N. thermophila strain N	Uninucleate and multinucleate syncytia	Pauci995	CoNuc67	+	16.4 (7.2–29); $n = 448$	HG530253	Aug 2011; Lake Zurich
Nuclearia sp. strain B3	Uninucleate	–	–	–	8.7 (5–14.2); $n = 100$	LN875120	Sep 2014; Lake Baldegg[b]
Nuclearia sp. strain A5	Uninucleate and multinucleate syncytia	–	–	–	9.2 (5.4–15.4); $n = 100$	LN875107	Sep 2014; Lake Hallwil[b]
N. pattersoni strain B4	Uninucleate	–	–	+	8.4 (5.4–15.3); $n = 100$	LN875111	Oct 2014; Lake Soppi[b]
N. pattersoni strain A2	Uninucleate	–	–	+	9.9 (6.5–17.8); $n = 100$	LN875110	Sep 2014; Lake Baldegg[b]
Nuclearia sp. strain NZ	Uninucleate	–	–	–	16.7 (10.6–28.4); $n = 100$	LN875112	Oct 2012; Lake Zurich[b]
Nuclearia sp. strain A1	Uninucleate	–	–	–	12.3 (8.2–18.3); $n = 106$	LN875113	Oct 2014; Lake Sempach
Nuclearia sp. strain D1	Uninucleate	–	–	–	11.9 (6.9–19.4); $n = 124$	LN875114	Oct 2014; Lake Sempach

[a] Amoebae lost bacterial ectosymbionts during long-term cultivation.
[b] Amoebal strains were isolated from the pelagic zone of the respective lake.

measured more than 3 months after isolation of the strains. Only for *N. thermophila* strain D6, additional measurements were taken right after isolation. For calculations of the cladistic tree, morphological characters were judged as either present or absent and each strain was attributed to one of three size classes: 1. x < 13 μm; 2. 13 μm < x < 20 μm; 3. x > 20 μm. The cladistic tree (Jaccard's similarity coefficient) was calculated with the Add-In software XLSTAT (Addinsoft).

Sequencing of the 18S rRNA genes (Nucleariidae)

DNA was extracted from aliquots (1.5 ml) of *Nuclearia* cultures with the GenElute Bacterial Genomic DNA Kit (Sigma). PCR with GoTaq® Green Master Mix (Promega) and the eukaryote-specific primers Euk328f and Euk329r (Moon-van der Staay, De Wachter and Vaulot 2001) were used to amplify the 18S rRNA genes. If gel elecrophoresis resulted in the detection of bands of expected size, PCR products were purified with QIAquick PCR Purification Kit (Qiagen) and Sanger sequenced with ABI BigDye chemistry on an ABI 3130x Genetic Analyzer (Applied Biosystems). In order to sequence the entire amplicons, the additional primers SR2f, SR2r, SR4f, SR6f, SR6r, SR8f, SR8r, SR10f and SR10r (Nakayama *et al.* 1998) were used. In seven cases (strains G, D, S4, D4, B6, B1 and B3), the direct sequencing was not successful. Here 18S rRNA genes were again amplified from the extracted DNA with Platinum PCR Super Mix High Fidelity (Invitrogen) and the primers Euk328f and Euk329r. Subsequently, PCR products were purified as mentioned above and cloned into *Escherichia coli* using a pGem-T Vector (Promega) according to the manual. Clones were screened for expected size inserts with the plasmid primers M13f and M13r. Positive clones were grown in liquid cultures, and plasmids were purified with GenElute Five-Minute Miniprep Kit (Sigma). Inserts of plasmids were sequenced in the same way as PCR products but plasmid primers were used instead of Euk328f and Euk329r.

Sequencing of the 16S rRNA genes (symbionts)

Two 16S rRNA gene clone libraries were constructed from *N. delicatula* strain D and strain G, respectively. About 130 *Nuclearia* cells were picked with a micropipette and washed in sterile water. After three freeze–thaw cycles, DNA was extracted with GenElute Bacterial Genomic DNA Kit (Sigma). Extracted DNA served then as template for amplification of 16S rRNA genes with Platinum PCR Super Mix High Fidelity (Invitrogen) and the primers GM3f and GM4r (Muyzer and Ramsing 1995). After purification of PCR products and ligation into the pGem-T Vector (Promega), they were cloned following the manufacturer's protocol. Positive *E. coli* clones were detected by screening with plasmid primers (size ~1.6 kbp) and their plasmids purified as described above. Sequencing of inserts was done with plasmid primers and the additional primer GM1f (Muyzer and Ramsing 1995). Partial 16S rRNA genes of the endosymbiont *Candidatus* Endonucleariobacter rarus from *N. thermophila* strain A and strain D6 were sequenced directly. The sequence of the probe CoNuc67 (Table 2) was used to design a specific primer (P1_CoNuc_f 5′-TAACAGAGTGTGTAGC-3′). PCR amplification with GoTaq Green Master Mix (Promega) was done with extracted DNA from these cultures using the forward primer P1_CoNuc_f and the reverse primer GM4r (positive control: ext. DNA from *N. thermophila* strain N; negative control: ext. DNA from *N. thermophila* strain B1). Subsequently purified PCR products were directly sequenced with the primers P1_CoNuc_f and GM4r as described above (LN875086–LN875088).

Table 2. Specific CARD-FISH probes applied in this study. Affiliations of the target bacteria to major taxonomic groups are given in brackets: AlRick85 (Alphaproteobacteria), Bu154 and Pauci995 (Betaproteobacteria), Del1424 (Deltaproteobacteria), CoNuc67 and Le827 (Gammaproteobacteria).

Probe (Reference)	Sequence (5′ to 3′)	Specificity	FA in %[a]	Hits in RDP[b]/Δ FA in % to the non-targets[c]
CoNuc67 (Dirren *et al.* 2014)	ATTGCTACACACTCTGTTACGG	'*Candidatus* Endonucleariobacter rarus'	70	0; 2; 31/30.5
Pauci995 (Dirren *et al.* 2014)	AATCTCTTCGGGATCTCTGACATG	*Paucibacter toxinivorans*	70	23; 77; 465/0
Bu154 (this study)	CGAACAGTTATCCCCCACTACC	*Inhella* sp. ectosymbiont of strain G	55	17; 14859; 29751/0
Le827 (this study)	CCCTAAGGCTTCCAACAGCC	'*Candidatus* Ovatusbacter abovo'	60	0; 1; 6/33.3
Del1424 (this study)	GCTCACGCGCTTCTGGCTTATAC	'*Candidatus* Turbabacter delicatus'	70	0; 0; 0/30.7
AlRick85 (this study)	CGTCTGCCACTAACATATGTGAGCT	'*Candidatus* Intestinusbacter nucleariae'	70	0; 0, 1/69.9

[a]Formamide concentrations in the hybridisation buffer.
[b]Number of hits with the 'Probe Match' tool in the RDP database: zero mismatches; one mismatch; two mismatches.
[c]Minimal difference in formamide concentrations between target and non-targets calculated with the 'Mismatch Analysis' tool from mathFISH.

Phylogenetic analyses

The software DNA Baser v3.5.0 (Heracle BioSoft) served as tool for assembling partial sequences. Chimeric sequences were detected and removed using Mallard and Pintail (Ashelford *et al.* 2005). For phylogenetic analyses, the ARB software package (Ludwig *et al.* 2004) with the SILVA database SSU Ref 111 (Pruesse *et al.* 2007) was used.

All available *Nuclearia* 18S rRNA gene sequences from described species, our isolates, and as outgroup two sequences from *Candida* sp. (AB013586 and EU348785) were included for phylogenetic tree reconstruction. Sequences were trimmed and aligned with the MAFFT aligner (Katoh and Standley 2013). Alignments were manually optimized and ambiguous regions (e.g. insertions in the V4, V7 and V8 domains) were removed resulting in 1501 positions with 150 distinct alignment patterns. Another phylogenetic tree including all our *N. delicatula* clones, *N. delicatula* (AF349563) and *N. simplex* (AF349566)/*N. moebiusi* (AF349565) as outgroup was calculated. In addition, sequences were aligned and trimmed as described above but none of the hypervariable regions were removed (2363 positions with 204 distinct alignment patterns).

The 16S rRNA gene sequences of symbionts were aligned with the SINA web aligner (www.arb-silva.de/aligner/). Five phylogenetic trees (*Ca.* Endonucleariobacter rarus: 1305 positions, 56 distinct patterns; ectosymbionts: 1417 positions, 199 distinct patterns; endosymbionts: 1558 positions, 827 distinct patterns; clone library strain G: 1383 positions, 617 distinct patterns; clone library strain D: 1415 positions, 769 distinct patterns) were calculated with our sequences and related sequences from the SILVA database (quality scores ≥88).

For the reconstruction of phylogenetic trees, maximum likelihood (ML) and Bayesian inference (BI) methods were used. Bootstrapped ML trees were calculated (1000 iterations) using the RAxML algorithm (Stamatakis, Hoover and Rougemont 2008). The parameters were GTR (general time reversible) model with a Γ distribution for rate heterogeneity among sites, with four discrete rate categories. BI was calculated using the ExaBayes software package (©The Exelixis Lab). The posterior probabilities from BI trees (four chains; 100 000 generations) were added to ML trees where trees of both methods were congruent. Full-length 16S rRNA gene sequences from clone libraries and 18S rRNA gene sequences of the *Nuclearia* strains were deposited in the EMBL database with the accession numbers LN875040–LN875170.

CARD-FISH and probe design

First, CARD-FISH with the general probes EUB I-III (Daims *et al.* 1999), ALF968 (Neef 1997), BET42a, GAM42a (Manz *et al.* 1992), CF319a (Manz *et al.* 1996), HGC69a (Roller *et al.* 1994) and VER47 (Buckley and Schmidt 2001) allowed for the identification of symbionts on a higher taxonomical level. Afterwards clusters of potential symbionts were chosen from phylogenetic trees of the 16S rRNA gene clone libraries. Specific probes were designed based on the sequences of these candidate clusters. Probe design with the dedicated ARB tool resulted in four specific CARD-FISH probes (Table 2). The Ribosomal Database Project (www.rdp.cme.msu.edu) and the web tool Mathfish (Yilmaz, Parnerkar and Noguera 2011) were used for *in silico* testing of the new probes. Appropriate formamide concentrations (for highest stringency) were determined empirically. Non-specific staining was addressed with the probe NON338 (Wallner, Amann and Beisker 1993). CARD-FISH on filters was done with differently labelled tyramids (fluorescein and Alexa546) following the previously published protocol (Dirren *et al.* 2014). In addition, CARD-FISH of amoebae on gelatine-coated glass slides and embedded in agarose were prepared.

Microscopy and photographic documentation

Differential interference and phase contrast images were acquired with a Canon EOS1000D controlled by the software AxioVision 4.8.2 (Zeiss) installed on an Axio Imager.M1 microscope (Zeiss). CARD-FISH preparations were analysed at the same microscope with epifluorescence microscopy (Zeiss optical filter sets: set 01, 10, 14 and 43) and by confocal laser-scanning microscopy (SP5-R, Leica Microsystems, Germany).

Transmission electron microscopy

Glutaraldehyde (final conc. 1.25 %) and osmium tetroxide (final conc. 1 %) were mixed and added to small volumes of *N. delicatula* strain D and strain G cultures (after centrifugation at 1000 g for 20 min and discarding of supernatants). Fixation was done on ice for 1 h followed by two washing steps (centrifugation for 10 min at 2000 g and exchanging of fixative solution with H_2O). Washed pellets were resuspended in melted agar (2 %). After hardening and cutting the agar block into smaller pieces (~10 mm^3), they were block stained with uranylacetat (1 %) for 1 h at room temperature. Subsequently, samples were dehydrated in an ethanol series (70%, 80%, 96% and 100%) and finally in propylenoxide, followed by embedding in epon-araldite. Ultrathin sections were cut with an Ultracut UCT (Leica) and poststained with lead citrate for 6 min. An electron microscope Philips CM100 equipped with a digital camera (Gatan Orius 1000) was used for the analysis of the TEM preparations.

RESULTS AND DISCUSSION

Morphological versus molecular phylogeny of *Nuclearia* spp.

For a long time, nucleariid amoebae were described using only morphological characters. However, the majority of these amoeboid species share many features used for their identification (see table 1 in Yoshida, Nakayama and Inouye 2009). It seems that some inadequately defined characters were even interpreted differently by researchers, e.g. if amoebae may form flattened/spherical cells, if a glycocalyx is present or absent and if the nucleolus is evident. This becomes obvious, when comparing fig. 11 in Patterson (1984), where the author stated the lack of a glycocalyx, with fig. 6 in Pernin (1976), where the presence of EPS was proven. In addition to these 'vague' characters, other features like the formation of multinucleate syncytia, cyst production and the appearance of branched filopodia might be rarely or not at all observed depending on culture and observation conditions. Even the cell size of single isolates may vary depending on culture conditions. We documented at least for one isolate a shrinkage of cells in the course of cultivation. The mean cell size of *N. thermophila* strain D6 decreased from initially 24.6 μm (day 7 after isolation, $n = 56$) to 15.7 μm (day 90, $n = 100$). Thus, most probably these inconsistencies and different interpretations of features led to redescriptions of species and incorrect identifications.

This assumption is additionally supported by the fact that two *N. simplex* isolates clustered in the 18S rRNA gene-based phylogenetic tree very distantly (Fig. 1A) with *N. moebiusi* and

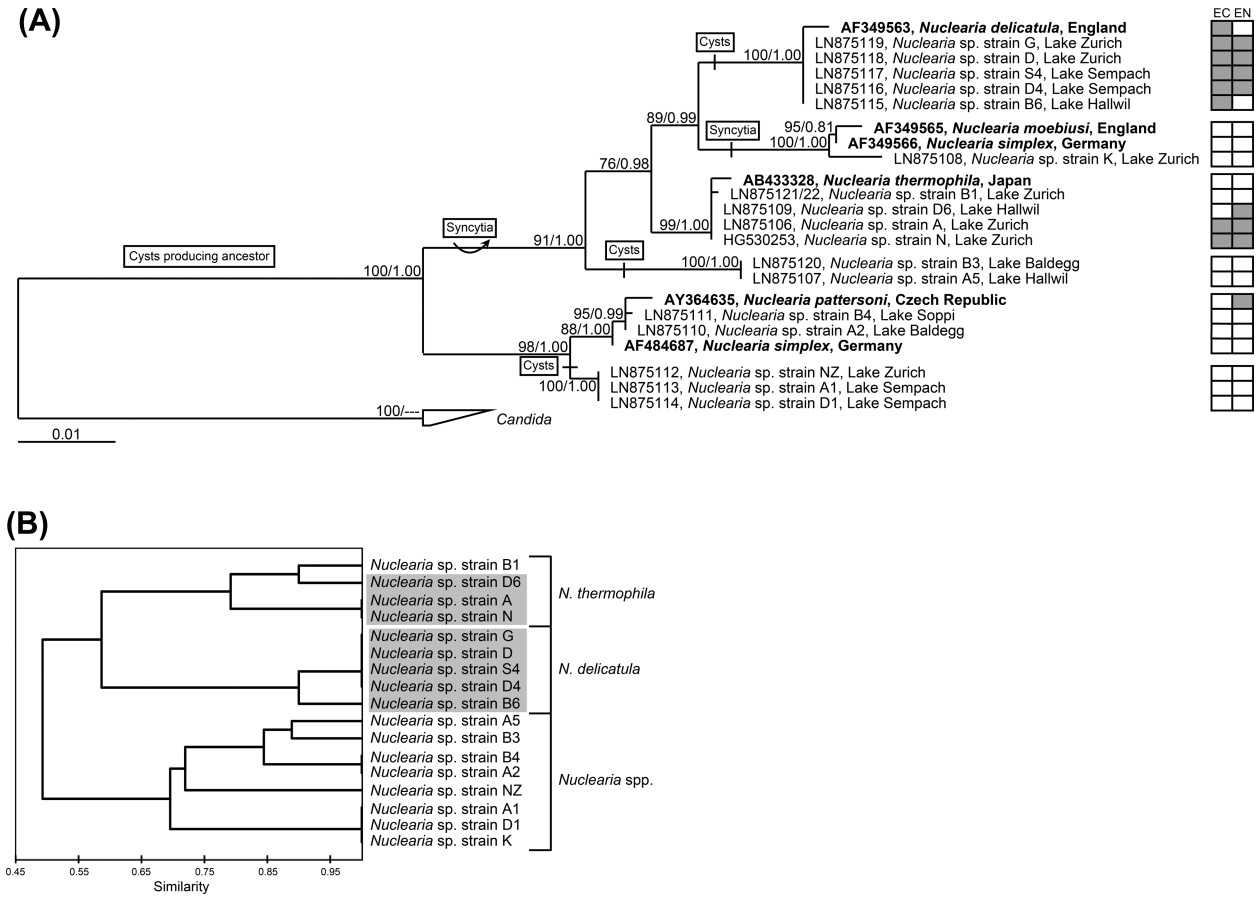

Figure 1. Phylogenetic analysis of the *Nuclearia* spp. isolates. (**A**) 18S rRNA gene based ML tree with posterior probabilities from BI; ML bootstrap value/BI probability. Described *Nuclearia* species are shown in bold and *Candida* was used as outgroup. Hypothetical gain (curved arrow) and loss (bar) of features 'cyst production' (Cysts) and 'formation of syncytia' (Syncytia) are shown. Detected ectosymbionts (EC) and endosymbionts (EN) are indicated with a filled square for the respective isolate. Scale bar: number of nucleotide substitutions per site. (**B**) Cladistic tree based on morphological characters of the *Nuclearia* spp. isolates. X-axis: similarity value (Jaccard coefficient). The affiliations of amoeboid isolates to described species are indicated on the right hand. Isolates with associated symbionts are grey shaded.

N. pattersoni, respectively. Because of this discrepancy, we considered the two as *N. simplex* identified isolates to belong to different species. Consequently, we will name these phylogenetic groups as *N. moebiusi* and *N. pattersoni* cluster, respectively. Moreover, two sequences of one and the same *N. moebiusi* isolate (AF349565 and AF484686) were included in phylogenetic trees by some authors (Dykova *et al.* 2003; Yoshida, Nakayama and Inouye 2009) which further caused confusions.

Nevertheless, in this study we partly worked with traditional morphological features for comparisons of our strains (Fig. 2 and Fig. S1, Supporting Information) with published species descriptions. To characterize our *Nuclearia* spp. isolates, we even included four additional features: benthic isolate, pelagic isolate, presence of ectosymbionts and presence of endosymbionts (Table 1). We checked if the morphological classification corresponded to the molecular phylogeny by performing a cladistic analysis based on presence/absence of characters. The cladistic tree (Fig. 1B) and the 18S rRNA gene-based ML tree (Fig. 1A) were in good accordance regarding the *N. delicatula* and the *N. thermophila* clusters. In both trees, they were sister groups including same isolates. In contrast, the third big cluster in the cladistical tree unified isolates from distant branches of the ML tree. Although the substructure of this third cluster reflected quite well the 18S rRNA gene-based phylogeny, two isolates clustered differently. In the cladistic tree, *Nuclearia* sp. strain NZ had no close relative and strain K formed together with strains A1 and D1 a group, which was not confirmed by molecular phylogeny. Taken together, only *N. delicatula* and *N. thermophila* strains could be identified solely by their morphological traits. For the affiliation of all other isolates, additional molecular information (18S rRNA genes) was needed.

Assignment of isolates to described species

The species descriptions of *N. delicatula* from Patterson (1984) and Cann (1986) are in good accordance with morphological features (Table 1) observed for all isolates in the *N. delicatula* cluster.

The morphological features described for *N. moebiusi* differed from what we observed for *Nuclearia* sp. strain K. We found spherical cells as well as a glycocalyx which was not reported for *N. moebiusi*. When considering the 'excavate cavities' (fig. 11 from Patterson 1984) to be the glycocalyx and additionally taking the trait 'spherical form' less restrictive, we can assign our isolate to this species (i.e. *N. moebiusi* strain K).

The morphological incongruences between *N. thermophila* strain N and the original species description of *N. thermophila* by Yoshida, Nakayama and Inouye (2009) were discussed in our previous study (Dirren *et al.* 2014). For the isolates clustering together with *N. thermophila*, we reported a good accordance with the characters earlier described for *N. thermophila* strain N. Only the formation of syncytia could not be documented for strains B1 and D6. The present results including morphological and

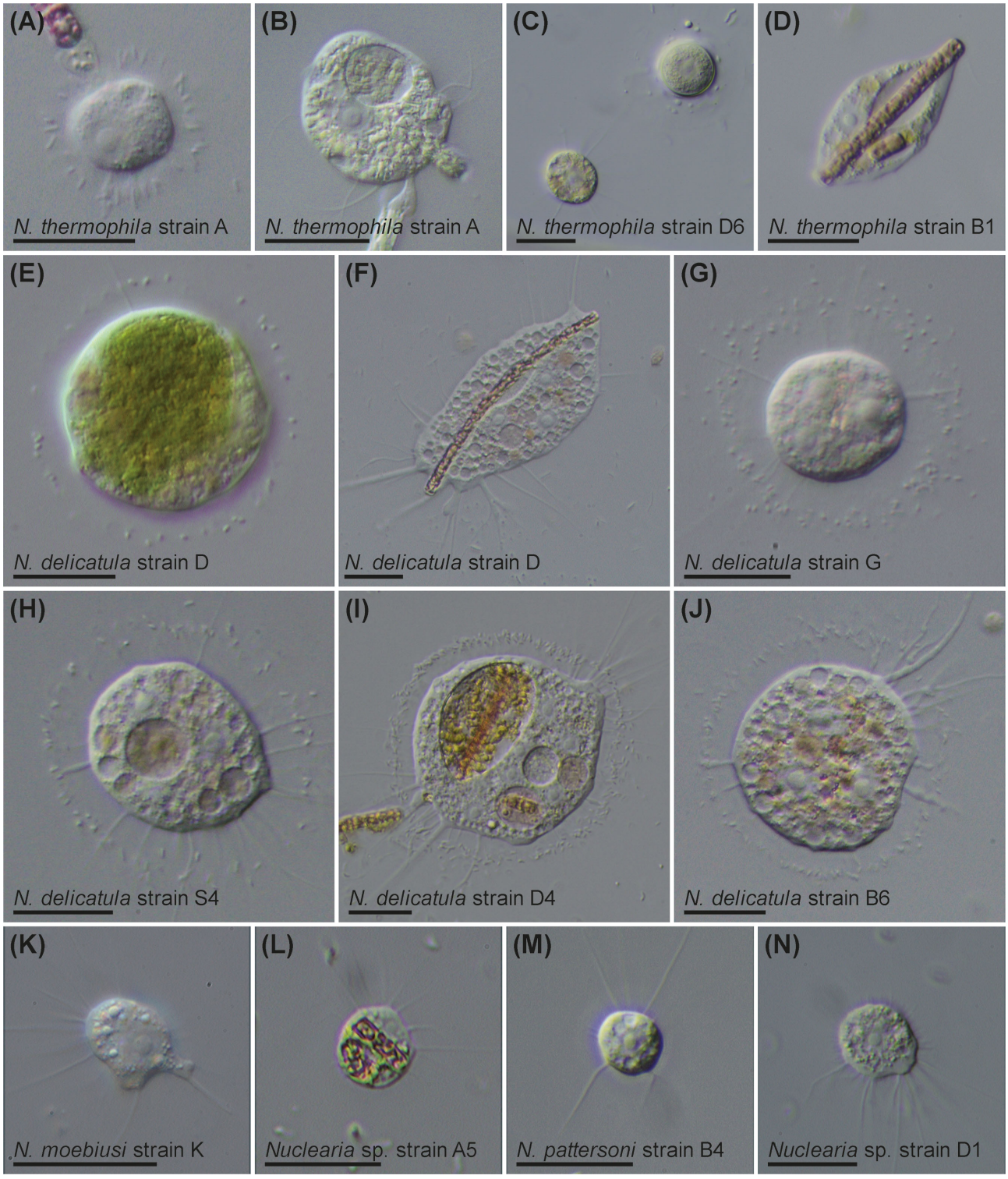

Figure 2. Light microscopical images of 12 *Nuclearia* spp. isolates. **(A)** Nucleariid cell attached to a *P. rubescens* filament surrounded by ectosymbiotic bacteria right after isolation. **(B)** Feeding individual after loss of ectosymbionts (3 months later). **(C)** Vegetative cell (left) and cyst (right) next to each other. **(D)** Elongated organism with phagocytised *P. rubescens* fragments. **(E)** Green cell (due to partly digested pigments of food organisms) colonized by ectosymbiotic bacteria 9 months after isolation. **(F)** Amoeboid multinucleated organism which lost ectosymbionts (3 years later). **(G)** Multinucleate spherical individual with symbiotic bacteria inside the glycocalyx. **(H)** Nearly spherical cell with radiating filopodia. Note food vacuoles and two nucleoli. **(I)** Feeding individual with a large food vacuole containing remnants of *P. rubescens* filaments at different states of digestion. Ectosymbiotic bacteria surround the multinucleate cell. **(J)** Organism partly attached to the surface colonized by symbiotic bacteria. Concentrated filopodia indicate the direction of locomotion. **(K)** Amoeboid cell with a prominent nucleolus. **(L)** Individual with ingested fragments of *P. rubescens*. **(M)** Spherical cell freely floating. **(N)** Amoeboid organism moving on surface. All pictures were taken with differential interference contrast (DIC) and scale bars indicate 20 μm.

phylogenetic analyses of four different isolates (strains B1, D6, A, N) thus justify their assignment to the species *N. thermophila*.

All described features for *N. pattersoni* (Dykova *et al.* 2003) except the presence of endosymbionts could be observed for *Nuclearia* sp. strain B4 and A2. Taking their phylogenetic close relatedness (Fig. 1A) into account, we can assign them to the species *N. pattersoni*.

The isolates *Nuclearia* sp. strain NZ, strain A1 and strain D1 built a sister group to the *N. pattersoni* cluster (Fig. 1A). Morphologically these three isolates were very similar and the lack of cysts was the only character differentiating them from *N. pattersoni* isolates. However, the phylogenetic distance (Fig. 1A) still does not allow for assigning them to the described species.

Finally, the two isolates *Nuclearia* sp. strain B3 and A5 formed a discrete new phylogenetic group. In spite of only minor morphological differences (e.g. formation of syncytia in strain A5) to isolates in the *N. moebiusi* and *N. pattersoni* clusters, we suppose that they form a new species. Phylogenetic reconstruction even points at a rather basal position, probably representing a sister group to *N. delicatula*, *N. moebiusi* and *N. thermophila*. We added hypothetical gains and losses of the features 'cyst production' and 'formation of syncytia' to the corresponding branches (Fig. 1A). The fact that we found cyst production for isolates all over the tree may indicate that the common ancestor was encysting. In contrast, the formation of syncytia was found only for isolates in one of the main branches and thus could be an acquired trait.

Variability of the nucleariid 18S rRNA gene copies

For all but seven *Nuclearia* isolates, PCR amplification of the 18S rRNA gene with general eukaryotic primers and direct sequencing was successful (LN875106–LN875114). In contrast, assembling of partial 18S rRNA gene sequences failed for *N. thermophila* strain B1, *Nuclearia* sp. strain B3 and all *N. delicatula* isolates (strains G, D, S4, D4 and B6). For *N. thermophila* strain B1, a poly-G region causing 'hard stops' during sequencing resulted in two non-overlapping partial sequences. The first part (~700 nt) and the second part (~1230 nt) of the 18S rRNA gene could thus not be assembled. Sequence qualities of all *N. delicatula* strains and *Nuclearia* sp. strain B3 dropped in regions containing homopolymers due to superposition of signals. This pointed to sequence variations in multiple 18S rRNA gene copies (e.g. different lengths of homopolymers). Therefore, PCR products of *N. delicatula* strains and *Nuclearia* sp. strain B3 were cloned and *de novo* sequenced resulting in partial sequences with high-quality scores even for regions containing homopolymers. Two to ten different clones were completely sequenced (LN875123–LN875170) for *N. delicatula* isolates and *Nuclearia* sp. strain B3. In order to exclude that interclone variation was introduced by PCR and sequencing errors, we reamplified 18S rRNA genes from cleaned-up plasmids of three *N. delicatula* strain D4 clones. The obtained sequences were identical to those generated by direct sequencing of inserts. Thus, detected interclone variations most probably originated from natural variations in 18S rRNA gene copies and were not artefacts.

Microheterogeneities in the nucleariid 18S rRNA genes have been already documented by Zettler *et al.* (2001). They mainly originate from size variations in the insertions inside the V4, V7 and V8 domains (sensu De Rijk *et al.* 1992). Pairwise sequence distances were calculated for each clone library of *N. delicatula* strains (G, D, S4, D4), *Nuclearia* sp. strain B3 and *N. thermophila* strain B1 (Fig. S2A, Supporting Information). Variations in the 18S rRNA gene copies of *N. thermophila* strain B1 (mean ± standard deviation: 0.21±0.07 %) were lower than those in *N. delicatula* strains (0.48±0.15 % to 0.63±0.24 %) and in *Nuclearia* sp. strain B3 (0.44±0.24 %). Intrastrain variations (distances of clone sequences: 0.58±0.05 %) were about three times higher than interstrain variations (distances of the consensus sequences: 0.17±0.07 %) for *N. delicatula* isolates. Thus, they could not be separated phylogenetically on the base of this marker gene (Fig. S2B, Supporting Information). When we calculated sequence similarity of *N. delicatula* (AF349563) and *N. delicatula* strain G without these variable parts in the V4, V7 and V8 domains, we got a high value of 99.7 %. In contrast, sequence similarity including the hypervariable stretches was only 94 %. In the same way, 18S rRNA gene copies in single isolates are mainly diverging (e.g. due to insertion and deletion of nucleotides) inside the homopolymers of hypervariable domains. Slipped-strand mispairing (Levinson and Gutman 1987) might be the mechanism behind this phenomenon. A slightly higher mutation rate could also be detected for the variable stretches in sequences from the *N. pattersoni* cluster (e.g. sequence similarity of the described *N. pattersoni* and *N. pattersoni* strain B4: with homopolymer region 99 % and without 99.2 %) but not within the *N. thermophila* cluster. The sequence similarity of *N. thermophila* (AB433328) and *N. thermophila* strain A was 99.6% with and without homopolymer regions.

Taken together, divergence and/or number of 18S rRNA gene copies vary between different *Nuclearia* species. Regarding their mutation rates, homopolymer regions can differ drastically from the rest of the sequence. And finally, accumulations of mutations in these regions seem to be species specific.

Associations of *Nuclearia* spp. with prokaryotes

In total 8 of our 17 isolates were associated with endosymbiotic and/or ectosymbiotic bacteria. Symbionts could be detected for all *N. delicatula* strains but not for *Nuclearia* isolates from three other clusters (Fig. 1A). Beside these homogeneous branches, also mixed groups were found. In the *N. thermophila* cluster, three out of five representatives had symbionts (Fig. 1A). The *N. pattersoni* cluster was also heterogeneous. It was only reported for *N. pattersoni* (Dykova *et al.* 2003) that this amoeba harboured a rickettsial endosymbiont.

The non-systematic appearance of symbiotic associations inside the genus *Nuclearia* indicates a species-dependent disposition. As far as we know such a high variability within a single genus has been described only for *Acanthamoeba* spp. (Fritsche *et al.* 1993; Horn *et al.* 1999; Horn 2008). Either some *Nuclearia* species evolved traits by which the probability to enter a symbiotic relationship increases or it is a plesiomorph character that has been partly lost. Considering their phylogenetic position within opisthokonts, it is of interest to search specifically for such traits in future genetic analysis. Probably, nucleariids have already specific genes and machineries which are involved in selecting and controlling of symbiotic partners (Bosch 2014). The question about the frequency of prokaryotic symbionts in unicellular opisthokonts still remains to be addressed. Today, it is not clear if the lack of knowledge simply derives from the low number of studies looking for symbiotic associations or if the highly diverse interactions inside the genus *Nuclearia* are an exceptional phenomenon.

Nuclearia thermophila isolates and their ectosymbionts

In a previous study (Dirren *et al.* 2014), we identified the ectosymbiont of *N. thermophila* strain N as the betaproteobacterium

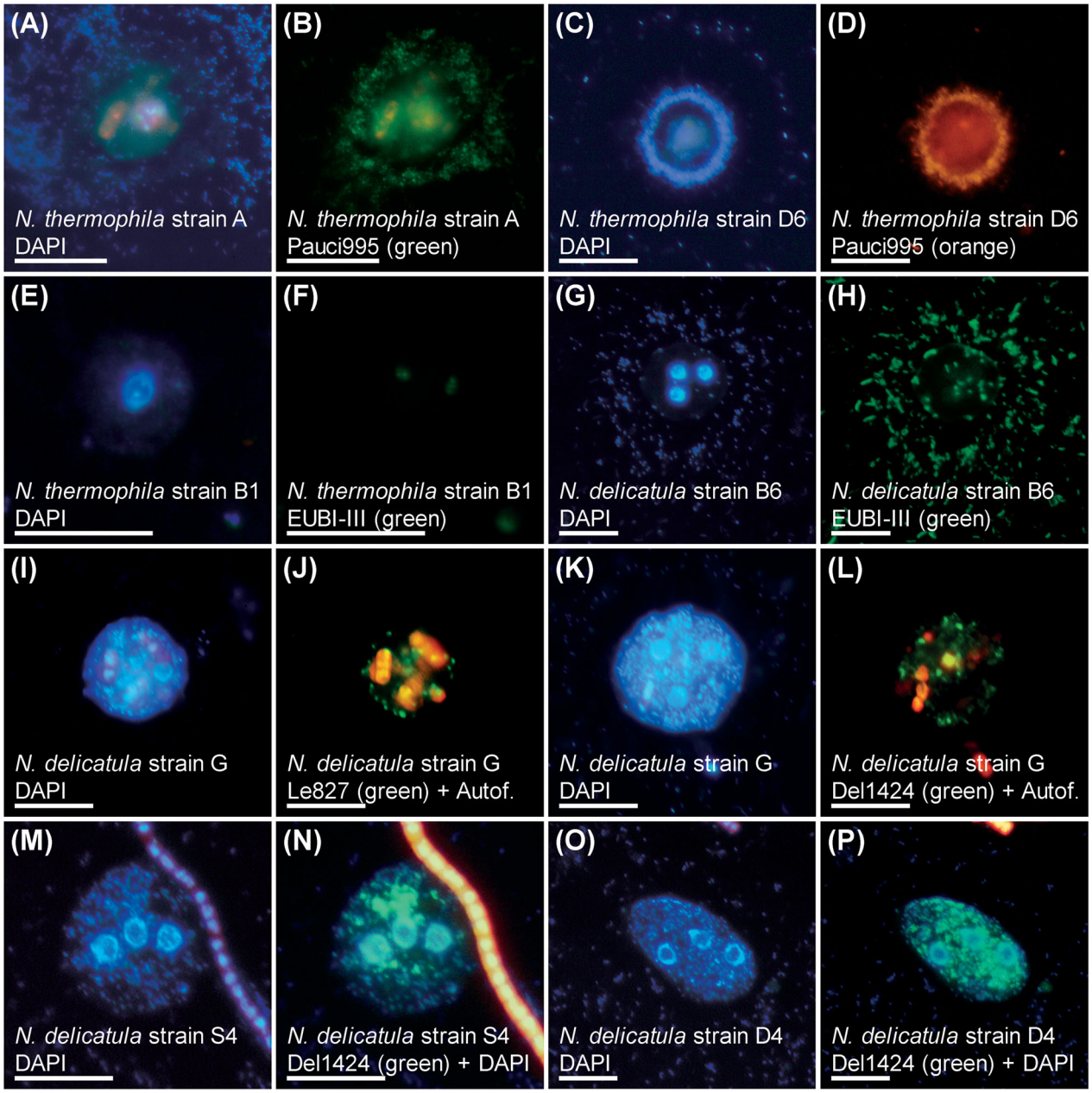

Figure 3. CARD-FISH of bacterial symbionts associated with (**A–F**) *N. thermophila* and (**G–P**) *N. delicatula* isolates. For abbreviations of applied oligonucleotide probes, see Table 2. Different fluorophore-specific filter sets were used to image the cells after hybridization. The first two and the last two columns of each row represent always the same cell. (A) Cell with ingested *P. rubescens* filaments and accompanying bacteria after DAPI staining. (**B**) Ectosymbiotic bacteria hybridized with the probe Pauci995. (**C**) Cell with well-preserved glycocalyx. Ectosymbionts are still arranged close to the cell surface. (**D**) The probe Pauci995 hybridized with ectosymbionts. (**E**) The nucleariid cell stained with DAPI. (F) No endosymbionts detected with the probe EUBI-III. (G) Three nuclei and ectosymbionts observed after DAPI staining. (**H**) No endosymbionts were detected with the probe EUBI-III. (**I**) Nuclei, endosymbionts and ingested *P. rubescens* filaments after DAPI staining. (**J**) Merged picture of the CARD-FISH signal and the autofluorescence. A small part of the endosymbionts are hybridized with the probe Le827. (**K**) Individual with three nuclei, endo- and ectosymbiotic bacteria after DAPI staining. (**L**) Merged picture of the CARD-FISH signal and the autofluorescence. The main part of endosymbionts hybridized with the probe Del1424. (**M**) Nucleariid cell with three nuclei and endosymbionts attached to a *P. rubescens* filament. (**N**) Merged picture of the CARD-FISH and the DAPI signal. One part of the endosymbiotic bacteria is hybridized with the probe Del1424. (**O**) Individual with three nuclei, endosymbionts and accompanying bacteria after DAPI staining. (**P**) Merged picture of the CARD-FISH and the DAPI signal. The major part of endosymbionts are hybridized with the probe Del1424. Scale bars represent 20 μm.

P. toxinivorans (Rapala *et al.* 2005) and designed the specific CARD-FISH probe 'Pauci995' (Table 2). Within the *N. thermophila* cluster, only strain A of our new isolates was also associated with ectosymbiotic bacteria right after isolation (Fig. 2A). Unfortunately during cultivation, these bacteria got lost (Fig. 2B) before CARD-FISH filters could be prepared. Although cells were surrounded by a glycocalyx, no ectosymbionts were observed for strain D6 (Fig. 2C; Fig. S1C, Supporting Information) and strain B1 (Fig. 2D). Since the ectosymbiont of strain N (*P. toxinivorans* strain SD41) was available as pure culture, we checked if the other strains could be infected with these bacteria. When we added an aliquot (1 ml) of a pure bacterial culture to the medium of ectosymbiont-free isolates, we observed a colonization of strains A and D6 (Fig. 3A–D). Surprisingly, this was not the case for strain B1. This

experiment indicated a highly specific interaction of *P. toxinivorans* strain SD41 with only one phylotype of the *N. thermophila* cluster (strain D6, A and N; see Fig. 1A). The fact that the ectosymbiont did not colonize the glycocalyx of the close relative strain B1 points to a distinct contribution of the host to this symbiosis.

The importance of a glycocalyx has been most extensively investigated for epithelial cells of the gastrointestinal tract (Moran, Gupta and Joshi 2011). The composition of glycoproteins produced by the host determines the physical (e.g. viscosity) and chemical (e.g. site for bacterial adhesion) nature of this extracellular structure and thus the interaction with bacteria. On the other hand, the composition of the glycocalyx can be modulated by bacteria in distinct ways (Hooper and Gordon 2001). This suggests a cross-talk between host and bacteria mediated by the glycocalyx. Furthermore, in the early branching metazoan *Hydra*, receptors, species-specific antimicrobial peptides (Bosch 2014) and even viruses (Bosch, Grasis and Lachnit 2015) have been shown to be main factors shaping the ectosymbiotic bacterial community. Unfortunately, the molecular interactions between the *N. thermophila* strains and *P. toxinivorans* are yet not studied.

Nuclearia thermophila isolates and their endosymbionts

In the *N. thermophila* cluster, three (A, D6 and N) out of four isolates harboured the gammaproteobacterial endosymbiont *Ca.* Endonucleariobacter rarus (Fig. 4A–H and Dirren *et al.* 2014). Hybridization with the specific probe CoNuc67 (Table 2) resulted in positive signals from all bacteria in strains A and D6 (Fig. 4C, G–H). In contrast, endosymbionts were missing in strain B1 (Fig. 3E and F) which additionally had a slightly divergent 18S rRNA gene sequence (Fig. 1A).

Interestingly, 18S rRNA gene sequences of strains D6, A and N were identical, but 16S rRNA gene sequences of their endosymbiont *Ca.* Endonucleariobacter rarus were slightly different. Endosymbionts of strains D6 and A formed a sister group to bacteria of strain N (Fig. 5A), although strains A and N were isolated from the same lake, and strain D6 from a 25 km distant lake.

Nuclearia delicatula isolates and their ectosymbionts

Four of our *N. delicatula* strains (D, G, S4 and D4) had both ectosymbionts (Figs 2E–I and 4Q–T) and endosymbionts (Figs 3I–P and 4I–P). Strain B6 was only associated with ectosymbionts (Figs 2J and 3G–H). Based on the 16S rRNA gene clone library of strain G (Fig. S3A, Supporting Information), three specific oligonucleotide probes were designed: Bu154, Le827 and Del1424 (Table 2). Ectosymbionts of strain G could be hybridized with the betaproteobacterial probe Bu154 (Fig. 4Q–T). The closest described relative (98.6% sequence similarity) to the cluster covered by this probe was *Inhella inkyongensis* (Song *et al.* 2009). Phylogeny of nucleariid's ectosymbionts (Fig. 5B) highlights that these ectosymbiotic bacteria are related (95.5% sequence similarity) to the earlier identified ectosymbiont of *N. thermophila* strain N (*P. toxinivorans*). *Inhella* sp. and *P. toxinivorans* have both sequence divergences to the bacteriochlorophyll *a* containing bacteria *Roseateles* (Suyama *et al.* 1999) and *Rubrivivax* (Willems, Gillis and De Ley 1991) of ~4% and ~5%, respectively. They form a metabolically diverse group sometimes referred to as '*Sphaerotilus-Leptothrix* group' (Spring 2006; Song *et al.* 2009) inside the family Comamonadaceae. As far as we know, a symbiotic live style has not been reported for any representative of this group.

Nucleariid amoebae are conspicuous concerning their nutrition: they can feed on harmful filamentous cyanobacteria, without being affected by toxic secondary metabolites (Dirren *et al.* 2014). In the previous study, we showed that *P. toxinivorans* was able to degrade microcystins, the cyanobacterial toxins stored in food organisms. In the case of *Inhella* sp., we have yet no proof for any similar metabolic capability. However, the spatial proximity to the host's cell surface suggests an exchange of metabolites between the symbiotic partners.

Nuclearia delicatula isolates and their endosymbionts

The gammaproteobacterial probe Le827 and the deltaproteobacterial probe Del1424 gave positive CARD-FISH signals for intracellular bacteria of *N. delicatula* strain G and no signals from bacteria in the cultivation medium. Endosymbionts hybridized with probe Le827 specific for a cluster of gammaproteobacteria were evenly distributed and represented a small part of total bacteria inside the cells (Figs 3I–J and 4P). Because of the homogenous distribution and their estimated abundance by CARD-FISH, we could assign this phylotype to distinct morphological features (morphotype 1) observed on TEM pictures (Fig. 6A and B). Bacteria had two membranes of a typical Gram-negative cell wall and an electron dense spot inside cells (Fig. 6C and D). They were localized in the cytoplasm and mostly surrounded by an electron translucent halo but never by an additional membrane. Some intracellular bacteria observed in *N. radians* display remarkable morphological similarities to bacteria in *N. delicatula* strain G (see Plate 4c from Cann and Page 1979). No described relatives of our endosymbiotic bacteria could be found in public databases. Apart from some sequences of uncultured gammaproteobacteria (highest sequence similarity 94.3%), the closest relatives were *Candidatus* Berkiella aquae (88.5% sequence similarity) and *Candidatus* Berkiella cookevillensis (88.1% sequence similarity) (Fig. 5C). These bacteria were found after infection inside the nucleus of *Acanthamoeba polyphaga* (Mehari *et al.* 2016). We never detected bacteria inside the nuclear membrane of strain G and endosymbionts differed morphologically from the recently characterized symbionts (Mehari *et al.* 2016, e.g. no electron dense spot). The 16S rRNA gene sequences of these symbiotic bacteria and strain G's endosymbiont are too much diverged to resolve their phylogenetic relationship based solely on this marker gene. Thus, corresponding branches had to be collapsed (low support values) in the phylogenetic tree (Fig. 5C). We propose the taxonomic status '*Candidatus* Ovatusbacter abovo' for the endosymbiont of *N. delicatula* strain G.

Double hybridization with the gammaproteobacterial probe Le827 and the deltaproteobacterial probe Del1424 showed different endosymbionts in strain G being hybridized (Fig. 4P). In contrast to the even distribution and low frequency of bacteria labelled with Le827, endosymbionts hybridized with Del1424 showed a lumped occurrence and were highly abundant (Figs 3K–L and 4P). These characteristics corresponded to the other prominent morphological phenotype (morphotype 2) seen on TEM pictures (Fig. 6A and B). Cells had again a typical Gram-negative cell wall structure (Fig. 6E and F) but in contrast to '*Candidatus* Ovatusbacter abovo' they were always surrounded by an additional host-derived membrane. Small vacuole-like structures harboured single cells (Fig. 6G and H) or multiple bacteria of morphotype 2 (Fig. 6E and F). We even detected these endosymbionts inside food vacuoles, often attached to the membrane of the vacuole, together with remnants of the food organism *P. rubescens* (Fig. 6B, G and H). In contrast to cyanobacterial cells, endosymbiotic bacteria seemed to be resistant to

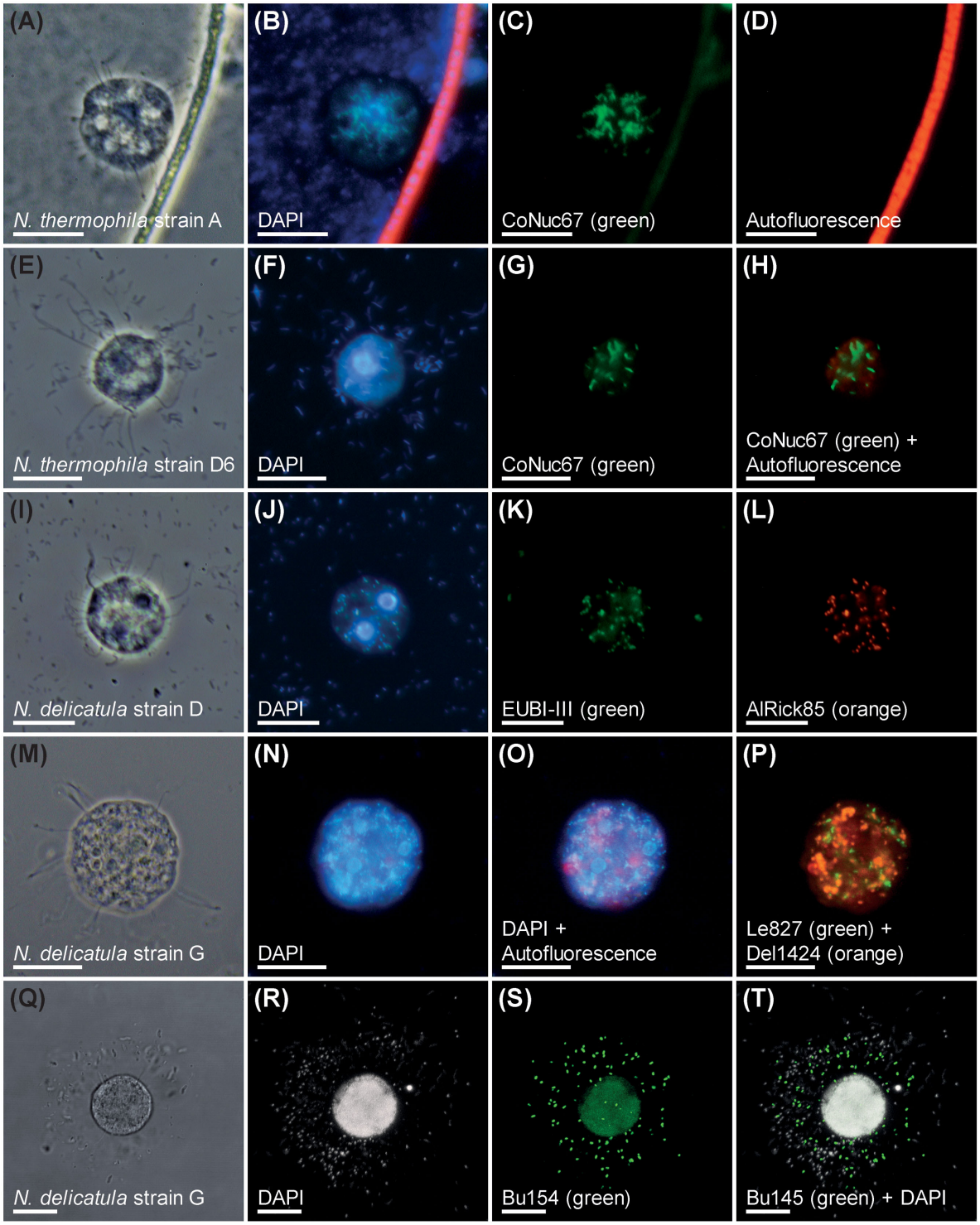

Figure 4. CARD-FISH preparations of (**A**–**H**) *N. thermophila* and (**I**–**T**) *N. delicatula* isolates embedded in (A–P) gelatine and (**Q**–**T**) agarose. Single nucleariid cells of different isolates are shown after hybridization. For abbreviations of applied oligonucleotide probes, see Table 2. Always the same cell is depicted in one row. Light microscopical pictures are placed in the first column; further columns represent epifluorescence images taken with fluorophore-specific filter sets. Pictures (Q–T) were recorded with a confocal laser scanning microscope. (A) Nucleariid cell next to a *P. rubescens* filament. (**B**) Endosymbiotic and accompanying bacteria after DAPI staining. (**C**) All endosymbionts hybridized with the probe CoNuc67. (**D**) Strong autofluorescence of the phototrophic cyanobacterium *P. rubescens*. (**E**) Cell with radiating filopodia. (**F**) Nucleus and bacteria stained with DAPI. (**G**) Hybridization of all endosymbionts with the probe CoNuc67. (**H**) Merged picture of autofluorescence (originating from ingested *P. rubescens*) and the CARD-FISH signal. (**I**) Nucleariid cell with two nuclei. (**J**) Endosymbionts visible after DAPI staining. (**K**) The oligonucleotide probe EUBI-III hybridized with endosymbionts and bacteria in the cultivation medium. (**L**) All endosymbionts hybridized specifically with the probe AlRick85. (**M**) Spherical cell with radiating filopodia. (**N**) Three nuclei and bacterial endosymbionts stained with DAPI. (**O**) Merged picture of autofluorescence (*P. rubescens* in food vacuoles) and DAPI. (**P**) Double hybridization with the two probes Le827 (few scattered bacteria) and Del1424 (many bacteria and lumped distribution). (**Q**) Spherical *Nuclearia* cell embedded in agarose. (**R**) Bacteria surrounding the cell stained with DAPI. (**S**) Ectosymbiotic bacteria hybridized with the probe Bu154. (**T**) Merged pictures of hybridized and DAPI-stained organisms. Scale bars represent 20 μm.

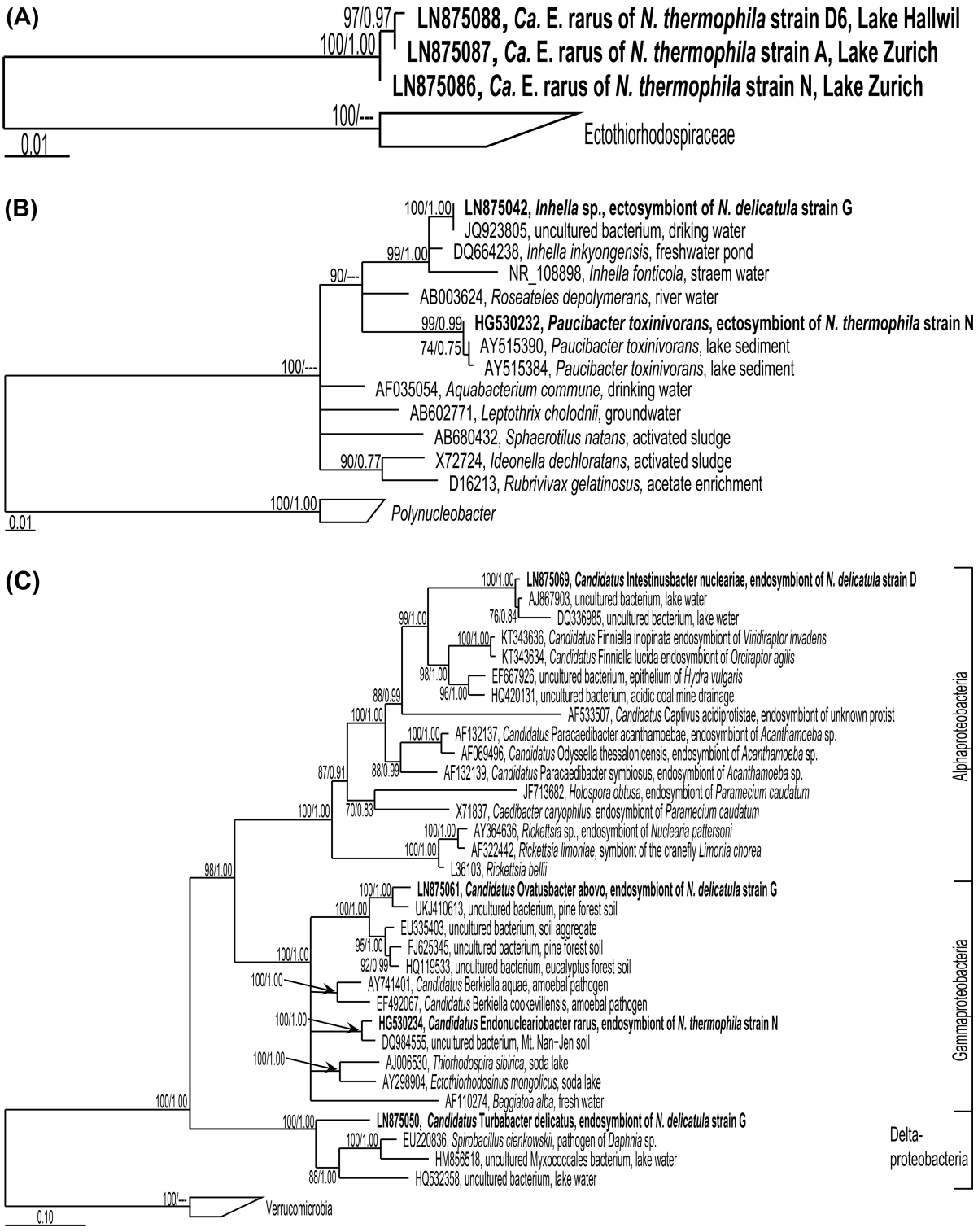

Figure 5. Phylogenetic analyses of (**A**) *Candidatus* Endonucleariobacter rarus, (**B**) ectosymbionts and (**C**) endosymbionts based on their 16S rRNA genes. Symbionts of *Nuclearia* spp. are shown in bold. ML trees with posterior probabilities from BI; ML Bootstrap value/BI probability. Branches with bootstrap values ≤60 were collapsed. Scale bars: numbers of substitutions per site. Ectothiorhodospiraceae, *Polynucleobacter* and Verrucomicrobia were used as outgroups, respectively.

digestion. This observation in combination with the fact that the deltaproteobacterial probe Del1424 did not hybridize with bacteria in the cultivation medium speaks against a possible role of these intracellular bacteria as food.

Usually bacterial pathogens are taken up by phagocytosis and then either prevent the fusion of lysosomes (e.g. *Legionella pneumophila*; Roy and Kagan 2000) or escape the phagosomes (e.g. *Rickettsia prowazekii*; Whitworth *et al.* 2005). Because of the facts that cyanobacterial cells were digested in food vacuoles and endosymbionts were never seen freely in the cytoplasm, there is no indication for any of these two strategies. TEM pictures of *A. castellanii* infected with the pathogenic symbiont

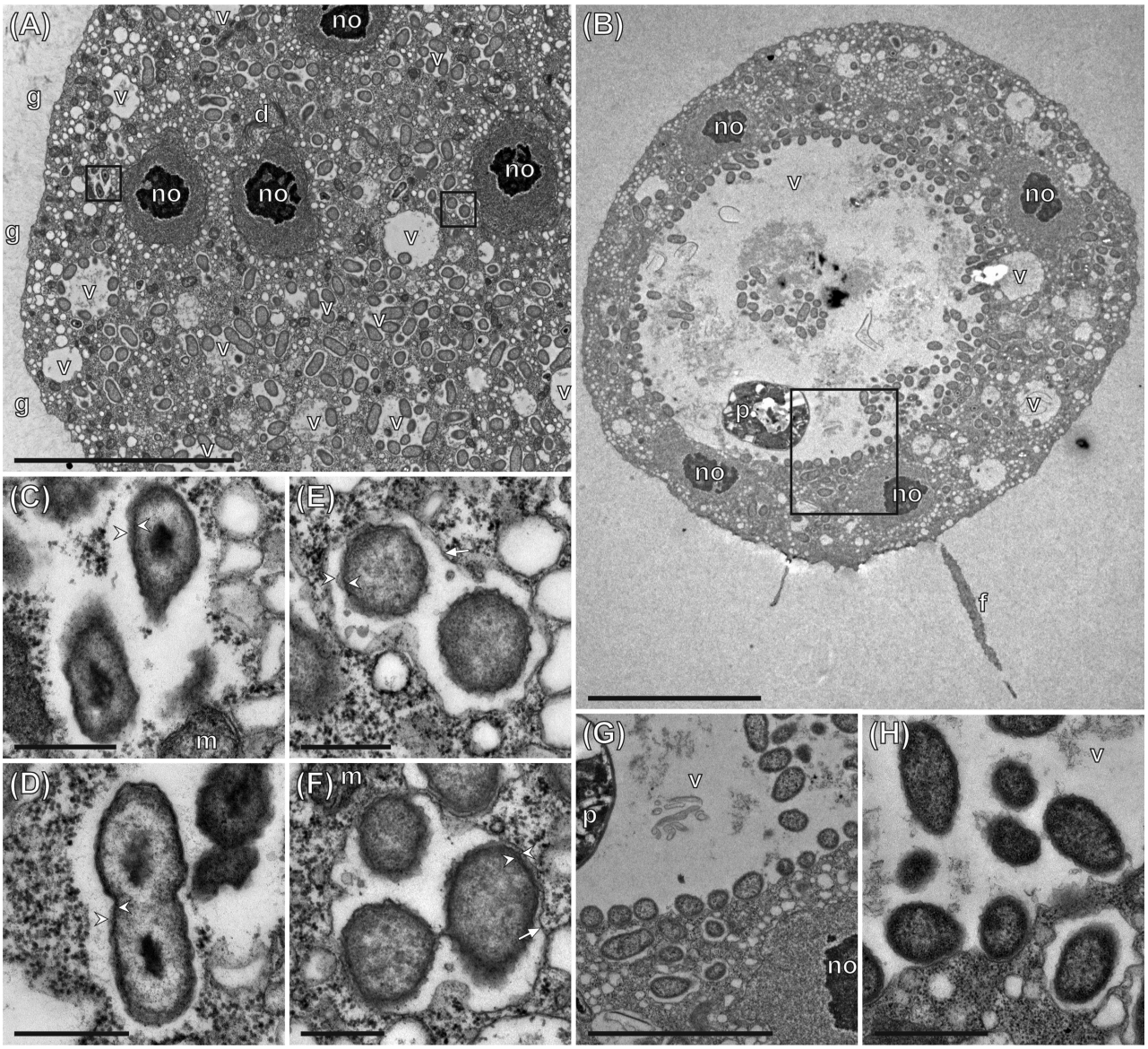

Figure 6. TEM images of *N. delicatula* strain G. (**A** and **B**) Overview of two different nucleariid cells displaying nuclei with their nucleoli (no) and numerous bacteria inside their cytoplasm. Magnifications of squares are shown in (**C**), (**E**) and (**G**), respectively. Two morphotypes of endosymbiotic bacteria can be distinguished. The less abundant morphotype 1 can be found freely inside the cytoplasm, whereas the prominent morphotype 2 is present in vacuole-like structures (v). (C) Two bacteria and (**D**) a dividing individual of morphotype 1 inside the nucleariid cell. A characteristic central electron-dense spot and a typical Gram-negative cell wall structure with two membranes (arrowheads) are visible. No peribacterial membrane is present, but an electron translucent halo surrounds the cell. (E and **F**) Cells having the characteristics of morphotype 2 are tightly packed inside a peribacterial membrane (arrow). The Gram-negative cell wall organization with two membranes (arrowheads) is visible. The cell content of this endosymbiont has a homogenous appearance on TEM pictures. (G) In the big central food vacuole (see overview B), an intact *P. rubescens* filament (p) and remnants of digested cyanobacteria can be seen. In addition to the food organism, bacteria of the morphotype 2 are present inside the food vacuoles (v). Many bacteria seem to be attached to the membrane. Additionally, single or few cells of this morphotype are enclosed in membranes apparently not connected to the food vacuole. (**H**) Higher magnification of the interface between food vacuole and cytoplasm. Bacteria of the morphotype 2 are attached to the membrane sometimes forming cavities. Bacteria seem to be intact and not digested. d, dictyosome; f, filopodium; g, glycocalyx; m, mitochondrion; no, nucleolus; p, *P. rubescens* filament; v, vacuole-like structures. Scale bars represent 10 μm in (A and B), 4 μm in (G), 1 μm in (H) and 500 nm in (C–F).

'*Candidatus* Jidaibacter acanthamoeba' (fig. 1 in Schulz *et al.* 2015) resemble conspicuously our observations of the frequent endosymbiont. In contrast to this accordance, types of the symbioses seem to differ. The regular exponential growth of the host *N. delicatula* speaks against a severe pathogenic nature of its endosymbiotic bacteria. Again, no close relatives of this endosymbiont belonging to the deltaproteobacteria were found in public databases. The closest relative (89.8% sequence similarity) was a pathogenic bacterium of daphnids named *Spirobacillus cienkowskii* (Rodrigues *et al.* 2008). None of the sequences included in the phylogenetic tree (Fig. 5C) clustered together with this endosymbiont of strain G. Thus, we propose the taxonomic status '*Candidatus* Turbabacter delicatus' for these bacteria. Specific hybridization with the deltaproteobacterial probe Del1424 showed that the endosymbiont was also present in cells of strains S4 and D4 (Fig. 3M–P). Like in strain G, not all of the intracellular bacteria were labelled. In contrast to the positive hybridization with the gammaproteobacterial probe Le827 with the other part of endosymbionts in strain G, no signal was obtained for strains S4 and D4. Most probably, these strains

additionally harboured other so far unidentified endosymbiotic bacteria.

The specific alphaproteobacterial probe AlRick85 was designed based on a cluster of sequences in the 16S rRNA gene clone library of *N. delicatula* strain D (Fig. S3B, Supporting Information). AlRick85 hybridized specifically with all endosymbiotic bacteria of this isolate (Fig. 4I–L). In public databases, no closely related sequences were found except for some uncultured bacteria. The closest characterized relatives were *Candidatus* Finniella inopinata (89.1% sequence similarity) and *Candidatus* Finniella lucida (88.4% sequence similarity) which are rickettsial endosymbionts of viridiraptorid amoeboflagellates (Fig. 5C). Sequences of the alphaproteobacterial endosymbiont of strain D affiliated with the recently established family *Candidatus* Paracaedibacteraceae (Hess, Suthaus and Melkonian 2016). This family is formed by endosymbionts of different protists. So far they were found in Rhizaria, Excavata and Amoebozoa. Here we report for the first time a representative of this family inside an opisthokont protist. TEM pictures proved that only one bacterial morphotype was found in the cytoplasm (Fig. 7A): Gram-negative bacterial cells with invaginated cell walls which were surrounded by an electron translucent halo (Fig. 7B and C). No additional host-derived membrane or electron-dense layer (which was observed for the endosymbionts of the viridiraptorid amoeboflagellates) was detected for this endosymbiont. The observed features were consistent with the descriptions for the members of the family *Candidatus* Paracaedibacteraceae. Because of a distinct phylogenetic clustering, several morphological differences and a new host habitat, we propose the provisional name '*Candidatus* Intestinusbacter nucleariae' for these endosymbiotic bacteria.

Description of '*Candidatus* Ovatusbacter abovo' (Gammaproteobacteria)

Etymology: L. masc. adj. *ovatus*, egg-shaped; N.L. masc. n. *bacter*, a rod; N.L. masc. n. *Ovatusbacter*, egg-shaped bacterium, inspired by the appearance on cross-sections (TEM), when cells looked like fried eggs. L. prefix. *ab*, from; L. nt. dat. sing. n. *ovo* of *ovum*, egg; L. *abovo* (*ab ovo*) mythological allusion to one of the two eggs of Leda which was the primary cause of the Trojan War; expression used to indicate an ancient origin.

Rod-shaped bacterium up to 1 μm in length (mean length: 0.65 μm and mean width: 0.34 μm; $n = 30$) with a typical Gram-negative cell wall structure and a characteristic central electron-dense spot observed by TEM. Basis of assignment: 16S rRNA gene sequence (accession number: LN875061) and positive signal with the specific CARD-FISH probe Le827 (5′-CCCTAAGGCTTCCAACAGCC-3′). So far only detected in the cytoplasm of *N. delicatula* strain G (accession number: LN875119), isolated from Lake Zurich (47°19′11.5″N, 8°33′10.1″E), Switzerland. Typically 50–200 cells could be observed inside this nucleariid host. Uncultured so far.

Description of '*Candidatus* Turbabacter delicatus' (Deltaproteobacteria)

Etymology: L. fem. n. *turba*, noisiness, swarm, mass; N.L. masc. n. *bacter*, a rod; N.L. masc. n. *Turbabacter,* rod-shaped bacterium appearing in masses. L. masc. adj. *delicatus*, spoilt, delicate, referring to the host species *N. delicatula* and to its lifestyle in a protected nutrient-rich niche.

Rod-shaped Gram-negative bacterium up to 1.69 μm in length (mean length: 1 μm and mean width: 0.48 μm; $n = 30$).

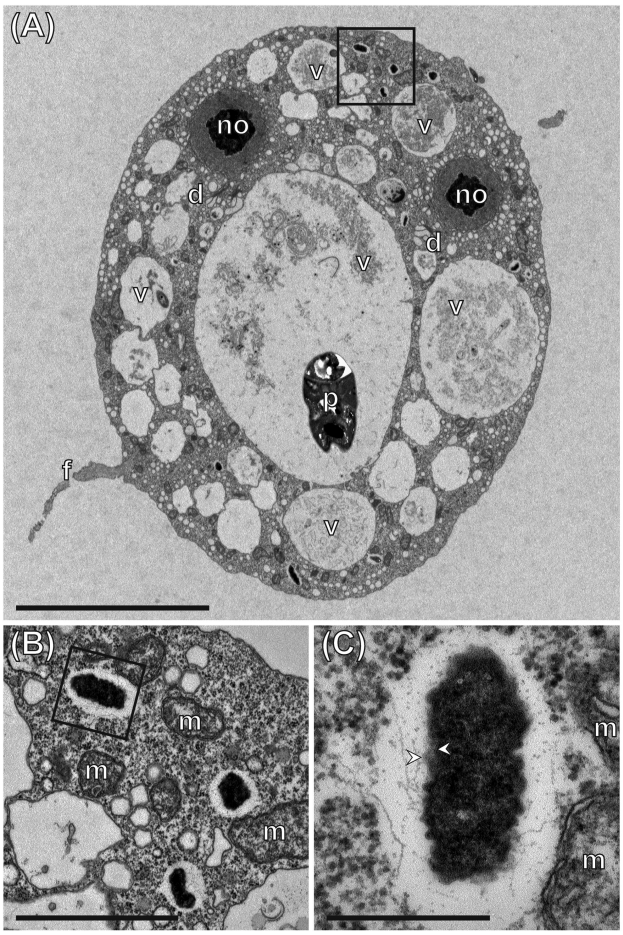

Figure 7. TEM images of *N. delicatula* strain D. (**A**) Overview showing the highly vacuolated (v) nucleariid cell with two prominent nucleoli (no) and a filopodium (f). Inside the big central food vacuole, a *P. rubescens* filament (p) and remnants of already digested cyanobacterial cells are visible. Only one morphotype of endosymbionts with homogenous electron-dense cell content is present. (**B**) Higher magnification of three endosymbionts (square in A). Bacteria are located freely in the cytoplasm surrounded by a pronounced electron-translucent halo. (**C**) Higher magnification of one bacterial cell (square in B). No peribacterial membrane but two membranes (arrowheads) of the Gram-negative cell wall are visible. d, dictyosome; f, filopodium; m, mitochondrion; no, nucleolus; p, *P. rubescens* filament; v, vacuole-like structures. Scale bars represent 10 μm in (A), 2 μm in (B) and 500 nm in (C).

Cells are found inside vacuole-like structures and food vacuoles (often attached to the membrane) but never freely in the cytoplasm. Basis of assignment: 16S rRNA gene sequence (accession number: LN875050) and positive signal with the specific CARD-FISH probe Del1424 (5′-GCTCACGCGCTTCTGGCTTATAC-3′). Up to now detected in three different *N. delicatula* isolates: strain G, strain S4 and strain D4 (accession numbers: LN875119, LN875117 and LN875116). Usually several hundreds of individuals were observed inside the host species which were isolated from two Swiss Lakes: Lake Zurich (47°19′11.5″N, 8°33′10.1″E) and Lake Sempach (47°08′15.8″N, 8°08′25.8″E). Uncultured so far.

Description of '*Candidatus* Intestinusbacter nucleariae' (Rickettsiales, Alphaproteobacteria)

Etymology: L. masc. adj. *intestinus*, internal; N.L. masc. n. *bacter*, a rod; N.L. masc. n. *Intestinusbacter*, rod-shaped bacterium

living internal (inside eukaryotic cells). N.L. fem. gen. sing. n. *nucleariae* from *Nuclearia*, taxonomic name of the single genus *Nuclearia* within the family Nucleariidae, indicating the affiliation of the host.

Rod-shaped bacterium up to 1.1 μm in length (mean length: 0.71 μm and mean width: 0.29 μm; $n = 18$) with Gram-negative invaginated cell wall organization and translucent halo (on conventional TEM pictures). Basis of assignment: 16S rRNA gene sequence (accession number: LN875069) and positive signal with the specific CARD-FISH probe AlRick85 (5′-CGTCTGCCACTAACATATGTGAGCT-3′). So far only detected in the cytoplasm of *N. delicatula* strain D (accession number: LN875118), isolated from Lake Zurich (47°19′11.5″N, 8°33′10.1″E), Switzerland. Uncultured so far.

SUPPLEMENTARY DATA

Supplementary data are available at FEMSEC online.

ACKNOWLEDGEMENTS

We thank Jakob Pernthaler (University of Zurich), Gianna Pitsch (University of Zurich) and Sebastian Hess (Dalhousie University) for fruitful discussions and Marvin Moosmann for the help with the isolation of amoebae. TEM imaging was performed with equipment and support of the Centre for Microscopy, University of Zurich.

FUNDING

This study was financed by the Swiss National Science Foundation (SNF 31003A_138473 and SNF 31003A_159842).

Conflict of interest. None declared.

REFERENCES

Alegado RA, King N. Bacterial influences on animal origins. *Cold Spring Harb Perspect Biol* 2014;**6**:a016162.

Artari A. Morphologische und biologische Studien über *Nuclearia delicatula* Cienk. *Zool Anz* 1889;**12**:408–16

Ashelford KE, Chuzhanova NA, Fry JC *et al.* At least 1 in 20 16S rRNA sequence records currently held in public repositories is estimated to contain substantial anomalies. *Appl Environ Microb* 2005;**71**:7724–36.

Bosch TC. Rethinking the role of immunity: lessons from *Hydra*. *Trends Immunol* 2014;**35**:495–502.

Bosch TC, Grasis J, Lachnit T. Microbial ecology in *Hydra*: Why viruses matter. *J Microbiol* 2015;**53**:193–200.

Buckley DH, Schmidt TM. Environmental factors influencing the distribution of rRNA from Verrucomicrobia in soil. *FEMS Microbiol Ecol* 2001;**35**:105–12.

Cann JP. The feeding behavior and structure of *Nuclearia delicatula* (Filosea: Aconchulinida). *J Protozool* 1986;**33**:392–6.

Cann JP, Page FC. *Nucleosphaerium tuckeri* nov. gen. nov. sp.- A new freshwater filose amoeba without motile form in a new family Nucleariidae (Filosea: Aconchulinida) feeding by ingestion only. *Arch Protistenk* 1979;**122**:226–40.

Casadevall A. Evolution of intracellular pathogens. *Annu Rev Microbiol* 2008;**62**:19–33.

Daims H, Bruhl A, Amann R *et al.* The domain-specific probe EUB338 is insufficient for the detection of all Bacteria: development and evaluation of a more comprehensive probe set. *Syst Appl Microbiol* 1999;**22**:434–44.

De Rijk P, Neefs J-M, Van De Peer Y *et al.* Compilation of small ribosomal subunit RNA sequences. *Nucleic Acid Res* 1992;**20**:2075–89.

Dirren S, Salcher MM, Blom JF *et al.* Ménage-à-trois: The amoeba *Nuclearia* sp. from Lake Zurich with its ecto- and endosymbiotic bacteria. *Protist* 2014;**165**:745–58.

Dykova I, Veverkova M, Fiala I *et al.* *Nuclearia pattersoni* sp. n. (Filosea), a new species of amphizoic amoeba isolated from gills of roach (*Rutilus rutilus*), and its rickettsial endosymbiont. *Folia Parasitol* 2003;**50**:161–70.

Franzenburg S, Walter J, Künzel S *et al.* Distinct antimicrobial peptide expression determines host species-specific bacterial associations. *P Natl Acad Sci USA* 2013;**110**:E3730–8.

Fraune S, Anton-Erxleben F, Augustin R *et al.* Bacteria-bacteria interactions within the microbiota of the ancestral metazoan *Hydra* contribute to fungal resistance. *ISME J* 2015;**9**:1543–56.

Fraune S, Bosch TC. Long-term maintenance of species-specific bacterial microbiota in the basal metazoan *Hydra*. *P Natl Acad Sci USA* 2007;**104**:13146–51.

Freeman MF, Gurgui C, Helf MJ *et al.* Metagenome mining reveals polytheonamides as posttranslationally modified ribosomal peptides. *Science* 2012;**338**:387–90.

Fritsche TR, Gautom RK, Seyedirashti S *et al.* Occurrence of bacterial endosymbionts in *Acanthamoeba* spp. isolated from corneal and environmental specimens and contact lenses. *J Clin Microbiol* 1993;**31**:1122–6.

Gast RJ, Sanders RW, Caron DA. Ecological strategies of protists and their symbiotic relationships with prokaryotic microbes. *Trends Microbiol* 2009;**17**:563–9.

Hess S, Suthaus A, Melkonian M. '*Candidatus* Finniella' (Rickettsiales, Alphaproteobacteria), novel endosymbionts of viridiraptorid amoeboflagellates (Cercozoa, Rhizaria). *Appl Environ Microb* 2016;**82**:659–70.

Hooper LV, Gordon JI. Glycans as legislators of host–microbial interactions: spanning the spectrum from symbiosis to pathogenicity. *Glycobiology* 2001;**11**:1R–10R.

Horn M. Chlamydiae as symbionts in eukaryotes. *Annu Rev Microbiol* 2008;**62**:113–31.

Horn M, Fritsche TR, Gautom RK *et al.* Novel bacterial endosymbionts of *Acanthamoeba* spp. related to the *Paramecium caudatum* symbiont *Caedibacter caryophilus*. *Environ Microbiol* 1999;**1**:357–67.

Huttenhower C, Gevers D, Knight R *et al.* Structure, function and diversity of the healthy human microbiome. *Nature* 2012;**486**:207–14.

Katoh K, Standley DM. MAFFT multiple sequence alignment software version 7: improvements in performance and usability. *Mol Biol Evol* 2013;**30**:772–80.

Kiers ET, West SA. Evolving new organisms via symbiosis. *Science* 2015;**348**:392–4.

Kikuchi Y, Hayatsu M, Hosokawa T *et al.* Symbiont-mediated insecticide resistance. *P Natl Acad Sci USA* 2012;**109**:8618–22.

Lema KA, Bourne DG, Willis BL. Onset and establishment of diazotrophs and other bacterial associates in the early life history stages of the coral *Acropora millepora*. *Mol Ecol* 2014;**23**:4682–95.

Levinson G, Gutman GA. Slipped-strand mispairing: a major mechanism for DNA sequence evolution. *Mol Biol Evol* 1987;**4**:203–21.

Liu Y, Steenkamp ET, Brinkmann H *et al.* Phylogenomic analyses predict sistergroup relationship of nucleariids and Fungi and paraphyly of zygomycetes with significant support. *BMC Evol Biol* 2009;**9**:272.

Lozupone CA, Stombaugh JI, Gordon JI *et al.* Diversity, stability and resilience of the human gut microbiota. *Nature* 2012;**489**:220–30.

Ludwig W, Strunk O, Westram R *et al.* ARB: a software environment for sequence data. *Nucleic Acid Res* 2004;**32**:1363–71.

McFall-Ngai M, Hadfield MG, Bosch TC *et al.* Animals in a bacterial world, a new imperative for the life sciences. *P Natl Acad Sci USA* 2013;**110**:3229–36.

Manz W, Amann R, Ludwig W *et al.* Phylogenetic oligodeoxynucleotide probes for the major subclasses of proteobacteria: problems and solutions. *Syst Appl Microbiol* 1992;**15**:593–600.

Manz W, Amann R, Ludwig W *et al.* Application of a suite of 16S rRNA-specific oligonucleotide probes designed to investigate bacteria of the phylum cytophaga-flavobacter-bacteroides in the natural environment. *Microbiol-UK* 1996;**142**:1097–106.

Mehari YT, Hayes BJ, Redding KS *et al.* Description of '*Candidatus* Berkiella aquae' and '*Candidatus* Berkiella cookevillensis', two intranuclear bacteria of freshwater amoebae. *Int J Syst Evol Micr* 2016;**66**:535–41.

Moon-van der Staay SY, De Wachter R, Vaulot D. Oceanic 18S rDNA sequences from picoplankton reveal unsuspected eukaryotic diversity. *Nature* 2001;**409**:607–10.

Moran AP, Gupta A, Joshi L. Sweet-talk: role of host glycosylation in bacterial pathogenesis of the gastrointestinal tract. *Gut* 2011;**60**:1412–25.

Muyzer G, Ramsing NB. Molecular methods to study the organization of microbial communities. *Water Sci Technol* 1995;**32**:1–9.

Nakayama T, Marin B, Kranz HD *et al.* The basal position of scaly green flagellates among the green algae (Chlorophyta) is revealed by analyses of nuclear-encoded SSU rRNA sequences. *Protist* 1998;**149**:367–80.

Neef A. Anwendung der In-situ-Einzelzell-Identifizierung von Bakterien zur Populationsanalyse in komplexen mikrobiellen Biozönosen. *Ph.D. Thesis*, Technische Universität München 1997.

Ouwerkerk JP, de Vos WM, Belzer C. Glycobiome: bacteria and mucus at the epithelial interface. *Best Pract Res Cl Ga* 2013;**27**:25–38.

Paracer S, Ahmadjian V. *Symbiosis: An Introduction to Biological Associations*. New York: Oxford University Press, 2000.

Patterson DJ. The genus *Nuclearia* (Sarcodina, Filosea): Species composition and characteristics of the taxa. *Arch Protistenk* 1984;**128**:127–39.

Pernin P. Study in vivo of an ameoba with pseudopodes filosa: *Nuclearia simplex* Cienkowski 1865 (Protozoa, Rhizopodea, Filosia, Aconchulinida). *Protistologica* 1976;**12**:555–62.

Pruesse E, Quast C, Knittel K *et al.* SILVA: a comprehensive online resource for quality checked and aligned ribosomal RNA sequence data compatible with ARB. *Nucleic Acid Res* 2007;**35**:7188–96.

Rapala J, Berg KA, Lyra C *et al.* *Paucibacter toxinivorans* gen. nov., sp nov., a bacterium that degrades cyclic cyanobacterial hepatotoxins microcystins and nodularin. *Int J Syst Evol Microbiol* 2005;**55**:1563–8.

Rodrigues JLM, Duffy MA, Tessier AJ *et al.* Phylogenetic characterization and prevalence of '*Spirobacillus cienkowskii*,' a red-pigmented, spiral-shaped bacterial pathogen of freshwater *Daphnia* species. *Appl Environ Microb* 2008;**74**:1575–82.

Rodríguez-Ezpeleta N, Brinkmann H, Burey SC *et al.* Monophyly of primary photosynthetic eukaryotes: green plants, red algae, and glaucophytes. *Curr Biol* 2005;**15**:1325–30.

Roller C, Wagner M, Amann R *et al.* *In situ* probing of gram-positive bacteria with high DNA G + C content using 23S rRNA targeted oligonucleotides. *Microbiol-UK* 1994;**140**:2849–58.

Roy CR, Kagan JC. *Evasion of Phagosome Lysosome Fusion and Establishment of a Replicative Organelle by the Intracellular Pathogen Legionella Pneumophila*. Austin: Landes Bioscience, 2000.

Schulz F, Martijn J, Wascher F *et al.* A rickettsiales symbiont of amoebae with ancient features. *Environ Microbiol* 2015, DOI: 10.1111/1462-2920.12881.

Smith JM. Generating novelty by symbiosis. *Nature* 1989;**341**:284–5.

Song J, Oh HM, Lee JS *et al.* *Inhella inkyongensis* gen. nov., sp. nov., a new freshwater bacterium in the order Burkholderiales. *J Microbiol Biotechn* 2009;**19**:5–10.

Spring S. The genera Leptothrix and Sphaerotilus. In: Dworkin M, Falkow S, Rosenberg E *et al.* (eds.) *The Prokaryotes*. New York: Springer, 2006, 758–77.

Stamatakis A, Hoover P, Rougemont J. A rapid bootstrap algorithm for the RAxML web servers. *Syst Biol* 2008;**57**:758–71.

Steenkamp ET, Wright J, Baldauf SL. The protistan origins of animals and fungi. *Mol Biol Evol* 2006;**23**:93–106.

Suyama T, Shigematsu T, Takaichi S *et al.* *Roseateles depolymerans* gen. nov., sp. nov., a new bacteriochlorophyll a-containing obligate aerobe belonging to the beta-subclass of the Proteobacteria. *Int J Syst Bacteriol* 1999;**49**:449–57.

Thrash JC, Boyd A, Huggett MJ *et al.* Phylogenomic evidence for a common ancestor of mitochondria and the SAR11 clade. *Sci Rep* 2011;**1**:13, DOI: 10.1038/srep00013.

Wallner G, Amann R, Beisker W. Optimizing fluorescent *in situ* hybridization with rRNA-targeted oligonucleotide probes for flow cytometric identification of microorganisms. *Cytometry* 1993;**14**:136–43.

Walsby AE, Avery A, Schanz F. The critical pressures of gas vesicles in *Planktorhrix rubescens* in relation tothe depth of winter mixing in Lake Zurich, Switzerland. *J Plankton Res* 1998;**20**:1357–75.

Whitworth T, Popov VL, Yu X-J *et al.* Expression of the *Rickettsia prowazekii pld* or *tlyC* gene in *Salmonella enterica* serovar typhimurium mediates phagosomal escape. *Infect Immun* 2005;**73**:6668–73.

Willems A, Gillis M, De Ley J. Transfer of *Rhodocyclus gelatinosus* to *Rubrivivax gelatinosus* gen. nov., comb. nov., and phylogenetic relationships with *Leptothrix*, *Sphaerotilus natans*, *Pseudomonas saccharophila*, and *Alcaligenes latus*. *Int J Syst Evol Micr* 1991;**41**:65–73.

Wylezich C, Karpov SA, Mylnikov AP *et al.* Ecologically relevant choanoflagellates collected from hypoxic water masses of the Baltic Sea have untypical mitochondrial cristae. *BMC Microbiol* 2012;**12**:1–13.

Yilmaz LS, Parnerkar S, Noguera DR. mathFISH, a web tool that uses thermodynamics-based mathematical models for *in silico* evaluation of oligonucleotide probes for fluorescence *in situ* hybridization. *Appl Environ Microb* 2011;**77**:1118–22.

Yoshida M, Nakayama T, Inouye I. *Nuclearia thermophila* sp. nov. (Nucleariidae), a new nucleariid species isolated from Yunoko Lake in Nikko (Japan). *Europ J Protistol* 2009;**45**:147–55.

Zettler LAA, Nerad TA, O'Kelly CJ *et al.* The nucleariid amoebae: more protists at the animal-fungal boundary. *J Eukaryot Microbiol* 2001;**48**:293–7.

Supplementary Figure S1

Light microscopical pictures of 16 *Nuclearia* spp. isolates. (A) A syncytium originating from the fusion of cells contains multiple nuclei. (B) Eight cysts next to a *Planktothrix rubescens* (cyanobacteria) filament. (C) Elongated cell with an ingested *P. rubescens* filament. (D) Cyst having a 'perfect' spherical shape and a central nucleus. (E) Completely engulfed *P. rubescens* filament by a nucleariid cell. The organism formed two cell bodies which might lead to cell division. (F) Multinucleate cells sometimes show cell divisions which look like budding. Only a small part of the cell splits off. (G) Spherical individual with four visible nucleoli and radiating filopodia. Inside the cell an intact *P. rubescens* filament and remnants of already digested cyanobacteria can be seen. Ectosymbiotic bacteria are nicely arranged around the cell. (H) Club-shaped nucleariid cell with two ingested *P. rubescens* filaments (or possibly one filament which was bended). (I) Amoeboid cell with multiple nuclei. (J) Nucleariid cell which adapted an amoeboid form. The prominent nucleolus and multiple filopodia are visible. (K) Spherical cell with a large food-vacuole. Bacteria thriving in the cultivation medium are attached to the surface of the glycocalyx. (L) Syncytium with four nuclei and radiating filopodia. Spirochaete bacteria seem to be attracted by the amoeba but do not enter the glycocalyx. (M) Cyst with a thick cell wall. (N) Amoeboid organism with concentrated filopodia indicating the direction of locomotion. (O) Cyst with hardly visible nuclei and a thick cell wall. (P) Spherical cell (not a 'perfect' sphere) floating in the water column. (Q) A spherical shaped individual with radiating filopodia. (R) Amoeboid cell attached to the surface. A prominent nucleolus and thick, sometimes branched, filopodia can be seen. (S) Spherical individual with a hardly visible nucleolus. (T) Cell which adapted an amoeboid form. A completely ingested *P. rubescens* filament and the nucleolus can be detected. All pictures were taken with Differential Interference Contrast (DIC), except pictures (J) and (L), where phase contrast was applied. Scale bars indicate 20 µm.

Supplementary Figure S1

Supplementary Figure S2

Comparison of the nucleariid 18S rRNA genes. (A) Box plot of the pairwise distances (in %) of sequences from six 18S rRNA gene clone libraries (of six different isolates). Boxes: 25^{th} to 75^{th} percentiles; whiskers: 10^{th} to 90^{th}; crosses: 5^{th} and 95^{th} percentiles. (B) ML tree with posterior probabilities from BI; ML Bootstrap value / BI probability. All *N. delicatula* sequences from five different clone libraries, the sequence of *N. delicatula* (AF349563) and *N. simplex* (AF349566) / *N. moebiusi* (AF349565) as outgroup were used for phylogenetic reconstruction.

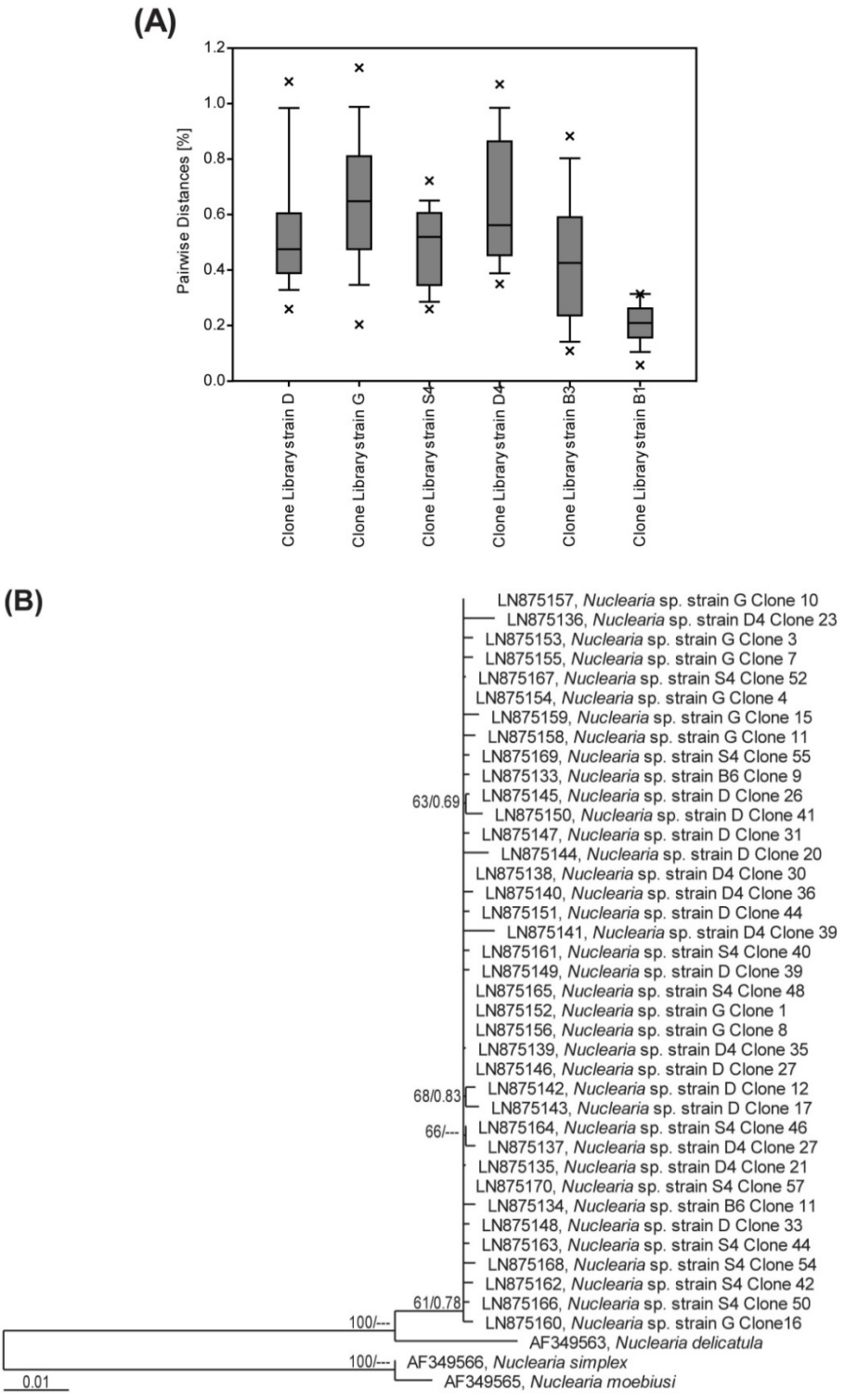

Supplementary Figure S2

Supplementary Figure S3

Phylogenetic analyses of two 16S rRNA clone libraries. ML trees with posterior probabilities from BI; ML Bootstrap value / BI probability. Branches with bootstrap values ≤ 50 were collapsed. Numbers in brackets represent the total number of partial sequences clustering with the respective group. Curly brackets represent the coverage of specific probes. Affiliations to higher taxonomic groups are indicated on the right side. Scale bar: number of nucleotide substitutions per site. (A) Phylogenetic tree of sequences from the clone library of the *N. delicatula* strain G culture and (B) of the *N. delicatula* strain D culture.

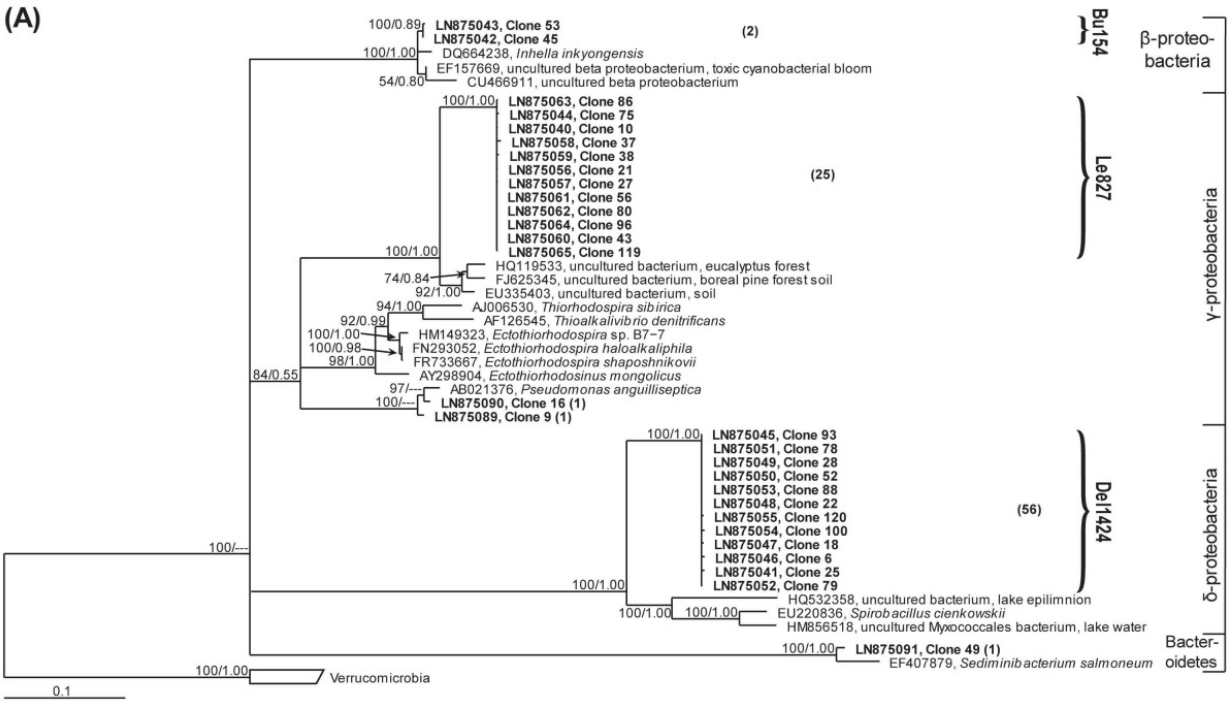

Supplementary Figure S3A

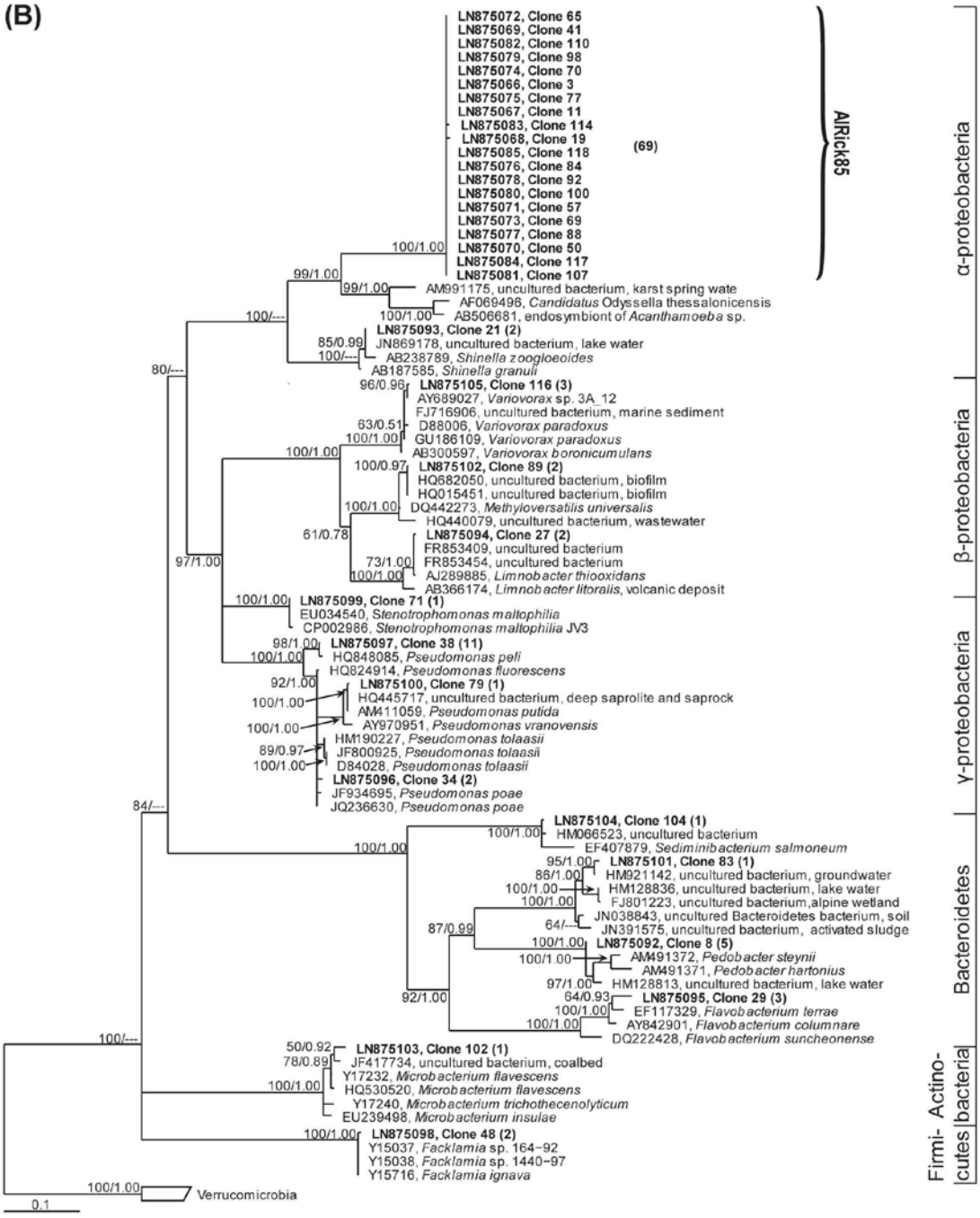

Supplementary Figure S3B

Article III

Dirren S, Pitsch G, Da Silva M & Posch T (in prep.) Feeding of *Nuclearia thermophila* and *Nuclearia delicatula* (Nucleariidae, Opisthokonta) on the toxic cyanobactetrium *Planktothrix rubescens*.

Grazing of *Nuclearia thermophila* and *Nuclearia delicatula* (Nucleariidae, Opisthokonta) on the toxic cyanobacterium *Planktothrix rubescens*

Sebastian Dirren, Gianna Pitsch, Marisa O. D. Silva and Thomas Posch[1]

Limnological Station, Department of Plant and Microbial Biology, University of Zurich, Seestrasse 187, CH-8802 Kilchberg, Switzerland

Running Title: Feeding behaviour of *Nuclearia* spp.

Number of pages (incl. references & figure legends):

Number of tables: 1

Number of figures: 5

Number of Supplementary Figures: ?

Intended as Research Article in 'European Journal of Protistology'

[1]Corresponding author:
Sebastian Dirren
Limnological Station, Department of Plant and Microbial Biology, University of Zurich
Seestrasse 187, CH-8802 Kilchberg, Switzerland
Phone: 0041 44 634 9214
Fax: 0041 44 634 9225
e-mail: s.dirren@limnol.uzh.ch

Abstract

During the last decades, the planktonic cyanobacterium *Planktothrix rubescens* became a dominant primary producer in many deep pre-alpine lakes. While altered physiochemical conditions due to lake warming (i.e. bottom up factors) seemed to favour this cyanobacterial species, its dominance is partly attributed to factors conferring grazing resistance (i.e. top down factors). The rigid structure of the cyanobacterial filaments and toxic secondary metabolites (e.g. microcystins) seem to protect against diverse grazers. Nonetheless, species of the protistan genus *Nuclearia* (Nucleariidae, Opisthokonta) have been reported to overcome this grazing protection. Time lapse video documentation enabled for the first time to catch the slow feeding process of *N. thermophila* and *N. delicatula*. Analysis of the feeding behaviour revealed that mechanical manipulation enables the efficient breakdown of *P. rubescens*. Growth experiments with different accompanying bacterial assemblages pointed to a pivotal role of prokaryotes. Their positive effect was not attributed to the degradation of the cyanobacterial toxin microcystin. Instead, potential contributions of unidentified bacterial species enhanced the breakdown of *P. rubescens*. The cyanobacterial toxin had no pronounced negative effects on *N. thermophila*. In contrast to the former assumption, *Paucibacter toxinivorans* the ectosymbiont of *N. thermophila* was not involved in the degradation of the microcystin variant contained in *P. rubescens*.

Introduction

In recent years, bloom forming cyanobacteria got in the focus of research as global warming and eutrophication seem to favour their occurrence in diverse ecosystems (O'Neil et al., 2012). Since many of these in mass occurring cyanobacteria produce a cocktail of toxic secondary metabolites (e.g. microcystins, anatoxins and lipopolysaccharides), they are a concern in heath and risk assessments (Carmichael, 2001). Beside this potential harmful aspect, they may play an important role as carbon source for heterotrophic organisms including bacteria, protozoa, metazoa and fungi (Sigee et al., 1999; Van Wichelen et al., 2016).

Planktothrix rubescens, a filamentous microcystin-producing cyanobacterium (Kurmayer et al., 2016), has become the dominant primary producer in the pelagial of many fresh water ecosystems, especially of deep pre-alpine lakes (Ernst et al., 2001; Jacquet et al., 2005; Posch et al., 2012). Kurmayer and Jüttner (1999) showed that the zooplankton species *Eudiaptomus gracilis*, *Cyclops abyssorum* and *Daphnia hyalina* have evolved strategies to co-exist with *P. rubescens*. According to the authors, the grazing resistance of the cyanobacterium was mainly attributed to chemical defence, whereas in other studies the filamentous form was considered as an equivalent or even more important factor (Oberhaus et al., 2007).

Microcystins are the quantitatively most prominent bioactive secondary metabolites of *P. rubescens* (Blom et al., 2001). The inhibition of protein phosphatases PP1 and PP2A and the induction of oxidative stress are the main mechanisms for their toxicity in animal cells (Campos and Vasconcelos, 2010). Cytotoxic impacts are generally assumed to affect all eukaryotes including protists. Whereas this is true for some protists like the amoeba *Acanthamoeba castellanii*, which was negatively affected (e.g. growth, physiological state and cytoskeleton) by ingested microcystin-producing cyanobacteria (Urrutia-Cordero et al., 2013), others like *Naegleria* sp. seemed to avoid or reject food particles containing this cyanotoxin (Liu et al., 2006). In contrast to these findings, certain protistan species feed actively on microcystin-containing cyanobacteria. No adverse effects of ingested toxic cyanobacteria was observed (e.g. long term cultures and regular exponential growth) for the ciliates *Obertrumia aurea*, *Trithigmostoma cucullulus* (own observations) and *Nassula* sp. (Combes et al., 2013), the flagellates *Monas guttula* (Li et al., 2011), *Diphylleia rotans* (Mohamed and Al-Shehri, 2013) and *Collodictyon* sp. ((Nishibe et al., 2002) and own observations), and the chrysophytes *Ochromonas* sp. (Wilken et al., 2010) and *Poterioochromonas* sp. (Ou et al., 2005; Zhang et al., 2010). An effective biological

degradation of microcystins was confirmed for many bacterial strains (Dziga et al., 2013). In eukaryotic organisms detoxification (e.g. glutathione S-transferase (Pflugmacher et al., 1998)) and mechanisms against oxidative stress (e.g. catalase (Ortiz-Rodríguez and Wiegand, 2010) / peroxidase (Jia et al., 2012)) play an important role to cope with the toxin. As far as we know, the only eukaryotes reported to degrade microcystins are the fungi *Trichaptum abietinum* (Jia et al., 2012), *Trichoderma citrinoviride* (Mohamed et al., 2014), the heterotrophic flagellate *Diphylleia rotans* (Mohamed and Al-Shehri, 2013), the chrysophytes *Ochromonas* sp. (Wilken et al., 2010) and *Poterioochromonas* sp. (Ou et al., 2005; Zhang et al., 2010).

The morphology of *P. rubescens* (~5 µm wide filaments up to 5 mm in length) is the other intrinsic factor conferring grazing protection. Many planktonic metazoans and protists are unable to ingest filaments which exceed their prey size range. Moreover, protistan grazers have problems to handle rigid trichomes which are formed by cyanobacterial cells. A specialized feeding apparatus and / or behaviour is needed to make filamentous cyanobacteria accessible as food source. Both attributes have been investigated in detail for *Pseudomicrothorax dubius*. This ciliate has a highly adapted cytopharyngeal basket to specifically ingest cyanobacterial filaments (Hausmann and Peck, 1979). The cytostructural adaption went along with the evolution of a sophisticated feeding behaviour. Two feeding strategies of *P. dubius* have been observed: Either individuals move along the filaments until they reach the tip, where ingestion is initiated or they attach to trichomes distantly from the tips and subsequently start phagocytosis after folding the filament (see video: https://av.tib.eu/media/9425?0). Similar feeding behaviours were documented for the ciliates *Tritigmostoma cucullulus* (Sudo et al., 1989) and *Obertrumia aurea* (Canter et al., 1990). Whereas flagellates belonging to the Collodictyonidae (e.g. *Diphylleia* sp. and *Collodictyon* sp. (Brugerolle et al., 2002)) ingest whole filamentous cyanobacteria with their ventral groove, no attack along the trichomes could be observed (unpublished observations). In contrast, amoeboid protists have no specialized feeding apparatus to graze on filamentous cyanobacteria. Although exact descriptions of the feeding behaviour is often missing, several amoebae are able to use cyanobacterial filaments as sole food source, e.g. *Acanthamoeba castellanii* (Wright et al., 1981), *Naegleria* sp. (Liu et al., 2006) among other amoebae (Dryden and Wright, 1987) and the nucleariid species *Nuclearia delicatula* (Artari, 1889; Cann, 1986), *N. radians* (formerly described as *Nucleosphaerium tuckeri* by Cann and Page (1979)), *N. thermophila* (Dirren et al., 2014), *N. moebiusi*, *N. pattersoni* and other undescribed species of the genus (Dirren and Posch, 2016; Yamamoto and Suzuki, 1984).

An interesting aspect of nucleariid species is the frequent association with endo- and ectosymbiotic bacteria. In our previous studies we characterized *N. delicatula* and *N. thermophila* isolates together with their symbionts (Dirren and Posch, 2016; Dirren et al., 2014). *Paucibacter toxinivorans*, the ectosymbiont of *N. thermophila*, was originally described as a microcystin-degrading (variants: microcystin-LR, microcystin-YR and nodularin) bacterium (Rapala et al., 2005). After the isolation of *N. thermophila*'s ectosymbiont, its ability to degrade the microcystin variant [Asp^3]microcystin-LR could be confirmed. Thus, it was assumed that these ectosymbiotic bacteria might degrade the microcystin contained in the food organism of its host (Dirren et al., 2014).

Here we report for the first time on the feeding behaviour of *N. thermophila* and *N. delicatula* ingesting toxic filamentous cyanobacteria, and combine these observations with microcystin measurements. Time lapse video documentation served as tool to record the slow feeding process. Quantifications of the cyanobacterium *P. rubescens*, its main toxin [D-Asp^3, *(E)*-Dhb^7]microcystin-RR, *N. thermophila* cells and accompanying bacteria (two different assemblages) gave insights into the dynamics of this complex system. Finally, we tested the hypothesis whether *N. thermophila*'s ectosymbiont *P. toxinivorans* is involved in the degradation of microcystin.

Key words: *Nuclearia*; feeding behaviour; microcystin; degradation; *Planktothrix*, cyanobacteria

Methods

Strains and cultures

Nuclearia thermophila strain N (HG530253) and *Nuclearia delicatula* strain G (LN875119) were isolated from Lake Zurich, Switzerland (47°19'11.5''N, 8°33'10.1''E), in the year 2011 and 2012, respectively. Single cells were picked and washed repeatedly in drops of sterile water to generate monoclonal xenic (plus bacteria) cultures. Isolates were kept in Tissue Culture Flask 25 cm^2 (TPP) on autoclaved mineral water (Cristalp) under a 12 h light (irradiance of 5-15 µmol $m^{-2}s^{-1}$) / 12 h dark cycle. The food organism *Planktothrix rubescens* BC 9307 (Walsby et al., 1998), originally isolated from Lake Zurich, was grown axenically. Fortnightly new batch cultures were established by adding an aliquot (~1 ml) of the *P. rubescens* culture to 10 ml mineral water and 200 µl of an old *Nuclearia* culture (stationary phase) as inoculum. The ectosymbiotic bacterium of *N. thermophila*, *Paucibacter toxinivorans* strain SD41 (HG792253), was isolated in a previous study (Dirren et al., 2014)

and cryopreserved in glycerol stocks (- 80° C). For the growth experiment, stocks were thawed and streaked onto R2 agar plates (Reasoner and Geldreich, 1985). Single colonies were then transferred to liquid R2 medium and grown until exponential growth phase. *N. thermophila* strain N and *N. delicatula* strain G have been deposited in the Culture Collection of Algae and Protozoa (CCAP) under the accession number CCAP 1552/5 and CCAP 1552/6, respectively.

Growth experiments

Three parallels of seven different set-ups (including control) were prepared as shown in Table 1. Whereas the exponentially growing *N. thermophila* culture served directly as inoculum, cells of *P. toxinivorans* were harvested and washed twice (centrifugation at 7000 g for 15 min and exchange of medium with autoclaved mineral water) before adding to the respective set-up. A stock culture of *P. rubescens* was poured over a sterilised steel sieve (mesh size: 71 µm) and cyanobacterial filaments were collected on a second steel sieve (mesh size: 32 µm). Cyanobacteria were washed with autoclaved mineral water (~1 L) and re-suspended in ~80 ml. One part (~22 ml) of washed filaments was used directly as food source (stock: *P. rubescens* 'intact'). The other part was subjected to a freeze/thaw cycle in order to break up cyanobacterial cells (stock: *P. rubescens* 'broken').

Water from the benthic zone of Lake Zurich (47°19'11.5''N, 8°33'10.1''E) was consecutively filtered twice over 0.8 µm pore size polycarbonate filters. The filtrate containing bacteria from Lake Zurich (stock: 'Lake Bacteria') was then used as medium in the respective set-ups. The following parameters were monitored for the different set-ups: cell counts of *N. thermophila* strain N, total bacterial abundances, biovolume of *P. rubescens* and microcystin concentrations. Unfortunately, after 235 h a contaminant (flagellate) was observed in one parallel of set-up 1 (Table 1), therefore data from this parallel were excluded from analysis. All other parallels of each set-up were highly congruent: growth parameters, densities and concentrations are subsequently reported as averages with corresponding standard deviations.

Quantification of cell abundances and biovolume

The growth of *N. thermophila* cells was followed by live counts in five drops of 20 µl on a daily basis (from day 3 to day 13) using an Axio Imager.M1 (Zeiss) microscope.

For the evaluation of bacterial abundances, 150 µl of fixed samples (fin. conc. 2 % formaldehyde) were stained with 4′,6-diamidino-2-phenylindole (DAPI, fin. conc. 7 µg ml^{-1}

for 2 min) and filtered onto polycarbonate membranes (0.2 µm pore size). Images of DAPI stained cells were acquired with an automated microscope (AxioImager Z1, Zeiss) controlled by the software AxioVision (Zeiss) and finally analysed as described previously (Zeder and Pernthaler, 2009; Zeder et al., 2009). Bacterial abundances were evaluated for the cultures (*N. thermophila* and *P. toxinivorans*) used for inoculation, the filtered lake water ('Lake Bacteria') and for all parallels at six time points during the experiment.

For the quantification of cyanobacterial biovolume, fixed samples (fin. conc. 2 % formaldehyde) were filtered (three replicates for each parallel) onto polycarbonate membranes (5 µm pore size). The total amount of filaments on filters had to be adjusted by using aliquots of different volumes (15 µl to 1500 µl). Subsequently, the image analysis software PlanktothriQuant (Zeder et al., 2010) was used for the quantification. This evaluation was done for the stock culture of *P. rubescens* (*P. rubescens* 'intact') and all parallels at two time points (after seven days and at the end of the experiment).

Microcystin measurement

Samples (1 ml) for microcystin measurements were subjected to two freeze/thaw cycles, followed by 20 min ultrasound treatment (water bath sonication), and finally frozen until analyses were done. After thawing, samples were mixed with methanol (fin. conc. 70 %), and filtered through a polyethersulphone syringe filter 0.2 µm (IC Acrodisc, Pall Corporation). [D-Asp^3, *(E)*-Dhb^7]microcystin-RR was analysed on a high performance liquid chromatography system (1260 Infinity series, Agilent Technologies) coupled with an API 5000 triple quadrupole mass spectrometer (AB Sciex). A C18 column Synergi Fusion-RP (50 x 2.00 mm, 4 µm particle size, Phenomenex) was applied to separate microcystins. Two solvents were used: 1 mM formic acid (Fluka) in water as solvent A and 100 % methanol (J.T. Baker, Avantor) as solvent B. The following gradient was applied: Solvent B from 20 % to 80 % in 5 min; B 100 % for 2.5 min and B 20 % for 2.5 min. The flow rate was kept at 1 ml min^{-1}. Nodularin (5 µg L^{-1}) was chosen as the internal standard and injected in an external vial after 6 min of sample injection. Dilutions of [D-Asp^3, *(E)*-Dhb^7]microcystin-RR were performed in order to prepare an accurate calibration curve in the range of 0.5–500 µg L^{-1}. Both toxins used as standards, were extracted and purified (99 %) through HPLC and their specific molar absorption coefficient was used to prepare accurate standard solutions. The software Analyst (version 1.6.1, AB Sciex) served as tool for data acquisition and microcystin quantification was done using the MultiQuant software (version 3.0.1, AB Sciex).

Microscopy: Photographic documentation and time lapse videos

Micrographs of living specimens (usually on slides with cover slip) were taken with a Canon EOS1000D installed on an Axio Imager.M1 (Zeiss). Camera and microscope were controlled by the software AxioVision (Zeiss). The inverted microscope Axio Vert.A1 (Zeiss) was used for observations of feeding behaviour (specimens were observed directly in culture flasks and petri dishes). Time lapse videos were acquired with an Axiocam 105 controlled by the dedicated module package available for the software Zen (Zeiss). Both microscopes were equipped with optics for differential interference and phase contrast.

Results

Morphology and locomotion of *Nuclearia* spp.

The main morphological difference between *N. thermophila* (Fig. 1a-b) and *N. delicatula* (Fig. 1c) was their size. Individuals of *N. thermophila* were uninucleated and spherical cells had body diameter of 16.4 µm on average (7.2 – 29 µm; n = 448). The multinucleate cells of *N. delicatula* were 26 µm on average (17.2 – 45.8 µm; n = 100). A glycocalyx surrounding the cell (a special feature of many *Nuclearia* spp.) was present in both investigated species. *N. thermophila* (cell diameter of ~16 µm) was typically surrounded by a glycocalyx with a thickness of ~15 µm. This structure could be seen as translucent halo around the cell body. Only ectosymbionts (few micrometres distant from the cell membrane) were observed inside the glycocalyx, other bacteria or detritus were not found in the extracellular matrix (Fig. 1). Our observations suggested a very dynamic nature of this structure. Fine filopodia elongated and retracted constantly through the translucent matrix apparently without facing resistance (Video 1). Additionally, big food particles could be moved through the glycocalyx without being hampered (Video 2). The plastic deformation during cell division and the formation of syncytia (see Figure S1 in Dirren et al. (2014)) further pointed to a highly manipulable character of the glycocalyx.

Despite the difference in size both nucleariid species displayed the same modes of locomotion. Nucleariid cells showed three different manifestations together with distinct types of cell motility. Individuals were either pelagic (Fig. 1a-c), attached with their filopodia to a substrate (Fig. 2a-c) or as amoeboid forms on the ground of culture flasks (Fig. 2d-f). Pelagic cells seemed to be capable of adjusting their vertical position, but currents in the waterbody mainly caused translocation in this state. After sedimentation, individuals used filopodia to attach to the ground followed by a horizontal movement of their cell bodies several micrometres above the ground (Fig. 2a-c and Video 1). Sliding on the outer borders of

the extracellular structure was characteristic for this type of cell motility. The required force was produced by forward pointing filopodia, continuously attaching to the substrate and pulling the cell body into the respective direction. During this mode of locomotion highest speeds were reached (1.14 µm s^{-1}; n = 16). Occasionally, spherical individuals used filopodia to pull cell bodies towards the ground which led to the transition into the amoeboid form (see Figure 1a from Surek and Melkonian (1980)). The subsequently movement was again dependent on forward pointing filopodia (Fig. 2d-f and Video 1). This cell motility was characterised by polarized cells emerging thick filopodia from a hyaline zone at their leading edge. No lobopodia or plasma streams were observed during this type of locomotion. Whereas the glycocalyx was still present, the thickness between cell membrane and substrate was reduced considerably to a few micrometres. In this way, the attaching and retracting filopodia allowed for the movement as amoeboid cells on surfaces. All of these three modes of cell motility were occasionally displayed by one and the same individual.

Feeding behaviour of *Nuclearia* spp.

The feeding behaviour of *N. thermophila* and *N. delicatula* were similar, but the larger cells of the later species were able to simultaneously ingest more food particles (Fig. 1d). Individuals of all three manifestations mentioned above actively fed on *P. rubescens* filaments. Whereas pelagic cells rather passively encountered cyanobacterial fragments, surface attached cells ‘searched’ the ground for food particles (Video 2). When nucleariids approached *P. rubescens* filopodia attached to cyanobacterial filaments. After attachment, individuals usually moved along filaments (by means of filopodia) until they reached a tip, where the feeding process was initiated. Filopodia were then used to pull fragments towards the cell body (Video 2). By this, the plasma membrane came in contact with the food and ingestion started. Subsequently, three ways of prey handling were observed. Filaments that were smaller than the nucleariid amoeba were taken up in one piece (Video 2). For filaments that were too large for being entirely ingested, two feeding behaviours were observed. First, spherical nucleariid cells engulfed only a little part of the filament, which was then moved constantly forwards and backwards (Video 2). Thereby the filament was sometimes ejected but usually contact was maintained by means of a big tube-like filopodium (Fig. 3a-b). During this mode of feeding, serial break-ups of cyanobacterial cells were observed (Fig. 3c). Particles which resulted from this break-up were then transported inside the pseudopodium towards the cell body and finally enclosed in food vacuoles (Fig. 3d). Second, elongation of the nucleariid cell led to the engulfment of the filament along the entire amoeba (Fig. 3e).

255 This was often followed by the bending of the fragment's outermost part (Fig. 3f). When
256 filaments did not break, they often snapped back into their straight conformation and bending
257 started again. After repetitive bending, small fragments eventually broke-off and were
258 enclosed in food vacuoles (Fig. 3g and Video 2). Occasionally, 'attacks' took place along
259 cyanobacterial filaments and not at the tips. After engulfment of filaments in the middle, they
260 were bended and finally broken (Video 2). This feeding behaviour was often observed for
261 large *N. delicatula* cells. After nucleariid cells had engulfed a cyanobacterial filament, they
262 were able to move along the filament occasionally even reaching the opposite tip (Video 2)
263
264 **Growth dynamics of *N. thermophila***
265 We studied effects of two distinct accompanying bacterial assemblages on the growth
266 of *N. thermophila*. A 'random' bacterial assemblage was generated as side effect of the
267 method applied to isolate amoebae. Bacteria (entitled as 'Culture assemblage') were not
268 selected for any special trait (e.g. efficiency, diversity or microcystin degradation) but rather
269 for optimal growth of nucleariids. Thus the long term culture of *N. thermophil*a probably did
270 not result in a 'natural' prokaryotic assemblage. For two set-ups an aliquot of this culture was
271 used as inoculum (see Table 1). Whereas in set-up 1 sterile mineral water served as medium
272 (only 'Culture assemblage'), lake water containing a natural bacterial assemblage was added
273 to set-up 2 ('Culture assemblage' + 'Lake bacteria').
274 Growth dynamics (lag, log and stationary / death phase) of *N. thermophila* in the two
275 set-ups were similar (Fig. 4a). While nucleariids together with the 'Culture assemblage' had a
276 shorter lag phase (set-up 1: 98 h; set-up 2: 122 h), higher cell abundances (set-up 1: 3373 cells
277 ml^{-1}; set-up 2: 4035 cells ml^{-1}) were reached when 'Lake bacteria' were present. Maximal
278 growth rates μ_{max} were 0.34 d^{-1} and 0.38 d^{-1} for set-up 1 and 2, respectively.
279 Bacterial growth dynamics in the two set-ups were similar (Fig. 4b). Inoculation led
280 immediately to an exponential increase of bacteria until a plateau was reached after 73 h. The
281 subsequent first stationary phase was shorter in set-up 1 (~47 h) than in the set-up 2 (~92 h).
282 This was followed by a second exponential growth leading to maximal abundances (after 312
283 h) of 4.4×10^7 cells ml^{-1} in set-up 1 and 6.1×10^7 cells ml^{-1} in set-up 2. Bacterial abundances
284 remained low in the control.
285 The biovolume of *P. rubescens* was strongly reduced after 312 h independently of the
286 accompanying bacterial assemblages. In the control variant we even observed an increase of
287 cyanobacterial biovolume (Fig. 4c).

In contrast to the very similar kinetics mentioned above, set-up 1 and 2 differed strikingly regarding the dynamics of microcystin concentrations (Fig. 4d). The same amount of *P. rubescens* 'intact' was added to these set-ups, resulting in a start concentration of 116 µg L^{-1}. In the control variant, microcystin concentrations were stable for 165 h and then increased to 177 µg L^{-1} after 311 h, which went in parallel with the increase of cyanobacterial biovolume. Cyanotoxin concentrations in set-up 1 increased slightly at the beginning. Thereafter, values fluctuated between 87 µg L^{-1} and 115 µg L^{-1}. Thus, there was virtually no net reduction of microcystins in the set-up with the 'Culture assemblage'. After a slight initial increase of microcystin concentrations in set-up 2, values continuously decreased to a minimum of 4 µg L^{-1}. Thus, in parallels where 'Lake Bacteria' were present, 96.6 % of the added microcystin was removed after 311 h.

Bacterial growth on intact and broken *Planktothrix rubescens* filaments

Growth curves of 'Lake Bacteria' and *P. toxinivorans* with either *P. rubescens* 'intact' or *P. rubescens* 'broken' as substrate are displayed in Fig. 5a. Compared to set-up 3 with 'intact' *P. rubescens*, 'Lake bacteria' showed higher growth rates when 'broken' filaments (set-up 4) were offered. Highest bacterial abundances were reached in set-up 4 with 7.4×10^7 cells ml^{-1} after 216 h and in set-up 3 with 6.8×10^7 cells ml^{-1} after 312 h. In the set-ups 5 and 6 *P. toxinivorans* did not grow at all independently whether *P. rubescens* was offered as 'intact' or 'broken' biovolumes (Fig. 5a).

The same amount of cyanobacterial biovolume (24.1 mm^3 L^{-1}) was added to all seven set-ups (including control) at the beginning of experiments (Fig. 4b and 5b). Since *P. rubescens* 'broken' filaments underwent freeze / thaw cycles, many cells were destroyed and thus their contents released as dissolved substances into the medium of the respective set-ups. Consequently, lower *P. rubescens* biovolumes were detected after 165 h (set-ups 4: 8.6 mm^3 L^{-1} and set- up 6: 11 mm^3 L^{-1}). When 'intact' cyanobacteria were offered to 'Lake bacteria' (set-up 3), their biovolume slightly increased at the beginning but subsequently decreased to about half (12.7 mm^3 L^{-1}) of the initial amount. Similarly, *P. rubescens* biovolume which was still intact after freeze / thaw cycles further decreased in set-up 4. In the variants were *P. toxinivorans* was inoculated, cyanobacterial biovolumes were not reduced due to bacterial activity. *Planktothrix rubescens* biovolume even increased in set-up 5 to a maximum of 35.8 mm^3 L^{-1}, which was higher than in the control (31.9 mm^3 L^{-1}).

Microcystin concentrations in the different set-ups are depicted in Fig. 5c. When *P. rubescens* 'broken' was offered to 'Lake bacteria' (set-up 4), microcystins were reduced

already after 73 h to about half (61 µg L^{-1}) of the starting concentration (116 µg L^{-1}), and to 20 µg L^{-1} at the end of the experiment. Thus, 83 % of the offered microcystins were degraded. When *P. rubescens* 'intact' was added to 'Lake Bacteria' (set-up 3), cyanotoxins were slowly reduced, resulting in a net decrease of 55 %. In the set-ups with *P. toxinivorans* micocystins were not degraded at all. We even noted increases of cyanotoxins in set-ups 5 and 6, which went in parallel with observations for the control.

Discussion

Glycocalyx of *Nuclearia* spp.

The glycocalyx is an extracellular structure composed of glycosylated proteins and lipids. A prominent and intensively studied example is the mucous layer of the gastrointestinal tract (Moran et al., 2011). There, glycoproteins and -lipids are anchored in the plasma membrane of epithelial cells forming the glycocalyx, which is covered by a second layer of secreted glycans. Similar extracellular structures have even been described for rather basal animals like corals (Rosenberg et al., 2007) and cnidarians (Fraune et al., 2015). Here, the glycocalyx serves as an interface between host and bacterial microbiota and seems to be a conserved trait. Thus, one of the main functions of the extracellular barrier is the selection of probiotic bacterial species and the defence against pathogens (Bosch et al., 2015; Ouwerkerk et al., 2013). Probably, this is also the case for the basal opisthokont family Nucleariidae. Most nucleariid species are surrounded by an extracellular structure composed of a mono- or a bilayer (see Table 1 in Yoshida et al. (2009)). Some species are associated with specific bacterial ectosymbionts living in the glycocalyx (e.g. *Inhella* sp. associated with *N. delicatula* and *P. toxinivorans* associated with *N. thermophila* (Dirren and Posch, 2016)). In relation to their small cell sizes, the dimensions of the extracellular layer are impressive. For *N. thermophila* the glycocalyx volume equals about two times the cell volume (Fig. 1). Our observations during cell division, formation of syncytia, transformation into the amoeboid morphotype and food uptake revealed a highly dynamic and manipulable character of this structure. It is not at all an amorphous passive layer, but a highly structured matrix probably precisely controlled by cellular mechanisms. Whereas the exclusion of bacterial invaders from the glycocalyx suggests high viscosity, big food particles can be moved through this structure seemingly without facing resistance. We propose two theses for this apparent dual character of the extracellular matrix. (i) Filopodia are able to generate sufficient physical force to counteract the resistance caused by viscosity. (ii) Chemical interactions of excreted factors

(e.g. proteases and lipases) with the glycoproteins and -lipids locally alter the proprieties of the matrix.

Considering the importance of the glycocalyx for many species including human beings, nucleariid amoebae could serve as model organisms in future experiment to address such hypotheses.

Cell motility of *Nuclearia* spp.

So far nucleariid species have been mainly isolated from benthic samples of lakes and ponds, and occasionally from the pelagial (see Table 1 in Dirren and Posch (2016)). Amoeboid and spherical morphotypes are likely adaptions to different environmental conditions. While the attachment on surfaces allows the colonisation of substrates, moving on substrates most probably increases the food encounter rates in the benthos. Horizontal translocation as planktonic forms might be important for dispersal and enables nucleariids to contact food sources in the pelagic realm (e.g. *P. rubescens*). *Planktothrix rubescens* regulates its buoyancy via intracellular gas vesicles (Walsby et al., 2004). Through the ingestion of cyanobacteria, nucleariids could make use of these buoyant organelles to detach and rise in the water column. In analogy to e.g. spines in other planktonic organisms, filopodia of nucleariids could decrease sedimentation rates of amoebae. The variable length and quantity of pseudopodia could even allow for a fine tuning of buoyancy.

As far as we know, the peculiar cell motility of spherical *Nuclearia* spp. has not been characterised yet. Due to the optical transparency of the extracellular matrix and the exclusive use of pseudopodia it looks like cells would be ‘walking’. In fact, spherical cells are sliding with the surface of the glycocalyx. Only filopodia seem to actively attach to the ground. Their retraction probably generates the force to pull the cell body forwards. Except the transformation of filopodia, no rolling or deformation of the cell body occurs during this kind of motility.

The cell motility of amoeboid nucleariids has some unusual characteristics. Models of amoeboid movement usually show the following sequence: First, lamellipodia and filopodia are formed at the leading edge and new adhesions under these protrusive structures are built. Then, the cell body with all its organelles is translocated forward. Finally, adhesions at the rear of the cell disassemble and the trailing edge retracts (see Figure 1 in Mattila and Lappalainen (2008)). In contrast to this classical model, no lamellipodia were observed for nucleariids. However, filopodia attach to the surface at the leading edge. Although the cell body is close to the surface, a thin layer of the glycocalyx still remains between the cell and

the ground. Thus, amoeboid nucleariid cells are actively attached only by filopodia. No pronounced translocation of cell organelles and no retraction of the trailing edge were observed. Backwards pointing filopodia are simply detached and retracted. Thus, only the attachment, detachment and retraction of filopodia causes cell movements.

Nuclearia thermophila* grazing on *Planktothrix rubescens

(with a little help from their little friends)

To date, the range of accepted food particles has been determined for only one nucleariid species (Surek and Melkonian, 1980). Nineteen out of 45 offered algal species served as sole food source for *Vampyrellidium perforans* (Surek and Melkonian, 1980). Based on ultrastructure this species was later assigned to the genus *Nuclearia* by Patterson et al. (1987). Interestingly, the three offered cyanobacterial species (*Anabaena cylindrica*, *Anabaena variabilis* and *Oscillatoria borneti*) did not support amoebal growth. Since feeding experiments by Surek and Melkonian (1980) were conducted exclusively with axenic cultures, the presence of bacteria in our experiments could explain why *P. rubescens* was indeed a suitable food source for amoebae (but see below).

Nuclearia thermophila caused breakdowns of *P. rubescens* populations by the combination of physical forces (e.g. bending of filaments) and chemical digestion (e.g. enzymes). Additionally, our results suggest, that direct and indirect interactions with heterotrophic bacteria influence growth success of *N. thermophila*.

Besides adverse physical conditions (i.e. abiotic factors) and cyanophages (Deng and Hayes, 2008), competition with bacteria and their excreted bio-active components could have a negative impact on *P. rubescens.* This might lead to cell apoptosis and partial degradation of cyanobacterial filaments, facilitating a further breakdown by grazing of *N. thermophila*. It is known that bacteria are able to release cyanobacteria-lysing factors, e.g. amino acids, (antibiotic) peptides, enzymes, steroids, alkaloids, phenol derivatives, pigments and glycolipids (see Suppl. Table 2 from Van Wichelen et al. (2016)). An accumulation of such bio-active components might be a prerequisite for successful feeding and growth of nucleariids. This thesis is supported by four observations. (i) The ‘Lake bacteria’ assemblage was able to lyse about half of offered cyanobacterial biovolume, even when grown alone with *P. rubescens* (Fig. 5b). The reported ability of many heterotrophic bacteria to degrade cyanobacteria is in line with this result (Van Wichelen et al., 2016). (ii) Different feeding behaviours of nucleariid cells might point to different physiological states of their food, *P. rubescens*. Bending of filaments by nucleariids probably indicates that physical forces are

423 required to attack ‘healthy’ cyanobacteria. When filaments were bended in newly inoculated
424 cultures, they often did not break but snapped back and the process of bending started again.
425 Insufficient bacterial degradation of cyanobacterial cells could explain these unsuccessful
426 attacks. (iii) Time lapse videos showed that the breakage of *P. rubescens* filaments often
427 coincides with an accumulation of bacteria (Video 2). Although the causative agent of cell
428 lysis cannot be clearly attributed to bacteria, chemotactic behaviour of certain bacteria
429 towards the cyanobacterium was evident. (iv) Growth dynamics of bacteria and *N.*
430 *thermophila* displayed a distinct succession in respective set-ups (Fig. 4a-b). While bacteria
431 grew immediately after inoculation, nucleariids were still in a lag-phase. Probably, during this
432 first bacterial growth phase cyanobacteria already started to degrade and break in smaller
433 filaments (e.g. caused by excreted bio-active substances). This could explain the subsequent
434 log-phase observed for *N. thermophila*. We documented even a more pronounced effect in a
435 preliminary growth experiment, where the addition of the ‘Culture assemblage’ from *N.*
436 *thermophila* to *N. delicatula* shortened the lag phase of the latter by 65 h (data not shown).
437 Consequently, the bacterial assemblage composition and probably excreted bio-active
438 substances might be crucial for the growth success of nucleariids.
439 Regarding the degradation of cyanobacteria there is a great discrepancy between lab
440 cultures and natural systems, e.g. the pelagial of deep pre-alpine lakes. In contrast to the
441 complete breakdown of *P. rubescens* populations in lab experiments with *N. thermophila*, this
442 cyanobacterial species seems to be protected from effective grazing in oligomesotrophic
443 lakes. Probably, this phenomenon is attributed to insufficient concentrations of cyanobacteria-
444 lysing substances. Low production, diffusion and dilution of these factors might be important
445 processes conferring grazing protection to *P. rubescens*.
446 In addition to positive effects of bacterial assemblages on *N. thermophila*, bacteria on
447 the other hand benefited from exponentially growing amoebae. The initial log-phase of
448 bacteria was probably linked to dissolved carbon sources (e.g. from damaged *P. rubescens*
449 cells), available already at the beginning of the experiment. Thus, their growth reached a
450 plateau after the depletion of these accessible substrates. Subsequently, a second log-phase
451 coincided with the growth dynamics of *N. thermophila*. This observation could be explained
452 by substrates released during grazing by nucleariids (i.e. sloppy feeding) and by exocytosis of
453 indigestible components. Unfortunately, we don’t know if this second bacterial log phase also
454 reflected a taxonomic shift within bacterial assemblages.
455 In contrast to this positive effect on *N. thermophila*, maximal cell abundances of ‘Lake
456 bacteria’ were higher (7.4×10^7 bacteria ml^{-1}) in set-ups with ‘broken’ *P. rubescens*, than in

457 set-ups where nucleariids were also present (6.1×10^7 bacteria ml^{-1}). This difference possibly
458 mirrors the competition of amoebae with bacteria for same resources. When only dissolved
459 substrates (i.e. sonicated *P. rubescens* cultures subsequently filtered through 0.2 µm pore
460 filter) were offered, *N. thermophila* was not growing (data not shown). From an evolutionary
461 perspective, phagocytosis is a crucial trait of heterotrophic protists to compete and survive in
462 a bacterial world. Although positive impacts on *N. thermophila* by the two accompanying
463 bacterial assemblages prevailed in our experiment, growth of nucleariids could be also
464 negatively affected by certain bacterial strains. Antagonistic effects might be direct (e.g.
465 spirillum-like bacteria feeding on the glycocalyx of *N. thermophila* see Figure 1I in Dirren et
466 al. (2014)) or indirect (e.g. competition of certain bacteria with bacterial 'helper' strains). In
467 sum, the interplay with accompanying bacteria is a crucial factor for the growth success of *N.*
468 *thermophila*.
469
470 **Degradation of microcystin**
471 The fact that microcystin (i.e. [D-Asp^3, *(E)*-Dhb^7]microcystin-RR) was reduced only
472 in the set-ups with 'Lake Bacteria' pointed to a bio-degradation caused by distinct bacterial
473 species. In contrast, no net degradation was monitored for the randomly generated 'Culture
474 assemblage', leading to an accumulation of cyanotoxins. Thus, two conclusions can be drawn:
475 (i) The microcystin variant of its food source was not degraded or covalently bound (e.g. via
476 the glutathione S-transferase) by *N. thermophila*. (ii) Instead the cyanotoxin was released in
477 the culture medium, where it would became available for bacterial degraders.
478 Our experiments gave no indications for negative effects of [D-Asp^3, *(E)*-
479 Dhb^7]microcystin-RR on *N. thermophila*, which contradicts the general assumption that
480 microcystins are harmful for all eukaryotes. This could be explained by two mechanisms. (i)
481 The inhibition of protein phosphatases PP1 and PP2A by microcystins is one of the main
482 causes for their toxicity (MacKintosh et al., 1990). Thus, structural variants of phosphatases
483 might not be affected. This was shown, e.g. for the ciliate species *Paramecium* sp. which
484 possess indeed different types of protein phosphatases. The lack of the specific targets in
485 combination with efficient export mechanisms would render the cyanotoxin harmless. (ii)
486 Since microcystins are not cell membrane permeable, transporters are needed for their uptake.
487 Members of the organic anion transporting polypeptide superfamily (Oatps) are known to
488 mediate the transport of microcystins (Faltermann et al., 2016). The transport of microcystins
489 was dependent on the specific Oatp and the microcystin variant (Fischer et al., 2005).
490 Unfortunately, it is not known which transporters are expressed by nucleariid species. But, if

nucleariid species lack the appropriate transporters, microcystins would not be taken up. Digestion thus could occur as follows: Cyanobacteria are digested inside food vacuoles and their cell content, including microcystins, is released. Subsequently, nutrients are actively absorbed by the nucleariids, but microcystins still remain inside vacuoles. Exocytose could finally lead to the release of cyanotoxins into the culture medium.

The ability of the ectosymbiont *P. toxinivorans* to degrade [Asp^3]microcystin-LR was previously shown (Dirren et al., 2014). Thus, a possible role in the degradation of cyanotoxins stored in the food source of *N. thermophila* seemed to be likely. In the current growth experiment no degradation of [D-Asp^3, *(E)*-Dhb^7]microcystin-RR could be attributed to *P. toxinivorans*. The ectosymbiont was harboured inside the glycocalyx of *N. thermophila* in set-up 1 and 2. However, only if 'Lake bacteria' were present (set-up 2), a degradation of cyanotoxins was monitored. Microcystin was not degraded when *P. toxinivorans* was confronted with 'intact' or 'broken' *P. rubescens* (set-ups 5 and 6). This findings suggest that the ectosymbiont *P. toxinivorans* is not able to degrade the [D-Asp^3, *(E)*-Dhb^7]microcystin-RR stored in the food source of its host *N. thermophila*.

Conclusion

Degradation dynamics of *P. rubescens* and its toxin differed remarkably in the various set-ups. Cyanobacterial filaments were almost completely eliminated after 312 h exclusively if *N. thermophila* was present. The combination of bacterial degradation together with the feeding activity of nucleariids caused an efficient breakdown of *P. rubescens*. *Nuclearia thermophila* did not degrade the microcystin variant originally stored in its cyanobacterial food. Taken together, two requirements have to be fulfilled for an efficient degradation of *P. rubescens* along with its toxin: Cyanobacterial filaments have to be partially degraded (e.g. unfavourable physiological conditions, cyanobacteria-lysing factors and / or cyanophages) and members of the bacterial assemblage should be able to degrade released microcystins.

The role of the ectosymbiont *P. toxinivorans* as microcystin-RR degrader could not be confirmed in the investigated system. Since nucleariid species have a broad prey range, the possible involvement of the ectosymbiont in the degradation of different microcystin variants (e.g. microcystin-LR) stored in alternative food sources should be addressed in future experiments. However, the close proximity of these ectosymbiotic bacteria to the host's membrane suggests an exchange of metabolites. Future experiments should address metabolic capabilities of the ectosymbiont to pinpoint the role of this associated bacterium for *N. thermophila*.

References

Artari, A., 1889. Morphologische und biologische Studien über *Nuclearia delicatula*, Cienk. Zool. Anz. 12, 408-416.

Blom, J.F., et al., 2001. High grazer toxicity of [D-Asp^3,*(E)*-Dhb^7]microcystin-RR of *Planktothrix rubescens* as compared to different microcystins. Toxicon 39, 1923-1932.

Bosch, T.C., et al., 2015. Microbial ecology in *Hydra*: Why viruses matter. J. Microbiol. 53, 193-200.

Brugerolle, G.u.y., et al., 2002. *Collodictyon triciliatum* and *Diphylleia rotans* (= *Aulacomonas submarina*) form a new family of flagellates (Collodictyonidae) with tubular mitochondrial cristae that is phylogenetically distant from other flagellate groups. Protist 153, 59-70.

Campos, A., Vasconcelos, V., 2010. Molecular mechanisms of microcystin toxicity in animal cells. Int. J. Mol. Sci. 11, 268-287.

Cann, J.P., 1986. The feeding behavior and structure of *Nuclearia delicatula* (Filosea: Aconchulinida). J. Protozool. 33, 392-396.

Cann, J.P., Page, F.C., 1979. *Nucleosphaerium tuckeri* nov. gen. nov. sp.- A new freshwater filose amoeba without motile form in a new family Nucleariidae (Filosea: Aconchulinida) feeding by ingestion only. Arch. Protistenk. 122, 226-240.

Canter, H.M., et al., 1990. The ecological significance of grazing on planktonic populations of cyanobacteria by the ciliate *Nassula*. New Phytol. 114, 247-263.

Carmichael, W.W., 2001. Health effects of toxin-producing cyanobacteria: “The CyanoHABs”. Hum. Ecol. Risk. Assess. 7, 1393-1407.

Combes, A., et al., 2013. Ciliate *Nassula* sp. grazing on a microcystin-producing cyanobacterium (Planktothrix agardhii): impact on cell growth and in the microcystin fractions. Aquat. Toxicol. 126, 435-441.

Deng, L.I., Hayes, P.K., 2008. Evidence for cyanophages active against bloom-forming freshwater cyanobacteria. Freshwater Biol. 53, 1240-1252.

Dirren, S., Posch, T., 2016. Promiscuous and specific bacterial symbiont acquisition in the amoeboid genus *Nuclearia* (Opisthokonta). FEMS Microbiol. Ecol. 92.

Dirren, S., et al., 2014. Ménage-à-trois: The amoeba *Nuclearia* sp. from Lake Zurich with its ecto- and endosymbiotic bacteria. Protist 165, 745-758.

Dryden, R.C., Wright, S.J.L., 1987. Predation of cyanobacteria by protozoa. Can. J. Microbiol. 33, 471-482.

Dziga, D., et al., 2013. Microbial degradation of microcystins. Chem. Res. Toxicol. 26, 841-852.

Ernst, B., et al., 2001. Presence of *Planktothrix* sp. and cyanobacterial toxins in Lake Ammersee, Germany and their impact on whitefish (Coregonus lavaretus L.). Environ. Toxicol. 16, 483-488.

Faltermann, S., et al., 2016. Comparative effects of nodularin and microcystin-LR in zebrafish: 1. Uptake by organic anion transporting polypeptide Oatp1d1 (Slco1d1). Aquat. Toxicol. 171, 69-76.

561 Fischer, W.J., et al., 2005. Organic anion transporting polypeptides expressed in liver and brain
562 mediate uptake of microcystin. Toxicol. Appl. Pharm. 203, 257-263.

563 Fraune, S., et al., 2015. Bacteria-bacteria interactions within the microbiota of the ancestral
564 metazoan *Hydra* contribute to fungal resistance. ISME J. 9, 1543-1556.

565 Hausmann, K., Peck, R.K., 1979. The mode of function of the cytopharyngeal basket of the ciliate
566 *Pseudomicrothorax dubius*. Differentiation 14, 147-158.

567 Jacquet, S., et al., 2005. The proliferation of the toxic cyanobacterium *Planktothrix rubescens*
568 following restoration of the largest natural French lake (Lac du Bourget). Harmful Algae 4, 651-672.

569 Jia, Y., et al., 2012. A fungus capable of degrading microcystin-LR in the algal culture of *Microcystis*
570 *aeruginosa* PCC7806. Appl. Biochem. Biotech. 166, 987-996.

571 Kurmayer, R., et al., 2016. Role of toxic and bioactive secondary metabolites in colonization and
572 bloom formation by filamentous cyanobacteria *Planktothrix*. Harmful Algae 54, 69-86.

573 Kurmayer, R., Jüttner, F., 1999. Strategies for the co-existence of zooplankton with the toxic
574 cyanobacterium *Planktothrix rubescens* in Lake Zurich. J. Plankton Res. 21, 659-683.

575 Li, J., et al., 2011. Biodegradation of microcystins by bacterial communities co-existing with the
576 flagellate *Monas guttula* and concurrent succession of community structures. J. Water Supply Res. T.
577 60, 352-363.

578 Liu, X.Y., et al., 2006. Feeding characteristics of an amoeba (Lobosea : *Naegleria*) grazing upon
579 cyanobacteria: Food selection, ingestion and digestion progress. Microb. Ecol. 51, 315-325.

580 MacKintosh, C., et al., 1990. Cyanobacterial microcystin-LR is a potent and specific inhibitor of
581 protein phosphatases 1 and 2A from both mammals and higher plants. FEBS Lett. 264, 187-192.

582 Mattila, P.K., Lappalainen, P., 2008. Filopodia: molecular architecture and cellular functions. Nat. Rev.
583 Mol. Cell Biol. 9, 446-454.

584 Mohamed, Z.A., Al-Shehri, A.M., 2013. Grazing on *Microcystis aeruginosa* and degradation of
585 microcystins by the heterotrophic flagellate *Diphylleia rotans*. Ecotox. Environ. Safe. 96, 48-52.

586 Mohamed, Z.A., et al., 2014. Growth inhibition of the cyanobacterium *Microcystis aeruginosa* and
587 degradation of its microcystin toxins by the fungus *Trichoderma citrinoviride*. Toxicon 86, 51-58.

588 Moran, A.P., et al., 2011. Sweet-talk: role of host glycosylation in bacterial pathogenesis of the
589 gastrointestinal tract. Gut 60, 1412-1425.

590 Nishibe, Y., et al., 2002. Grazing on *Microcystis aeruginosa* by the heterotrophic flagellate
591 *Collodictyon triciliatum* in a hypertrophic pond. Aquat. Microb. Ecol. 29, 173-179.

592 O'Neil, J.M., et al., 2012. The rise of harmful cyanobacteria blooms: The potential roles of
593 eutrophication and climate change. Harmful Algae 14, 313-334.

594 Oberhaus, L., et al., 2007. Grazing of two toxic *Planktothrix* species by *Daphnia pulicaria*: potential for
595 bloom control and transfer of microcystins. J. Plankton Res. 29, 827-838.

596 Ortiz-Rodríguez, R., Wiegand, C., 2010. Age related acute effects of microcystin-LR on *Daphnia*
597 *magna* biotransformation and oxidative stress. Toxicon 56, 1342-1349.

598 Ou, D., et al., 2005. Effects of microcystins on and toxin degradation by *Poterioochromonas* sp.
599 Environ. Toxicol. 20, 373-380.

600 Ouwerkerk, J.P., et al., 2013. Glycobiome: Bacteria and mucus at the epithelial interface. Best. Pract.
601 Res. Cl. Ga. 27, 25-38.

602 Patterson, D.J., et al., 1987. The ultrastructure of *Vampyrellidium perforans* Surek & Melkonian and
603 its taxonomic position among the naked filose amoebae. J. Protozool. 34, 63-67.

604 Pflugmacher, S., et al., 1998. Identification of an enzymatically formed glutathione conjugate of the
605 cyanobacterial hepatotoxin microcystin-LR: the first step of detoxication. Biochim. Biophys. Acta
606 1425, 527-533.

607 Posch, T., et al., 2012. Harmful filamentous cyanobacteria favoured by reduced water turnover with
608 lake warming. Nature Clim. Change.

609 Rapala, J., et al., 2005. *Paucibacter toxinivorans* gen. nov., sp nov., a bacterium that degrades cyclic
610 cyanobacterial hepatotoxins microcystins and nodularin. Int. J. Syst. Evol. Microbiol. 55, 1563-1568.

611 Reasoner, D.J., Geldreich, E.E., 1985. A new medium for the enumeration and subculture of bacteria
612 from potable water. Appl. Environ. Microbiol. 49, 1-7.

613 Rosenberg, E., et al., 2007. The role of microorganisms in coral health, disease and evolution. Nat.
614 Rev. Micro. 5, 355-362.

615 Sigee, D.C., et al., 1999. Biological control of cyanobacteria: principles and possibilities. Hydrobiologia
616 395, 161-172.

617 Sudo, R., et al., 1989. Predation and deodorization of musty odor-producing filamentous algae by the
618 protozoa *Trithigmostoma cucullulus*. Water Sci. Technol. 21, 1743-1746.

619 Surek, B., Melkonian, M., 1980. The filose amoeba *Vampyrellidium perforans* nov. sp. (Vampyrellidae,
620 Aconchulinida): Axenic culture, feeding behaviour and host range specifity. Arch. Protistenk. 123,
621 166-191.

622 Urrutia-Cordero, P., et al., 2013. Effects of harmful cyanobacteria on the freshwater pathogenic free-
623 living amoeba *Acanthamoeba castellanii*. Aquat. Toxicol. 130–131, 9-17.

624 Van Wichelen, J., et al., 2016. The common bloom-forming cyanobacterium Microcystis is prone to a
625 wide array of microbial antagonists. Harmful Algae 55, 97-111.

626 Walsby, A.E., et al., 1998. The critical pressures of gas vesicles in *Planktorhrix rubescens* in relation
627 tothe depth of winter mixing in Lake Zurich, Switzerland. J. Plankton Res. 20, 1357-1375.

628 Walsby, A.E., et al., 2004. Comparison of the Depth Where Planktothrix rubescens Stratifies and the
629 Depth Where the Daily Insolation Supports Its Neutral Buoyancy. New Phytol. 162, 133-145.

630 Wilken, S., et al., 2010. Microcystins do not provide anti-herbivore defence against mixotrophic
631 flagellates. Aquat. Microb. Ecol. 59, 207-216.

632 Wright, S.J.L., et al., 1981. *Acanthamoeba castellanii*. a predator of cyanobacteria. J. Gen. Microbiol.
633 125, 293-300.

634 Yamamoto, Y., Suzuki, K., 1984. Light and electron microscope observations and prey specificities of
635 an algophorous amoeba from Japanese freshwater. J. Gen. Appl. Micrbiol. 30, 411-417.

636 Yoshida, M., et al., 2009. *Nuclearia thermophila* sp. nov. (Nucleariidae), a new nucleariid species
637 isolated from Yunoko Lake in Nikko (Japan). Europ. J. Protistol. 45, 147-155.

638 Zeder, M., Pernthaler, J., 2009. Multispot live-image autofocusing for high-throughput microscopy of
639 fluorescently stained bacteria. Cytom. Part A 75A, 781-788.

640 Zeder, M., et al., 2009. A small population of planktonic *Flavobacteria* with disproportionally high
641 growth during the spring phytoplankton bloom in a prealpine lake. Environ. Microbiol. 11, 2676-
642 2686.

643 Zeder, M., et al., 2010. Automated quantification and sizing of unbranched filamentous
644 cyanobacteria by model-based object-oriented image analysis. Appl. Environ. Microbiol. 76, 1615-
645 1622.

646 Zhang, X., et al., 2010. The effect of *Poterioochromonas* abundance on production of intra- and
647 extracellular microcystin-LR concentration. Hydrobiologia 652, 237-246.

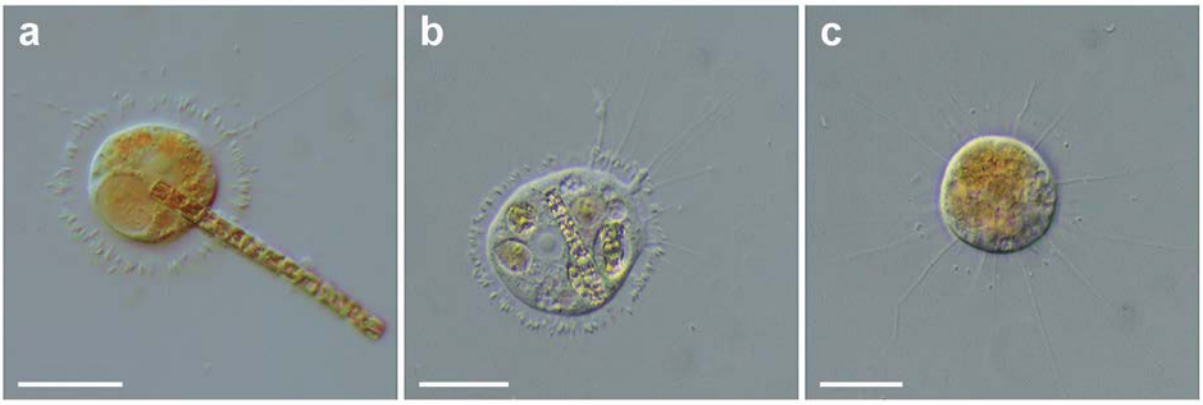

Figure 1

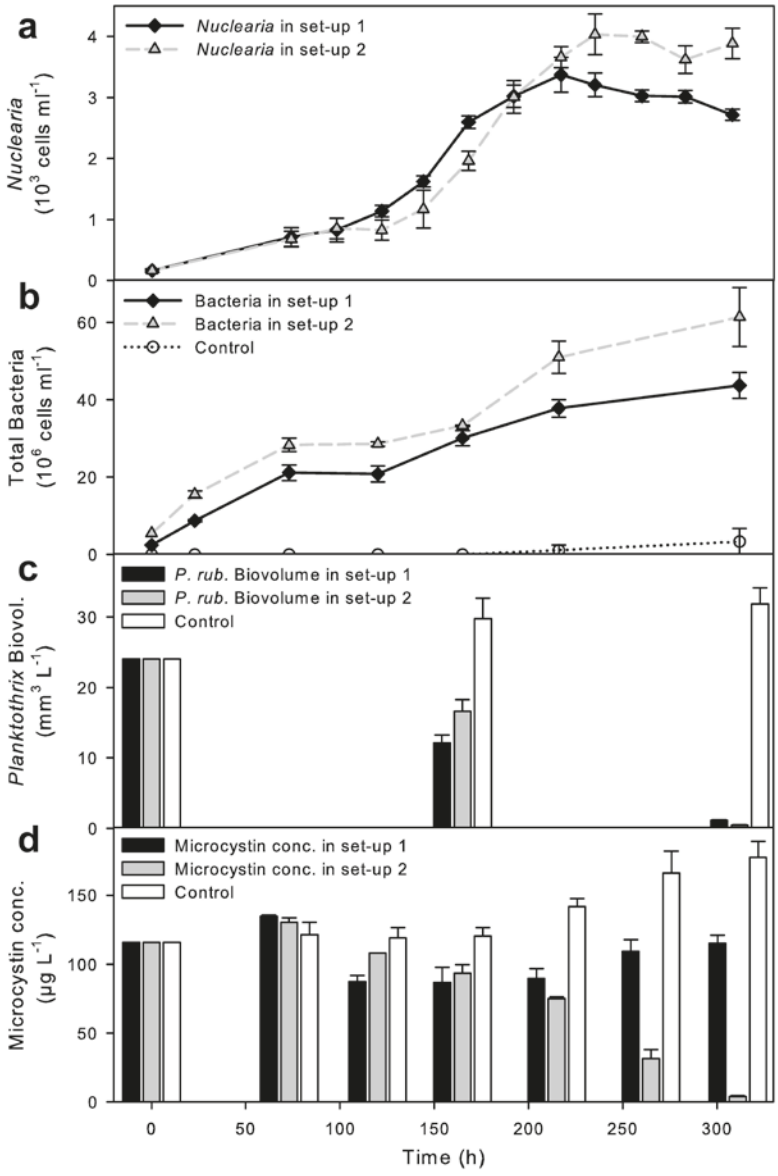

Figure 4

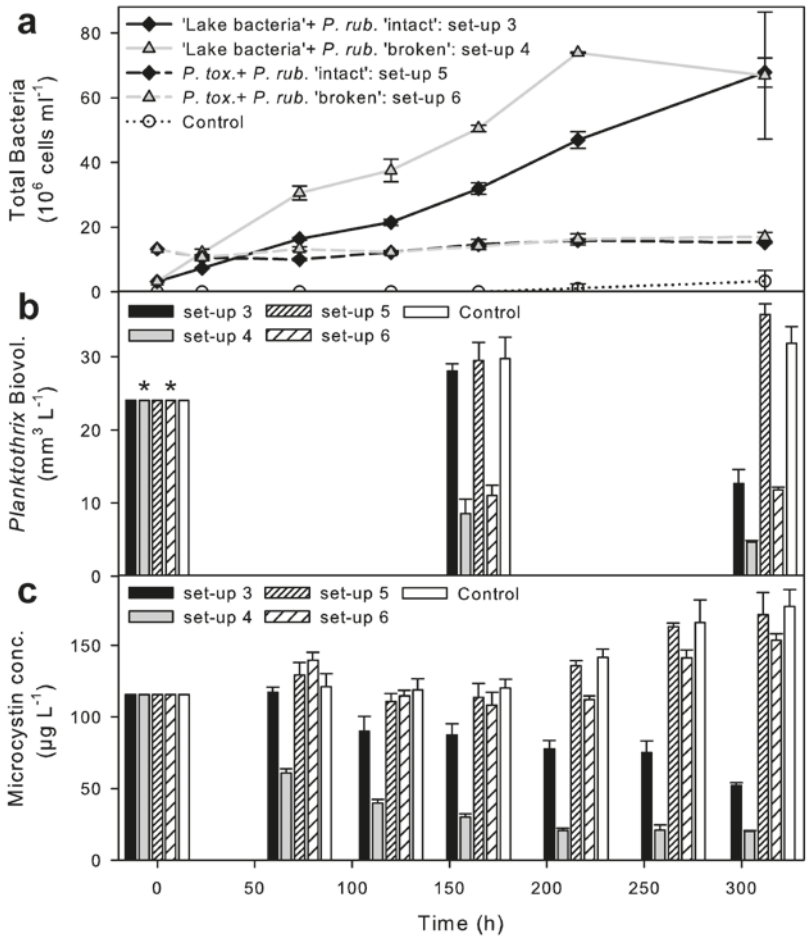
a
'Lake bacteria'+ P. rub. 'intact': set-up 3
'Lake bacteria'+ P. rub. 'broken': set-up 4
P. tox.+ P. rub. 'intact': set-up 5
P. tox.+ P. rub. 'broken': set-up 6
Control
Total Bacteria (10^6 cells ml^-1)
b
set-up 3
set-up 5
Control
set-up 4
set-up 6
Planktothrix Biovol. (mm^3 L^-1)
c
Microcystin conc. (µg L^-1)
Time (h)

Figure 5

Article IV

Pitsch G, Adamec L, Dirren S, Nitsche F, Šimek K, Sirová D & Posch T (accepted) The green *Tetrahymena utriculariae* n. sp. (Ciliophora, Oligohymenophorea) with its endosymbiotic algae (*Micractinium* sp.), living in traps of a carnivorous aquatic plant. *Journal of Eukaryotic Microbiology*.

The Journal of Eukaryotic Microbiology

ISOP Published by the International Society of Protistologists

Journal of Eukaryotic Microbiology ISSN 1066-5234

ORIGINAL ARTICLE

The Green *Tetrahymena utriculariae* n. sp. (Ciliophora, Oligohymenophorea) with Its Endosymbiotic Algae (*Micractinium* sp.), Living in Traps of a Carnivorous Aquatic Plant

Gianna Pitsch[a], Lubomír Adamec[b], Sebastian Dirren[a], Frank Nitsche[c], Karel Šimek[d], Dagmara Sirová[d,e] & Thomas Posch[a]

a Limnological Station, Department of Plant and Microbial Biology, University of Zurich, Kilchberg 8802, Switzerland
b Institute of Botany CAS, Section of Plant Ecology, Třeboň 379 82, Czech Republic
c Institute for Zoology, General Ecology, Biocenter, University of Cologne, Cologne 50674, Germany
d Biology Centre CAS, Institute of Hydrobiology, České Budějovice 370 05, Czech Republic
e Faculty of Science, University of South Bohemia, České Budějovice 370 05, Czech Republic

Keywords
Ciliates; life cycle; mixotrophy; symbiotic algae; Tetrahymenida; *Utricularia*.

Correspondence
T. Posch, Limnological Station, Department of Plant and Microbial Ecology, University of Zurich, Seestrasse 187, Kilchberg 8802, Switzerland
Telephone number: +41-44-634-9224;
FAX number: +41-44-634-9225;
e-mail: posch@limnol.uzh.ch

Received: 12 July 2016; revised 5 September 2016; accepted September 5, 2016.

doi:10.1111/jeu.12369

ABSTRACT

The genus *Tetrahymena* (Ciliophora, Oligohymenophorea) probably represents the best studied ciliate genus. At present, more than forty species have been described. All are colorless, i.e. they do not harbor symbiotic algae, and as aerobes they need at least microaerobic habitats. Here, we present the morphological and molecular description of the first green representative, *Tetrahymena utriculariae* n. sp., living in symbiosis with endosymbiotic algae identified as *Micractinium* sp. (Chlorophyta). The full life cycle of the ciliate species is documented, including trophonts and theronts, conjugating cells, resting cysts and dividers. This species has been discovered in an exotic habitat, namely in traps of the carnivorous aquatic plant *Utricularia reflexa* (originating from Okavango Delta, Botswana). Green ciliates live as commensals of the plant in this anoxic habitat. Ciliates are bacterivorous, however, symbiosis with algae is needed to satisfy cell metabolism but also to gain oxygen from symbionts. When ciliates are cultivated outside their natural habitat under aerobic conditions and fed with saturating bacterial food, they gradually become aposymbiotic. Based on phylogenetic analyses of 18S rRNA and mitochondrial *cox1* genes *T. utriculariae* forms a sister group to *Tetrahymena thermophila*.

THE genus *Tetrahymena* (Ciliophora, Oligohymenophorea) includes probably the best and most intensively studied ciliate species at present (Collins 2012; Kher et al. 2011; Plattner et al. 2009). A quick literature search (August 2016) in the Web Of Science™ Core Collection remarkably reflects the extensive research activities. Using the term "*Tetrahymena*" in the online search field "Topic" resulted in ~10,330 hits. This value even exceeds search results obtained for the ciliate genus *Paramecium* (~5,940 hits). In contrast with nearly all other ciliates, some *Tetrahymena* species can be grown as pure osmotrophs in axenic cultures (Cassidy-Hanley 2012), i.e. without accompanying bacteria. This aspect also contributes to the wide use of *Tetrahymena* strains as model organisms (Collins 2012).

In nature these primarily bacterivorous ciliates can be found in all freshwater habitats, with a clear preference for the benthic zone (Doerder and Brunk 2012). Nevertheless, a few *Tetrahymena* species were described to be facultative or obligate parasites (e.g. of insects; Jerome et al. 1996), whereas others are even histophagous (Strüder-Kypke et al. 2001). At present, more than 40 species within the genus were described (Lynn and Doerder 2012; Quintela-Alonso et al. 2013), i.e. ciliates got a species name although the precision and extent of species descriptions varied. On the one hand, a few species have been characterized in detail based on morphological features in combination with molecular marker genes (e.g. Quintela-Alonso et al. 2013). On the other hand, several species were named solely on the basis of molecular or

biochemical methods but adequate descriptions of their morphological characteristics and life cycles are still missing (e.g. *Tetrahymena farahensis* which was described based on sequences by Zahid et al. 2014). However, this is an ambivalent aspect, as a "pure morphology based discrimination" of several known *Tetrahymena* species seems to be impossible (Lynn and Doerder 2012). Thus, nowadays combinations of classical approaches with molecular phylogenetic analyses are needed, based not only on 18S rRNA but mainly on the mitochondrial cytochrome *c* oxidase subunit 1 (*cox1*) genes (Chantangsi et al. 2007; Kher et al. 2011).

Nevertheless, all currently described *Tetrahymena* species from natural habitats have two characteristics in common: (i) No natural species was reported to harbor symbiotic algae, as it is known for several representatives of various freshwater genera (*Coleps, Euplotes*, *Paramecium*, *Stokesia* – to name just a few examples). (ii) All *Tetrahymena* species are aerobic ciliates and thus live in oxygenated habitats, although ciliates seem to prefer and tolerate microaerobic zones (Doerder and Brunk 2012).

Here, we present the "first" green *Tetrahymena* species, i.e. the ciliate harbors symbiotic green algae. Ciliates were discovered in a real exotic habitat—they live as symbionts in traps of the aquatic carnivorous plant *Utricularia reflexa* (Lentibulariaceae, Lamiales). The green *Tetrahymena* form a central element of the microbial food web in the anoxic trap fluid. For a detailed description of the autecology of this *Tetrahymena* species we refer to our accompanying manuscript by Šimek et al. (2016). Here, we give a detailed morphological and molecular characterization of the ciliate including its life cycle, resulting in the description of the new species *Tetrahymena utricullariae* n. sp. Ciliates were isolated and maintained as green but also as aposymbiotic cultures outside their natural habitat. Finally we investigated if algal symbionts were "typical" endosymbionts (in terms of taxonomic affiliation) described for ciliate hosts.

MATERIALS AND METHODS

Trap fluids and cultivation of ciliates and algae

The aquatic plant *U. reflexa* Oliv. originates from the Okavango Delta, Botswana and is cultivated at the Institute of Botany CAS (Třeboň, Czech Republic) since the year 2005. Whole plant shoots were transferred in 1-liter aquaria to the University of Zurich (Switzerland) in the years 2014 and 2015. For a detailed description of the plant itself and its cultivation conditions we refer to Adamec (2012, 2015) and Šimek et al. (2016).

To gain living ciliates, single traps were cut from the shoot and transferred into a small drop (300 μl) of 0.2 μm pre-filtered mineral water (Volvic, France). The trap wall was opened with two dissecting needles to release ciliates in the surrounding water. Most stages of the complex life cycle could be already observed after the opening of traps. In vivo observations were done with a Zeiss Axio Imager M1 (Zeiss, Jena, Germany) at magnifications of 100–1,600X with bright-field, phase and interference contrast. Photomicrographs were taken with a Canon EOS 1000D controlled by the software AxioVision (Zeiss). Single green ciliates were collected with a sterilized glass pipette. For the cultivation of ciliates we tried both, to create clonal isolates and cultures originating from several individuals. First, ciliates were transferred in 96 microwell plates (each well containing 200 μl of pre-filtered Volvic). Plates were kept at aerobic conditions at 18 °C, and at a 12 h day (10 μmol/m^2/s)/12 h night cycle. Half of the wells were amended with each 50 μl of a mixed bacterial suspension growing on wheat grains. In case of obvious growth of ciliates in wells, cells were transferred into Tissue Culture Flasks 25 cm^2 (TPP®; Techno Plastic Products AG, Switzerland), filled with 50 ml of pre-filtered Volvic (either enriched with bacteria or not). Cultures of green ciliates could be maintained in a freshwater medium WC (Guillard and Lorenzen 1972) and Volvic (1:1) mixture for several months. Nevertheless, several ciliate isolates kept under aerobic conditions with over-saturating bacterial food gradually lost their algal symbionts (during several weeks) – even when cultures were grown at a 12 h day/12 h night cycle. Here, ciliates switched toward complete heterotrophy, feeding exclusively on bacteria.

For the isolation of algal symbionts, single green ciliates were gently squeezed in a small drop (20 μl) of 0.2 μm pre-filtered Volvic with a dissecting needle until cell rupture happened and algal symbionts were released. Several algal cells were collected with a sterilized ultrafine glass capillary and transferred into 96 microwell plates. Each well contained 200 μl of freshwater medium WC. When successful growth was observed, algae were transferred to Tissue Culture Flasks 25 cm^2 (TPP®), filled with 30 ml of freshwater medium WC.

Silver impregnations

For the quantification of algal symbionts per ciliate we applied the quantitative protargol staining (QPS) method (Skibbe 1994 with modifications after Pfister et al. 1999). This method allowed for the collection of a high number of ciliates for silver impregnation. Samples were fixed with Bouin's solution (picric acid, formaldehyde, and acetic acid) adjusting a final concentration of 5% (vol/vol, Pfister et al. 1999). Subsamples (100–300 μl) were filtered on 0.8 μm pore-size cellulose nitrate filters (with counting grid; Sartorius) and silver impregnation with protargol was conducted according to the protocols mentioned above.

For analyses of ciliary patterns and measurements of morphometric parameters we used the protargol impregnation "Procedure A" after Foissner (2014). Silverline patterns were characterized after the dry silver nitrate staining procedure (Foissner 2014). Fixed specimens were observed with the microscopic equipment described above. Measurements of morphometric parameters (Table 1) derived from a green clonal culture and were done with the image analysis software Lucia (Laboratory Imaging, Prague).

Table 1. Morphometric parameters of living trophonts and theronts, and protargol impregnated trophonts of the green ciliate species *Tetrahymena utricullariae* n. sp.isolated from *Utricularia reflexa*

Symbiont bearing green ciliates	Average	M	SD	SE	CV	Min	Max	*n*
Body, length – living trophonts (μm)	36.7	36.7	4.0	0.7	11.0	30.0	45.3	31
Body, width – living trophonts (μm)	27.4	27.7	2.1	0.4	7.8	21.8	30.1	31
Body, volume – living trophonts (μm^3)	14,543	14,766	2,985	536	21.0	7,988	20,214	31
Body, length – living theronts (μm)	49.8	49.1	5.8	1.3	11.5	41.0	59.0	20
Body, width – living theronts (μm)	20.1	19.8	2.3	0.5	11.2	17.2	25.4	20
Number of algal symbionts per ciliate	52.0	49.5	15.7	2.5	30.1	26.0	89.0	40
Size of living algal symbionts (μm)	5.9	5.8	0.6	0.1	11.1	4.8	7.3	31
Body, length – protargol impregnated trophonts (μm)	32.6	33.7	4.4	0.9	13.6	22.9	38.2	25
Body, width – protargol impregnated trophonts (μm)	19.7	19.6	2.0	0.4	10.3	14.6	23.3	25
Anterior body end to buccal cavity, distance (μm)	3.7	3.6	0.9	0.2	24.5	2.2	5.7	25
Anterior body end to macronucleus, distance (μm)	11.1	10.9	2.3	0.5	20.3	5.7	16.8	25
Anterior body end to excretory pore, distance (μm)	26.5	26.6	3.7	1.4	13.8	20.1	32.0	7
Macronucleus, length (μm)	9.6	9.5	1.7	0.3	17.9	6.5	13.6	25
Macronucleus, width (μm)	8.4	8.2	1.5	0.3	18.4	5.2	12.8	25
Micronucleus, length (μm)	4.3	4.4	0.5	0.1	11.7	3.2	5.4	25
Micronucleus, width (μm)	3.1	3.2	0.4	0.1	13.8	2.2	3.9	25
Buccal cavity, length (μm)	6.9	6.9	1.0	0.2	14.1	5.1	8.3	25
Buccal cavity, width (μm)	3.9	3.8	0.8	0.2	19.8	2.4	5.4	25
Adoral membranelle number 1, length (μm)	3.4	3.4	0.4	0.1	13.2	2.5	4.2	25
Adoral membranelle number 2, length (μm)	3.4	3.4	0.5	0.1	13.5	2.7	4.4	25
Adoral membranelle number 3, length (μm)	1.8	1.8	0.3	0.1	15.5	1.2	2.3	25
Excretory pores, number	1.3	1.0	0.5	0.2	38.0	1.0	2.0	7
Somatic kineties, number	23.0	23.0	0.9	0.2	3.9	21.0	25.0	25
Postoral kineties, number	2.0	2.0	0.0	0.0	0.0	2.0	2.0	25
Kinetids in a dorsal kinety, number	36.5	36.0	4.7	0.9	13.0	30.0	46.0	25
Aposymbiotic ciliates								
Body, length – living trophonts (μm)	40.5	41.0	5.1	0.9	12.6	26.2	48.1	31
Body, width – living trophonts (μm)	24.2	24.1	1.9	0.3	7.9	19.5	27.8	31
Body, volume – living trophonts (μm^3)	12,649	13,157	3,131	562	25	5,186	17,858	31
Body, length – living theronts (μm)	51.1	51.8	3.2	0.6	6.3	43.9	56.0	26
Body, width – living theronts (μm)	16.5	16.3	2.0	0.4	12.2	12.7	21.0	26

CV, coefficient of variation in %; M, median; Max, maximum; Min, minimum; *n*, number of measured specimens; SD, one standard deviation; SE; standard error of average.

Algal symbionts were identified as *Micractinium* sp. Data based, if not mentioned otherwise, on mounted, protargol impregnated trophonts from a green clonal culture. In addition morphometric parameters of living trophonts and theronts of an aposymbiotic culture are listed.

DNA extraction and sequencing

DNA from a clonal aposymbiotic *T. utricullariae* culture was extracted with the DNeasy Blood and Tissue kit (Qiagen, Vento, the Netherlands). The aposymbiotic culture originated from a symbiont bearing clonal culture (basis for morphometric measurements) which was kept under aerobic conditions with over-saturating bacterial food. Subsequently, the partial *cox1* gene was amplified using Platinum® PCR Super Mix High Fidelity (Invitrogen), the forward primer COI-FW 5′-ATGTGAGTTGATTTTATAGAGCAGA-3′ (Chantangsi et al. 2007) and the reverse primer FolB 5′-TA AACTTCAGGGTGACCAAAAAATCA-3′ (Folmer et al. 1994). The PCR reaction was performed under the following conditions: initial denaturation at 94 °C for 180 s, five cycles of 94 °C for 30 s, 45 °C for 60 s, 68 °C for 75 s and 35 cycles of 94 °C for 30 s, 55 °C for 60 s, 68 °C for 75 s, and final extension at 68 °C for 600 s (modified from Strüder-Kypke and Lynn 2010). GenElute™ PCR Clean-Up Kit (Sigma, St. Louis, MO) served as tool for the purification of the PCR products, which were subsequently sequenced with the same primers and ABI BigDye chemistry on an ABI 3130x Genetic Analyzer (Applied Biosystems, Waltham, MA).

The amplification of the 18S rRNA gene of *T. utricullariae* was done with GoTaq® Green Master Mix (Promega, Madison, WI) and the primer pair EK82f 5′-GAAACTGC GAATGGCTC-3′ (Auinger et al. 2008)/EUK239r 5′-TGATCC TTCYGCAGGTTCAC-3′ (Moon-van der Staay et al. 2001). The conditions for the PCR were as follows: denaturation at 94 °C for 300 s, 30 cycles of 94 °C for 15 s, 50 °C for 60 s, 72 °C for 180 s and a final extension of 300 s at 72 °C. PCR products were purified and sequenced as described above.

In order to sequence the ribosomal genes (18S rRNA gene, ITS1, 5.8S rRNA gene and ITS2) of the algal symbiont, DNA was extracted with the DNeasy Blood and Tissue kit (Qiagen) from a pure culture. PCR reactions were

run using GoTaq® Green Master Mix (Promega) and the following primer pairs: EUK238f 5′-ACCTGGTTGATCCTGC CAG-3′/EUK239r (Moon-van der Staay et al. 2001) and INT-4F 5′-TGGTGAAGTGTTCGGATTGG-3′/HLR3R 5′-TCCC AAACAACCCGACTCT-3′ (Hoshina et al. 2005) under the previously described conditions. The generated amplicons were purified and sequenced as described above. All sequences were deposited in GenBank with the accession numbers (LT605001 – LT605003).

Phylogenetic analysis

Two phylogenetic trees for *T. utriculariae* n. sp. (18S rRNA and *cox1* genes) and one for the algal symbiont (18S rRNA gene combined with ITS2) were calculated with different tools. The online aligner SINA (Pruesse et al. 2012) and the software package ARB (Ludwig et al. 2004) were used for the alignment and manual curation of the 18S rRNA genes (1,613 positions). Only sequences of *Tetrahymena* spp. (52 isolates) which had additionally available *cox1* sequences were included in the analysis (see Table S1). Sequences from the genus *Ichthyophthirius* (KJ690571 and U17354) were used as outgroup. The RAxML algorithm (Stamatakis et al. 2008) served as tool for the calculation of a bootstrapped (1,000 iterations) maximum likelihood (ML) tree using the GTR (General Time Reversible) model with Γ distribution for rate heterogeneity among sites. Posterior probabilities (four chains; 100,000 generations) from Bayesian interference (BI) obtained with the ExaBayes software package (©The Exelixis Lab) were added to the ML tree where topologies of the trees generated by the two different methods were congruent. Finally, branches with low bootstrap support (< 50%) were collapsed.

The phylogenetic analysis of the *cox1* sequences was built based on the alignment by Quintela-Alonso et al. (2013). The alignment was supplemented and calculated again with all newly available sequences of *Tetrahymena cox1* genes from GenBank using the freely available software Unipro UGENE 1.23. Short sequences (≤ 634 nt) together with duplicates (identical sequences with two accession numbers) were deleted (Table S1) and the alignment was manually corrected. In total, it compromised 188 sequences (987 positions) of *Tetrahymena* isolates along with seven sequences of *Ichthyophthirius multifiliis* as outgroup. For the phylogenetic analysis we applied the neighbor-joining algorithm with an interior-branch-test (Dopazo 1994; Li 1989; Nei et al. 1985; Rzhetsky and Nei 1992), implemented in the program MEGA v7.014 (Tamura et al. 2011), using the Jukes Cantor distance model with 1,000 replicates and pairwise deletion (Quintela-Alonso et al. 2013). As previously described, the interior branch test is highly appropriate in cases where the tree topology is predefined (Sitnikova 1996). Finally, the phylogenetic distance was calculated by using the pairwise distance, also supplied by MEGA.

The phylogenetic analysis of the algal symbiont (Chlorophyta, Trebouxiophyceae, Chlorellaceae) was done based on the concatenated 18S rRNA gene sequence (without introns) and the ITS2 sequence (2,219 positions). Primary sequence information combined with their individual secondary structures increases the accuracy and robustness of the resulting phylogenetic tree (reviewed in Wolf et al. (2014)). Thus, the state of the art methodology recently described by Heeg and Wolf (2015) was applied for the phylogenetic reconstruction of Chlorellaceae including the algal symbiont of *T. utriculariae*. From this publication we also extracted the 60 sequences (concatenated 18S rRNA gene and ITS2) with individual secondary structures (see file S1 of the supporting information in Heeg and Wolf (2015)). First, the secondary structures had to be added to the gene sequences of the algal symbiont. The RNA structure was taken from *Actinastrum hantzschii* FM205841 (99.76% sequence similarity) and the secondary structure of its ITS2 was predicted by homology modeling using a relevant template (Selig et al. 2008). Subsequently, a "xfasta file" (sequence-structure information of the concatenated 18S rRNA gene + ITS2) of the algal symbiont was generated and added to the 60 extracted Chlorellaceae sequences (with *Chloroidium ellipsoideum* FM946015 and *Chlorella saccharophila* FM946000 as outgroup). The software 4SALE v1.7 (Seibel et al. 2008) was subsequently used for a global multiple sequence alignment with simultaneous consideration of the primary sequence and the secondary structure. Using this alignment a ML tree was calculated with "phagorn" (Schliep 2011) which is implemented in R (R Core Team 2014). We used the R script available from the 4SALE homepage at http://4sale.bioapps.biozentrum.uni-wuerzburg.de. Finally, a BI tree was calculated as described above using the alignment generated with 4SALE. In case of congruent topologies of both trees, posterior probabilities were added to the ML tree.

RESULTS

Description of *Tetrahymena utriculariae* n. sp

Sizes of living symbiont bearing trophonts (Table 1) are 36.7 × 27.4 μm ($n = 31$), resulting in an average cell volume of 14,543 μm^3. Measurements on protargol-impregnated ciliates show a shrinkage of fixed and stained specimens (Table 1). Ovate ciliate cells (trophonts) are neither very flexible nor contractile. The globular macronucleus of protargol-impregnated specimens (9.6 × 8.4 μm) is in the central or slightly posterior position (Fig. 1B, 2B). The micronucleus (4.3 × 3.1 μm) is positioned at the macronucleus (Fig. 1B, 2C), sometimes difficult to see in vivo but clearly recognizable after staining with DNA specific dyes (e.g. DAPI) or after protargol impregnation. The oral apparatus is typical for the genus *Tetrahymena*. It consists of one undulating membrane on the right side of the buccal cavity and three oral membranelles on the left (Fig. 1A and Table 1). The buccal cavity has a size of 6.9 × 3.9 μm on average in portargol-impregnated specimens (Table 1). The contractile vacuole is slightly subterminal and has in most cases one and occasionally two excretory pores in dorsal position (Fig. 1B). Trophonts have on average 23 somatic kineties including two

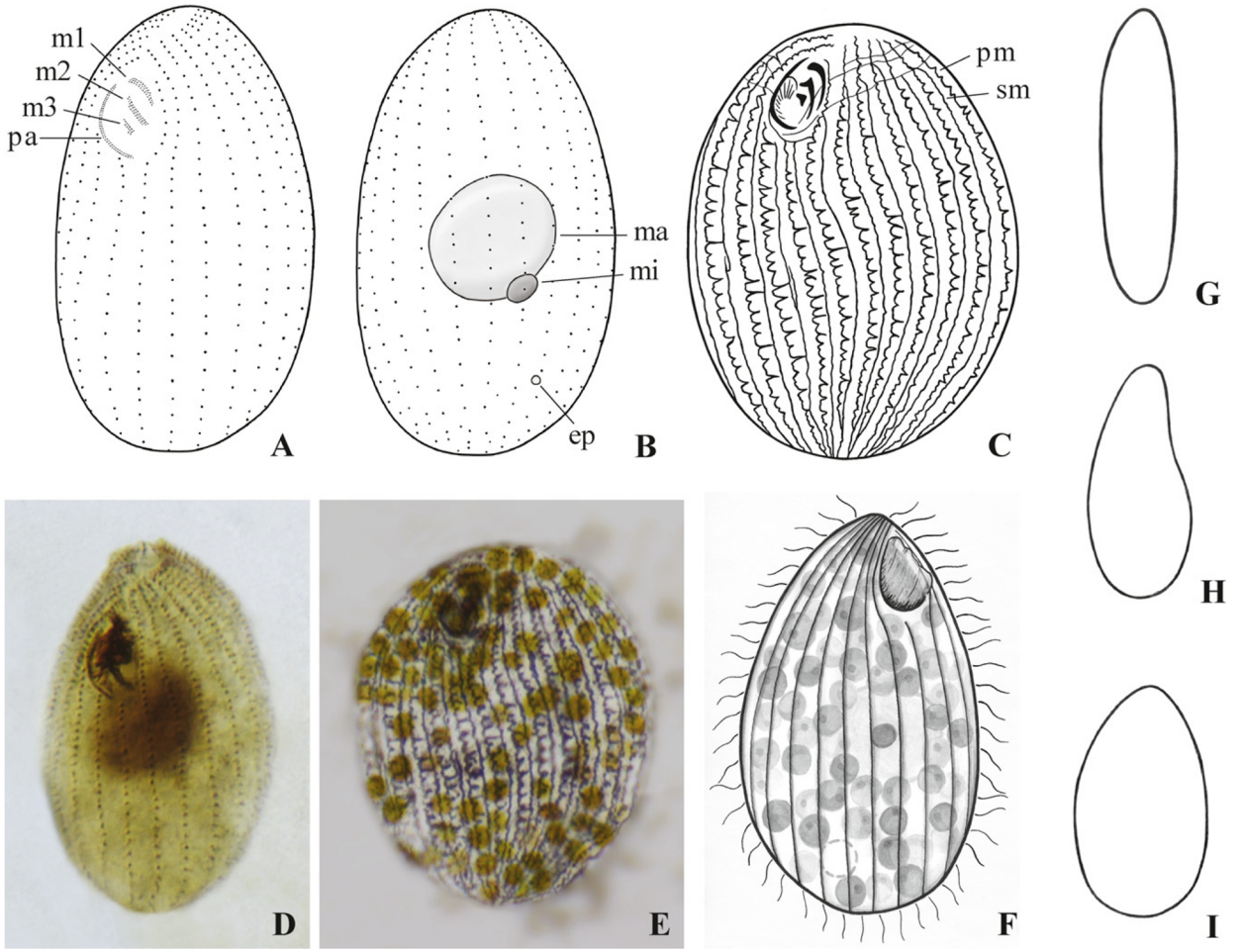

Figure 1 *Tetrahymena utriculariae* n. sp. after protargol impregnation (**A, B, D**), after "dry" silver nitrate impregnation (**C, E**), and from life (**F–I**). (A, B) Ciliary pattern of ventral and dorsal side of a trophont. (C) Silverline pattern of ventral side of a trophont. (D) Photomicrograph of a protargol stained green trophont, ventral view. (E) Photomicrograph of a "dry" silver nitrate impregnated green trophont, ventral view. (F) Right lateral view of a living green trophont. (G–I) Shape of a typical theront (G), lateral (H) and ventral (I) view of a typical trophont. ep, excretory pore; m1–m3, adoral membranelles; ma, macronucleus; mi, micronucleus; pa, paroral membrane; pm, primary silverline meridian; sm, secondary silverline meridian.

postoral kineties (Fig. 1A, B and Table 1). The silverline pattern (Fig. 1C,E) is of type 2, i.e. it shows primary meridians connecting the kinetids and secondary meridians (for further explanation of silverline patterns we refer to Quintela-Alonso et al. 2013). Trophonts harbor on average 52 algal symbionts (average diameter and standard deviation of living algae = 5.9 ± 0.6 μm) uniformly distributed within the ciliate cell (Fig. 2 and Table 1).

Tetrahymena utriculariae shows a "*Tetrahymena pyriformis* – like" life cycle (Fig. 2, 3). The real dominant life stage in trap fluids are green trophonts. Besides trophonts, conjugating individuals, dividers, and occasionally resting cysts could be observed. In stressed clonal cultures we could induce the formation of theronts. These elongated, spindle-shaped cells (49.8 × 20.1 μm; Table 1) show a higher swimming speed than gliding trophonts. Theronts have one clearly recognizable (in vivo) elongated caudal cilium (Fig. 2H) which is not observed for trophonts.

The cultivation of green ciliates under aerobic conditions and sufficient bacterial food particles resulted occasionally in a loss of algal symbionts. We could even generate algal free, aposymbiotic ciliate cultures. Sizes of living aposymbiotic trophonts are 40.5 × 24.2 μm (n = 31), resulting in an average cell volume of 12,649 μm^3 (Table 1). These aposymbiotic isolates can be maintained for several months, however, only by regular feeding with new bacterial food sources. We observed all life stages documented for the green counterparts also for the aposymbiotic cells (Fig. 2, 3), except conjugating cells. However, aposymbiotic ciliates can be re-infected by the addition of the isolated algal symbiont within several weeks (Šimek et al. 2016). Notably, colorless ciliates were never observed in trap fluids.

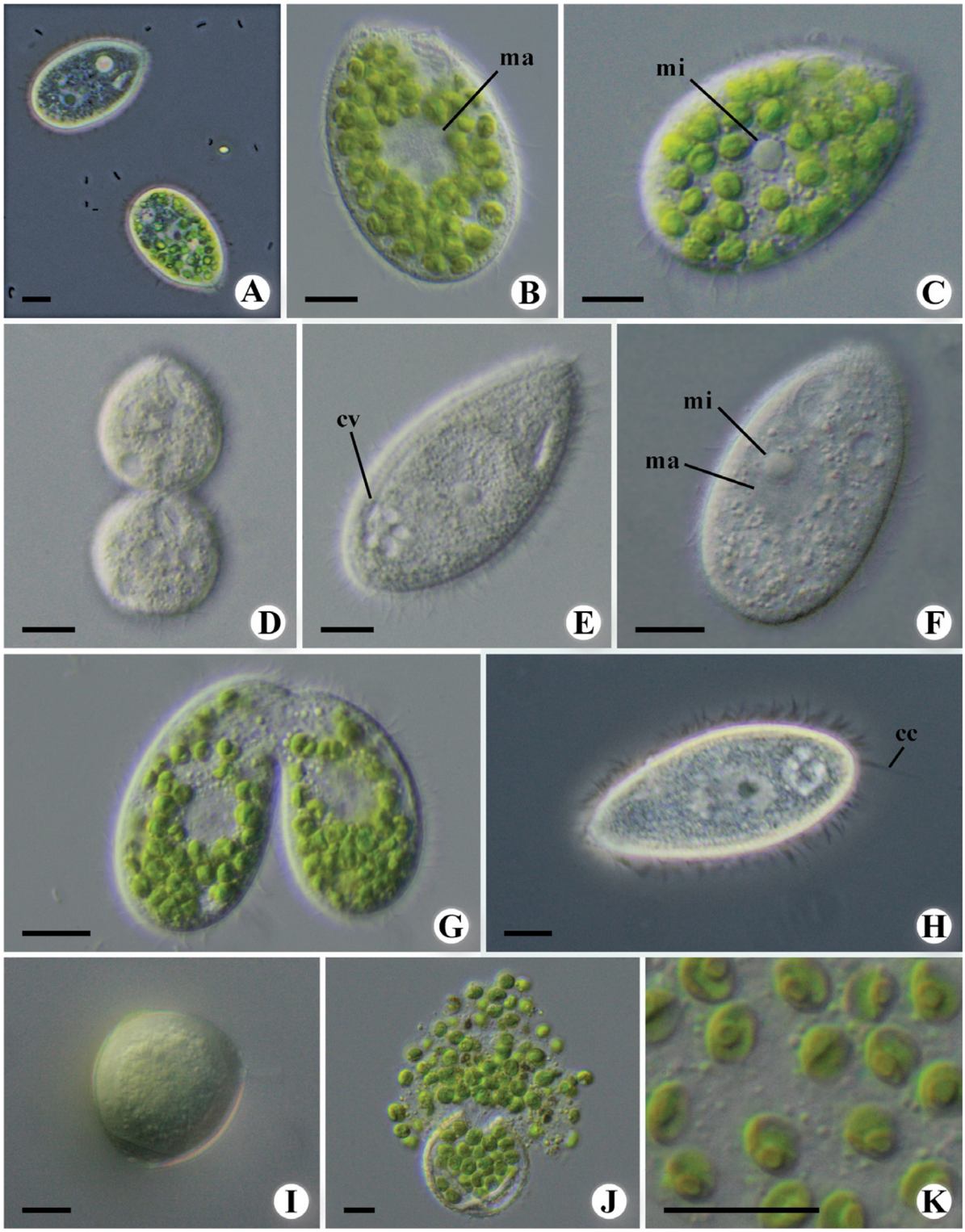

Figure 2 Photomicrographs of living green and aposymbiotic *Tetrahymena utriculariae* n. sp. (**A**) An aposymbiotic and a green trophont. (**B, C**) Green trophonts. (**D**) Late, aposymbiotic divider. (**E, F**) Aposymbiotic trophonts. (**G**) Conjugation pair of green ciliates. (**H**) Aposymbiotic theront. (**I**) Resting cyst. (**J**) A green cyst was dissected under microscopic control. (**K**) The isolated algal symbiont *Micractinium* sp. cc, caudal cilium; cv, contractile vacuole; ma, macronucleus; mi, micronucleus. Scale bars = 10 μm.

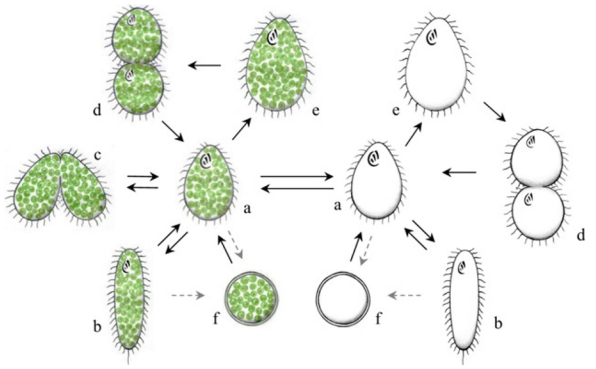

Figure 3 Observed stages within life cycles of green (left) and aposymbiotic (right) *Tetrahymena utricullariae* n. sp. Observed transformations are indicated by black arrows. Possible, but not observed transformations are shown by dashed gray arrows. a, throphont; b, theront; c, conjugation pair; d, cell dividers; e, enlarged trophont before cell division; f, resting cyst. Modified from Lynn and Doerder (2012).

Molecular identity and phylogenetic analysis of *Tetrahymena utricullariae*

The partial 18S rRNA gene sequence of *T. utricullariae* (1,643 unambiguous nucleotides, GC content 43.21%) was deposited under the accession number LT605001 at GenBank. The next hit at public databases for the 18S rRNA gene was *Tetrahymena malaccensis* (M26360) with a similarity of 99.76%. The sequence of the partial *cox1* gene (985 unambiguous nucleotides) was deposited under the accession number LT605002 at GenBank. The highest similarity (90.26%) was found with a *cox1* sequence of *T. thermophila* (GU439297).

As the phylogenetic analysis of the 18S rRNA gene alone (Fig. S1) was not sufficient, the *cox1* gene was used to determine the phylogenetic position of *T. utricullariae* (Fig. 4). In total 188 sequences were implemented in the analysis (Table S1), which showed a highly similar topology as previously published analyses (Chantangsi et al. 2007; Kher et al. 2011; Quintela-Alonso et al. 2013). The new species nested with medium support on a separate branch between the *T. thermophila* cluster (Fig. 4), containing 28 highly similar sequences, one sequence of *T. malaccensis*, one sequence of *T. farahensis* and a cluster of 10 sequences from a new *Tetrahymena* species, yet unnamed (Kher et al. 2011). The difference of the new species compared to its probably next relative, *T. thermophila*, was 9.74%, while the distance to *T. malaccensis* (EF070291) was 11.37%.

Habitat and ecology of *Tetrahymena utricullariae*

Tetrahymena utricullariae numerically dominates the eukaryotic community of commensals/mutual partners in traps of *U. reflexa*, reaching abundances of up to 50,000 cells per milliliter of trap fluid (Šimek et al. 2016). Green *T. utricullariae* inside traps are bacterivorous, with individual ingestion rates ranging from 260 to 340 bacteria/ciliate/h. Due to the high numbers of ciliates inside trap

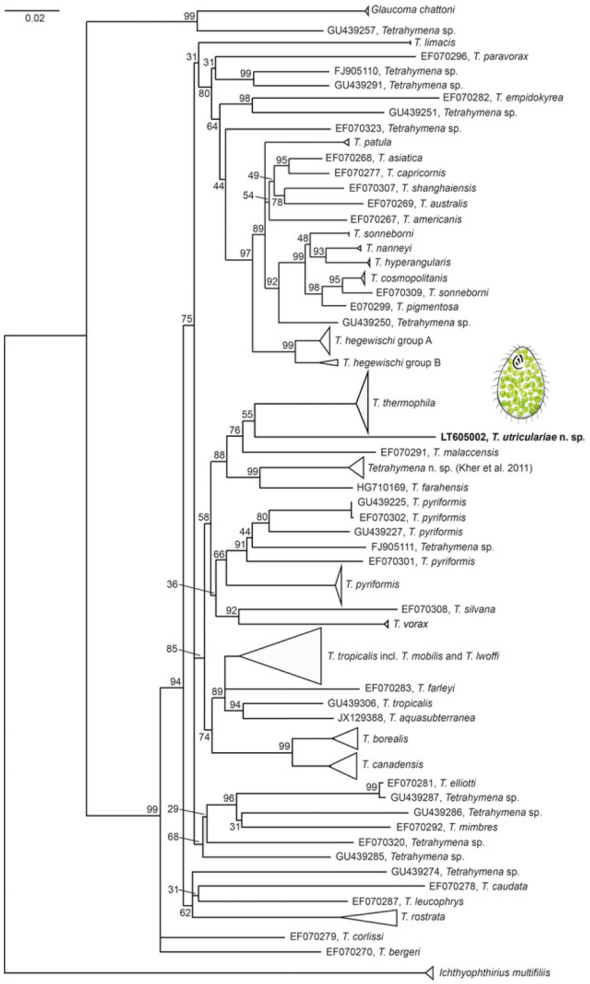

Figure 4 Phylogenetic analysis of 189 *Tetrahymena* isolates including *T. utricullariae* n. sp. (bold). A neighbor-joining tree was generated with an interior-branch test based on *cox1* gene sequences. *Ichthyophthirius multifiliis* was used as outgroup. Accession numbers for sequences inside collapsed cluster are listed in Table S1. Numbers at the branches represent bootstrap values. Scale bar: number of substitutions per site.

fluids, their total grazing rates lead to a fast bacterial turnover (Šimek et al. 2016).

The biogeography of *U. reflexa* is not confined to Botswana but the plant is endemic to Africa. We checked numerous feeding traps of seven other *Utricularia* species (*U. australis*, *U. bremii*, *U. aurea*, *U. inflata*, *U. purpurea*, *U. stygia*, *and U. vulgaris)* for the occurrence of *T. utricullariae*, however, at present we have to state that this ciliate species could be only found in *U. reflexa* (for further details see Šimek et al. 2016).

Molecular identity and phylogenetic analysis of the algal symbiont

The sequence of the algal symbiont, spanning almost the entire 18S rRNA gene, the ITS1, the 5.8S rRNA gene, the

ITS2 and the partial 28S rRNA gene (2,681 nt), was deposited under the accession number LT605003 at GenBank. The next hit at public databases was *Micractinium* sp. ehime (JX889639) with a sequence similarity of 98.5%. In the recent publication from Heeg and Wolf (2015) a detailed phylogenetic analysis of taxa belonging to the Chlorellaceae (sensu stricto + species name available) was conducted. Sequence-structure analysis of the 18S rRNA genes and the ITS2 genes alone was compared with the phylogenetic reconstruction using both of these genes in combination. The authors assumed to have more accuracy using the concatenated data set. For reasonable comparison, we thus followed their approach and included the same taxa and merely added the sequence of the algal symbiont (Fig. 5). According to our phylogenetic analysis, the algal symbiont clustered with high bootstrap support inside the *Micractinium* spp. cluster, basal to *M. pusillum* (FM205875), *M. belenophorum* (FM205879 and FM205880), and *A. hantzschii* (FM205841, FM205884). This was also true for the BI tree but the algal symbiont directly clustered with *M. pusillum* making up the sister group to the two *M. belenophorum* and the two *A. hantzschii* sequences (no posterior probabilities for the respective branches). The relative great distance and the separated positioning prevented us from affiliating the algal symbiont to a described species. It rather represents a novel species in the genus *Micractinium*.

DISCUSSION

Morphological comparison with congeners

A morphological comparison of *T. utriculariae* with closely related congeners (*T. farahensis*, *T. malaccensis*, *T. thermophila*) is difficult as the first two species were established without clear morphological descriptions (Table 2). We had to exclude the phylotype *Tetrahymena* n. sp. presented by Kher et al. (2011) from the comparison as it was only characterized by *cox1* gene sequences without defining a type strain (see Table S1 for further details).

The most striking difference within the congeners concerns the presence/absence of symbiotic algae in natural ciliate populations. Only *T. utriculariae* harbors endosymbionts, although this character may be lost under defined culture conditions (aerobic cultivation with dense bacterial food organisms). *Tetrahymena utriculariae* can form cysts, which was observed neither for *T. thermophila* nor for *T. malaccensis* (Table 2). All three species have at least in natural populations a micronucleus. The morphological comparison of *T. utriculariae* with the closest relative, *T. thermophila* (Collins 2012), shows some slight differences: *T. utriculariae* has on average 23 kineties (range 21–25), whereas *T. thermophila* has on average 17–21 kineties (range 15–25). The average number of kinetids in a kinety are 36.5 and 30 for *T. utriculariae* and *T. thermophila*, respectively. *Tetrahymena utriculariae* has usually one excretory pore (range one to two), whereas *T. thermophila* has on average two (range 1–3). A clear difference is obvious from the sizes of living trophonts. Even the aposymbiotic trophonts of *T. utriculariae* (on average 40.5 × 24.2 μm) are by 10 μm smaller than typical specimens of *T. thermophila* (on average 50 × 30 μm; Collins 2012).

Morphological comparison with similar species

Tetrahymena is a young genus-group name (Furgason 1940) and its type species, *T. pyriformis* (*T. geleii* is considered as a synonym; Aescht 2001), was classified in various other genera, e.g. *Glaucoma*, *Leucophrys*, and *Sathrophilus* (Foissner et al. 1994). Thus, we did a literature search for species showing similarities to *T. utriculariae* in the genus *Tetrahymena* and the mentioned genera.

Dujardin (1838) described a green species, *Glaucoma viridis*, which might have some similarities to *T. utriculariae*. In June 1837, the author discovered a mass development of *G. viridis* in an old wine barrel, containing tartar (dried rest of the wine) and rainwater. Obviously, quality of the one month old water was not the best anymore as the author spoke about '*l'eau s'était putréfiée*', meaning moldy water (Dujardin 1841). *Glaucoma viridis* had a size of 30–50 μm and a buccal cavity which seemed to be typical for the genus *Glaucoma* (see figure G4 on Plate 15 in Dujardin 1838 and figure 9 on Plate 8 in Dujardin 1841). Nevertheless, the buccal cavity spanned over at least one-third of the total cell length. This morphological feature allows the differentiation between *G. viridis* and *T. utriculariae*. According to Dujardin (1841), *G. viridis* contained several green "large" vacuoles which had "twelve to thirteen nodules". However, the author did not describe if these green vacuoles were ingested or symbiotic algal cells (likewise it is not obvious from the original drawings mentioned above). Unfortunately, there seems to be no other record of this species after the description by
Dujardin (1838, 1841).

Within the genus *Sathrophilus* we found one species similar to *T. utriculariae*. *Sathrophilus chlorophagus* (Kahl 1931) Corliss, 1960 has a similar size and shape (see figure 60, panel 33 in Kahl 1931). Free living specimens harbored often small green algae but were occasionally colorless. Cells had one elongated caudal cilium, conspicuous long cilia and a large buccal cavity which spanned over one-third of the total cell length. The latter two morphological features allow the differentiation between *S. chlorophagus* and *T. utriculariae*. *Sathrophilus chlorophagus* was abundant in a pond during winter but the exact type locality was not defined. Again, we could not find new records of this species after the description by Kahl (1931).

Another green ciliate with a similar shape as *T. utriculariae* was described by Penard (1922) as *Ophryoglena viridis* (see figure 146 in Penard 1922). Nevertheless, the ciliature of the buccal cavity, the high number of postoral kineties and the larger size of *O. viridis* (80 × 54 μm) allow a clear differentiation between the two species.

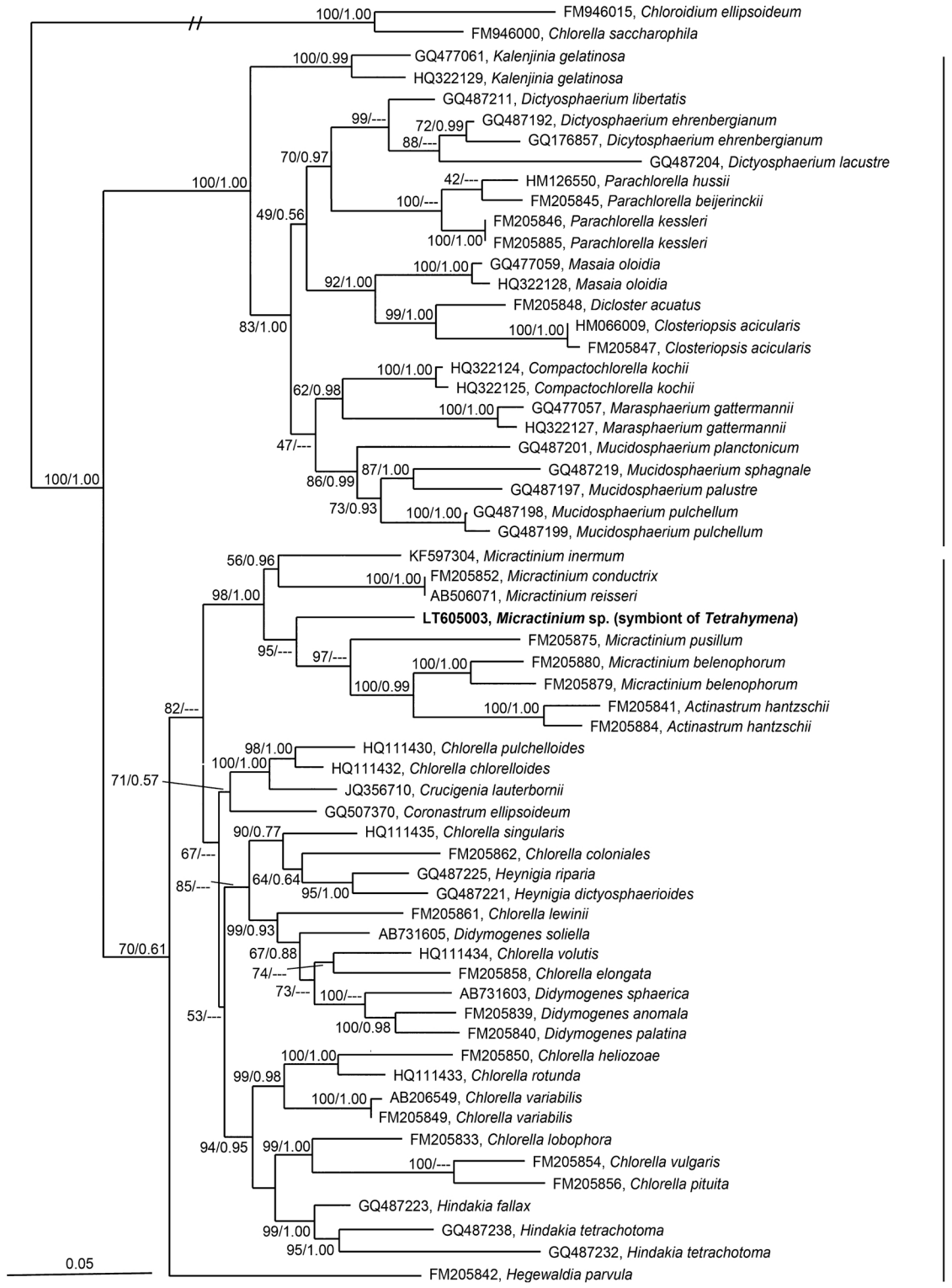

Figure 5 Maximum likelihood (ML) tree with posterior probabilities from Bayesian interference (BI) based on the concatenated ITS2 + 18S rRNA gene sequence-structure of 61 chlorellacean isolates. *Chloroidium saccharophilum* and *Chloroidium ellipsoideum* were used as outgroup. The algal symbiont (bold) affiliated with the *Micractinium* cluster. Numbers at the branches represent ML bootstrap value/BI posterior probabilities. Scale bar: number of substitutions per site.

Table 2. Brief characterization of *Tetrahymena* species related to *Tetrahymena utriculariae* n. sp. according to the *cox1* gene phylogeny

	Habitat	Algal endo-symbionts	Cysts	Mating	Micronucleus present (+)/ absent (−)	*Cox1* gene GenBank accession number	18S rDNA GenBank accession number	References
Tetrahymena utriculariae n. sp.	Traps of the aquatic plant *Utricularia reflexa*[a]	Yes[b]	Yes	Conjugation	+	LT605002	LT605001	This study
Tetrahymena farahensis	Wastewater treatment plant, Pakistan	No	Nd	Nd	Nd	HG710169	HE820726	Zahid et al. (2014)
Tetrahymena malaccensis	Swamp, K. Rantau Abang, Malaysia	No	No	Conjugation	+	EF070291	M26360	Simon et al. (1985)
Tetrahymena thermophila	Woods Hole, USA[c]	No	No	Conjugation	+/−	EF070310	M10932	Nanney and McCoy (1976)

Nd, not determined.

A detailed morphological comparison with the closest congener, *T. thermophila*, is given in the text. Table modified from Lynn and Doerder (2012).

[a]A detailed discussion of the type locality is given in the text.

[b]Symbiont bearing cultivated specimens may lose their symbionts when kept under aerobic conditions and dense bacterial food organisms. Nevertheless, we never found aposymbiotic cells in the natural habitat of *T. utriculariae*, i.e. in the traps of *Utricularia reflexa*.

[c]Strain B derived from a cross between wild strains WH-6 and WH-14.

Phylogenetic analysis and relation to other *Tetrahymena* species

The *cox1* gene is considered the most reliable DNA barcode to discriminate among different *Tetrahymena* species, as it is improving the resolution of most clades within the phylogenetic analysis, compared to the 18S and 28S rRNA gene (Chantangsi et al. 2007; Lynn and Strüder-Kypke 2006; Simon et al. 2008). When comparing phylogenetic analyses of 18S rRNA (Fig. S1) and *cox1* (Fig. 4) genes, a similar topology in general, with few exceptions, is recovered, indicating a monophyletic character of the genus *Tetrahymena*.

In our analysis of the *Tetrahymena cox1* dataset we recovered a topology supporting previous studies (Kher et al. 2011; Lynn and Doerder 2012; Quintela-Alonso et al. 2013). The application of the interior-branch-test, which is suitable for a given topology, increased the reliability and hence the bootstrap support within the tree (Quintela-Alonso et al. 2013; Sitnikova 1996). Analyzing the genetic distance of the *cox1* gene compared to other species, revealed a high distance of 9.74%. The intraspecific difference found regarding the *cox1* gene was described previously to range from 0% to 3.5%, with *T. thermophila* having the largest intraspecific range (Doerder 2014). Based on the high genetic distance, the ecological/physiological characteristics, and the habitat specificity (Šimek et al. 2016) we describe the strain from Třeboň (Czech Republic) as a new species, *T. utriculariae* n. sp.

Phylogenetic analysis of the algal symbiont (Chlorophyta, Trebouxiophyceae, Chlorellaceae)

Surprisingly, the addition of only one taxon, the algal symbiont of *T. utriculariae*, to the selected sequences of Heeg and Wolf (2015) changed the topology of the phylogenetic tree remarkably (compare our Fig. 5 with fig. 7 in Heeg and Wolf (2015)). Whereas the structure inside the *Parachlorella*-clade could be reproduced, there were structural changes inside the *Chlorella*-clade. Most conspicuous was the difference between the topologies concerning the *Micractinium* spp. isolates to which the algal symbiont clustered. In contrast with the polyphyly of this genus in the 18S rRNA + ITS2 gene tree from Heeg and Wolf (2015), in our tree all *Micractinium* spp. made up a monophyletic cluster including only two additional sequences from *A. hantzschii*. In contrast with this discrepancy regarding the two trees based on the concatenated data set, the phylogenetic ITS2 tree (Heeg and Wolf 2015) also revealed the monophyly of *Micractinium* spp. It would be tempting to claim the algal symbiont to be the missing link connecting the two parts of the *Micractinium* spp. cluster in the 18S rRNA + ITS2 gene tree. But since the importance of taxon sampling was reported earlier and also pointed out by Heeg and Wolf (2015), it should probably rather be treated as an extreme example illustrating the impact of taxon sampling on phylogenetic analysis.

Symbiosis with the alga *Micractinium* sp

Mutualistic symbioses between freshwater ciliates and green algae (often affiliated with Chlorophyta) can be found in various genera (e.g. *Askenasia*, *Coleps*, *Euplotes*, *Halteria*, *Paramecium*, *Stokesia*, *Vorticella*, etc. – for an overview see Foissner et al. (1999)). In nearly all cases, we find within the same genus both, "obligate" green and colorless species. The best studied symbiosis with algae concerns the species *Paramecium bursaria*. It is a real mutual relationship, whereby both partners profit from each other (see Fujishima and Kodama (2014) and

references therein). However, it was also shown, that ciliates can lose their symbionts due to experimental manipulations, e.g. cultivation in complete darkness with sufficient bacterial food. Nearly all algal symbionts can live outside the hosts as free cells, thus they can be successfully cultivated in monocultures (Pröschold et al. 2011). A reinfection of aposymbiotic *P. bursaria* (Summerer et al. 2007) but also of other ciliate species with isolated algal strains is possible within a few days to weeks (see also fig. 4 in Šimek et al. 2016).

All these aspects are also valid for *T. utricularlae* and its symbiont *Micractinium* sp., thus it seems to be a well-established ciliate algae symbiosis. However, one might speculate about the origin of this symbiosis. In principle, there are two ways how algae are taken up by ciliate hosts: (i) by incidental ingestion or (ii) by repetitive phagocytosis of algae as positively selected food source (Fujishima and Kodama 2014). As most *Tetrahymena* species are rather bacterivorous, an incidental incorporation of algal cells seems more likely. In case of *T. utricularlae* we suppose that the lack of oxygen in traps (Adamec 2007) was the major selective force driving the evolution of this ciliate alga symbiosis. Notably, caught metazoan prey first dies in traps of *U. reflexa* due to anoxic conditions and not primarily due to enzymatic lysis (Adamec 2007). All *Tetrahymena* species are aerobes, as they don't have adequate organelles, i.e. hydrogenosomes which are found in anaerobic ciliates. Thus, the symbiosis with oxygen producing algae is the prerequisite for *T. utricularlae* to survive in this habitat. That algal symbionts can indeed supply their ciliate hosts with oxygen was already demonstrated for *Paramecium bursaria* (Reisser 1980) and natural ciliate assemblages (Finlay et al. 1996).

Bacterial uptake rates of *T. utricularlae* (Šimek et al. 2016) may point to a second role of algal symbionts. Individual bacterial ingestion rates were low in comparison to other similar sized bacterivorous ciliate species and thus not allowing for the assumed rapid ciliate growth in trap fluid. Probably algal symbionts do also support *T. utricularlae* with diverse metabolites, however, we have no proof yet for this assumption.

Interestingly, Nakajima et al. (2009, 2013)) could induce the uptake of a green alga (*Micractinium* sp. ehime) as symbiont by *T. thermophila* in a five year long-term co-cultivation microcosm, with *Escherichia coli* as bacterial food source. It seemed that even a more cooperative algal phenotype evolved after five years of co-cultivation which allowed the ciliate ancestor a longer lifespan in experimental tests (Germond et al. 2013). However, ciliates were permanently confronted with an extraordinary high number of algae ($5*10^6$ algal cells/ml) during co-cultivation (Nakajima et al. 2009), which does not reflect natural circumstances. In contrast, numbers of *Micractinium* sp. in trap fluids of *U. reflexa* were always below the limit of detection and also abundances reported for freshwater systems are much lower. However, it is remarkable that the *Micractinium* sp. strain used in their experiment was found to be next hit in public databases to the algal symbiont of *T. utricularlae*. In combination with the close relatedness of the hosts, this opens up speculations about an ancient origin of the symbiosis between *T. thermophila* and *Micractinium* sp. Most probably prerequisites for the seemingly "de novo" established symbiosis reported by Nakajima et al. (2009, 2013)), have been acquired already during a former coexistence. In other words ancestors of the symbiotic partners might have lived together and established the symbiotic interaction already in former times.

Habitat specificity of *Tetrahymena utricularlae*

Its natural environment, fluids inside traps of *U. reflexa*, is a harsh habitat, characterized by (i) very low, often anoxic conditions (Adamec 2007), (ii) low pH values (average 5.1), but (iii) extremely high concentrations of dissolved nutrients (Sirová et al. 2009). We checked numerous feeding traps of seven other *Utricularia* species, but detected *T. utricularlae* only in two *U. reflexa* populations form Botswana and Zambia (see also Šimek et al. 2016). It is important to note that *U. reflexa* is endemic to Africa. The here studied aquatic plants have been collected in the Okavango Delta (Botswana) and are cultivated at the Institute of Botany CAS (Třeboň, Czech Republic) since 2005. Thus, we have to debate whether *T. utricularlae* invaded plants during cultivation in the culture collection, or ciliates were transported together with *U. reflexa* inside the feeding traps at that time. The aquaria with *U. reflexa* are not covered, thus, it cannot be excluded that *T. utricularlae* has been introduced from the Czech nature, e.g. also with zooplankton used for plant feeding. However, several arguments supply the second thesis that this ciliate species was transferred together with *U. reflexa* from Africa to Europe: (i) *T. utricularlae* has been found neither in other native Czech *Utricularia* species nor in species of the same genus which have been co-cultivated for several months together with *U. reflexa* (for further details see Šimek et al. 2016). (ii) Green ciliates were discovered in cultivated *U. reflexa* already in August 2009 (see fig. 2A in Płachno et al. 2012) but ciliates were miss-identified as *Paramecium bursaria*. The anterior position of the cytostome and cell shapes, documented in fig. 2A of Płachno et al. (2012), definitely speak for the first photographic evidence of *T. utricularlae*. We have observed this ciliate species for the first time in the year 2014 in the Czech Republic, when we inspected fresh trap fluids of *U. reflexa*. (iii) All autecological data about *T. utricularlae* indicate that ciliates are not only commensals but probably have a mutualistic relationship with *U. reflexa*, forming a complex symbiosis (Šimek et al. 2016). Ciliates are protected inside the traps from predators and supported with bacterial food and probably saturating dissolved nutrients. On the other hand, ciliates are efficient and, moreover, the only regulators of the bacterial standing stock inside traps. It is very unlikely, that this relationship developed within a few years during the period when *U. reflexa* was cultivated in Třeboň (Czech Republic). (iv) *T. utricularlae* seems to be not a cosmopolitan species. Regarding the extensive research activities on *Tetrahymena* and related

genera, the peculiar green species would have been noticed by morphologists or recently, its sequence would have appeared in sequencing data. Both evidences were not provided until now (but see also our comparison with similar species records above).

In summary, arguments prevail which speak for an endemic, very specialized ciliate species. Concerning the type locality we mention that *U. reflexa* plants were collected from the Okavango Swamp north from Maun in Botswana. However, our type material of *T. utriculariae* was isolated from *U. reflexa* specimens cultivated in the aquatic plant collection of the Institute of Botany CAS, Section of Plant Ecology in Třeboň (Czech Republic). To get a final proof that *T. utriculariae* is indeed a common symbiont of African *U. reflexa* plants it will be worth to conduct an expedition to the Okavango Delta in the near future.

TAXONOMIC SUMMARY

Class Oligohymenophorea de Puytorac et al., 1974
Order Tetrahymenida Fauré-Fremiet in Corliss, 1956
Family Tetrahymenidae Corliss, 1952
Genus *Tetrahymena* Furgason, 1940
Tetrahymena utriculariae n. sp.

Diagnosis. Green ciliates with symbiotic algae of the genus *Micractinium* (Chlorophyta, Chlorellaceae). Size of living ovate trophonts 36.7 × 27.4 μm on average. Theronts (49.8 × 20.1 μm) ellipsoidal. On average 52 algae per ciliate cell. One globular macronucleus. One globular micronucleus. Contractile vacuole subterminal. On average 23 somatic kineties including two postoral ones. Cytostome typical for the genus. Life cycle includes trophonts, theronts, conjugating cells, dividing cells and occasionally resting cysts. Theronts with one elongated caudal cilium. Aposymbiotic specimens (without algal symbionts) with same life cycle, except conjugating cells (not observed up to now).

Type material. The slide with the protargol-impregnated symbiont bearing holotype and several paratypes as well as a paratype slide with "dry" silver-nitrate impregnated symbiont bearing and aposymbiotic ciliates have been deposited in the Biology Centre of the Museum of Natural History in Upper Austria, Linz, under the accession numbers 2016/116 and 2016/117, respectively. Relevant specimens have been marked by black circles on the coverslip. In addition, one paratype QPS (quantitative protargol staining) slide with several symbiont bearing specimens has been also deposited (accession number 2016/118).

Type habitat. Inside carnivorous traps of the submerged aquatic plants *Utricularia reflexa*.

Type locality. Okavango Swamp north from Maun in Botswana (for some uncertainties see discussion). *Utricularia reflexa* specimens, from which the type material of *T. utriculariae* was isolated, are cultivated in the aquatic plant collection of the Institute of Botany CAS, Section of Plant Ecology, 379 82 Třeboň, Czech Republic.

Etymology. The species-group name *utriculariae* refers to the aquatic plant *Utricularia reflexa*. *Utriculariae* is the genitive of *Utricularia* and means that the described ciliates are closely associated with these plants. Up to now, the ciliate species was only detected in the carnivorous traps of
U. reflexa.

Gene sequence. The GenBank accession numbers for the partial 18S rRNA and *cox1* gene sequences of the ciliate are LT605001 and LT605002 respectively. The GenBank accession number for the partial 18S rRNA gene, the ITS1, the 5.8S rRNA gene, the ITS2 and the partial 28S rRNA gene of the symbiotic algae (*Micractinium* sp.) is LT605003.

ACKNOWLEDGMENTS

This study was supported by the Swiss National Science Foundation (310030E-160603/1) awarded to Thomas Posch and the Grant of the Czech Science Foundation (13-00243S) awarded to Karel Šimek. Additional support provided the grant of the Faculty of Science, University of South Bohemia (GAJU 04-145/2013/P). The study was also partly supported (to Lubomír Adamec) by the Long-term research developmental project (RVO 67985939). We also thank Bettina Eugster and Estelle Bruni for their excellent laboratory assistance. Finally, we thank two anonymous reviewers for their valuable comments on the first version of the article.

LITERATURE CITED

Adamec, L. 2007. Oxygen concentrations inside the traps of the carnivorous plants *Utricularia* and *Genlisea* (Lentibulariaceae). *Ann. Bot.*, 100:849–856.

Adamec, L. 2012. Firing and resetting characteristics of carnivorous *Utricularia reflexa* traps: physiological or only physical regulation of trap triggering? *Phyton (Horn, Austria)*, 52:281–290.

Adamec, L. 2015. Regulation of the investment in carnivory in three aquatic *Utricularia* species: CO_2 or prey availability? *Phyton (Horn, Austria)*, 55:131–148.

Aescht, E. 2001. Catalogue of the generic names of ciliates (Protozoa, Ciliophora). *Denisia*, 1:1–350.

Auinger, B. M., Pfandl, K. & Boenigk, J. 2008. Improved methodology for identification of protists and microalgae from plankton samples preserved in lugol's iodine solution: combining microscopic analysis with single-cell PCR. *Appl. Environ. Microbiol.*, 74:2505–2510.

Cassidy-Hanley, D. M. 2012. *Tetrahymena* in the laboratory: strain resources, methods for culture, maintenance, and storage. *Methods Cell Biol.*, 109:239–276.

Chantangsi, C., Lynn, D. H., Brandl, M. T., Cole, J. C., Netrick, N. & Ikonomi, P. 2007. Barcoding ciliates: a comprehensive study of 75 isolates of the genus *Tetrahymena*. *Int. J. Syst. Evol. Microbiol.*, 57:2412–2425.

Collins, K. 2012. *Tetrahymena thermophila*. Methods in cell biology, Vol 109. Academic Press, Amsterdam. 452 p.

Doerder, F. P. 2014. Abandoning sex: multiple origins of asexuality in the ciliate *Tetrahymena*. *BMC Evol. Biol.*, 14:112–125.

Doerder, F. P. & Brunk, C. 2012. Natural populations and inbred strains of *Tetrahymena*. *Methods Cell Biol.*, 109:277–300.

Dopazo, J. 1994. Estimating errors and confidence intervals for branch lengths in phylogenetic trees by a bootstrap approach. *J. Mol. Evol.*, 38:300–304.

Dujardin, F. 1838. Mémoires sur l'organisation des Infusoires. *Ann. Sci. Nat. Zool. (Sér. 2)*, 10:230–315.

Dujardin, F. 1841. Histoire naturelle des zoophytes. Infusoires, comprenant la physiologie et la classification de ces animaux, et la manière de les étudier à l'aide du microscope. Libraire Encyclopédique de Roret, Paris. 648p.

Finlay, B. J., Maberly, S. C. & Esteban, G. F. 1996. Spectacular abundance of ciliates in anoxic pond water: contribution of symbiont photosynthesis to host respiratory oxygen requirements. *FEMS Microbiol. Ecol.*, 20:229–235.

Foissner, W. 2014. An update of 'basic light and scanning electron microscopic methods for taxonomic studies of ciliated protozoa'. *Int. J. Syst. Evol. Microbiol.*, 64:271–292.

Foissner, W., Berger, H. & Kohmann, F. 1994. Taxonomische und ökologische Revision der Ciliaten des Saprobiensystems. Band III: Hymenostomata, Prostomatida, Nassulida. *Informationsberichte des Bayer. Landesamtes für Wasserwirtschaft*. Issue 1/94.

Foissner, W., Berger, H. & Schaumburg, J. 1999. Identification and ecology of limnetic plankton ciliates. *Bavarian State Office for Water Management*, Issue 3/99.

Folmer, O., Black, M., Hoeh, W., Lutz, R. & Vrijenhoek, R. 1994. DNA primers for amplification of mitochondrial cytochrome c oxidase subunit I from diverse metazoan invertebrates. *Mol. Mar. Biol. Biotechnol.*, 33:294–299.

Fujishima, M. & Kodama, Y. 2014. Insights into the *Paramecium-Holospora* and *Paramecium-Chlorella* symbioses. *In:* Hausmann, K. & Radek, R. (ed.), Cilia and flagella. Ciliates and flagellates. Ultrastructure and cell biology, function and systematics, symbiosis and biodiversity. Schweizerbart'sche Verlagsbuchhandlung, Stuttgart. p. 203–227.

Furgason, W. H. 1940. The significant cytostomal pattern of the "*Glaucoma-Colpidium* group" and a proposed new genus and species, *Tetrahymena geleii*. *Arch. Protistenkd.*, 94:224–266.

Germond, A., Kunihiro, T., Inouhe, M. & Nakajima, T. 2013. Physiological changes of a green alga (*Micractinium* sp.) involved in an early-stage of association with *Tetrahymena thermophila* during 5-year microcosm culture. *Biosystems*, 114:164–171.

Guillard, R. R. L. & Lorenzen, C. J. 1972. Yellow-green algae with chlorophyllide c. *J. Phycol.*, 8:10–14.

Heeg, J. S. & Wolf, M. 2015. ITS2 and 18S rDNA sequence-structure phylogeny of *Chlorella* and allies (Chlorophyta, Trebouxiophyceae, Chlorellaceae). *Plant Gene*, 4:20–28.

Hoshina, R., Kato, Y., Kamako, S. & Imamura, N. 2005. Genetic evidence of "American" and "European" type symbiotic algae of *Paramecium bursaria* Ehrenberg. *Plant Biol.*, 7:526–532.

Jerome, C. A., Lynn, D. H. & Simon, E. M. 1996. Description of *Tetrahymena empidokyrea* n.sp., a new species in the *Tetrahymena pyriformis* sibling species complex (Ciliophora, Oligohymenophorea), and an assessment of its phylogenetic position using small-subunit rRNA sequences. *Can. J. Zool.*, 74:1898–1906.

Kahl, A. 1931. Urtiere oder Protozoa I: Wimpertiere oder Ciliata (Infusoria) 2. Holotricha ausser den im 1. Teil behandelten Prostomata. *Tierwelt Dtl.*, 21:181–398.

Kher, C. P., Doerder, F. P., Cooper, J., Ikonomi, P., Achilles-Day, U., Küpper, F. C. & Lynn, D. H. 2011. Barcoding *Tetrahymena*: discriminating species and identifying unknowns using the cytochrome c oxidase subunit 1 (*cox-1*) barcode. *Protist*, 162:2–13.

Li, W. H. 1989. A statistical test of phylogenies estimated from sequence data. *Mol. Biol. Evol.*, 6:424–435.

Ludwig, W., Strunk, O., Westram, R., Richter, L., Meier, H., Yadhukumar, Buchner, A., Lai, T., Steppi, S., Jobb, G., Förster, W., Brettske, I., Gerber, S., Ginhart, A. W., Gross, O., Grumann, S., Hermann, S., Jost, R., König, A., Liss, T., Lüßmann, R., May, M., Nonhoff, B., Reichel, B., Strehlow, R., Stamatakis, A., Stuckmann, N., Vilbig, A., Lenke, M., Ludwig, T., Bode, A. & Schleifer, K. H. 2004. ARB: a software environment for sequence data. *Nucl. Acid Res.*, 32:1363–1371.

Lynn, D. H. & Doerder, F. P. 2012. The life and times of *Tetrahymena*. *Methods Cell Biol.*, 109:9–27.

Lynn, D. H. & Strüder-Kypke, M. C. 2006. Species of *Tetrahymena* identical by small subunit rRNA gene sequences are discriminated by mitochondrial cytochrome c oxidase I gene sequences. *J. Eukaryot. Microbiol.*, 53:385–387.

Moon-van der Staay, S. Y., De Wachter, R. & Vaulot, D. 2001. Oceanic 18S rDNA sequences from picoplankton reveal unsuspected eukaryotic diversity. *Nature*, 409:607–610.

Nakajima, T., Matsubara, T., Ohta, Y. & Miyake, D. 2013. Exploitation or cooperation? Evolution of a host (ciliate)-benefiting alga in a long-term experimental microcosm culture. *Biosystems*, 113:127–139.

Nakajima, T., Sano, A. & Matsuoka, H. 2009. Auto-/heterotrophic endosymbiosis evolves in a mature stage of ecosystem development in a microcosm composed of an alga, a bacterium and a ciliate. *Biosystems*, 96:127–135.

Nanney, D. L. & McCoy, J. W. 1976. Characterization of the species of the *Tetrahymena pyriformis* complex. *Trans. Am. Microsc. Soc.*, 95:664–682.

Nei, M., Stephens, J. C. & Saitou, N. 1985. Methods for computing the standard errors of branching points in an evolutionary tree and their application to molecular data from humans and apes. *Mol. Biol. Evol.*, 2:66–85.

Penard, E. 1922. Études sur les infusoires d'eau douce. Georg & Cie, Genève. 331p.

Pfister, G., Sonntag, B. & Posch, T. 1999. Comparison of a direct live count and an improved quantitative protargol stain (QPS) in determining abundance and cell volumes of pelagic freshwater protozoa. *Aquat. Microb. Ecol.*, 18:95–103.

Płachno, B. J., Łukaszek, M., Wołowski, K., Adamec, L. & Stolarczyk, P. 2012. Aging of *Utricularia* traps and variability of microorganisms associated with that microhabitat. *Aquat. Bot.*, 97:44–48.

Plattner, H., Sehring, I. M., Schilde, C. & Ladenburger, E.-M. 2009. Pharmacology of ciliated protozoa – drug (in)sensitivity and experimental drug (ab)use. *Int. Rev. Cell Mol. Biol.*, 273:163–218.

Pröschold, T., Darienko, T., Silva, P. C., Reisser, W. & Krienitz, L. 2011. The systematics of *Zoochlorella* revisited employing an integrative approach. *Environ. Microbiol.*, 13:350–364.

Pruesse, E., Peplies, J. & Glöckner, F. O. 2012. SINA: accurate high-throughput multiple sequence alignment of ribosomal RNA genes. *Bioinformatics*, 28:1823–1829.

Quintela-Alonso, P., Nitsche, F., Wylezich, C., Arndt, H. & Foissner, W. 2013. A new *Tetrahymena* (Ciliophora, Oligohymenophorea) from groundwater of Cape Town, South Africa. *J. Eukaryot. Microbiol.*, 60:235–246.

Reisser, W. 1980. The metabolic interactions between *Paramecium bursaria* Ehrbg. and *Chlorella* spec. in the *Paramecium bursaria*-symbiosis. *Arch. Microbiol.*, 125:291–293.

Rzhetsky, A. & Nei, M. 1992. A simple method for estimating and testing minimum-evolution trees. *Mol. Biol. Evol.*, 9:945–967.

Schliep, K. P. 2011. Phangorn: phylogenetic analysis in R. *Bioinformatics*, 27:592–593.

Seibel, P. N., Müller, T., Dandekar, T. & Wolf, M. 2008. Synchronous visual analysis and editing of RNA sequence and secondary structure alignments using 4SALE. *BMC Res. Notes*, 1:1–7.

Selig, C., Wolf, M., Müller, T., Dandekar, T. & Schultz, J. 2008. The ITS2 Database II: homology modelling RNA structure for molecular systematics. *Nucl. Acid Res.*, 36:D377–D380.

Šimek, K., Pitsch, G., Salcher, M. M., Sirová, D., Shabarová, T., Adamec, L. & Posch, T. (2016). Ecological traits of the algae-bearing *Tetrahymena utriculariae* (Ciliophora) from traps of the aquatic carnivorous plant *Utricularia reflexa*. *J. Eukaryot. Microbiol.* DOI: 10.1111/jeu.12368.

Simon, E., Meyer, B. & Preparata, R. 1985. New wild *Tetrahymena* from Southeast Asia, China, and North America, including *T. malaccensis*, *T. asiatica*, *T. nanneyi*, *T. caudata*, and *T. silvana* n. spp. *J. Protozool.*, 32:183–189.

Simon, E. M., Nanney, D. L. & Doerder, F. P. 2008. The "*Tetrahymena pyriformis*" complex of cryptic species. *Biodivers. Conserv.*, 17:365–380.

Sirová, D., Borovec, J., Černá, B., Rejmánková, E., Adamec, L. & Vrba, J. 2009. Microbial community development in the traps of aquatic *Utricularia* species. *Aquat. Bot.*, 90:129–136.

Sitnikova, T. 1996. Bootstrap method for interior-branch test for phylogenetic trees. *Mol. Biol. Evol.*, 13:605–611.

Skibbe, O. 1994. An improved quantitative protargol stain for ciliates and other planktonic protists. *Arch. Hydrobiol.*, 130:339–347.

Stamatakis, A., Hoover, P. & Rougemont, J. 2008. A rapid bootstrap algorithm for the RAxML web servers. *Syst. Biol.*, 57:758–771.

Strüder-Kypke, M. C. & Lynn, D. H. 2010. Comparative analysis of the mitochondrial cytochrome c oxidase subunit I (COI) gene in ciliates (Alveolata, Ciliophora) and evaluation of its suitability as a biodiversity marker. *Syst. Biodivers.*, 8:131–148.

Strüder-Kypke, M. C., Wright, A.-D., Jerome, C. & Lynn, D. H. 2001. Parallel evolution of histophagy in ciliates of the genus *Tetrahymena*. *BMC Evol. Biol.*, 1:5.

Summerer, M., Sonntag, B. & Sommaruga, R. 2007. An experimental test of the symbiosis specificity between the ciliate *Paramecium bursaria* and strains of the unicellular green alga *Chlorella*. *Environ. Microbiol.*, 9:2117–2122.

Tamura, K., Peterson, D., Peterson, N., Stecher, G., Nei, M. & Kumar, S. 2011. MEGA5: molecular evolutionary genetics analysis using maximum likelihood, evolutionary distance, and maximum parsimony methods. *Mol. Biol. Evol.*, 28:2731–2739.

Wolf, M., Koetschan, C. & Müller, T. 2014. ITS2, 18S, 16S or any other RNA – simply aligning sequences and their individual secondary structures simultaneously by an automatic approach. *Gene*, 546:145–149.

Zahid, M. T., Shakoori, F. R., Zulifqar, S., Jahan, N. & Shakoori, A. R. 2014. A new ciliate species, *Tetrahymena farahensis*, isolated from the industrial wastewater and its phylogenetic relationship with other members of the genus *Tetrahymena*. *Pak. J. Zool.*, 46:1433–1445.

SUPPORTING INFORMATION

Additional Supporting Information may be found online in the supporting information tab for this article:

Figure S1. Maximum likelihood (ML) tree with posterior probabilities from Bayesian interference (BI) based on the 18S rRNA gene sequences of 52 *Tetrahymena* and two *Ichthyophthirius* isolates as outgroup.

Table S1. Species of *Tetrahymena* and *Ichthyophthirius* used for *cox1* and 18S rRNA gene analyses.

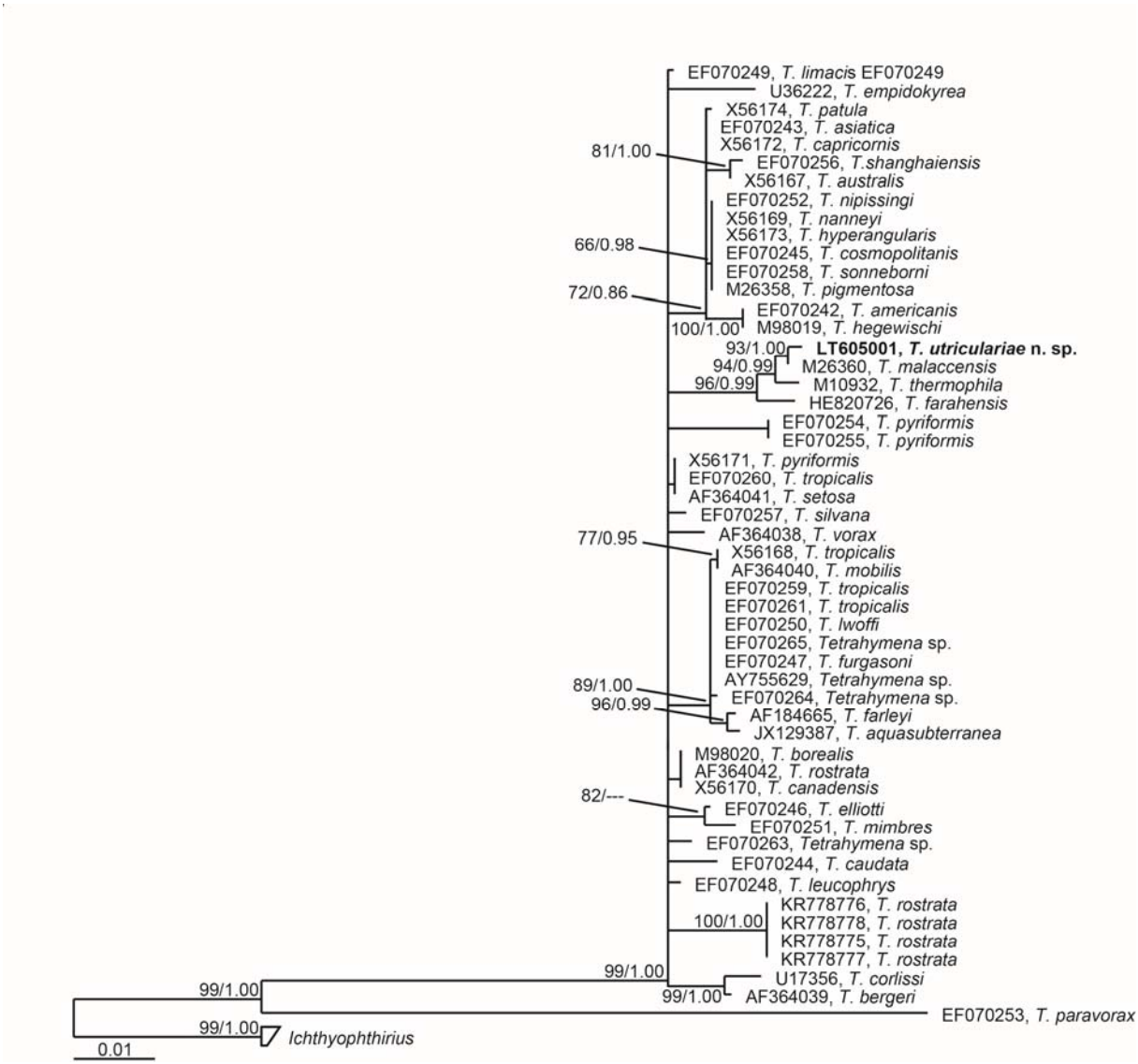

Figure S1. Maximum likelihood (ML) tree with posterior probabilities from Bayesian interference (BI) based on the 18S rRNA gene sequences of 52 *Tetrahymena* and two *Ichthyophthirius* isolates as outgroup. Branches with low bootstrap support (<50) were collapsed. Numbers at the branches represent ML bootstrap values / BI posterior probabilities. Scale bar: number of substitutions per site.

General discussion

Cultures versus single cell genomics

The basis of this PhD thesis was the laborious isolation and cultivation of protists. Cultures of more than 17 isolates affiliated with the genus *Nuclearia* were established and are still maintained (Article I and II). The adjustment of adequate culture conditions and the use of suitable food sources are essentially a try and error approach. Unfortunately, attempts to generate axenic *Nuclearia* cultures failed because the treatment with antibiotics had lethal effects on eukaryotic cells. Thus, protistan cultures are in fact microcosms of one eukaryotic and several prokaryotic species. The presence of several different species implies *per se* interactions in these small but already complex systems. Bottleneck effects (i.e. regular preparation of new cultures) and other random changes can cause taxonomic shifts in accompanying bacterial assemblages (Fraser et al., 2009), which might vice versa strongly affect the growth of nucleariid cells (e.g. interactions with bacteria influence the growth success of nucleariids, see Article III). Consequently, cultures of *Nuclearia* spp. are most likely not stable systems during long term cultivation. Thus, they have to be continuously checked and controlled by microscopy. This time consuming task is a great issue for culture collections. During the last years all except one single nucleariid culture disappeared from the lists of public culture collections. In order to foster further work on already characterised *Nuclearia* species, it is essential to make them available for other researchers. Therefore, we sent five strains of different species to the Culture Collection of Algae and Protozoa (CCAP). Unfortunately due to unknown reasons only one of these cultures can be ordered so far.

Although single cell genomics is a promising culture-independent tool to study protists (e.g. see Yoon et al. (2011)), cultivation is still needed to study phenotypic features such as morphological characteristics, ecophysiological aspects, cell cycles and behaviour. Analyses of genomic information might be used to formulate hypotheses, but evidences from additional methods are nonetheless required to test them. Since DNA extraction destroys specimens, it is not trivial to find ways to test the hypotheses. Modern molecular techniques are constantly improving and researchers are aware of their drawbacks, thus more sophisticated methodologies might be available in future. In the meantime, ‘the old fashioned cultivation’ of microorganisms in general and protists in particular is still essential. Whenever cultivation is possible it is the most convenient and cheapest approach to get meaningful information about an organism in a short period of time. Sequencing of marker genes of an isolate allows not only its identification and phylogenetic analyses, but it is an excellent link between information originating from cultures and findings from studies dealing with genomic information (e.g. from environmental samples).

Molecular markers

The small subunit of the ribosomal RNA (SSU rRNA) is widely used as molecular marker for the identification and the phylogenetic analysis of microorganisms. In general this molecule is particularly suited (Woese, 1987) due to its conserved structure and universal presence in prokaryotes (i.e. 16S rRNA) as well as eukaryotes (i.e. 18S rRNA). Sequences of the gene encoding for the SSU rRNA are usually rather easily obtained using PCR amplification and Sanger sequencing. Unfortunately, it seems that the SSU rRNA is not the marker gene of choice for every taxonomic group. Studies during the last decades showed different marker genes to be best suited for different protistan lineages (Pawlowski et al., 2012).

Before I started my work, six 18S rRNA gene sequences of at least partly characterised *Nuclearia* spp. isolates were available in public databases. Thus, in order to compare own isolates with described species this marker gene was my first choice. After readily sequencing the gene from *N. thermophila* strain N and subsequent phylogenetic analyses (Article I) it still appeared to be a good marker for nucleariids. Even though highly variable stretches complicated the phylogenetic reconstruction (e.g. they had to be excluded from the analysis, see Article II), the quick amplification and sequencing still favoured this marker gene. It was not before the many unsuccessful attempts to sequence the 18S rRNA genes of *N. delicatula* isolates, that drawbacks regarding this marker became obvious. Microheterogeneities in the nucleariid 18S rRNA gene copies of single isolates have already been reported by Zettler et al. (2001). They manly originate from size variations in the insertions inside the V4, V7 and V8 domains (sensus De Rijk et al. (1992)). Thus, variations in length of homopolymers, which are found inside these domains, led to the superposition of signals during sequencing. Since direct sequencing resulted in ambiguous sequences, clone libraries of the 18S rRNA genes of *N. delicatula* isolates had to be constructed. Sequencing consequently turned out to be both more time consuming as well as more costly. While the same was found for *Nuclearia* sp. strain B3, another issue hampered the sequencing of *N. thermophila* strain B1: A poly-G region in the 18S rRNA gene of this isolate causing ‘hard stops’ resulted in two non-overlapping partial sequences. In Article II we analysed these species specific differences quantitatively based on the constructed clone libraries. In summary, divergences and/or number of 18S rRNA gene copies vary between different *Nuclearia* species. In terms of their mutation rates, homopolymer regions can differ drastically from the rest of the gene. And finally, accumulations of mutations in these regions seem to be species specific.

Our studies revealed considerable limitations of this marker gene. Unfortunately, in nucleariids the amplification of another often used marker, namely the mitochondrial cytochrome c oxidase subunit I gene (*cox1*), failed so far (unpublished data). In order to facilitate the identification and phylogenetic analyses of sequences originating from *Nuclearia* spp. (e.g. isolates and environmental samples), further marker genes should be tested.

In contrast to nucleariids, the *cox1* gene is well established as molecular maker for ciliates of the genus *Tetrahymena*. It improves the resolution of most clades in the phylogenetic tree, compared to analyses based on 18S and 28S rRNA genes (Chantangsi et al., 2007; Lynn and Strüder-Kypke, 2006; Simon et al., 2008). For the identification and phylogenetic analyses of *Tetrahymena utricularіae* n. sp. (Article IV) both the 18S rRNA and the *cox1* gene were sequenced. In line with previous studies, phylogenetic reconstructions based on either of these markers resulted in trees differing strikingly in resolution and bootstrap supports. The 18S rRNA gene of *T. utricularіae* had a sequence similarity of 99.8 % to the closest relative *T. malaccensis*, which would not allow for a clear separation of these two species. In contrast the *cox1* gene sequence of *T. uticularіae* was most similar to the sequence of *T. thermophila*, and this marker showed a rather low sequence similarity of 90.3 %. Based on this divergence a clear separation was possible (e.g. usually an intraspecific range of 0 % to 3.5 % is expected for *Tetrahymena* species, see Doerder (2014)).

The identification and phylogenetic analysis of the algal symbiont of *T. utricularіae* (Article IV) asked for an additional third molecular marker, namely the internal transcribed spacer 2 (ITS2). This region between the 5.8S rRNA and the 28S rRNA genes is increasingly used for phylogenetic analyses of many eukaryotic linages. The comparably fast evolving sequence enables low-level analyses (e.g. for *Chlorella*; see Hoshina et al. (2005)). In contrast to its sequence, the secondary structure of the ITS2 is highly conserved (Selig et al., 2008) allowing the phylogenetic reconstruction on a higher level (e.g. throughout the Eukaryota; see Schultz et al. (2005)). Furthermore, the combination of primary sequence information with their individual secondary structures increases the accuracy and robustness of phylogenetic trees (e.g. reviewed in Wolf et al. (2014)). These characteristics make the ITS2 marker a great tool for phylogenetic reconstructions of the Chlorellaceae (e.g. see Hoshina (2014) and Luo et al. (2010)). Since the sequencing of the 18S rRNA gene from the algal symbiont revealed its affiliation to the Chlorellaceae, we decided to work with the state of the art methodology using sequence-structure information from the concatenated data set of the ITS2 and the 18S rRNA genes (Article IV). For reasonable comparison, we thus followed the approach from Heeg and Wolf (2015) including the same taxa and merely added the sequence of the algal symbiont. Surprisingly, the addition of only one taxon, the algal symbiont of *T. utricularіae*, to the selected sequences of Heeg and Wolf (2015) changed the topology of the phylogenetic tree remarkably. While the structure inside the *Parachlorella*-clade could be reproduced, there were structural changes inside the *Chlorella*-clade (see figure 5 in Article IV and figure 7 in Heeg and Wolf (2015)). The differences between the topologies concerning the *Micractinium* spp. isolates to which the algal symbiont clustered were remarkable. In contrast with the polyphyly of this genus in the 18S rRNA + ITS2 gene tree from Heeg and Wolf (2015), in our tree all *Micractinium* spp. made up a monophyletic cluster including only two additional sequences from *Actinastrum hantzschii*. It would be tempting to claim the algal symbiont to be the missing link connecting the two parts of the *Micractinium* spp. cluster. But since the importance of taxon sampling was reported earlier and also pointed out by Heeg and Wolf (2015), it should probably rather be treated as an extreme example illustrating the impact of taxon sampling on phylogenetic analysis.

Morphological versus molecular phylogeny in the genus *Nuclearia*

The comparison of morphological features with molecular phylogenetic analyses of *Nuclearia* sp. strain N (Article I) revealed contradicting results. While we found a very high 18S rRNA gene sequence similarity (99.6 %) of our isolate with the described *N. thermophila* (Yoshida et al., 2009), several morphological features differed remarkably. In contrast to the original species description our isolate had a (i) glycocalyx harbouring (ii) ectosymbiotic bacteria, (iii) bacterial endosymbiont inside the cytoplasm, (iv) different mean cell size, and the production of (v) syncytia and (vi) cysts could be documented. Considering the few features traditionally used for the characterisation of nucleariids (see table 1 in Yoshida et al. (2009)) these morphological discrepancies would most likely have been interpreted as sufficient to discriminate between two independent species (in the absence of molecular information). At that time these differences also prevented us from assigning the isolate to the species *N. thermophila*.

In Article II we systematically characterised 17 *Nuclearia* spp. isolates based on both morphological and molecular (i.e. 18S rRNA gene) features. We wanted to know to which extent the morphological classification mirrored the molecular phylogeny. Thus, a cladistic analysis based on presence/absence of morphological characters was compared with the phylogenetic reconstruction from the 18S rRNA gene analysis. The cladistic tree and the molecular based maximum likelihood (ML) tree were in good accordance regarding the *N. delicatula* and the *N. thermophila* clusters. In both trees, they were sister groups including same isolates (see figure 1 in Article II). In contrast, the third big cluster in the cladistic tree unified isolates from distant branches of the ML tree. In other words only *N. delicatula* and *N. thermophila* strains could be identified solely by their morphological traits. For the affiliation of all other isolates, additional molecular information (i.e. 18S rRNA genes) was needed. Two isolates previously as *N. simplex* identified clustered very distantly in the 18S rRNA gene-based tree. This fact supported the assumption about the severe difficulties of morphological discrimination and suggested a misidentification of these isolates. Thus, it is likely that due to missing diagnostic morphological features, isolates belonging to different species have been identified as *N. simplex*. On the other hand it might be that *N. simplex* described by Cienkowski was later redescribed as *N. moebiusi*, *N. pattersoni* or *N. thermophila*. Since there is no obvious way to resolve this problem, we propose to use the mentioned species, from which molecular as well as morphological information is available.

Taken together 12 of our 17 strains could be assigned to described species based on morphology in combination with molecular information (Article II). For isolates clustering together with *N. thermophila*, we reported a good accordance with the characters earlier documented for *Nuclearia* sp. strain N (Article I). Thus, the obtained results including morphological and phylogenetic analyses of four different isolates (strains B1, D6, A and N) justified their affiliation to the species *N. thermophila*. While five isolates could be affiliated to *N. delicatula*, two isolates to *N. pattersoni* and one to *N. moebiusi,* it was not possible to assign the remaining five strains. In the phylogenetic tree a sister group to the *N. pattersoni* cluster was formed by three of these isolates. Further, two strains made up a distinct rather deep-branching cluster without described representatives. They obviously belong to a new, so far undescribed species. Considering their basal position in the phylogenetic tree, a

formal species description should be done including additional analyses of ultrastructure and genome sequencing.

It is remarkable that we isolated representatives of all the described species from which 18S rRNA gene sequences were available from only two Swiss Lakes (i.e. Lake Zurich and Lake Baldegg). In other words all of the four known nucleariid phylotypes were found in a rather small geographic area. The genus additionally includes seven 'accepted' merely morphological described species (i.e. including *N. simplex*, discussed earlier). In order to further address the diversity of nucleariids and to possibly get isolates of the mentioned morphospecies, sampling and isolation should be continued and extended to a broader geographic area. Adding other substrates (e.g. green algae like *Spirogyra* sp. or *Chlorogonium* sp.) for enrichments might also result in cultures of so far uncultivated representatives of the genus.

The diverse symbiotic associations of *Nuclearia* spp.

In Article I we characterised for the first time a nucleariid isolate (i.e. *N. thermophila* strain N) in combination with its bacterial ecto- and endosymbionts. The ectosymbiotic bacteria inside the glycocalyx belonged exclusively to one betaproteobacterial species, namely *Paucibacter toxinivorans* (Rapala et al., 2005). This finding pointed to a controlled and specific association. Surprisingly, loss of the associated bacteria did not result in any obvious negative effects for *N. thermophila*. Consequently, the symbiosis can be characterised as facultative interaction. In contrast, endosymbionts were always present in the cells of *N. thermophila* strain N and we speculated about an obligate nature of this association. The very constant number of endosymbiotic bacteria per nucleariid cell over the entire growth cycle supported this conclusion. Since the phylogenetic analysis of the 16S rRNA gene sequence from the gammaproteobacterial endosymbiont showed a very low sequence similarity with entries from public databases (i.e. about 10 % sequence divergence to the closest described relatives in the genus *Ectothiorhodosinus*), we decided to establish a new genus and a new species. Endosymbiotic bacteria usually get the provisional status of a *Candidatus* because they are often not cultivable outside their host. Thus, we characterised the endosymbiont of *N. thermophila* strain N and named it *Candidatus* Endonucleariobacter rarus.

In Article II we systematically analysed the association of 17 *Nuclearia* spp. isolates with bacterial symbionts. Eight of these nucleariids had endo- and/or ectosymbionts. Symbiotic bacteria could be detected for all *N. delicatula* strains but not for *Nuclearia* isolates from three other phylogenetic clusters. Beside these homogeneous branches, also mixed groups were found. In the *N. thermophila* cluster, three out of five representatives had symbionts. The *N. pattersoni* cluster was also heterogeneous. Only *N. pattersoni* (Dykova et al. 2003) was found to harbour an endosymbiont. It was conspicuous that strains of *N. thermophila* were associated with the same endosymbiont even when isolated from different lakes. This suggested a specific and obligate interaction. In contrast, two isolates of *N. delicatula* originating from the same lake harboured different endosymbiotic bacteria. Here the symbiont acquisition seemed to be rather promiscuous.

This non-systematic appearance of symbiotic associations inside the genus *Nuclearia* indicates a species-dependent disposition. Either some *Nuclearia* species evolved traits by which the probability to enter a symbiotic relationship increased or it is a plesiomorph character that has been partly lost. Considering their phylogenetic position within opisthokonts, it is of interest to search specifically for such traits in future genetic analysis. Probably, nucleariids have already specific genes and machineries which are involved in selecting and controlling of symbiotic partners (Bosch, 2014). The question about the frequency of prokaryotic symbionts in unicellular opisthokonts still remains to be addressed. Today, it is not clear if the lack of knowledge simply derives from the low number of studies looking for symbiotic associations or if the highly diverse interactions inside the genus *Nuclearia* are an exceptional phenomenon.

In total we characterised five novel symbionts (Article I and Article II), two ectosymbiont and four endosymbionts. Comparable with our first study (Article I) the betaproteobacterial ectosymbiont of *N. delicatula* strain G (Article II) could be affiliated to a genus (i.e. *Inhella*), whereas for none of the novel endosymbionts close relatives were found in public databases. The three endosymbionts of *N. delicatula* isolates belong to the alpha-, gamma- and deltaproteobacteria and were named *Ca.* Intestinusbacter nucleariae, *Ca.* Ovatusbacter abovo and *Ca.* Turbabacter delicatus, respectively. Uncovering an already high diversity in only a few nucleariid isolates and the detection of additional so far unidentified symbionts suggests that we still are only scratching the surface of the diversity of symbionts.

Through the study of our nucleariid isolates we further gained evidence for the facultative nature of the associations with ectosymbionts in general (i.e. frequent loss of ectosymbiotic bacteria during long term cultivation, see Article II). It is remarkable, that we also have indications for the loss or at least the quantitative reduction of *Ca.* Turbabacter delicatus in the course of cultivation. Recently we noticed by performing CARD-FISH with specific probes, that this endosymbiont was not detectable in some cultures of *N. delicatula* strain G anymore. Originally, cells had numerous endosymbionts inside food vacuoles and small vacuole-like structures (Article II). In order to confirm the possible loss of *Ca.* Turbabacter delicatus, *N. delicatula* strain G cultures were prepared for TEM. While the typical morphotype of the second endosymbiont *Ca*. Ovatusbacter abovo was still observed inside nucleariids (Fig. 3A-E), the *Ca.* Turbabacter delicatus morphotype was indeed not detected anymore. Instead, another so far unknown endosymbiotic morphotype was localised in the cytoplasm (Fig. 3F-J). One possible explanation would be, that the new symbiont was already present from the beginning on, but overlooked due to its low abundance at that time. Thus, *Ca.* Turbabacter delicatus might have been replaced by the newly discovered endosymbiont. Such a replacement could point to a functional redundancy of these symbionts. However, it would be likely that they have to some extent the same ecological niche. If culture conditions favoured the newly detected endosymbiotic bacteria, *Ca.* Turbabacter delicatus could have been outcompeted by the newly discovered endosymbiont (Lefèvre et al., 2004).

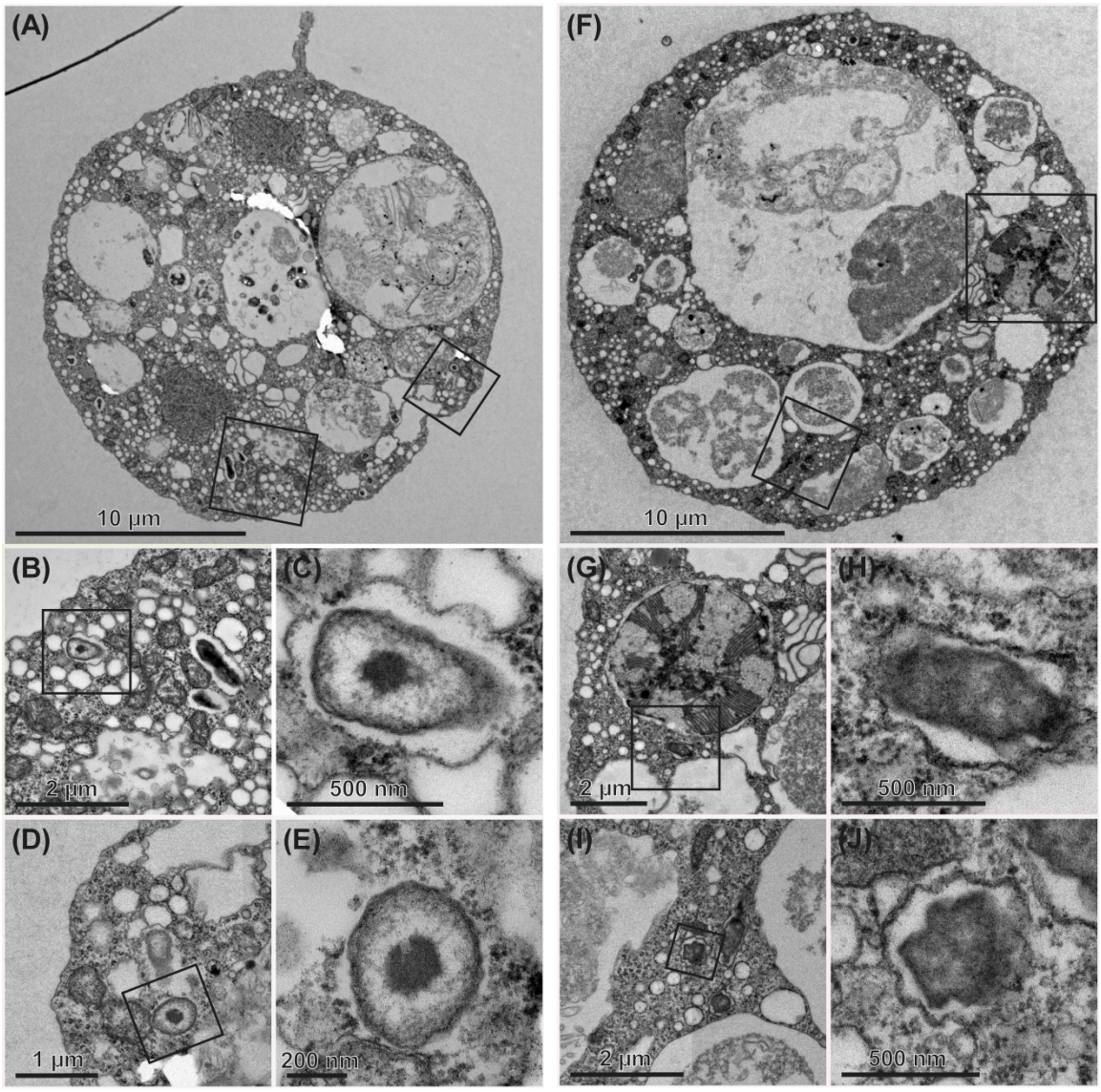

Fig. 3: TEM images of *N. delicatula* strain G. A and F: Overview of two different specimens. Magnifications of squares are shown in (B), (D) and (G), (I), respectively. B-E: *Ca.* Ovatusbacter abovo with its typical morphology localised freely in the cytoplasm. Magnification of square in (B) is shown in (C) and magnification of square in (D) is shown in (E). G-J: New bacterial morphotype observed inside *N. delicatula* strain G. Endosymbiotic bacterium surrounded by a peribacterial membrane. Magnification of square in (G) is shown in (H) and magnification of square in (I) is shown in (J).

Nuclearia thermophila feeding on 'toxic' *Planktothrix rubescens*

In a preliminary growth experiment we offered two different *Planktothrix rubescens* strains to *N. thermophila*. It is known that different *P. rubescens* strains produce and store different toxic secondary metabolites (Kurmayer et al., 2016). While strain A7 was shown to produce microcystins (Blom et al., 2001), strain 63 does not synthesise this cyanotoxin. The axenic strain A7 was originally isolated from Lake Zurich (Walsby et al., 1998) and it routinely serves as food source for nucleariid cultures. After a lag-phase *N. thermophila* strain N usually showed exponential growth (Fig. 4A). Surprisingly, no log-phase was observed, if the non-microcystin-producing strain was offered to *N. thermophila* (Fig. 4B). Since microcystin is generally considered to be toxic for all eukaryotic cells (Campos and Vasconcelos, 2010; Urrutia-Cordero et al., 2013), we rather expected an adverse effect of microcystin on the growth of *N. thermophila*. Beside the production of microcystin, the presence of accompanying bacteria was an important difference between the two strains of *P. rubescens*. Strain 63 was not grown as axenic culture, thus we cannot exclude that the accompanying bacterial assemblage was responsible for the main impact on the growth of *N. thermophila*.

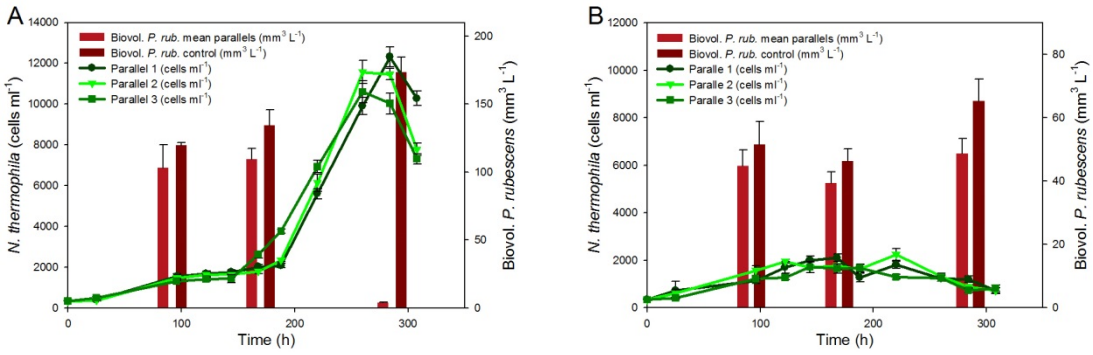

Fig. 4: Growth curves (lines: abundances) of *N. thermophila* (three replicates) on different *P. rubescens* strains (bars: biovolume). A: *P. rubescens* strain A7 was almost completely depleted. The growth curves of nucleariids show an initial lag-phase, followed by exponential growth. B: No exponential growth was observed when *P. rubescens* strain 63 served as food source. Cyanobacterial biovolumes did not decrease during the experiment.

Based on these findings, we designed new experiments to study effects of different accompanying bacterial assemblages on the growth success of nucleariids. Interesting results were obtained by adding the accompanying bacteria of *N. thermophila* to cultures of *N. delicatula* (Fig. 5A). The lag-phase of the latter nucleariid species was shortened by about one third after adding the accompanying bacteria of *N. thermophila*. However, no growth stimulation of *N. thermophila* was induced when conducting the experiment the other way around (Fig. 5B). No exchange of ecto- and endosymbionts was evident during these experiments. Thus, distinct members of the bacterial assemblage from *N. thermophila* cultures were probably responsible for positive effects on the growth of *N. delicatula*. Consequently, we formulated two possible hypotheses: (i) Adverse impacts of the toxin microcystin stored in the food of *Nuclearia* spp. might be reduced by bacterial degradation. (ii) The breakdown of *P. rubescens* filaments might be accelerated by the presence of specific bacterial factors. Thus, if distinct bacterial species would produce bio-active components against cyanobacteria, this could have a positive impact on the growth of nucleariid cells.

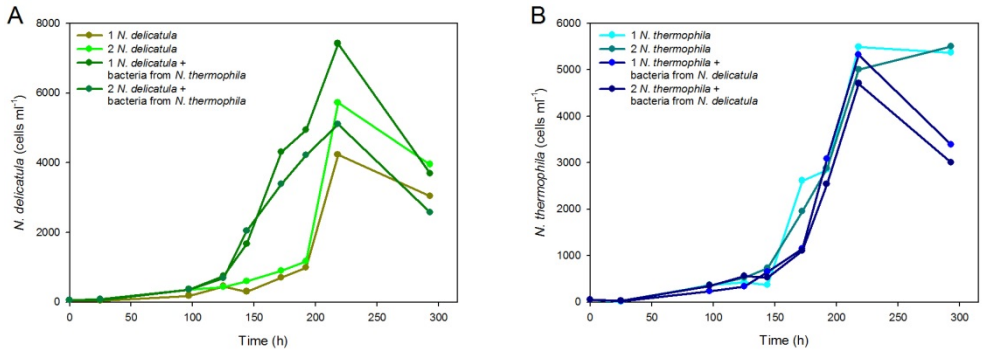

Fig. 5: Growth curves of *N. delicatula* and *N. thermophila* with different accompanying bacterial assemblages (two replicates for each set-up). A: *N. delicatula* started the log-phase about 65 h earlier, when supernatants of *N. thermophila* cultures were added. B: The addition of accompanying bacteria from *N. delicatula* had no effect on the growth success of *N. thermophila*.

In order to test the hypotheses further growth experiments were performed. We wanted to elucidate in more detail how two different accompanying bacterial assemblages influence the growth of *N. thermophila* (Article III). On the one hand a random bacterial assemblage was generated as side effect of the isolation method used for nucleariid cells. These accompanying bacteria (entitled as 'Culture assemblage') were not selected for any special trait (e.g. efficiency, diversity or microcystin degradation) but rather for optimal growth of nucleariids. Thus the long term culture of *N. thermophila* probably did not result in a 'natural' prokaryotic assemblage (set up 1). On the other hand a second bacterial community (set up 2) was generated by adding lake water containing a natural bacterial assemblage ('Culture assemblage' + 'Lake bacteria'). As sole food source we offered *P. rubescens* strain A7, which was shown to produce [D-Asp^3, *(E)*-Dhb^7]microcystin-RR (Blom et al., 2001). During the growth experiment we monitored the following parameters: cell counts of *N. thermophila* and total bacteria, the biovolume of *P. rubescens* and microcystin concentrations. Based on results of this experiment we could show that growth dynamics of *N. thermophila* cells depend on the bacterial assemblage. Beside effects of the accompanying bacteria on the nucleariid cells, different dynamics of the microcystin concentrations in the two set-ups could be monitored. While microcystin was reduced only in the set-up with 'Lake bacteria', no net degradation was detected for the randomly generated 'Culture assemblage'. Instead cyanotoxins accumulated in the culture medium during the experiment. Thus, two conclusions were drawn: (i) The microcystin variant of its food source was not degraded nor covalently bound (e.g. via the glutathione S-transferase, see Pflugmacher et al. (1998)) by *N. thermophila*. (ii) Instead the cyanotoxin was released in the culture medium, where it became available for bacterial degraders. The experiments gave no indications for negative effects of [D-Asp^3, *(E)*-Dhb^7]microcystin-RR on *N. thermophila*, which contradicts the general assumption that microcystins are harmful for all eukaryotes. This could be explained by two mechanisms. (i) The inhibition of protein phosphatases PP1 and PP2A by microcystins is the main cause for their toxicity (MacKintosh et al., 1990). Nonetheless, the structural variants of the nucleariid phosphatases might not be affected. The lack of the specific targets in combination with efficient export mechanisms would render the cyanotoxin harmless. (ii) Since microcystins are not cell membrane permeable, transporters are needed for their uptake. Members of the organic anion transporting polypeptide superfamily (Oatps) are known to mediate the transport of microcystins (Faltermann et al., 2016). This transport is dependent on the specific Oatp and the microcystin variant (Fischer et al., 2005). Unfortunately, it is not known yet which transporters are expressed by nucleariid species. But, if nucleariid species lack the appropriate

transporters, microcystins would not be taken up. Exocytose could finally lead to the release of cyanotoxins into the culture medium.

The results presented in Article III contradicted our hypotheses about the positive effect of bacterial microcystin degradation on nucleariids. On the other hand we have now indications that the bacterial lysis of cyanobacteria might play a role for the growth success of *Nuclearia* cells. Partial cell lysis and fragmentation of cyanobacterial filaments caused by complete lysis of cells (i.e. within a filament) could facilitate their break-down by nucleariids. When we offered *P. rubescens* filaments as sole food source to 'Lake bacteria' alone, about half of the cyanobacterial cells were lysed after 300 h (Article III). It has been previously shown that many bacterial strains have an antagonistic effect on cyanobacteria (e.g. see the review from Van Wichelen et al. (2016)). Bio-active substances (e.g. see suppl. table 2 from Van Wichelen et al. (2016)) produced by bacteria are most likely responsible for cell lysis. An accumulation of such bacterial factors might be a prerequisite for successful break-down of *P. rubescens* filaments by nucleariids. We assume that types of factors are dependent on the bacterial species present in the culture medium. Further their concentrations are most likely dependent on the composition of these species. Thus, different compositions of accompanying bacteria would have different impacts on the growth success of *Nuclearia* cells. This assumption could explain the observed influences of different bacterial assemblages on nucleariids (Article III). In future studies this issue should be address in more detail. The identification of the responsible bacterial species and their bio-active factors might give new insights into the investigated system. Furthermore, such studies could be of great importance for the understanding of *P. rubescens*' grazing resistance in natural environments. In contrast to the dynamics in cultures, the cyanobacterial filaments seem to be protected against grazers in the pelagial of many fresh water ecosystems (Ernst et al., 2001; Jacquet et al., 2005; Posch et al., 2012). Considering interactions between *Nuclearia* (or other grazers) and bio-active factors produced by distinct bacterial species might offer some explanation for the increasing dominance of *P. rubescens* in these environments.

Apart from the growth dynamics and the question about the fate of microcystins, we investigated the cell motility and the feeding behaviour of nucleariids (Article III). Time laps video documentation allowed to visualise for the first time the otherwise imperceptible motion of nucleariid cells. In this way we were able to add another dimension to the knowledge about these rather exotic organisms. The produced movies are vivid examples of how these creatures live in the microscopic world. Such visualised information is, to my opinion, a large profit not only for didactic purposes but for a more holistic understanding of protists in general. Using such video material is a good opportunity to pass some of our fascination for protists. We are about to submit Article III, which will include the mentioned movies in the online version. For the printed article we produced drawings to illustrate the details of cell motility and feeding behaviour.

The role of *Paucibacter toxinivorans* for *Nuclearia thermophila*

Most of the nucleariid species are surrounded by an extracellular matrix (see table 1 in Yoshida et al. (2009)). This so-called glycocalyx might be important for the protection from pathogens and for the selection of ectosymbionts (Bosch, 2014; Bosch et al., 2015). While other bacteria are generally excluded from the glycocalyx of *N. thermophila* strain N, the ectosymbiont *P. toxinivorans* can be localised nicely arranged several micrometres distant from the eukaryotic cell membrane (Article I, II and III). Unfortunately, the extracellular matrix is only poorly conserved using conventional preparation techniques for TEM samples. To study the ultrastructure of the nucleariid glycocalyx in more detail, we switched to the high pressure freezing / freeze substitution method (for an example see Fraune et al. (2015)). Samples of *N. thermophila* strain N were prepared with this method. Beside the detection of the formerly described endosymbiont *Ca.* Endonucleariobacter rarus (Fig. 6 A-D), two layers of the glycocalyx (Fig. 6 A and E, Fig. 7) could be seen on TEM images.

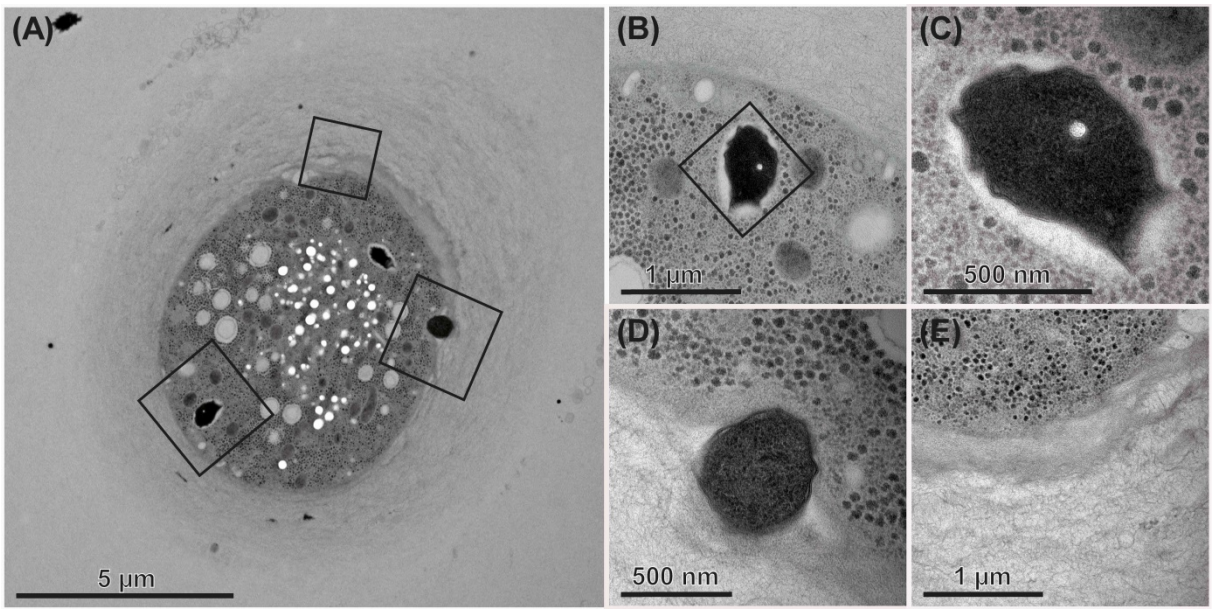

Fig. 6: High pressure freezing / freeze substitution TEM images of *N. thermophila* strain N. A: Overview of a nucleariid cell with partly preserved glycocalyx. Magnifications of squares are shown in (B), (D) and (E). B-D: *Ca.* Endonucleariobacter rarus with its typical morphology. B-C: Endosymbiotic cell localised inside the cytoplasm with a peribacterial membrane. Magnification of square in (B) is shown in (C). D: Exocytosis of a single endosymbiotic cell displaying the characteristics of *Ca.* Endonucleariobacter rarus. E: The glycocalyx is composed of two different layers.

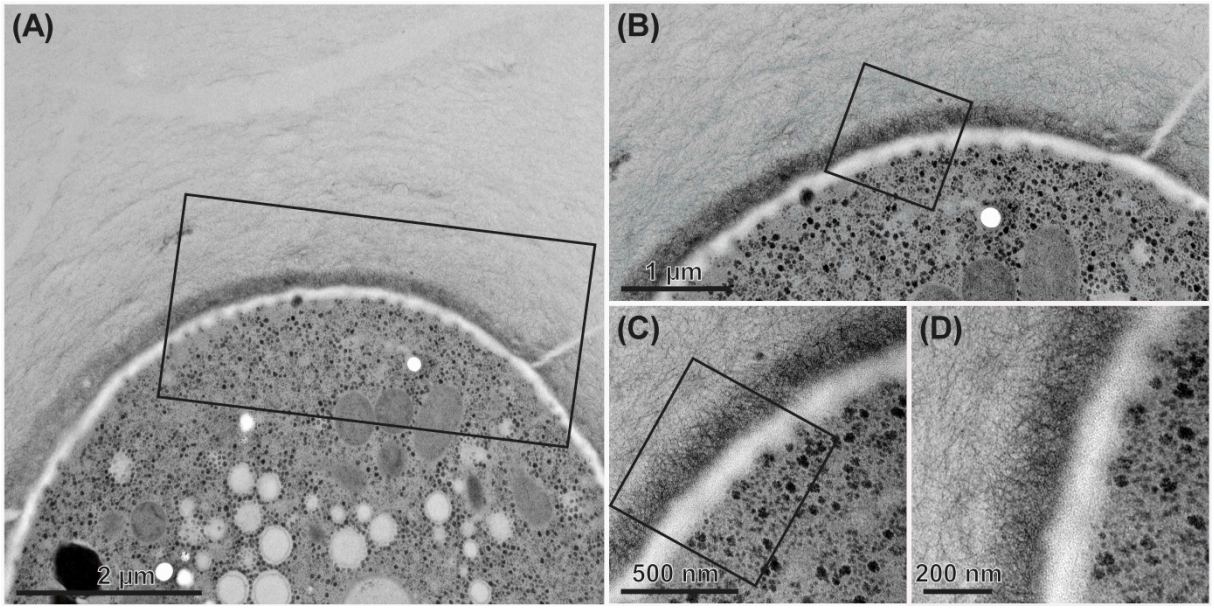

Fig. 7: High pressure freezing / freeze substitution TEM images of *N. thermophila* strain N. A: Overview of a nucleariid cell with partly preserved glycocalyx. Magnification of square is shown in (B). B-D: Two layers with different electron densities can be distinguished. Magnification of square in (B) is shown in (C) and magnification of square in (C) is shown in (D).

It is characteristic for the high pressure freezing / freeze substitution method that the quality of conservation can vary remarkably not only between different cells but even within the same cell. Thus, many sections of TEM preparations should be analysed to find a region representing a near-native state. Until now we only imaged a limited number of sections originating from a few cells. The generated images are already promising, but in near future TEM of further sections might result in images with fewer artefacts caused by ice crystals (e.g. note the fine structures in the glycocalyx Fig. 6 and 7). Unfortunately, *P. toxinivorans* was not detected directly in the glycocalyx on the analysed images as it is the case *in vivo* (Article I, II and III). Nonetheless, the two layers with different electron densities might explain why ectosymbiotic bacteria are localised several micrometres distant from the eukaryotic cell. Most probably *P. toxinivorans* is not able to penetrate this second dense layer of the glycocalyx, which directly covers the nucleariid cell membrane.

The role of *P. toxinivorans* for *N. thermophila*, was the subject of a series of experiments. Since the isolation of this ectosymbiont was successful (Article I) and cultivation in pure culture was possible, we were able to design growth experiments to investigate the nature of the symbiosis (i.e. mutualistic, commensal or parasitic). However, the symbiotic interaction seemed to be more complex than expected. Beside the monoculture of the ectosymbiont, we used different *N. thermophila* strains for experiments. While strain N was associated with *P. toxinivorans*, strain A had no ectosymbionts within its glycocalyx. The two nucleariid strains showed strikingly different growth dynamics (Fig. 8A). We speculated that the addition of ectosymbionts to symbiont-free nucleariids would result in growth stimulation. As expected, the ectosymbiont colonised the glycocalyx of strain A cells (Article II). Unfortunately, high variations between replicates did not allow for a clear interpretation (Fig. 8B). Probably, the accompanying bacterial assemblage had a greater impact on the growth success of *N. thermophila* than the presence of *P. toxinivorans* (e.g. Article III).

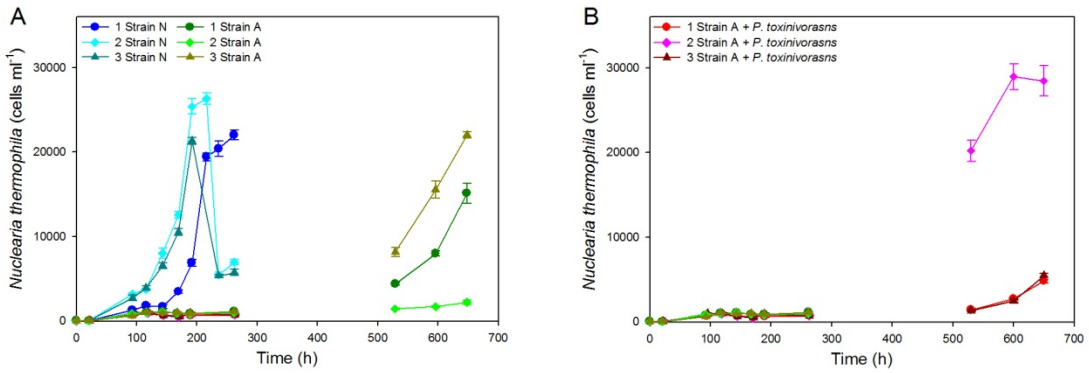

Fig. 8: Growth curves of *N. thermophila* strain N and strain A with *P. rubescens* as food source (three replicates per set-up). A: Different growth dynamics were observed for the two strains. B: The addition of the ectosymbiont *P. toxinivorans* had no pronounced effect on the growth of strain A in two out of three replicates.

P. toxinivorans strain 2C20T was originally described to be able to degrade different microcystin variants (Rapala et al., 2005). Since we proved that the ectosymbiont *P. toxinivorans* could degrade the microcystin variant [Asp^3]microcystin-LR (Article I), a possible involvement in the degradation of the toxin contained in the food source of its host was assumed. To further study the ectosymbiont's capability to degrade microcystin variants produced by *P. rubescens*, we conducted experiments with bacterial monocultures. For this purpose, strain 2C20T was ordered from a culture collection for comparative experiments. Surprisingly, only strain 2C20T was able to degrade the dominant microcystin variant ([D-Asp^3, *(E)*-Dhb^7]microcystin-RR) present in *P. rubescens* (Fig. 9).

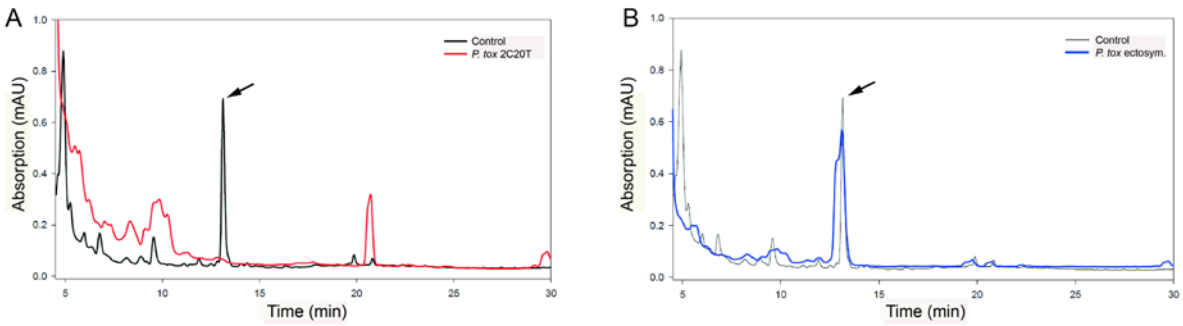

Fig. 9: HPLC chromatograms of extracted peptides from cultures of *P. toxinivorans* strain 2C20T (*P. tox* 2C20T) and the prokaryotic ectosymbiont (*P. tox* ectosym.) of the amoeba *Nuclearia thermophila*. The peak of [D-Asp^3, *(E)*-Dhb^7]microcystin-RR (arrows) is present in the control variant (i.e. *P. rubescens* extract without bacteria) A: Microcystin was degraded by *P. toxinivorans* strain 2C20T. B: The ectosymbiont *P. toxinivorans* did not efficiently degrade the offered microcystin.

These findings contradicted our assumption that ectosymbionts are involved in the degradation of microcystins stored in the food source of their host (Article I). In Article III we thus addressed this issue in detail under more 'realistic' conditions. We monitored batch cultures where the [D-Asp^3, *(E)*-Dhb^7]microcystin-RR-producing *P. rubescens* strain A7 served as sole food source for *N. thermophila*. In these experiments nucleariid cells were associated with the ectosymbiont *P. toxinivorans*. Two different set-ups with different artificially produced bacterial assemblages were generated (see above). Apart from these 'co-cultures' additional monocultures of the ectosymbiont were set up. As substrates in these cultures either 'broken' or 'intact' *P. rubescens* filaments were offered. Growth experiments revealed that only in one set-up of the 'co-cultures' (i.e. with 'Lake bacteria', see Article III) microcystin was degraded. Since *P. toxinivorans* was always present in the

glycocalyx of *N. thermophila*, the microcystin degradation could not be attributed to the ectosymbiont. This was also true for the set-ups of the monocultures, in which the offered microcystin variant was also not degraded. Consequently, the role of the ectosymbiont *P. toxinivorans* as degrader of [D-Asp^3, *(E)*-Dhb^7]microcystin-RR could not be confirmed in the investigated system. Since nucleariid species have a broad prey range, the possible involvement of the ectosymbiont in the degradation of different microcystin variants (e.g. microcystin-LR) stored in alternative food sources (e.g. *Microcystis* sp.) should be addressed in future experiments. While neither negative nor positive effects of the ectosymbiont on *N. thermophila* could be elucidated so far, there are indications that the ectosymbiotic bacteria profit from nucleariids. The fact that no growth of the ectosymbiont was monitored in neither of the monocultures could reflect the dependence of these bacteria on substrates released by nucleariid cells. This assumption is in line with the close proximity of the ectosymbiont to the host's membrane, which would allow for an exchange of metabolites (Croft et al., 2005). Taken together, it seems that at least the ectosymbiont profits from the symbiotic association. Thus, here we are probably dealing with a facultative symbiosis of a commensal.

Growth experiments did not elucidate the role of *P. toxinivorans* for *N. thermophila*. In order to study possible metabolic activities of the ectosymbiont, we decided to sequence its genome. After DNA extraction from a pure culture, we used the Illumina TruSeq® DNA PCR-Free kit for the library preparation. Subsequently, the library was sequenced on the MiSeq platform (Illumina). This resulted in 2 409 054 reads, which were assembled using the A5-miseq algorithm. The assembly of the 67 contigs led to 38 scaffolds with a total size of 6 260 015 bp. After excluding the scaffold originating from the sequencing control (i.e. bacteriophage phiX), we obtained a draft genome of the ectosymbiont *P. toxinivorans*. The RAST home page served as tool for the rapid annotation (Table 1). Most probably a more sophisticated assembly will reduce the number of scaffolds and it might even be possible to close the genome using additional Sanger sequencing of certain regions. Based on the ectosymbiont's genome, we will try to generate hypotheses about its metabolic activities in the glycocalyx of *N. thermophila*.

Table 1: Draft genome of the ectosymbiont *P. toxinivorans* analysed by RAST.

Size (bp)	Number of scaffolds	GC content (%)	Number of subsystems	Number of coding sequences	Number of RNAs
6 254 381	**37**	**65.9**	**475**	**5484**	**58**

Since the symbiosis of *N. thermophila* with *P. toxinivorans* was found to be a facultative association, the extent of genetic adaptions in the symbionts' genome is most likely not very pronounced. Consequently, it will not be trivial to find evidences for such adaptions (e.g. specific transporters and metabolic pathways), from which metabolic activities could be deduced. Although the genome sequencing of endosymbiotic bacteria is more complicated (e.g. due to the absence of a pure culture and the low number of bacteria inside the eukaryotic cell), the interpretation might be simpler due to more genetic adaptions (e.g. genome reduction (Moran, 1996) and low GC content (Sloan and Moran, 2012)). In future studies we intend to analyse genomes of nucleariid endosymbionts to address interesting questions about the functional aspects of the characterised symbioses.

References

Artari, A., 1889. Morphologische und biologische Studien über *Nuclearia delicatula*, Cienk. Zool. Anz. 12, 408-416.

Bary, A.d., 1879. Die Erscheinung der Symbiose. Verlag von Karl J. Trübner, Strassburg.

Blom, J.F., et al., 2001. High grazer toxicity of [D-Asp^{3},*(E)*-Dhb^{7}]microcystin-RR of *Planktothrix rubescens* as compared to different microcystins. Toxicon 39, 1923-1932.

Bosch, T.C., 2014. Rethinking the role of immunity: lessons from *Hydra*. Trends Immunol. 35, 495-502.

Bosch, T.C., et al., 2015. Microbial ecology in *Hydra*: Why viruses matter. J. Microbiol. 53, 193-200.

Campos, A., Vasconcelos, V., 2010. Molecular mechanisms of microcystin toxicity in animal cells. Int. J. Mol. Sci. 11, 268-287.

Cann, J.P., Page, F.C., 1979. *Nucleosphaerium tuckeri* nov. gen. nov. sp.- A new freshwater filose amoeba without motile form in a new family Nucleariidae (Filosea: Aconchulinida) feeding by ingestion only. Arch. Protistenk. 122, 226-240.

Chantangsi, C., et al., 2007. Barcoding ciliates: a comprehensive study of 75 isolates of the genus *Tetrahymena*. Int. J. Syst. Evol. Microbiol. 57, 2412-2423.

Cienkowski, L., 1865. Beiträge zur Kenntniss der Monaden. Arch. Mikrosk. Anat. 1, 203-232.

Croft, M.T., et al., 2005. Algae acquire vitamin B12 through a symbiotic relationship with bacteria. Nature 438, 90-93.

De Rijk, P., et al., 1992. Compilation of small ribosomal subunit RNA sequences. Nucl. Acid. Res. 20, 2075-2089.

Dirren, S., Posch, T., 2016. Promiscuous and specific bacterial symbiont acquisition in the amoeboid genus *Nuclearia* (Opisthokonta). FEMS Microbiol. Ecol. 92.

Dirren, S., et al., 2014. Ménage-à-trois: The amoeba *Nuclearia* sp. from Lake Zurich with its ecto- and endosymbiotic bacteria. Protist 165, 745-758.

Doerder, F.P., 2014. Abandoning sex: multiple origins of asexuality in the ciliate *Tetrahymena*. BMC Evol. Biol. 14, 112-112.

Dykova, I., et al., 2003. *Nuclearia pattersoni* sp. n. (Filosea), a new species of amphizoic amoeba isolated from gills of roach (*Rutilus rutilus*), and its rickettsial endosymbiont. Folia Parasitol. 50, 161-170.

Ernst, B., et al., 2001. Presence of *Planktothrix* sp. and cyanobacterial toxins in Lake Ammersee, Germany and their impact on whitefish (Coregonus lavaretus L.). Environ. Toxicol. 16, 483-488.

Faltermann, S., et al., 2016. Comparative effects of nodularin and microcystin-LR in zebrafish: 1. Uptake by organic anion transporting polypeptide Oatp1d1 (Slco1d1). Aquat. Toxicol. 171, 69-76.

Fischer, W.J., et al., 2005. Organic anion transporting polypeptides expressed in liver and brain mediate uptake of microcystin. Toxicol. Appl. Pharm. 203, 257-263.

Franzenburg, S., et al., 2013. Distinct antimicrobial peptide expression determines host species-specific bacterial associations, Proc. Natl. Acad. Sci., pp. E3730-E3738.

Fraser, C., et al., 2009. The bacterial species challenge: making sense of genetic and ecological diversity. Science 323, 741-746.

Fraune, S., et al., 2015. Bacteria-bacteria interactions within the microbiota of the ancestral metazoan *Hydra* contribute to fungal resistance. ISME J. 9, 1543-1556.

Heeg, J.S., Wolf, M., 2015. ITS2 and 18S rDNA sequence-structure phylogeny of *Chlorella* and allies (Chlorophyta, Trebouxiophyceae, Chlorellaceae). Plant Gene 4, 20-28.

Hess, S., et al., 2012. Shedding light on vampires: the phylogeny of vampyrellid amoebae revisited. PloS one 7, e31165.

Hoshina, R., 2014. DNA analyses of a private collection of microbial green algae contribute to a better understanding of microbial diversity. BMC Res. Notes 7, 592.

Hoshina, R., et al., 2005. Genetic evidence of “American” and “European” type symbiotic algae of *Paramecium bursaria* Ehrenberg. Plant Biology 7, 526-532.

Huttenhower, C., et al., 2012. Structure, function and diversity of the healthy human microbiome. Nature 486, 207-214.

Jacquet, S., et al., 2005. The proliferation of the toxic cyanobacterium *Planktothrix rubescens* following restoration of the largest natural French lake (Lac du Bourget). Harmful Algae 4, 651-672.

Kurmayer, R., et al., 2016. Role of toxic and bioactive secondary metabolites in colonization and bloom formation by filamentous cyanobacteria *Planktothrix*. Harmful Algae 54, 69-86.

Lefèvre, C., et al., 2004. Endosymbiont phylogenesis in the dryophthoridae weevils: evidence for bacterial replacement. Mol. Biol. Evol. 21, 965-973.

Leidy, J., 1879. Fresh-water rhizopods of North America. Government Printing Office, Washington.

Lema, K.A., et al., 2014. Onset and establishment of diazotrophs and other bacterial associates in the early life history stages of the coral *Acropora millepora*. Mol. Ecol. 23, 4682-4695.

Liu, Y., et al., 2009. Phylogenomic analyses predict sistergroup relationship of nucleariids and Fungi and paraphyly of zygomycetes with significant support. BMC Evol. Biol. 9, Article No.: 272.

Lozupone, C.A., et al., 2012. Diversity, stability and resilience of the human gut microbiota. Nature 489, 220-230.

Luo, W., et al., 2010. Generic concept in *Chlorella*-related coccoid green algae (Chlorophyta, Trebouxiophyceae). Plant Biology 12, 545-553.

Lynn, D.H., Strüder-Kypke, M.C., 2006. Species of *Tetrahymena* identical by small subunit rRNA gene sequences are discriminated by mitochondrial cytochrome c oxidase I gene sequences. J. Eukaryot. Microbiol. 53, 385-387.

MacKintosh, C., et al., 1990. Cyanobacterial microcystin-LR is a potent and specific inhibitor of protein phosphatases 1 and 2A from both mammals and higher plants. FEBS Lett. 264, 187-192.

Margulis, L., 1992. Biodiversity: molecular biological domains, symbiosis and kingdom origins. Biosystems 27, 39-51.

Martin, W.F., et al., 2015. Endosymbiotic theories for eukaryote origin. Phil. Trans. R. Soc. B 370, 20140330.

Mereschkowsky, C., 1905. Über Natur und Ursprung der Chromatophoren im Pflanzenreiche, Biol. Central., 25 ed, Leibzig.

Mereschkowsky, C., 1910. Theorie der zwei Plasmaarten als Grundlage der Symbiogenesis, einer neuen Lehre von der Entstehung der Organismen, Biol. Central., 30 ed, Leibzig.

Mignot, J.P., Savoie, A., 1979. Ultrastructural observations on *Nuclearia simplex* Cienkowski (Protozoa, Rhizopodea, Filosia). Protistologica 15, 23-32.

Mitchell, D.R., 2007. The evolution of eukaryotic cilia and flagella as motile and sensory organelles. Adv. Exp. Med. Biol. 607, 130-140.

Moran, N.A., 1996. Accelerated evolution and Muller's rachet in endosymbiotic bacteria. Proc. Natl. Acad. Sci. USA 93, 2873-2878.

Nowack, E.C.M., Melkonian, M., 2010. Endosymbiotic associations within protists. Phil. Trans. R. Soc. B 365, 699-712.

Patterson, D.J., 1984. The genus *Nuclearia* (Sarcodina, Filosea): species composition and characteristics of the taxa. Arch. Protistenk. 128, 127-139.

Pawlowski, J., et al., 2012. CBOL Protist Working Group: Barcoding eukaryotic richness beyond the animal, plant, and fungal kingdoms. PLoS Biol. 10, e1001419.

Pflugmacher, S., et al., 1998. Identification of an enzymatically formed glutathione conjugate of the cyanobacterial hepatotoxin microcystin-LR: the first step of detoxication. Biochim. Biophys. Acta 1425, 527-533.

Posch, T., et al., 2012. Harmful filamentous cyanobacteria favoured by reduced water turnover with lake warming. Nature Clim. Change.

Rapala, J., et al., 2005. *Paucibacter toxinivorans* gen. nov., sp nov., a bacterium that degrades cyclic cyanobacterial hepatotoxins microcystins and nodularin. Int. J. Syst. Evol. Microbiol. 55, 1563-1568.

Rodríguez-Ezpeleta, N., et al., 2005. Monophyly of primary photosynthetic eukaryotes: green plants, red algae, and glaucophytes. Curr. Biol. 15, 1325-1330.

Sagan, L., 1967. On the origin of mitosing cells. J. Theor. Biol. 14, 255-274.

Schultz, J., et al., 2005. A common core of secondary structure of the internal transcribed spacer 2 (ITS2) throughout the Eukaryota. RNA 11, 361-364.

Selig, C., et al., 2008. The ITS2 Database II: homology modelling RNA structure for molecular systematics. Nucl. Acid. Res. 36, D377-D380.

Simon, E.M., et al., 2008. The "*Tetrahymena pyriformis*" complex of cryptic species. Biodivers. Conserv. 17, 365-380.

Sloan, D.B., Moran, N.A., 2012. Genome reduction and co-evolution between the primary and secondary bacterial symbionts of psyllids. Mol. Biol. Evol.

Steenkamp, E.T., et al., 2006. The protistan origins of animals and fungi. Mol. Biol. Evol. 23, 93-106.

Thrash, J.C., et al., 2011. Phylogenomic evidence for a common ancestor of mitochondria and the SAR11 clade. Sci. Rep. 1, 13.

Urrutia-Cordero, P., et al., 2013. Effects of harmful cyanobacteria on the freshwater pathogenic free-living amoeba *Acanthamoeba castellanii*. Aquat. Toxicol. 130–131, 9-17.

Van Wichelen, J., et al., 2016. The common bloom-forming cyanobacterium *Microcystis* is prone to a wide array of microbial antagonists. Harmful Algae 55, 97-111.

Walsby, A.E., et al., 1998. The critical pressures of gas vesicles in *Planktorhrix rubescens* in relation tothe depth of winter mixing in Lake Zurich, Switzerland. J. Plankton Res. 20, 1357-1375.

Woese, C.R., 1987. Bacterial evolution. Microbiol. Rev. 51, 221-271.

Wolf, M., et al., 2014. ITS2, 18S, 16S or any other RNA — simply aligning sequences and their individual secondary structures simultaneously by an automatic approach. Gene 546, 145-149.

Yoon, H.S., et al., 2011. Single-cell genomics reveals organismal interactions in uncultivated marine protists. Science 332, 714-717.

Yoshida, M., et al., 2009. *Nuclearia thermophila* sp. nov. (Nucleariidae), a new nucleariid species isolated from Yunoko Lake in Nikko (Japan). Europ. J. Protistol. 45, 147-155.

Zettler, L.A.A., et al., 2001. The nucleariid amoebae: more protists at the animal-fungal boundary. J. Eukaryot. Microbiol. 48, 293-297.

Contributions at scientific congresses

Congress (venue, date)	Title of contribution
5th Swiss Microbial Ecology congress SME (Murten, Switzerland, 05.02.2013)	Oral presentation: The amoeba *Nuclearia* sp. from Lake Zurich live in concert with ecto- and endosymbiotic bacteria
32nd Meeting of the German Society for Protozoology (Warth-Weiningen, Switzerland, 28.02.2013)	Oral presentation: Ménage-à-trois: The amoeba *Nuclearia* sp. from Lake Zurich with its ecto- and endosymbiotic partners
1st EMBO Conference on Aquatic Microbial Ecology SAME13 (Stresa, Italy, 10.09.2013)	Oral presentation: Ménage-à-trois: The amoeba *Nuclearia* sp. from Lake Zurich with its ecto- and endosymbiotic partners
27th general assembly of the Swiss Society of Hydrology and Limnology SGHL (Lausanne, Switzerland 16.11.2013)	Oral presentation: Ménage-à-trois: The amoeba *Nuclearia* sp. from Lake Zurich with its ecto- and endosymbiotic partners
33nd Meeting of the German Society for Protozoology (Essen, Germany, 12.02.2014)	Poster: *Nuclearia* spp. from Lake Zurich feeding on *Planktothrix rubescens*
15th International Symposium an Microbial Ecology ISME (Seoul, South-Korea, 26.08.2014)	Oral presentation: *Nuclearia* spp. from Lake Zurich with their associated symbionts
34st Meeting of the German Society for Protozoology (Magdeburg, Germany 05.03.2015)	Oral presentation: Promiscuous or conservative symbiont acquisition in the genus *Nuclearia*?
7th European Concress of Protistology ECOP in partnership with ISOP (Sevilla, Spain 07.09.2015)	Oral presentation: Promiscuous and conservative symbiont acquisition in the genus *Nuclearia*

Selected abstracts of oral presentations:

Abstract I: Presentation abstract for SAME13

TUESDAY 10 SEPTEMBER 2013
OS-5. Giving and getting: lifestyles of attached and symbiotic microbes

12:15 *MÉNAGE-À-TROIS*: THE AMOEBA *NUCLEARIA* SP. FROM LAKE ZURICH WITH ITS ECTO- AND ENDOSYMBIOTIC PARTNERS

Sebastian Dirren, Limnological Station, University of Zurich (Switzerland)
Coauthors: Salcher MM, Pernthaler J, Schweikert M, Posch T

We present a fascinating triad relationship between a eukaryotic amoeba and its two bacterial partners. As the benthic amoeba feeds on toxic filamentous cyanobacteria (*Planktothrix rubescens*), we hypothesized that symbiotic bacteria may be involved in the degradation of toxic metabolites. For the identification of the three microbial partners we used morphological features as well as molecular methods like cloning and sequencing of the small subunit rRNA, and fluorescence *in situ* hybridisation. The morphological characteristics of the amoeba isolated from Lake Zurich allowed for a confident affiliation to the genus *Nuclearia*. However, for species identification we obtained an ambiguous image. Sequence comparisons favoured the affiliation of our isolates to the species *N. thermophila* but several observed morphological features are in strong contradiction to the original description. Isolates from Lake Zurich live in symbiosis with ecto- and endosymbiotic bacteria. The ectosymbiont is localized regularly arranged inside a layer of extracellular polymeric substances provided by the amoeba. It was identified as *Paucibacter toxinivorans*, a bacterium that was originally isolated through enrichment with the cyanobacterial toxin microcystin. Thus, *P. toxinivorans* may indeed increase the fitness of the nucleariid amoeba, being involved in the detoxification of its toxic food. The endosymbiont was observed by transmission electron microscopy to be enclosed in symbiosomes inside the amoebal cytoplasm. According to the 16S rDNA sequence, this bacterium belongs to *Gammaproteobacteria* but it could not be grouped into any established genus. Therefore, we propose the provisional name *Candidatus* Companero nuclearis for these bacteria that have until now never been found free-living nor in a symbiotic association. Additionally, we have never observed endosymbiont-free amoebae of our isolates, which might indicate that this interaction is an obligate symbiosis. In contrast, ectosymbiotic bacteria may be lost, still enabling the amoeba to survive. We highlight that the presented microbial *Ménage-à-trois* may serve as a wonderful model system to study very basic symbiotic interactions between pro- and eukaryotes.

Abstract II: Presentation abstract for ECOP / ISOP

PROMISCUOUS AND CONSERVATIVE SYMBIONT ACQUISITION IN THE GENUS NUCLEARIA

Sebastian Dirren (Limnological Station, Institute of Plant Biology, University of Zurich, Switzerland), Michaela M. Salcher (Biology Centre of the Academy of Sciences of the Czech Republic, Institute of Hydrobiology, Ceské Budejovice, Czech Republic), Thomas Posch (Limnological Station, Institute of Plant Biology, University of Zurich, Switzerland).

Intimate associations between organisms have been observed for a long time. Knowing that such associations are manifold, we use the term symbiosis in a very general manner. We simply call the phenomenon of a close living together of dissimilar organisms a 'symbiosis'. We focused on members of the amoeboid genus *Nuclearia* (Opisthokonta, Nucleariidae) which often live in symbiosis with ecto- and endosymbiotic bacteria. We isolated 16 *Nuclearia* strains from five different Swiss lakes, of which 7 strains were associated with symbionts. The isolated amoebae were characterized morphologically as well as by their 18S rDNA. Phylogenetic analyses resulted in four already established monophyletic branches (made up by the six so far sequenced species of the genus) and an additional cluster formed by two new isolates. A very heterogeneous picture emerged by highlighting *Nuclearia* strains with associated symbionts. Apart from one cluster which included only *Nuclearia* spp. with symbiotic bacteria and two clusters with no symbionts, we also found mixed clusters which were composed of amoebae with and without symbionts. By analysing 16S rRNA genes of symbiotic bacteria, the picture got even more 'obscure'. Although already seven different symbiotic bacterial strains have been identified, it seems that we still are only scratching the surface of the symbionts' diversity. Furthermore, the characters of the symbioses seem to be different depending on the host species. *Nuclearia thermophila* harboured the same endosymbiont even when isolated from different lakes. This points to a rather conservative and obligate interaction. However, we also found two isolates of *Nuclearia delicatula* to be associated with different endosymbiotic bacteria. Here the symbiont acquisition seems to be more promiscuous. As far as we know there are no other documented cases of opisthokont protists with prokaryotic symbionts. This is especially remarkable considering the importance of symbiotic interactions for higher opisthokonts. Thus, Nucleariidae represents an ideal model group to study the basic principles of symbioses.

Poster presented at the DGP in Essen

Nuclearia spp. from Lake Zurich feeding on *Planktothrix rubescens*

Dirren Sebastian, Salcher M. Michaela, Posch Thomas

Universität Zürich[UZH]

Limnological Station, University of Zurich, CH-8802 Kilchberg, Switzerland, s.dirren@limnol.uzh.ch

We explored the so far hidden diversity of Nucleariid amoebae in the prealpine Lake Zurich, Switzerland. *Nuclearia* spp. (Opisthokonta, Nucleraiidae) were enriched and kepti n culture using the toxic cyanobacterium *Planktothrix rubescens* as sole source off ood. Molecular (18S rRNA gene; Fig.1) and morphological characterisation (Tab.1) was done for five differenti solates (Fig.2-6). Three *Nuclearia* spp. (Fig.2, 4 and 5) were associated with an ectosymbiont (inside a mucous layer) as well as one or two phylotypes of endosymbiotic bacteria inside the cell. In the case oft he symbionts sequencing of the 16S rDNA and hybridisation with specific probes (CARD-FISH) was used for their phylogenetic identification (Fig.7).

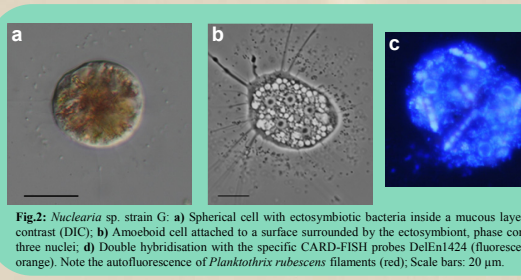

Fig.2: *Nuclearia* sp. strain G: **a)** Spherical cell with ectosymbiotic bacteria inside a mucous layer (not visible), differential interference contrast (DIC); **b)** Amoeboid cell attached to a surface surrounded by the ectosymbiont, phase contrast (PC); **c)** DAPI-stained cell with three nuclei; **d)** Double hybridisation with the specific CARD-FISH probes DelEn1424 (fluorescein; green) and LeEn827 (ALEXA546; orange). Note the autofluorescence of *Planktothrix rubescens* filaments (red); Scale bars: 20 µm.

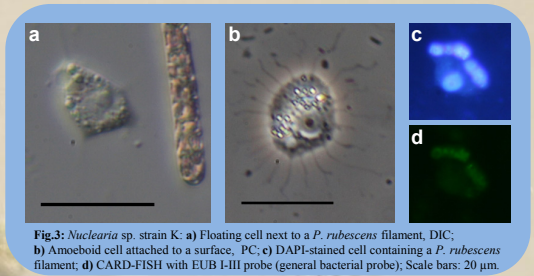

Fig.3: *Nuclearia* sp. strain K: **a)** Floating cell next to a *P. rubescens* filament, DIC; **b)** Amoeboid cell attached to a surface, PC; **c)** DAPI-stained cell containing a *P. rubescens* filament; **d)** CARD-FISH with EUB I-III probe (general bacterial probe); Scale bars: 20 µm.

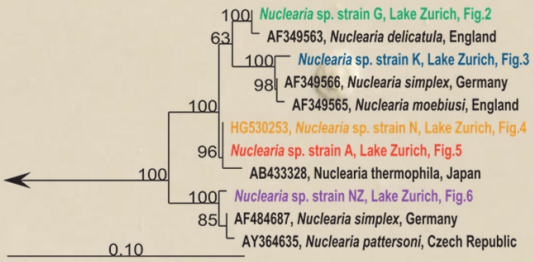

Fig.1: Bootstrapped (node labels in %) Maximum Likelihood tree (1000 iterations) based on the conserved regions of the 18S rDNA of *Nuclearia* spp. (diff. colours) isolated from Lake Zurich (Switzerland) related to all described *Nuclearia* species; Scale bar: 10 % sequence divergence.

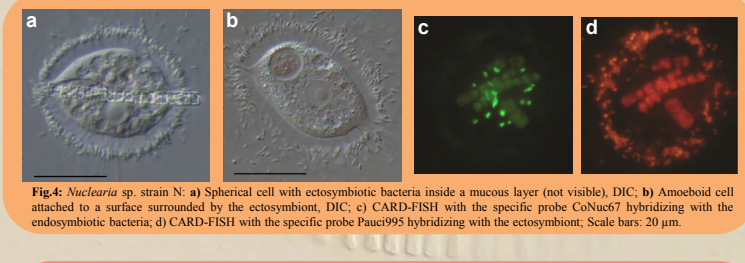

Fig.4: *Nuclearia* sp. strain N: **a)** Spherical cell with ectosymbiotic bacteria inside a mucous layer (not visible), DIC; **b)** Amoeboid cell attached to a surface surrounded by the ectosymbiont, DIC; c) CARD-FISH with the specific probe CoNuc67 hybridizing with the endosymbiotic bacteria; d) CARD-FISH with the specific probe Pauci995 hybridizing with the ectosymbiont; Scale bars: 20 µm.

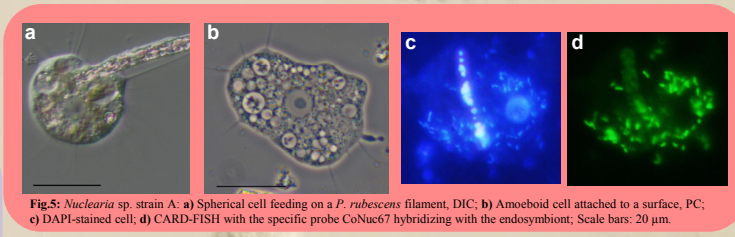

Fig.5: *Nuclearia* sp. strain A: **a)** Spherical cell feeding on a *P. rubescens* filament, DIC; **b)** Amoeboid cell attached to a surface, PC; **c)** DAPI-stained cell; **d)** CARD-FISH with the specific probe CoNuc67 hybridizing with the endosymbiont; Scale bars: 20 µm.

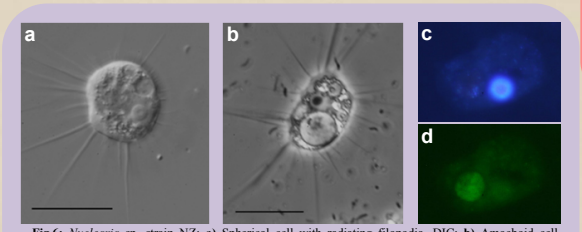

Fig.6: *Nuclearia* sp. strain NZ: **a)** Spherical cell with radiating filopodia, DIC; **b)** Amoeboid cell attached to a surface, PC; **c)** DAPI-stained cell; **d)** CARD-FISH with EUB I-III probe (general bacterial probe); Scale bars: 20 µm.

	Nuclearia sp. strain N *Nuclearia* sp. strain A	*Nuclearia* sp. strain G	*Nuclearia* sp. strain NZ	*Nuclearia* sp. strain K
Spherical form	yes	yes	yes	yes
Amoeboid	yes	yes	yes	yes
Nucleus	1 (up to ~20: syncytia)	multinucleate	uninucleate	uninucleate
Nucleolus	evident; round	evident; round/ irregular outline	evident; round	evident; round
Extracellular matrix	yes	yes	yes	yes
Cysts	yes	no	no	no
Filopodia	branched and knobbed	branched and knobbed	branched and knobbed	branched and knobbed
Cell size	7.2 - 29 µm; mean: 16.2 µm; n: 718	17.2 - 45.8 µm; mean: 25.5 µm; n: 60	10.6 - 28.4 µm; mean: 16.7 µm; n: 100	3.8 - 15.1 µm; mean: 9.8 µm; n: 100

Tab.1: Morphological characteristics of *Nuclearia* spp. from Lake Zurich.

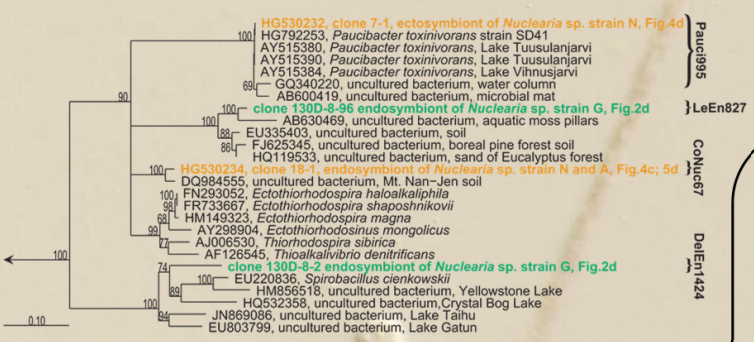

Fig.7: Bootstrapped (node labels in %) Maximum Likelihood tree (1000 iterations) based on the 16S rDNA of *Nuclearia* spp. symbionts (diff. colours) and closely related sequences from public databases. Coverage of the specific CARD-FISH probes is indicated with curly brackets; Scale bar: 10 % sequence divergence.

FNSNF
Fonds National Suisse
Schweizerischer Nationalfonds
Fondo Nazionale Svizzero
Swiss National Science Foundation

This research is financed by the Swiss National Science Foundation (SNF 31003A-138473).

We found an unexpected high diversity of Nucleariid amoebae in Lake Zurich. Since more than half oft he isolates were associated with various symbionts (ecto- and endosymbionts), symbiosis seems to be a prominent phenomenon in this group. Four oft he five characterized *Nuclearia* spp. showed unique morphological characters (Tab.1) and additionally affiliated with different clusters in the genus (Fig.1). Two isolates (strain N and A) had the morphology, symbionts (strain A lostt he ectosymbiont during cultivation) and 18S rDNA phylogeny in common, thus we consider them to belong to the same species. In total we isolated four different species, two oft hem being associated with ecto- as well as with endosymbiotic bacteria and two living without symbionts. All endosymbionts have been found neither free-living nor in symbiotic associations (~10 % sequence divergence to the closest described relatives; Fig.7).

Curriculum Vitae

Personal Data

Full name: Sebastian Dirren

Date of Birth: 27.01.1984 | Place of Birth: Visp, Switzerland | Nationality: Swiss

Work Address: Limnological Station | Seestr. 187 | 8802 Kilchberg | Switzerland

Private Address: Dorfstr. 8 | 3944 Unterbäch | Switzerland

Education

2005-2009	Bachelor in Biology, University of Zurich
2009-2010	German language and literature studies, University of Zurich
2010-2012	Master in Microbiology, entitled "*Nuclearia* sp. and its symbiotic associations", supervised by Dr. Thomas Posch, Limnological Station, University of Zurich
Since 2012	PhD-student, supervised by Dr. Thomas Posch, Limnological Station, University of Zurich
Since 2012	Member of the Science Zurich Graduate School, Microbiology and Immunology (MIM)

Awards

Oct 2013	Master thesis awarded by the Foundation for Hydrobiology-Limnology (Hydrobiologie-Limnologie-Stiftung für Gewässerforschung); Zurich
Feb 2015	Poster prize (second place) at the conference of the German Society for Protozoology, Essen (Germany)

External acquired skills

Nov 2011	Transmission Electron Microscopy: Conventional preparation and photomicrography; 2 weeks supervised by Dr. Michael Schweikert, University of Stuttgart
Nov 2014	Transmission Electron Microscopy: Conventional preparation and photomicrography; 2 weeks supervised by Dr. Michael Schweikert, University of Stuttgart
Nov 2015	Library preparation for Illumina sequencing: 1 week at Genetic Diversity Centre (GDC) supervised by Dr. Stefan Neuenschwander, ETH of Zurich.
Jan 2016	Transmission Electron Microscopy: High pressure freezing / freeze substitution method; 1 week at the Centre for Microscopy and Image Analysis supervised by Dr. Andres Käch, University Zurich

Publications

Dirren S, Salcher MM, Blom JF, Schweikert M & Posch T (2014) Ménage-à-trois: The amoeba *Nuclearia* sp. from Lake Zurich with its ecto- and endosymbiotic bacteria. *Protist* 165: 745-758.

Dirren S & Posch T (2016) Promiscuous and specific bacterial symbiont acquisition in the amoeboid genus *Nuclearia* (Opisthokonta). *FEMS Microbiology Ecology* 92.

Dirren S, Pitsch G, Da Silva M & Posch T (in prep.) Feeding of *Nuclearia thermophila* and *Nuclearia delicatula* (Nucleariidae, Opisthokonta) on the toxic cyanobactetrium *Planktothrix rubescens*.

Pitsch G, Adamec L, Dirren S, Nitsche F, Šimek K, Sirová D & Posch T (accepted) The green *Tetrahymena utriculariae* n. sp. (Ciliophora, Oligohymenophorea) with its endosymbiotic algae (*Micractinium* sp.), living in traps of a carnivorous aquatic plant. *Journal of Eukaryotic Microbiology*.

Teaching Experience

Mar 2013	Planning of project and supervision of student groups during the block course Bio290; Aquatic Microbial Ecology, University of Zurich
Apr 2014	Planning of project and supervision of student groups during the block course Bio290; Aquatic Microbial Ecology, University of Zurich
Mar 2015	Planning of project and supervision of student groups during the block course Bio290; Aquatic Microbial Ecology, University of Zurich
Mar 2016	Planning of project and supervision of student groups during the block course Bio290; Aquatic Microbial Ecology, University of Zurich

Supervision of students during internships

Sep-Nov 2014	Internship by Marvin Moosmann; Project entitled “A look beyond the nose: Seven new *Nuclearia* strains from Lake Hallwil and Lake Baldegg”, Limnological Station, University of Zurich
Jul-Aug 2015	Internship by Natalie Wickli; Project entitled “Feeding behaviour and comparative growth experiment of the eukaryotic amoeba *Nuclearia*”, Limnological Station, University of Zurich

Acknowledgment

There are many people who supported me during the last years. First, I would like to thank Thomas Posch: You were a great 'Doktorvater', always helping me when help was needed. It was wonderful to work together with somebody who was as enthusiastic about new discoveries as me. Nobody else knows better than you, that scientific discussions can be improved with a beer or two. Although sometimes ingenious ideas the next day turned out to be not that brilliant as they seemed at first glance, it was always a lot of fun spending evenings at the lake with you. Next I wish to thank Jakob Pernthaler for giving me the opportunity to do my PhD at the Limnological Station in Kilchberg. Discussions with you were always a source for inspirations and new inputs. Moreover I am thankful to Leo Eberl for all the useful suggestions during the committee meetings. Further I want to thank Michaela Salcher: Thank you so much for your practical tips and tricks in the lab and all the discussions about science and other things during your time at the Limnological Station. Afterwards, it was great to have somebody in the Czech Republic, who invited us or brought some good beers back to Zurich. The boat trip on the Vitava was great fun. Then I am very grateful to Gianna Pitsch: Thank you for everything. It is wonderful to spend time with you not only in the lab or in front of a screen showing a manuscript, but also climbing the walls of beautiful mountains in the midst of unforgettable sceneries. It is a present to have found a good friend, a work colleague and a partner for life combined in one person - what more could one wish for? Next I would like to thank Marisa Da Silva for measuring all the microcystin samples. It was nice to work together with you on the project about the feeding of *Nuclearia* and the degradation of microcystin. Moreover I am thankful to Stefan Neuenschwander: Many thanks not only because you kept all the things clean even from evil DNA, but also for all the further help and helpful suggestions. Thank you for the help with the genome sequencing and all the scientific discussions. Apart from that, it was great that we sometimes managed to persuade you to join us to the climbing gym or the 'Klettergarten'. Further I would like to thank Bettina Eugster: You were a great help in the lab, always keeping the things at their right place. It was nice that you accompanied me to Stuttgart for TEM and that you were always ready to help. Moreover I am thankful to Michael Schweikert for the invitation to Stuttgart and for introducing me to the world of TEM imaging. Apart from the gained skills, thank you for the continuous and enjoyable entertainment. Then I wish to thank Andres Käch for showing me how to prepare samples with the high pressure freezing / freeze substitution method for TEM. Further I am thankful to Judith Blom for the microcystin and all the HPLC measurements. The sampling of Lake Zurich and other sampling campaigns would not have been possible without Eugen Loher: Many thanks that you are the best boat captain and that you fixed all the broken things. You were the most important contact person for questions about technical issues and IT problems. Thank you also for all the small useful gadgets you built. Administration is not the most joyful work, but nonetheless it is necessary for a PhD. I am very thankful to Astrid Kunz: Thank you for taking over these sometimes disagreeable administrative tasks and for all our cakes, snacks and deserts. I also wish to thank Ester Eckert: It was great fun to spend time with you, no matter if in the lab, at lunch or after work. Although we had sometimes different views, discussions were always interesting and entertaining. Another person who broad a lot of enthusiasm to the group, was Marie-Ève Garneau: Thank you for proof reading my first manuscript and of

course for the wild parties you organised. Additionally, I want also thank all the members of the Limnological Station, who were not directly involved in my projects but were always there for discussions and non-work related activities: Yana Yankova, Natalia Krempaska, Karel Hornak, Daniel Marty, Esther Kohler, Estelle Bruni, Michael Baumgartner and Jörg Villiger. Further, I was lucky to get motivated students during the student coursed at the Limnological Station: Tamara Schlegel, Nathalie Amacker, Alexandra Barmettler, Annika Hunziker, Gabriela Purtschert, Jeanine Brantschen and Saskia Senn. I want to thank all of you for the valuable work you did. Such small projects often uncovered new aspects and were an important enrichment of my PhD. Two other students I supervised during an internship were also a great help: Marvin Moosmann and Natalie Wickli. I was happy that after Marvin's first frustration and his fear of never finding a *Nuclearia*, the project turned out to be very successful. Basically, Marvin isolated many different *Nuclearia* strains, of which some even belong to a new species. Last but not least I would like to thank my Parents: You were always there for me and supported me in many ways. You believed in me and I could always count on you. Thank you very much.